Specific separation- and detection strategies for the characterization of acid-functional polymers

Brooijmans, T.

Publication date
2022

Document Version
Final published version

Specific separation- and detection strategies for the characterization of acid-functional polymers

Ton Brooijmans

SPECIFIC SEPARATION- AND DETECTION STRATEGIES FOR THE CHARACTERIZATION OF ACID-FUNCTIONAL POLYMERS

Ton Brooijmans

Specific separation- and detection strategies for the characterization of acid-functional polymers

Ton Brooijmans

2022

Specific separation- and detection strategies for the characterization of acid-functional polymers

PhD thesis, University of Amsterdam, The Netherlands

ISBN:	978-94-6458-506-3
Cover design:	Anita Dredor | www.skinque.com
Image design:	Ton Brooijmans, base vector images by www.freepik.com
Lay-out:	Publiss | www.publiss.nl
Print:	Ridderprint | www.ridderprint.nl

UNIVERSITEIT VAN AMSTERDAM

Specific separation- and detection strategies for the characterization of acid-functional polymers

ACADEMISCH PROEFSCHRIFT

ter verkrijging van de graad van doctor
aan de Universiteit van Amsterdam
op gezag van de Rector Magnificus
prof. dr. ir. P.P.C.C. Verbeek
ten overstaan van een door het College voor Promoties ingestelde commissie,
in het openbaar te verdedigen in de Agnietenkapel
op vrijdag 4 november 2022, te 13.00 uur

door
Ton Franciscus Henricus Brooijmans
geboren te Waalwijk

Promotiecommissie

Promotores:	Prof. dr. R.A.H. Peters *Universiteit van Amsterdam* Prof. dr. ir. P.J. Schoenmakers *Universiteit van Amsterdam*
Copromotores:	Dr. B.W.J. Pirok *Universiteit van Amsterdam*
Overige leden:	Prof. dr. A.C. van Asten *Universiteit van Amsterdam* Dr. W. Radke *PSS Polymer Standards Service* Dr. ir. P.J.C.H. Cools *Grace, Columbia* Prof. dr. M.R. van Bommel *Universiteit van Amsterdam* Prof. dr. S. van der Wal *Universiteit van Amsterdam* Prof. dr. C.E. Koning *Rijksuniversiteit Groningen* Prof. dr. G.J.M. Gruter *Universiteit van Amsterdam*

Faculteit der Natuurwetenschappen, Wiskunde en Informatica

When hope and love has been lost
And you fall to the ground
You must find a way
When the darkness descends
And you're told it's the end
You must find a way
When God decides to look the other way
And a clown takes the throne
We must find a way
Face the firing squad
Against all the odds
You will find a way

From Dig Down - Simulation Theory
Lyrics by Matt Bellamy

Table of contents

Between you getting out of bed and reading this thesis, you may not know but you have touched a multitude of different polymers / macromolecules. Really. The textile covers you sleep under are dyed and printed using (chemically modified) starch derivatives such as algin, guar gum and carboxymethylcellulose. Stepping out of bed, depending on which floor you have in your bedroom, you will touch a topcoat of polyurethane, a UV-curable polymer or a polyacrylate. The bathroom is also filled with polymers, be it in your shampoo, hair gel, toothpaste or your polyester/nylon towel. Your morning newspaper (and if you are reading this thesis as hardcopy) uses pigments which are glued to the paper using – indeed: polymers. The application area for polymers is endless, and the life as we know it today would not be possible without polymers. In a more literal sense this is also true: the energy source for the majority of life (plants, animals, bacteria, fungi) is glycogen – a polysaccharide polymer. Early man used polymer products such as wool or hemp to stay warm, the Mayans and Aztecs made balls from natural rubber to play their famous ball game named pokolpok. In modern Spanish it is known as "pelota maya" and it is still played in certain Mexican regions. Before 1000 AD, this little polymer ball literally decided over life and death – talk about losing your head over a ballgame.

The Pelota Maya ball court at Chichén Itzá, Yucatan Peninsula – Mexico (Picture by Ton Brooijmans, 2009)

Similar to coating formulations, where polymers act as the binding ingredient – polymers are one of the most important classes of materials which keep our society together.

CHAPTER 1

General Introduction

1.1 Water-borne polymers

Synthetic polymers have been around for over a hundred years, the first man-made polymers were celluloid (a thermoplastic plant-derived polymer, made of a blend of nitrocellulose and camphor) and Bakelite (the first synthetic polymer, prepared by a condensation reaction between phenol and formaldehyde). Both polymer types, although useful for decades, have been outperformed by newer polymer types. A more specific application for synthetic polymers are coatings, intended to provide certain properties to the surface of an object. A class of polymers that is rapidly gaining ground in global applications are the water-borne coatings, which are replacing the traditional solvent-borne coatings. These solvent-borne coatings release a large amount of volatile organic compounds (VOCs) upon drying of the coatings. These VOCs originate from the solvent used in the resins/binders and additives in the coatings. Water-borne coatings use water as the diluent, which is also released upon drying of the coating – and thus immensely more friendly for people and environment. The polymers in these coating solutions are dispersed in water as nanometer- to micrometer-sized particles, using surface-active species to stabilize the particles. A schematic representation of such a particle is shown in Figure 1.1.

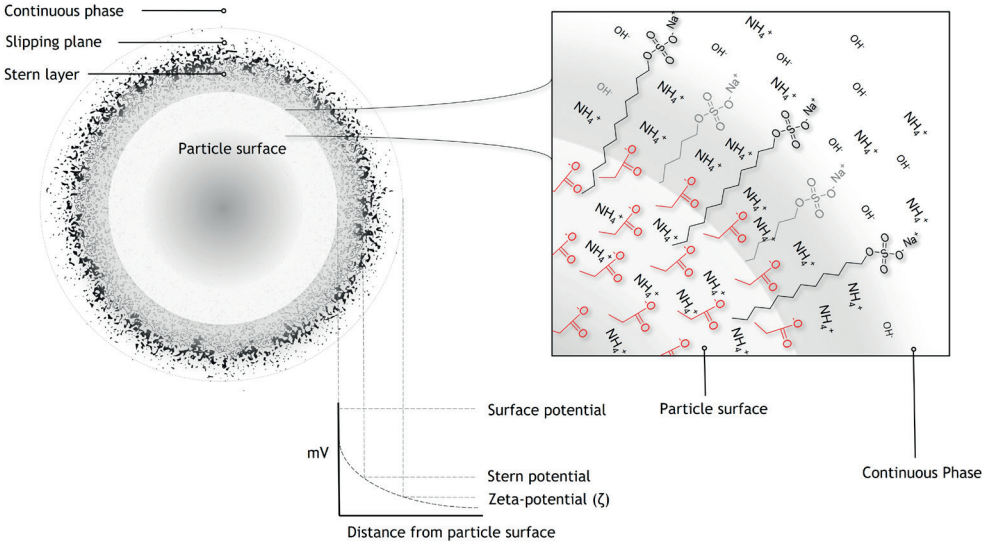

Figure 1.1. Schematic representation of the surface of a colloidal polymer particle. Particle surface shows presence of deprotonated acrylic acid monomer functionality and adsorbed surfactant molecules.

A multitude of water-borne polymer chemistries have been developed over the years, including polyolefins, polyamides, polyesters, polyurethanes, polyacrylics and many hybrids of the aforementioned chemistries. The most frequently used water-borne particle chemistries in current commercial applications are polyurethanes and polyacrylics, mostly due to superior dispersion stability, flexible synthesis routes and end-product performance. Polyacrylics are found in a wide variety of applications, including wall paints, pressure-sensitive adhesives, paper- and plastic coatings, ink formulations and joinery applications [1-3], while water-borne polyurethanes are mostly used in high-end markets such as the automotive industry, tactile coatings and leather applications due to their great elasticity and flexibility, combined with very durable coating surfaces [4-6]. Also, the high degree of adhesion to various substrates makes polyurethanes very suitable for primer applications. Both polyacrylics and polyurethanes are also increasingly applied in coating and printing of food packaging.

1.1.1 Polyacrylics

Although acrylic acid was first synthesized in 1843, the use of acrylic acid and its esters in water-borne acrylic emulsions had to wait for commercialization in the 1950's.

Water-borne acrylics are synthesized using emulsion polymerization [7], which is a form of free-radical polymerization. In contrast to solvent- or bulk polymerization, the continuous phase during the reaction is water. Next to the significantly reduced environmental impact upon release of the water during the coating drying process compared to solvent-borne coatings, another significant advantage is obtained using water as a continuous phase. During emulsion polymerization, the polymers are formed as droplets within this continuous phase. The polymers within these droplets may achieve molar masses which are far beyond the mass range that can be achieved during solvent- or bulk polymerization processes – mainly due to viscosity limitations of dissolved polymers. In water-borne polymers, molar mass build-up does not have a significant effect on resin viscosity as the polymers are not dissolved in the continuous phase. This enables a different range of polymer properties to be achieved with respect to coating durability as higher molar mass / crosslinking result in better chemical- and physical resistances.

Radical polymerization of acrylics takes places in a three-step process, consisting of initiation (I), propagation (II) and termination (III), which is shown in Figure 1.2. Initiator (R-R) is thermally dissociated into two radicals (R·), which may react with monomer units (M). Upon growth of the polymer chain, the polymer radical may lose its reactivity

by recombination with another polymeric radical chain or a low molar mass radical R·, proton abstraction from a different chain (disproportionation) or a chain transfer reaction (X, which may be a monomer, polymer, solvent or a chain transfer agent), which transfers the radical to a different chemical species.

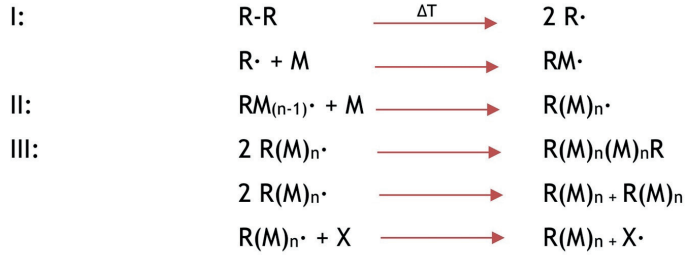

Figure 1.2. Radical polymerization process, three phases can be discerned: initiation (I), propagation (II) and termination (III).

In emulsion polymerization, the initiation phase takes place in the water phase, which contains stabilizing chemicals – most commonly surfactants or pre-formed polar (acrylic) oligomers capable of micelle formation. Water-soluble radical initiators such as persulphates and hydrophilic peroxides are commonly used in this process. These initiators produce radicals through thermal dissociation and rapidly react with acrylic monomer units which are present in the water phase. After this radical oligomer chain achieves a certain chain length and thus, a lower water-solubility, these radical monomer chains transfer into micelles which are formed by the surfactants present in the water phase above their critical micelle concentration (CMC). Within the micelles, polymerization continues and is supplied by diffusion of the monomer from the monomer droplets into the water phase and into the micelles. A schematic representation is shown in Figure 1.3. The hydrophilicity of the monomers used is an important consideration, as a (small) degree of water-solubility is required to properly perform emulsion polymerization. Many different monomers with varying acrylic ester lengths and functionalities are available, including acrylic- and methacrylic acid. These carboxylic acid monomers are specifically used to impart better particle stability by incorporating them into the polymer backbone and deprotonating them using (in)organic bases.

More water-soluble monomers, such as the acidic monomers mentioned above, obviously have a higher chance to undergo radical initiation in the water phase. As such, these monomer types are likely one of the first to undergo radical propagation.

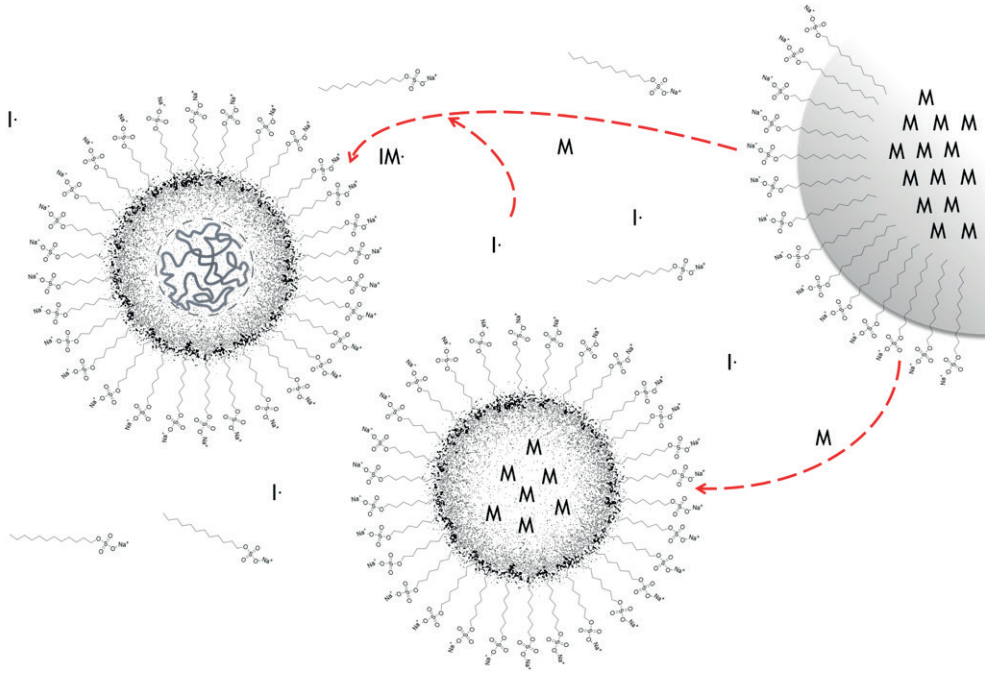

Figure 1.3. Schematic representation of emulsion polymerization. Monomers are indicated by M, initiator molecules by I. From right to left: a monomer droplet (stabilized in water by adsorbed surfactant), a monomer-swollen polymer particle and a resulting (fully reacted) polymer particle.

1.1.2 Polyurethanes

The first polyurethanes were made in 1937 by Bayer *et al.* [8] as a replacement for rubber, and one of the initial applications for this novel chemistry was the synthesis of flexible polyurethane foam [9, 10]. Commercial applications were introduced in the 1950's. To this date, polyurethanes are still widely used in many applications such as resilient foam, elastomeric wheels and tires. A specific application for polyurethanes was found in coatings, as this material combines coating durability, flexibility and abrasion resistance with good adhesion to various substrates – making it widely applicable.

Polyurethanes are synthesized by the reaction of di- or tri-isocyanates with multifunctional alcohols. This reaction is slow at room temperature but is considerably faster at higher temperatures and/or upon addition of a catalyst. The nature and structure of the catalyst has a strong influence on the polyurethane reaction profile, resulting in different selectivity between monomer units. This different buildup in turn results in polymer with different properties. Traditionally used catalysts include tertiary amines such as triethylamine

(which is also a common neutralizing base for water-borne carboxylic functionality), 1,8-diazabicyclo(5.4.0)undec-7-ene and organometallic catalysts. This latter class is under increasing pressure from a regulatory perspective, specifically the organotin catalysts (which have been one of the most frequently used in the synthesis of polyurethanes) pose a significant risk for human safety. Less toxic alternatives such as bismuth salts [11] are finding more and more applications by many resin suppliers.

Viscosity of the alcohol/isocyanate reaction mixture will rapidly build upon formation of longer chains of so-called prepolymer. In a second reaction step, the isocyanate-functional prepolymer may be reacted with an extension agent, which is commonly a diamine. In the case of a water-borne polyurethane system (or more correctly, a polyurethane-urea) the dispersion step and the extension step are performed simultaneously [12]. Depending on the desired chemistry, the extension agent may be added to the water prior to addition of urethane prepolymer (pre-extension) or after (post-extension). In the latter case, a more significant fraction of the isocyanate groups will react with water. This results in the formation of primary amine end groups that may react further with isocyanate end groups attached to other polymer molecules, resulting in chain extension under formation of a urea group (Figure 1.4).

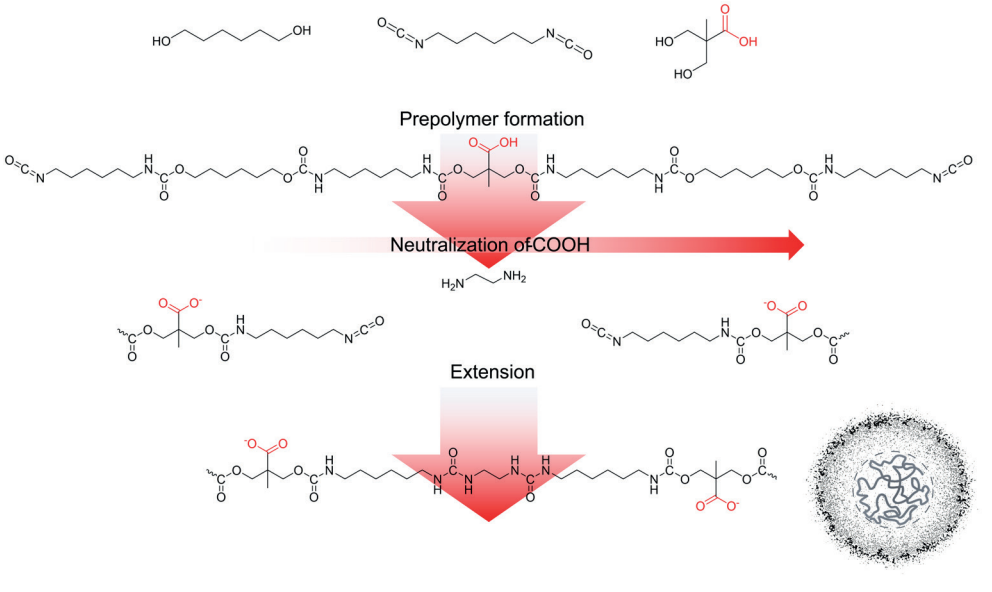

Figure 1.4. Theoretical representation of the synthesis of a polyurethane-urea polymer, consisting of hexanediol, hexane diisocyanate and dimethylolpropanoic acid. Extension is performed by addition of the polyurethane prepolymer to an aqueous solution of ethylenediamine, resulting in particle formation.

Although the choice of diisocyanate monomers is relatively limited, the polyol types that can be used are not. Soft segments can be incorporated using polyether polyols such as polyethylene glycol (PEG), polypropylene glycol (PPG) or polytetramethylene glycol (PTMG, also known as polytetrahydrofuran - PTHF) or combinations, which are already polymeric building blocks. Next to these frequently used soft segment types, polyester polyols or polycarbonate diols can be used. These polyols can be built from a wide range of diols and dicarbonates. The large variety in monomer types enables polymer scientists to synthesize and fine-tune polyurethane resins with many different final properties.

1.1.3 Polymer microstructure

As the choices with respect to polymer composition and processing are virtually endless, the polymer architectures that can be built from these choices are equally vast. The synthesis of polymers results in the creation of polymer chains which show heterogeneity, *i.e.* not all resulting polymer chains or particles are created with equal chemical and morphological microstructure [13]. Many types of heterogeneity exist in polymer microstructure, of which the molecular weight distribution (MWD), chemical composition distribution (CCD), degree-of-branching distribution and functionality-type distribution (FTD) are well-known examples. A graphical representation of these modes of heterogeneity is shown in Figure 1.5.

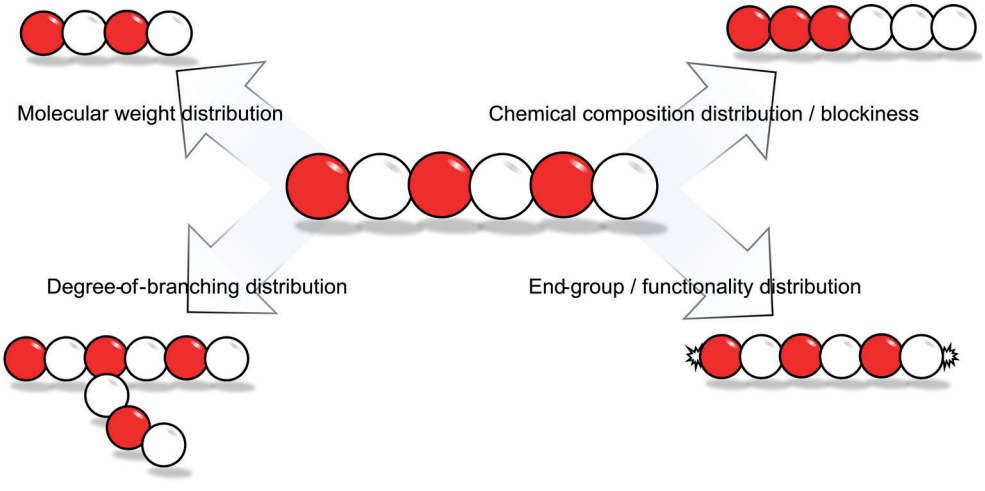

Figure 1.5. Schematic representation of different modes of molecular heterogeneity in macromolecules.

These types of molecular heterogeneity exist simultaneously, so (for instance) a copolymer – consisting of monomer A, B and C - could have an enriched fraction of A in the low- or high molar mass, preferentially B as a blocky section, and/or C as a branching unit. The presence of all these superimposed modes of heterogeneity results in very complex macromolecules. If information is required on how these materials are built up, analytical techniques can be applied. Next to spectroscopic techniques such as nuclear magnetic resonance (NMR) or infrared spectroscopy (IR), these complex systems can be separated by chromatographic techniques. Depending on the type of separation that is performed, a certain aspect (or combinations of aspects) of these polymers may be characterized, such as the molecular weight distribution. Achieving separations which are purely based on a single aspect of the polymer heterogeneity is not a trivial task, as often one distribution influences the analysis of another distribution (*e.g.* the molecular weight distribution of a polymer has an effect on the chemical composition distribution analysis). The separation of these complex systems (preferably as a single-parameter separation) can enable detailed insights in the polymeric microstructure. The chemical microstructure determines the organization / behavior of molecules in water-borne coating particles (mesostructure) and the properties of the final coating surface (macrostructure). It is therefore crucial to understand the microstructure of these polymers, so that this chemical information can be correlated with meso- and macrostructural properties. This knowledge could enable the development of tailor-made polymer microstructures. This can result in the creation of polymers which have superior performance (such as adhesion, durability, flexibility), are more environmentally friendly and/or have a more cost-efficient profile. The need to obtain more insights into the polymer microstructure results in many novel chromatographic optimizations or developments with regard to separating polymer species.

1.1.4 Acid functionality

The incorporation of monomer units with a specific functionality, other than used to construct the polymer itself, can be utilized to provide polymers with additional features. Examples of these functional monomers are:

i. Hydroxy-functional (meth)acrylates, which can provide reactivity towards isocyanates in two-component systems when incorporated through radical polymerization [14] or ultraviolet (UV) curing reactivity when incorporated through reaction with isocyanates in urethane chemistry [15].

ii. Diacetoneacrylamide, which is a frequently used ketone-functional monomer in radical polymerizations. This monomer type may react with substances like adipic dihydrazide in a post-application crosslinking reaction [16]. This Schiff-

base reaction primarily takes place at low pH, which is achieved upon drying of the coating (by evaporation of neutralizing bases such as ammonia). Similar functional groups can also be incorporated in polyester- or polyurethane backbones by ketone-functional dialcohols or diacids such as α-ketoglutaric acid.

iii. (Meth)acrylic acid, which is one of the most frequently used functional monomers in water-borne acrylic polymers. These acidic monomer types are the basis of all acrylic monomers as those are prepared from esterification of alcohols with (meth)acrylic acid, but acid monomers may also be used unmodified. The pendant acid groups that are obtained in a polymer backbone are used to provide additional stability of water-borne polymer particles and to provide more durability and adhesion to certain substrates [17, 18]. Polyurethane polymers almost exclusively use dimethylolpropanoic acid, an acid-functional dialcohol for similar purposes [19, 20].

The acid functionality in water-borne resins is of importance, as it directly impacts various aspects of the synthesized polymers, such as colloidal stability and end-product coating properties. The polymer microstructure with respect to this functional monomer is of crucial importance, as the way in which it is incorporated (sequence order, block length) directly influences the polymer properties [21, 22]. By combining data of many chromatographic and/or spectroscopic techniques, information regarding the polymer microstructure can be obtained. For instance, fractional monomer conversion measurements can describe the incorporation of monomer units as a function of the polymerization time [23]. Although this is very useful information, it is unknown where the reacted monomers are incorporated – we only know these monomers are incorporated somewhere in the polymer. Spectroscopic techniques such as infrared spectroscopy (IR) and nuclear magnetic resonance spectroscopy (NMR) are also often applied for the characterization of water-borne polymers [24-27]. Hyphenation of these techniques with separation systems is particularly promising for revealing polymer microstructure [28]. However, the acid monomer is, composition-wise, often used in the low percentile region in water-borne polymers. This poses sensitivity challenges for named spectroscopic techniques to accurately characterize the acid functionality. To be able to prepare water-borne resins with optimized properties and performance, there is a need to direct these properties towards the desired direction. In order to do so, however, the polymer microstructure with respect to the acid-functionality must be understood.

In the following paragraphs, a literature review is described on various conventional polymer analysis techniques which are frequently applied for the characterization of (water-borne) resins. Next to this, recent developments associated with these techniques

and their possibilities with respect to insights on the polymer microstructure are discussed. This is by no means a comprehensive list of all research efforts in these techniques, but it should provide an overview of the main technologies and approaches, the possibilities and the drawbacks associated with these polymer analysis approaches. None of the described techniques / published works provides selective information regarding the incorporated acid groups, which is a gap which was addressed in the research chapters of this thesis (Chapters 2 to 6).

1.2 Size-exclusion chromatography

A well-established technique often used for polymer analysis is size exclusion chromatography (SEC), also known as gel permeation chromatography (GPC). SEC can be applied to obtain molecular weight (MW) averages and/or the molecular weight distribution of a polymer sample [29]. It is an entropy-based process: polymers are separated according to their hydrodynamic volume by exclusion from a porous packing material. Small molecules penetrate the pores in the stationary phase material which will extend the residence time in the column, larger molecules are more excluded from these pores, meaning larger molecules will elute earlier [30-37]. This is schematically shown in Figure 1.6.

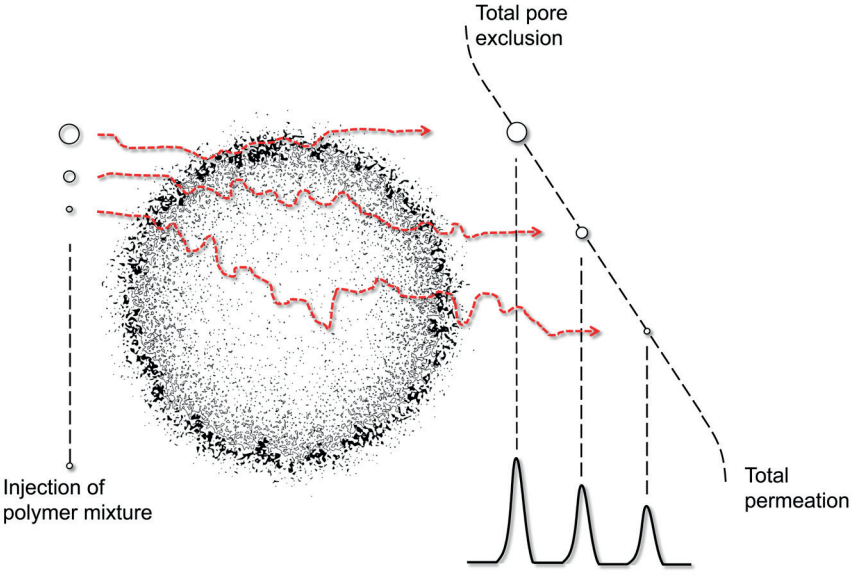

Figure 1.6. Schematic representation of the size-exclusion chromatography process using fully porous stationary phase particles. Polymers of various sizes are separated by their ability to enter particle pores.

Under perfect SEC-conditions, (no interactions between polymer and stationary phase and/or other polymer chains, or $0 \leq K \leq 1$) the behavior of polymers can be described by the following equation:

$$V_E = V_{ex} + KV_p \tag{1}$$

in which V_E is the elution volume, V_{ex} is the interstitial or exclusion volume of the column and V_p is the total pore volume of the packing. K is the distribution constant, which is, in liquid chromatography, defined as follows:

$$K = \frac{[c]_s}{[c]_m} \tag{2}$$

where $[C]_s$ is the concentration of the polymer in the pore volume ("stationary phase") and $[C]_m$ is the concentration of the polymer in the interstitial volume (mobile phase)[38].

In SEC, K has limits of $0 \leq K \leq 1$, meaning the separation mechanism is entirely controlled by entropy. If $K > 1$, interactions occur between the analyte and the column, which is unwanted in SEC. For very large molecules, K will be 0, meaning they do not penetrate the pores and elute in the exclusion volume (V_{ex}). Very small molecules which can easily penetrate the pores have a K value of 1, meaning it will elute in the total column liquid volume [39].

Different molecular weight averages can be obtained using SEC, such as M_n, M_w and M_z. The number-average molecular weight M_n is calculated by dividing the sum of the weight of all fractions divided by the number of molecules:

$$M_n = \frac{\sum(N_i M_j)}{\sum N_1} \tag{3}$$

In this equation, N_i corresponds to the number of i^{th} molecules with M_i as molecular weight. The weight-average molecular weight M_w can be calculated using the following equation:

$$M_w = \frac{\sum(N_i M_j^2)}{\sum(N_i M_j)} \tag{4}$$

As can be derived from the formula, the weight-average molecular weight is the sum of the weight times the molecular weight of all fractions, divided by the total weight. Finally, M_z is calculated via the following equation:

$$M_z = \frac{\sum(N_i M_j^3)}{\sum(N_i M_j^2)} \tag{5}$$

Stationary phases for SEC are available in a variety of pore sizes. The pore size is chosen based on the molecular weight of the analytes to be separated. In general, SEC columns can be either "single" pore size with narrow pore-size distribution or mixed-bed ("linear") with a broad pore-size distribution [37]. For columns with a single pore size, the molecular weight range which can be analyzed is limited, yet the resolution is high. These columns are often used when the molecular weight range of a sample is known. Mixed-bed columns provide a larger separation range but with less resolution. These columns are often used for screening experiments of samples to determine which single porosity column to use, or to analyze polymer blends of different molecular weights [35, 37]. Also, multiple columns of different pore sizes can be used in series, increasing the resolution and/or separation range [32, 37].

SEC columns are available in different particle sizes. Plate height and column permeability decreases with decreasing particle diameter, providing increased resolution. Generally, particle sizes around 3 µm can be applied for lower MWD polymers. For high-molar-mass polymers and high viscous solvents (such as dimethyl sulfoxide, trichlorobenzene), 10 to 20 µm particles are applied. For intermediate cases, particle sizes of 5 to 10 µm are available [37]. Small beads have higher optimal flow rates, but generate higher backpressures [35]. To withstand these pressures, rigidity of the packing is an important factor [40].

Columns packed with spherical polystyrene-divinylbenzene (PSDVB) copolymer gels are often used for non-aqueous SEC. Samples which can, for example, be analyzed using PSDVB columns are polystyrene (PS), polymethyl methacrylate (PMMA), polyolefins etc. Other common polymer packings used for non-aqueous SEC are acrylate- or polyester-based. These packings are of medium polarity. Examples of samples which are commonly analyzed using these columns are polyurethanes and polyimides. In aqueous SEC, hydrophilic polymer gels are used as column packing. These columns can be used with aqueous solutions with pH values between 2 and 10 [40]. Any other high-performance liquid chromatography (HPLC) column of which the pore-size distribution is appropriate can be used for SEC, regardless of its surface chemistry. However, non-size-exclusion effects must be absent, and the pore volumes must be large enough [32, 40]. To meet the first criterium, certain mobile phase compositions and column temperatures must be chosen to ensure interaction and/or charge exclusion between the polymer and stationary phase is minimized. When the polarities of stationary phase, mobile phase and the sample are perfectly balanced, the separation will solely be governed by exclusion effects, meaning the system will be in SEC mode [30, 36-38]. If the system is not completely in SEC mode, analytes may interact with the column and will be retarded, resulting in incorrect lower molecular weight estimations [35].

In aqueous mobile phases, more parameters (*e.g.* pH, ionic strength, organic modifier addition etc.) have to be adjusted to ensure no specific interactions take place. Also, charged functional groups of polymers in aqueous solutions may interact with the stationary phase [30, 32]. To prevent interactions between analytes and analytes and stationary phase, salts or 10 to 20 percent water-miscible organic solvent may be added to the mobile phase. Aqueous SEC can obviously only be applied to natural and synthetical water-soluble polymers [40]. For polymers only soluble in organic solvents, non-aqueous SEC must be applied. Since most industrial polymers are insoluble in aqueous environments (despite being water-borne), non-aqueous SEC is more commonly applied than aqueous SEC [39, 40].

One of the limitations of SEC is that the separation is based on hydrodynamic volume. Hydrodynamic volume does not only depend on molecular weight, but also on polymer topology and chemical nature in relation to the solvent. This means a calibration curve is only truly valid for samples with the same chemistry and topology as the reference materials [34, 35, 37, 41]. The use of an on-line viscometer with universal calibration can be used to overcome this problem. By applying this detector in combination with a concentration detector, absolute molecular weight measurements are possible [34, 37] using the Mark-Houwink equation:

$$[\eta] = K_{MH} M^{a} \tag{6}$$

Here, M is the molecular weight of an analyte. $[\eta]$ is the intrinsic viscosity of the sample. a and K_{MH} are coefficients for a given polymer dissolved in a specific solvent at a certain temperature [40, 42]. If the values of K and a are known for both calibration standard and sample, no viscometer (thus no universal calibration) is needed, assuming the hydrodynamic volume $[\eta]\ x\ M$ is equal for co-eluting polymers. The molecular weight for the sample can then be calculated as [42]:

$$logM_{1} = \left(\frac{1}{a_{1} + 1}\right) \log\left(\frac{K_{2}}{K_{1}}\right) + \left(\frac{a_{2} + 1}{a_{1} + 1}\right) logM_{2} \tag{7}$$

However, when the values of the Mark-Houwink coefficients are not known, an on-line viscometer must be used to determine the intrinsic viscosity. This is performed for standards with known molecular weights. A calibration curve is obtained, with which the molecular weight of the sample can be determined [18].

Light scattering detection is another way of determining a polymer's molecular weight by use of incident light of a certain wavelength. M_{w} is measured based on the following equation [43]:

$$\frac{K'c}{R_\theta} = \frac{1}{MwP(\theta)} + \frac{2A_2c}{P(\theta)} + \frac{3A_3c^2}{P(\theta)} + \cdots \tag{8}$$

where

$$K' = \left(\frac{2\pi^2 n^2}{\lambda_0^4 N_{av}}\right)\left(\frac{dn}{dc}\right)^2 (1 + cos^2\,\theta) \tag{9}$$

In these equations, K' is a constant, ϑ is the angle between the incident and observed light, R_θ is the difference in the Rayleigh scattering factor between the polymer solution and the solvent, c is the polymer concentration, $P(\vartheta)$ is the particle scattering function, A_i represents virial coefficients, n is the refractive index, λ_0 is the incident light wavelength, N_{av} represents Avogadro's number and dn/dc is the refractive index increment of the polymer solution. The particle scattering function $P(\vartheta)$ is dependent on the geometry and size of polymer molecules with respect to the wavelength of the incident light. Measuring R_θ and $P(\vartheta)$ and extrapolating the data for zero concentration and zero angle will give the absolute M_w [43].

Limitations in SEC analysis are band broadening and limited resolution [30]. These limitations complicate MWD determination, molecular weight average determinations and separation of polymer blends. The separation efficiency in chromatography can be described by the plate height H. The lower the plate height, the higher the separation efficiency. Plate height can be described by the Van Deemter equation [39]:

$$H = Ad_p + \frac{BD_m}{u} + C\frac{d_p{}^2 u}{D_m} \tag{10}$$

In this equation, A, B and C are coefficients, d_p is the particle diameter of the stationary phase, u is the interstitial velocity (average velocity in the domain outside the particles) and D_m is the diffusion coefficient of the polymer in the mobile phase. For comparison of separation efficiencies between methods, the reduced velocity and reduced plate height were introduced. ud_p/D_m is equal to the reduced velocity n, and H/d_p is equal to the reduced plate height h. Incorporating this into the Van Deemter equation results in the following equation [39, 44]:

$$h = A + \frac{B}{v} + Cv \tag{11}$$

A, B and C describe the three factors contributing to band broadening, causing deterioration of separation efficiency. One source of band broadening is eddy diffusion, the A-term in the Van Deemter equation [39]. Eddy diffusion occurs within the SEC column, as

molecules take different flow pathways through the packed bed towards the detector [40, 45]. In addition to eddy diffusion, longitudinal diffusion occurs: the B-term. Due to molecular diffusion, slight dispersion in both directions of the average flow rate occurs. In SEC, however, longitudinal diffusion is generally regarded as insignificant due to the slow diffusion of macromolecules in solution [44]. Lastly, band broadening can occur due to the resistance of an analyte to mass transfer, the C-term in the Van Deemter equation. This band broadening occurs for both mobile phase and stationary phase. For the mobile phase, the liquid near the packing material moves slower than the liquid in the center of the path, causing molecules in the center of the flow path to migrate faster. For the stationary phase, some analytes penetrate pores, while others move with the solvent. Large molecules with low diffusion coefficients are more prone to this effect [39, 40, 44]. The C-term is considered to be the largest contributor to band broadening in SEC [40].

The resolution of two adjacent peaks in chromatography is defined as follows:

$$R_S = + \frac{2(V_{R2} - V_{R1})}{w_1 + w_2} \tag{12}$$

V being the elution volume and *w* being the peak width at the baseline. In SEC, it must be taken into account that the separation is based on molecular size in solution. For that reason, the resolution for a SEC column can be defined as a specific resolution:

$$R_{SP} = + \frac{2(V_{R2} - V_{R1})}{w_1 + w_2} \log \left(\frac{M_2}{M_1} \right) \tag{13}$$

SEC is considered a technique with limited selectivity and limited resolution. Since separation in SEC is based on hydrodynamic volume, sample components of the same hydrodynamic volume cannot be separated. Also, polymer distributions with small differences in hydrodynamic volume cannot be separated with high resolution [46]. Resolution, however, can be increased by *e.g.* coupling multiple columns in series, decreasing stationary phase particle size and increasing temperature.

1.2.1 Non-aqueous SEC

As can be seen in Table 1.1, a great variety of (co)polymers has been analyzed employing non-aqueous SEC, also with a large variety in solvent systems. Frequently, additives were added to the mobile phase. For tetrahydrofuran (THF), butylated hydroxytoluene (BHT) was present in several published methods. This material is added as antioxidant to prevent autooxidation and polymerization of the solvent. Lithium bromide or lithium chloride are additives of choice for dimethylacetamide (DMAc), dimethylformamide

(DMF) and N-methylpyrrolidone (NMP). These lithium salts suppress hydrogen bonding and polar interactions between charges along the polymer chains and the mobile phase by neutralizing the ionic groups within the polymer. Additionally, the hydrodynamic volume of the polymers is decreased, since repulsive forces between the ionic groups are eliminated by neutralization [34, 47]. Acetic acid was used as additive in non-aqueous SEC methods for similar reasons [34].

For non-aqueous SEC, a variety of column packings were used. Most methods used a PSDVB-packed column. Caltabiano *et al.* [32] used a variety of common RP and HILIC columns for the separation of PMMA and PS standards. Medium polarity columns, such as fluoro-phenyl (130Å) and cyano (80Å), provided elution of PS and PMMA of similar molecular weights at the same elution volume. The molecular weight of the PS standards ranged from 580 to 51,200 $g.mol^{-1}$, and the molecular weights for the PMMA standards ranged from 550 to 46,890 $g.mol^{-1}$. For the cyano column, a mobile phase composition of 70/30 THF/acetonitrile (MeCN) was used. The fluoro-phenyl column was used with 60/40 THF/MeCN as mobile phase. These mobile phase compositions are different for both columns as the nature of the stationary phases are different, and as such interactions with the analytes are different. As is previously discussed, these interactions are unwanted in SEC analysis.

Moyses and Ginzburg [48] separated high molecular weight poly(phenylene ether) using a Hypercarb porous graphite carbon (PGC) column with trichlorobenzene (TCB) as eluent. PGC columns are normally used as stationary phase for RPLC-analysis of polar analytes. The result of the SEC analysis was compared to SEC analysis on a PSS PSDVB High-Speed linear M column using chloroform as mobile phase. Although the PGC column is not designed for SEC-analysis, it performed very well in this mode. Four PS standards, ranging from 575 to 281,700 $g.mol^{-1}$ were separated within two minutes, which is typical of rapid SEC. The poly(phenylene ether) sample was separated using a two Polypore columns within 25 minutes. A similar chromatogram was obtained using the PGC column within 5 minutes. Since a single column with increased pore size compared to the Polypore columns is used, there is an increase in the high molecular weight cutoff and a decrease in resolution in the low molecular weight range. Despite this, the PGC column provides a dynamic range of separation, which covers one or two decades in molecular weight.

Pirok *et al.* [49] used a column packed with core-shell particles, also known as superficially porous particles, for the SEC analysis of PS standards. Core-shell particles consist of a solid core and a porous shell. The pore volume is reduced compared to fully porous particles due to the solid core. Because of the reduced pore volume, core-shell particles had not been applied for SEC, despite the demonstrated high efficiency

in LC [50]. From the research of Pirok *et al.* it can be concluded that SEC analysis can be performed using a core-shell column packing. In fact, a similar or better resolution can be obtained more rapidly compared to fully porous particles as stationary phase. Schure and Moran [51] also demonstrated the possibility of SEC analysis for polystyrene standards using core-shell particles, comparing the results to separations using fully porous particles. It was concluded that core-shell particles can perform faster SEC separations with good resolution. However, fully porous particles outperform core-shell with respect to specific resolution when time is not critical.

A custom pentaerythritol-based monolithic column is used for polystyrene analysis by Kurganov *et al.* [52]. During the production of these columns, monolithic sorbents are synthesized in the columns, occupying the whole inner space. Advantages of monolithic columns are high porosity and enhanced permeability to flow. Both advantages could be beneficial for fast, efficient SEC separations [53, 54]. In the research by Kurganov *et al.*, the custom-made monolithic columns were compared to PSDVB and poly(ethylene glycol dimethacrylate) monolithic columns. The custom monolithic columns have a higher non-flow-through pores fraction compared to the other studied columns, resulting in a more efficient separation of polymers up to 10^5 g.mol^{-1}. As a logical result, the achieved resolution in this molar mass range is considerably higher [52].

In ultrahigh-pressure UHP-SEC, conventional UHPLC columns with sub-2 µm particles are used for the size-based separation of macromolecules. Higher flow rates can be used, decreasing analysis time significantly, yet separation efficiency remains high. UHP-SEC was first described by Uliyanchenko *et al.* [55] using a BEH C18 packed column with average pore size of 130Å. Using this packing material, a SEC separation of polystyrene standards up until 52,400 g.mol^{-1} was achieved in less than one minute using THF as mobile phase. Separation of higher molecular weight polymers is possible, but separation will then be based on hydrodynamic chromatography (HDC; see section 1.2.4).

The drawback of UHP-SEC is possible deformation of polymeric analytes due to high (shear) stress. Coiled polymer chains can be transferred into a stretched shape, which was observed by Uliyanchenko *et al.* [56]. Also, some studies show indications that polymer degradation may take place [37, 39]. The Deborah number can be used to calculate whether deformation of analytes takes place. This number can be calculated using the following equation:

$$De = k_{PB}\left(\frac{u}{d_p}\right)\frac{6.12\phi\eta r_G^{\,2}}{RT} \tag{14}$$

k_{PB} is a constant which depends on the structure of the packed bed, having a value of 9.1 for a randomly packed bed. u Is the flow rate per unit area of empty column, d_p is the particle diameter, η is the mobile phase viscosity, ϕ the Flory-Fox parameter, r_G the radius of gyration of the polymer, R the gas constant and T the absolute temperature. Around $De \approx 0.5$, a gradual transition from a coiled to stretched shape takes place. When polymers are stretched ($De > 0.5$), elution takes place in slalom chromatography (SC) mode [56]. The larger stretched molecules will experience more difficulties passing through the channels between particles because their direction must change frequently. Elution order is from small to large, opposite to SEC elution [39, 56]. The change between the three separation mechanisms, SEC, HDC and SC, is visualized in Figure 1.7, in which the molecular weights of polymer standards are plotted as a function of elution time. As the molecular weight increases, the separation mechanism changes from SEC to HDC to SC.

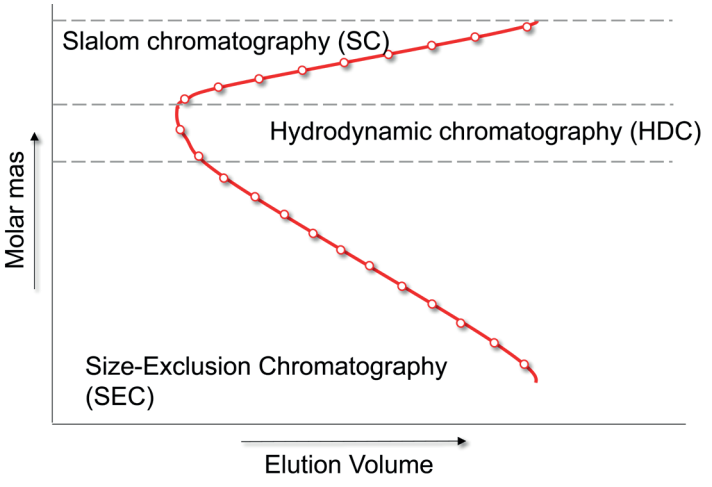

Figure 1.7. Schematic representation of a change in separation modes upon increase in polymer molar mass [84].

Even though slalom chromatography may potentially offer high selectivity separations, the separation of polydisperse synthetic polymers may cause complications. If the critical polymer size for which $De = 0.5$ falls within the MWD, part of the distribution will be eluted in SEC or HDC mode. The other part will be eluted in SC mode, meaning small and large particles will elute at the same time. Accurate MWD information cannot be obtained in this case. In addition to that, when too much stress is applied to the polymer, covalent bonds in the already stretched polymers can break. This leads to an increase in low-MW polymers, resulting in inaccurate MWD determinations [39].

Table 1.1. Selected applications of non-aqueous size-exclusion chromatography

Analyte	Column	Mobile phase	Ref
Poly((2-dec-9-enyl)-2-oxazoline)	2x PLgel Mixed-D	Chloroform with 4% TEA	[54]
Poly(2-ethyl hexyl acrylate-*co*-MAA)	Styragel HR2, HR4 and HR6	THF	[57]
Poly(2-phenyl-2-oxazoline)	2x PLgel Mixed-D	Chloroform with 4% TEA	[54]
Poly((2-phenyl-2-oxazoline)-*co*-((2-dec-9-enyl)-2-oxazoline)	2x PLgel Mixed-D	Chloroform with 4% TEA	[54]
Poly(3-hydroxyvalerate-*co*-hydroxybutyrate)	PLgel PDVB	Chloroform	[58]
Poly(ε-caprolactone) diols	HSPgel HR1.0, 2.5, 4.0, MB-M	THF	[59]
Poly(ε-caprolactone-*block*-PS)	3x PLgel Mixed-C+ PLgel Mixed-C guard	THF	[60]
Polyacrylate nanoparticles	3x Phenomenex experimental core-shell	THF	[61]
Polybutadiene	2x PLgel Mixed-C	THF	[62]
Poly(n-BA-*stat*-AA)	PSS GRAM Linear XL	DMAc with 50 mM LiCl and 50 mM acetic acid	[63]
Poly(butylene adipate)	Ultrastyragel HR4, HR3, HR2 and HR1	THF	[64]
Polydihydrosilane	Shodex KF-806L + Shodex guard column	Cyclohexene	[65]
Poly(ethyl diazoacetate-*co*-benzyl diazoacetate)	2x PLgel MiniMix-C	Chloroform	[66]
Poly(ethylene-2,6-naphthalate)	3x Shodex KF806L	1,1,1,3,3,3-hexafluoro-2-propanol with 0.01 M triethylammonium nitrate	[67]
Poly(EO-*block*-ε-caprolactone)	3x PLgel Mixed-D + PLgel guard column	Chloroform	[68]
Polyimides, isomerized	2x PLgel Mixed-B-LS	DMF with 0.1 M LiBr or 3.1 mM TBAB	[69]
Polyisobutylenes, high molecular weight	Styragel HR0.5, 1, 3, 4, 5 and 6	THF	[70]
Polymethylsilane and polycarbosilane	2x Jordi Gel DVB Mixed bed + Jordi Gel DVB precolumn	THF	[71]
PMMA	Shodex KF-804L Shodex KF-805L	THF	[72]
PMMA	XSelect CHS Fluoro-Phenyl	60/40 THF/MeCN	[32]
PMMA	Zorbax SB-CN	70/30 THF/MeCN	[32]
PMMA	3x PLgel MiniMix-C	THF	[73]
Poly(MMA-*co*-BA)	PSS SDV High-Speed Linear M	THF	[74]

Table 1.1. Continued

Analyte	Column	Mobile phase	Ref
Poly(MMA-*co*-BA)	PSS SDV High-Speed Linear M	DMSO with 0.1 M $NaNO_3$	[74]
Poly(MMA-*graft*-S)	3x PSS SDV, 10^3, 10^5 and 10^6Å + PSS SDV guard	THF	[75]
Polypropene	2x PLgel Mixed-B	TCB	[76]
Poly(ethene-*co*-propylene), alkyl-substituted	2x Tosoh TSKgel GMH_{HR}-H Mixed-bed	THF	[77]
Poly(phenylene ether)	Hypercarb	TCB	[48]
PS	2x PLgel Mixed-C	THF	[78]
PS	XSelect CHS Fluoro-Phenyl	60/40 THF/MeCN	[32]
PS	Zorbax SB-CN	70/30 THF/MeCN	[32]
PS	Custom DVB column	Methylene chloride	[79]
PS	Custom monolithic column of pentaerythritol derivatives containing three or four acrylic groups	DCM	[79]
PS	2x PLgel Mixed-C + PLgel guard	THF with 0.125% BHT	[80]
PS	2x Phenomenex silica C18 core-shell Phenomenex silica core-shell	THF	[49]
PS nanoparticles	3x Phenomenex experimental core-shell	THF	[61]
PS, high molecular weight	Styragel HR0.5, 1, 3, 4, 5 and 6	THF	[70]
PS	Custom core-shell particle column	THF	[51]
Poly(S-*block*-butadiene)	PSS SDV High-Speed Linear M	Chloroform	[81]
Poly(S-*block*-n-butyl acrylate)	2x PLgel Mixed-C + PLgel guard	THF, BHT stabilized	[82]
Poly(S-*co*-maleic acid)	PSS Gram 30 and 3000Å + PSS Gram precolumn	DMAc	[83]
Poly(S-*block*-THF)	3x PLgel Mixed-C + PLgel Mixed-C guard	THF	[84]
Poly(2-ethyl-2-oxazoline)	Acquity APC-XT	Methanol	[85]
Polyethylene oxide (PEO)	Prototype BEH diol	MeOH with 20 mM NH_4Ac	[86]
PMMA	Prototype BEH diol	THF	[86]
PMMA	Acquity APC XT	DMAc with 50 mM LiCl	[85]
PS	Prototype BEH diol	THF	[86]
PS	Acquity UPLC C18 BEH	THF	[55]

1.2.2 Aqueous SEC

In aqueous SEC, columns with hydrophilic polymer packings were used mainly (Table 1.2). Caltabiano *et al*. [87] used common RP and hydrophilic interaction chromatography (HILIC) columns for the SEC analysis of sodium polystyrene sulfonate. The columns investigated were Luna HILIC and ACE 3 C_{18}, C_4, phenyl and cyano columns. The Luna HILIC column showed the best performance, with near-ideal SEC elution at 10 to 60°C using 80/20 0.2 M Na_2SO_4 / THF or 70/30 0.2 M Na_2SO_4 / MeCN as mobile phase. The cyano column demonstrates a near-ideal SEC elution with 80/20 0.2 M Na_2SO_4 / THF, but only at 40 to 60°C. Similarly, the near-ideal SEC elution can be performed using the C_{18} column and 70/30 0.2 M Na_2SO_4 / MeCN, but only between 20 and 50°C. In this research, organic solvent was added to the mobile phases to minimize hydrogen bonding of the sulfonate groups with non-ionized residual silanol groups of the stationary phase.

Interaction between analytes and stationary phases in aqueous SEC can, beside addition of organic solvent to the mobile phase, be reduced or eliminated by increasing the ionic strength. Generally, ionic strengths exceeding 50 mM should be applied to eliminate interactions between analytes and silica stationary phases [39]. In several of the selected methods, sodium chloride is added to increase ionic strength [88-90]. Buffers are sometimes used to regulate ionization of the analytes, simultaneously reducing or eliminating analyte-stationary phase interactions as a result of buffer concentration [91-93].

Table 1.2. Selected applications of aqueous size-exclusion chromatography

Analyte	Column	Mobile phase	Ref
Polyacrylic acid, methylated	3x PSS Suprema, 100, 1000 and 3000Å + PSS Suprema guard	0.1 M Na_2HPO_4 (pH 9)	[91]
Polyacrylic acid, sodium salt	G6000 and G3000 PWXL	Phosphate-buffered saline	[93]
Polyacrylic acid and poly(ethyl acrylate) copolymers	Shodex OH pak SB-804HQ	20 mM ammonium acetate pH 9	[92]
Poly(acrylamide-co-N,N-dimethylacrylamide)	PL Aquagel-OH 60, 50, 40 and 30	MilliQ with 0.5 M acetic acid and 0.5M NaCl	[88]
Polyethylene glycol	2x PL Aquagel-OH Mixed-H	Water with 0.02% NaN_3	[94]
Polymethacrylic acid, methylated	3x PSS Suprema, 100, 1000 and 3000Å + PSS Suprema guard	0.1 M Na_2HPO_4 (pH 9)	[91]
Sodium polystyrene sulfonate	Luna HILIC	0.2 M Na_2SO_4 / THF 80/20 or 0.2 M Na_2SO_4 / MeCN 70/30	[87]
Sodium polystyrene sulfonate	ACE 3C18-300	0.2 M Na_2SO_4 / MeCN 70/30, 20-50°C	[87]
Sodium polystyrene sulfonate	ACE 3CN-300	0.2 M Na_2SO_4 / THF 80/20, 40-60°C	[87]
Poly(*N*-vinyl formamide)	Custom glycidyl methacrylate – Ethylene glycol dimethacrylate column	0.2 M NaCl	[90]
Poly(*N*-vinyl formamide)	3x Ultrahydrogel, 120, 250 and 2000Å	80/20 water/MeCN with 0.15 M NaCl and 0.03 M NaH_2PO_4	[89]

1.2.3 Gradient SEC

Gradient SEC, a separation mode which combines features of SEC and interaction LC, was first applied by Schollenberger and Radke [95]. The concept is visualized in Figure 1.8. In gradient SEC, the sample is dissolved in a strong eluent, meaning interaction of the analytes with the stationary phase is minimized/eliminated and the polymers elute in SEC-mode. Columns with small pore sizes are used to prevent the polymers from penetrating the pores. A gradient with increasing eluent strength is applied but is started before sample introduction. After injection, the polymers will escape from the solvent band because the solvent molecules are significantly smaller compared to the polymers. As such, the solvent molecules will penetrate all pores. Since the polymers migrate through the column at higher velocity, they will experience changing mobile phase compositions. At a certain eluent composition, the polymer will be adsorbed onto the stationary phase and cannot continue migrating through the column at higher velocity than the solvent molecules. This eluent composition is called the adsorption threshold. The polymers will migrate with the same velocity as the surrounding solvent molecules and will elute at the adsorption threshold solvent composition.

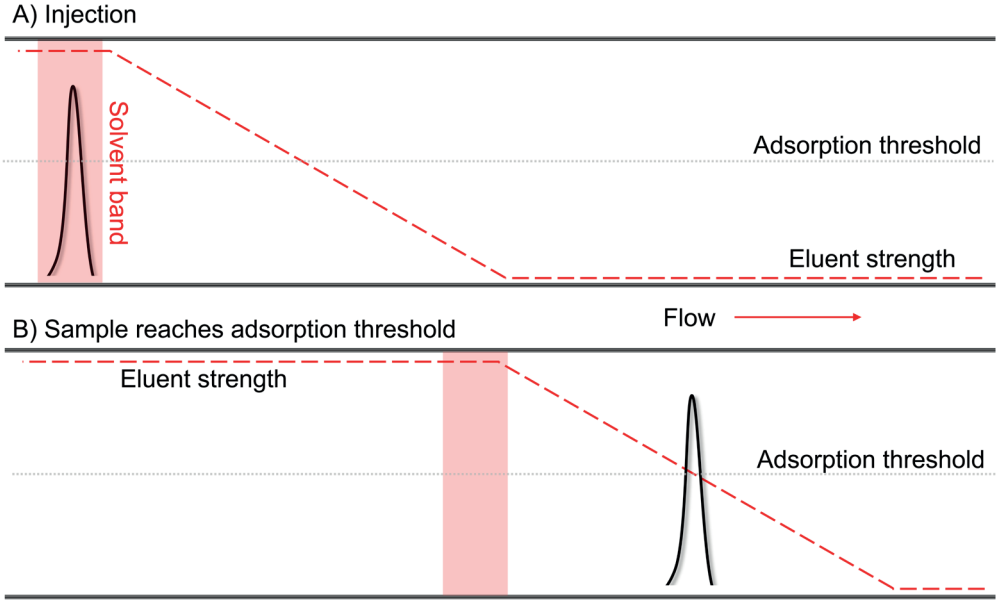

Figure 1.8. Representation of the SEC-gradient concept: A. After injection, B. At the adsorption threshold/ threshold of solubility.

Table 1.3. Gradient SEC applications

Analyte	Column	Mobile phase	Ref
Poly (butyl acrylate) (PBA)	Proteema SEC	0/100 to 100/0 THF/MeOH	[96]
Poly(butyl acrylate-*stat*-acrylic acid)	Proteema SEC	96/4 to 0/100 CHCl3/DMAc	[63]
Poly(methyl methacrylate-*stat*-methacrylic acid)	Proteema SEC	95/5 to 50/50 CHCl3/DMAc	[97]
Poly(methyl methacrylate)	Proteema SEC	0/100 to 100/0 THF/MeOH	[96]
Poly(methyl methacrylate) and polystyrene mixture	Proteema SEC	0/100 to 100/0 THF/$CHCl_3$	[95]

In this case, polymers will precipitate at the threshold of solubility, after which they will move through the column by a precipitation-redissolution mechanism. The polymers will elute at the threshold of solubility mobile phase composition. The adsorption threshold or threshold of solubility differs for chemically different molecules. Chemically different molecules with the same hydrodynamic volume can, thus, be separated by applying a SEC-gradient.

Gradient SEC was applied for the separation of PS and PMMA of similar hydrodynamic size by using a chloroform to THF gradient based on adsorption [95]. In another article [96], Schollenberger and Radke attempted a solubility-based separation of PMMA, poly(t-butyl acrylate, P-tBA) and poly(n-butyl acrylate, P-nBA) by applying a methanol (MeOH) to THF gradient. Poly(t-BA) and PMMA were separated successfully, but poly(n-BA) elutes at a similar elution volume to PMMA. However, the concept of solubility-based separation by applying a SEC-gradient was proven. Maier *et al.* [63] separated p(MMA-*stat*-MAA) copolymers with different MAA contents using a chloroform to DMAc gradient based on adsorption. Finally, poly(n-BA-*stat*-AA)s were separated with respect to the AA content. For this, a chloroform to DMAc gradient was applied as well, separating on differences in adsorption.

1.2.4 Hydrodynamic chromatography (HDC)

Where SEC separates polymers based on hydrodynamic volume in solution by means of porous packing materials, HDC separates polymers either in the interparticle space between packing material particles or in narrow capillaries. HDC is a solution- or dispersion-phase separation method, in which separation is governed by the parabolic flow profile in a narrow channel, as visualized in Figure 1.9. Large molecules are sterically excluded from the walls and will be driven to the center of the channel. Here, the particles experience higher average velocities due to the flow profile: faster streamlines are in the middle of the cylindrical tube [39, 98]. This results in earlier elution of large molecules or particles compared to small molecules or particles, meaning elution order is the same as in SEC [99].

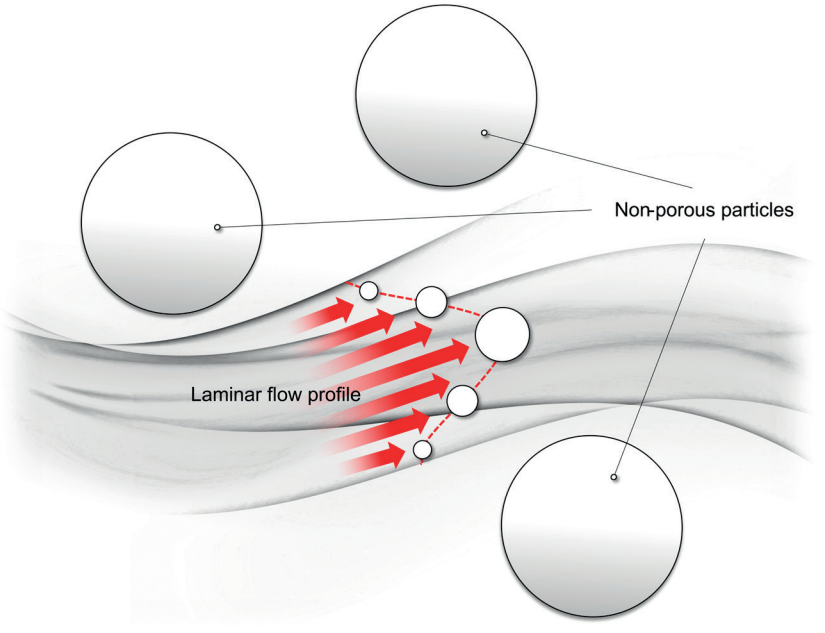

Figure 1.9. Schematic representation of separation in HDC mode, governed by the laminar flow profile.

For effective separation, the analytes should be relatively large compared to the channel. The aspect ratio for a given column is defined as the ratio of the radius of the analyte *(r_a)* to that of the flow channel *(r_c)*:

$$\lambda = \frac{r_A}{r_C} \tag{15}$$

For the HDC-effect to occur, the value of the aspect ratio must be roughly 0.01 - 0.4 [61, 100]. Capillaries with extremely small internal diameters (less than 10 μm) can be used for HDC [39, 101]. Separation can also take place in the interstitial space between particles in packed columns. The use of non-porous particles or porous particles of pore size substantially smaller than the analyte size prevents the analytes from penetrating any pores. Pore penetration by the analytes would lead to SEC-based separations. In addition, the packing material should be inert, minimizing non-HDC enthalpic interactions [99].

Size determinations by HDC are based on calibration, relating the elution volumes/times of monodisperse latex dispersions to known particle size. More specifically, a calibration plot of the retention volume/time versus latex diameter is used to determine the particle size of latex samples [101]. If elution would be controlled by the hydrodynamic effect

only, the elution rate of a colloid would be insensitive to the chemical nature and surface charge. However, electrostatic and van der Waals interactions between stationary phase and analytes are often present, resulting in non-ideal HDC. These interactions can be different for each polymer. Calibration of HDC using, for example, polystyrene latexes, can therefore not always be applied universally [101].

Mobile phases in HDC are chosen based on the surface chemistry of the capillary or column and on the sample nature. When non-HDC interactions arise between the analytes and the column/capillary, addition of salts or surfactants to the mobile phase may be helpful to minimize these effects [101]. Also, the selected buffer determines the application range. As the ionic strength increases, the electrical double layer of the analytes and that of the surface will decrease, causing the HDC separation range to shift to larger particles since electrostatic repulsions are minimized [61].

Many different additives can be added to the mobile phases. Pirok *et al.* [61, 102] used purified water with HNa_2PO_4, sodium lauryl sulfate (SLS), Brij L23 and sodium azide for polyacrylate and polystyrene nanoparticle analysis. HNa_2PO_4 was added to increase ionic strength, screening electrostatic repulsion between the analytes and stationary phase. These electrostatic repulsions originate from the overlap of electrical double layers around the particles and the stationary phase. Finally, sodium azide was added to the mobile phase for preventing bacterial growth [61].

Brewer and Striegel [103] used the same mobile phase additives, except sodium azide was replaced with formaldehyde. Formaldehyde is added for the same reason as sodium azide, prevention of bacterial growth [61]. Op de Beeck *et al.* [104] used a sodium borate buffer as mobile phase, with Triton X-100 added as surfactant.

When dissolved polymers instead of dispersed polyacrylate and polystyrene nanoparticles were analyzed, organic solvents were used for the mobile phases. Edam *et al.* [105] used THF as mobile phase for the analysis of PS and PMMA between 2 kDa and 1.1 MDa. Similar experiments were done by Korolev *et al.* [106, 107], using dichloromethane as mobile phase for PS separation by HDC.

Columns have been designed specifically for HDC, such as PL-PSDA cartridges [61, 102] or PS-1 HDC [103]. Edam *et al.* [105] performed solvent-based HDC analysis of PMMA and polystyrene using a custom PSDVB monolithic column. Columns with pore sizes as small as 75 nm were prepared, which enabled separation via HDC for $0.02 < \lambda < 0.2$, corresponding to molecular weights between 20 and 523 kDa. For $\lambda < 0.02$, SEC is the main separation mechanism. In the publication by Korolev *et al.* [106], the use

Table 1.4. Selected HDC applications

Analyte	Column	Mobile phase	Ref
Polyacrylate latexes PS latexes	PL-PSDA cartridge type-2	MilliQ with HNa_2PO_4, SLS, Brij L23 and sodium azide	[61]
PMMA latexes	2x PS-1 HDC	MilliQ with 0.002 M HNa_2PO_4, 0.2% Brij-35, 0.2% formaldehyde, 0.05% SDS; pH 7.5	[103]
PMMA	PS-DVB monolithic column	THF	[105]
PS latexes	2x PS-1 HDC	MilliQ with 0.002 M HNa_2PO_4, 0.2% Brij-35, 0.2% formaldehyde, 0.05% SDS; pH 7.5	[103]
PS	PS-DVB monolithic column	THF	[105]
PS	DVB monolithic column	DCM	[106]
PS	Unmodified quartz capillary	DCM	[107]
PS latexes, fluorescently labeled	Silicon micropillar channel capillary	3 mM sodium borate with 0.5 g/L Triton X-100; pH 9.2	[104]

of an unmodified quartz capillary for monolithic column preparation was described. Monolithic microporous polymers based on divinylbenzene were prepared in the capillary. The advantage of using monolithic columns, is that the size of the channels is determined by the reaction mixture and the synthesis conditions, providing custom channel sizes within wide limits [106].

In another publication [79], Korolev *et al.* used a similar unmodified quartz capillary with a diameter of 5 µm, but without filling. Separation of a mixture of polystyrene standards was successfully achieved, but the observed data was not consistent with the theoretical model. For this reason, additional experiments were needed to fully understand HDC separation in hollow capillaries.

1.2.5 Limitations of SEC for analysis of acid-functional polymers

The described separation modes are applicable for water-borne polymers (aqueous SEC obviously for water-soluble polymers only). Non-aqueous SEC is the mode of choice to obtain the molar mass distribution of non-water-soluble of polymers. The incorporation of acid monomers does not necessarily influence the separation of acid-functional polymers, although the presence of functional groups in the polymers may provide additional challenges in obtaining a purely entropy-based separation process. The information obtained by SEC does not yield any information regarding the incorporation of the acid monomer. In gradient SEC, it is possible to obtain a clear separation between polymers with a difference in content of acid monomer. Gradient SEC has a broad application range with respect to the relative content of acid monomer, polymers with up to 50% of acid monomer were eluted with good integrity [97]. This mode of separation (using the polymer acid content to change the adsorption characteristics) will however only be applicable for copolymers within the same chosen subset of comonomers. The change of the comonomer type or the addition of a third monomer type will change the adsorption/desorption characteristics of the polymer and change the elution behavior. In such cases, obtaining information regarding the incorporation of the acid monomer will be challenging.

1.3 Interaction chromatography (ILC)

Interaction chromatography is a general term for a collection of separation modes which, contrary to SEC, are driven by a combination of enthalpic and entropic effects. These separation modes are used to characterize the chemical composition distribution of

polymer samples. Such characterization techniques are useful in the case that describing only the molar mass distribution is not sufficient to explain the properties of a polymeric material. Interaction chromatography is thus most frequently applied in assessing the heterogeneity of copolymers. Different modes can be discerned, of which several are discussed below (gradient SEC, which was discussed in the previous paragraph can also classify as an interaction chromatography method as it uses attributes of both SEC and interaction chromatography). Techniques such as temperature gradient interaction chromatography (TGIC) are not discussed in detail, as this is not (yet) applied for the characterization of water-borne polymer systems but primarily for non-polar species such as polyolefins [62, 78, 80, 108].

Polymer analysis using interaction chromatography (or gradient polymer elution chromatography, GPEC) is a HPLC technique for separation mainly based on chemical composition. The mobile phase consists of a mixture of a weak eluent and a strong eluent for the sample, with a programmed composition (gradient). At the start of the separation process, a weak eluent composition is used. After the polymer is injected, it precipitates onto the column due to low solubility in the non-solvent. Subsequently, the mobile phase strength is increased, causing the precipitated polymers to slowly redissolve. Polymer separation is achieved by retention of different polymers, based on differences in chemical composition (and/or end groups) and molecular weights [109, 110]. The polymer fractions may also physically interact with the stationary phase [29, 109, 110], resulting in a favorable partitioning of the polymers from the mobile phase to the stationary phase. Thus, retention is not only governed by solubility, but also by adsorption effects; separation is based on both enthalpic and entropic effects [39, 96, 111-113].

ILC can be applied to determine several types of polymer distributions, such as the chemical composition distribution (CCD) or functionality type distribution (FTD) of a polymer sample. Different types of polymer distributions have been discussed in the Introduction and are topic of many publications [39, 109, 110, 114]. Under certain solvent compositions, the interaction between the fractions and the stationary phase is mainly based on adsorption. This means retention depends on chemical composition and molecular weight. Longer polymer chains possess more interacting units, meaning they will be more strongly retained than smaller chains. As such, low-MW fractions will be eluted first [38, 39]. Under gradient conditions, molecular-weight-dependent elution is stronger for low-MW polymers. For polymers above 100 $kg.mol^{-1}$, molecular weight independence is often observed [29, 39, 113].

For CCD determination of copolymers, the ILC behavior of homopolymers or of copolymers with known compositions must be studied. The difference in retention times of the homopolymers must be sufficiently high in order to obtain a high resolution for CCD determination. The CCD of a sample can be calculated from a calibration curve of standards with known chemical compositions [29]. In several publications, CCD determination is performed under critical conditions (liquid chromatography at critical conditions; LCCC), which is further described in paragraph 1.3.3. However, since LCCC is an isocratic elution technique, a requirement is that all functionality or chemical composition fractions elute with one eluent composition. Especially for low-MW polymers, ILC can provide detailed information on FTD or CCD within a polymer sample [113] although confounding molar mass effects can complicate this analysis.

Conventional HPLC columns, such as C_{18}, cyano, amino or unmodified silica, are used as stationary phase in ILC, meaning ILC can be reversed-phase (RP-ILC) or normal phase (NP-ILC). In NP, adsorption interactions are generally much stronger than in reversed-phase. Most functional (end) groups are more polar than the polymer backbone. For this reason, NP-ILC is frequently applied for FTD determinations, and also often for CCD determinations [115, 116]. Since in RP-ILC, adsorption interactions are weaker, non-solvents must be applied for the analytes to be retained by the stationary phase. The use of non-solvents may result in precipitation of the polymeric analytes. Redissolution of the polymers into the mobile phase and/or desorption from the stationary phase is molecular weight-dependent, which results in an increased dependence of molecular weight on retention in RP-ILC [116].

For selection of the mobile phase components, the solubility of the analytes and the eluent strength must be considered. The mobile phase composition at the start of the analysis is mainly non-solvent, causing the polymer sample to precipitate and/or interact with the stationary phase at the top of the column. The mobile phase composition must be changed to a solvent that is capable of dissolving and/or desorbing all sample fractions. Some large polymers will be strongly adsorbed on the column and may not be eluted. When only part of the entire sample elutes from the column, MWD, CCD or FTD determinations cannot be done accurately [39]. THF, acetonitrile and methanol are commonly used strong solvents/eluents in RP-ILC of low-molecular-weight analytes. Many higher-molecular-weight polymers are insoluble in acetonitrile and methanol, which is why THF is more often used. The non-solvent component of the mobile phase can be another organic solvent, but water is also frequently applied [113].

Often in isocratic LC analysis modes, such as SEC, the sample is dissolved in the mobile phase. In ILC, however, sample precipitation can also occur in the injector because the initial mobile phase composition consists mainly of non-solvent. For this reason, the sample is ideally dissolved in a good solvent which is a weak eluent [117]. Alternatively, a higher percentage of strong eluent can be used for sample dissolution, but this may lead to breakthrough peaks. Breakthrough peaks appear when part of the sample passes through the column together with the strong solvent band without interacting with the stationary phase. In case this effect occurs, accurate analysis is impossible. Therefore, using a weak eluent as sample solvent is preferred [113, 118].

Like in SEC, mass transfer is slow, meaning the Van Deemter C-term dominates band broadening at room temperature [39, 44]. In addition to that, diffusion of macromolecules in solution is minimal, meaning longitudinal diffusion (Van Deemter B-term) is minimal.

Similar to SEC, ILC can be performed at elevated temperatures (HT-ILC). This is often applied to polymers which are insoluble in any solvent at room temperature, such as polyolefins. Temperature increase leads to a lower mobile phase viscosity and thus a higher analyte diffusion coefficient. This causes a decrease in reduced velocity ν, resulting in reduced plate height according to the Van Deemter equation. This means separation efficiency is improved when performing ILC at elevated temperatures. Also, flow rates can be increased without considerably increasing backpressure, resulting in faster separations. Even though the interactions between the analyte and stationary phase decrease with increasing temperature, HT-ILC allows for more efficient and faster separation of polymer samples [39, 113].

Another way to reduce analysis time is the use of columns packed with sub-2 µm particles at pressures up to 100 MPa: UHP-ILC. Not only is analysis possible at higher speed, but resolution also increases, which can be derived from the Van Deemter equation. This cannot be applied without boundaries, as the attainable plate number (and thus resolution) decreases at a certain point upon decrease of the maximum column length due to pressure limitations. Also, several groups have reported on a potential risk of polymer deformation or even degradation when performing UHP-ILC, although this may hold true only for very high molar-mass polymers [39, 56]

.

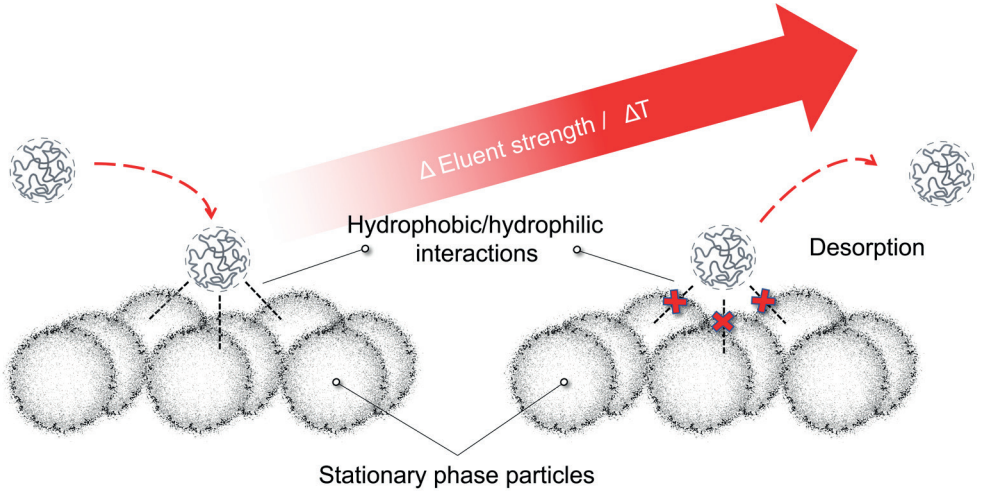

Figure 1.10. Schematic representation of adsorption/desorption processes as found in interaction chromatography.

C18 columns were often applied for polymer analysis, next to unmodified silica columns. C18 columns are mainly used for separation based on chemical composition [54, 58, 73, 119]. Molecular weight dependence on elution is often observed, specifically for polymers below 50 kg.mol^{-1}. Also, some publications show the separation of polymers according to degree of branching [74, 80, 120, 121] or to block length [122]. The degree of branching is observed to be molecular-weight dependent, understandably with higher degrees of branching in higher-molecular-weight polymers. NP columns are more often used for block copolymer analysis [74, 81, 82, 91, 123] due to their selectivity for polar functionalities. Separation according to degree of branching on NP columns was not found in the selected articles. However, chain-end-based separation of polybutadiene and polystyrene was seen, using an isocratic eluent composition [124].

All published HT-ILC methods found so far used a Hypercarb porous graphite carbon (PGC) column for polymer separation. PGC columns were developed as an alternative to octadecyl silyl (ODS) phases. The columns are built up of two-dimensional graphitic sheets with sp^2 hybridized carbon atoms in hexagonal arrangement. The sheets are kept together through van der Waals interactions [125, 126]. Similar to ILC separations using conventional stationary phases, retention is thought to occur through a combination of interactions between mobile phase, stationary phase and the analytes. Hydrogen bonding between the analytes and mobile phase discourage retention. However, hydrophobic

interactions promote retention by 'pushing' analytes towards the PGC surface. Dispersive forces between nonpolar analytes and the PGC contribute to retention. Also, the PGC surface is polarizable, meaning polar analytes can be retained through charge induction [126, 127]. PGC columns give increased retention of both polar and non-polar analytes compared to reversed-phase silica-based columns. In addition, an increased selectivity for structurally similar analytes has been observed. Large planar molecules are strongly retained, whereas highly branched molecules exhibit limited retention [125].

The reason PGC columns are used in HT-ILC, is their resistance to extreme conditions. Compared to silica-based stationary phases, PGC columns can be used at a broader pH value range. Where ODS columns can generally withstand pH values ranging from 2 to 8, PGC columns are compatible with mobile phases from pH 0 to 14. In addition, PGC is chemically stable in aggressive mobile phases and at high temperatures up to 200°C. In comparison: most silica-based stationary phases (such as ODS) cannot be used at temperatures exceeding 60°C [126] or extreme pH conditions. In addition, PGC has high rigidity and mechanical stability, as it can withstand pressures up to 100 MPa - which is ascribed to the intertwined nature of the material. The intertwined nature also causes the material to be resistant to swelling or shrinking [128]. In comparison: ODS stationary phases have similar mechanical stability and also allow use up to 100 MPa. For PSDVB and other polymer packings, however, low mechanical strength is typically encountered. These packings suffer from excessive shrinkage and swelling upon changes in eluent composition [129, 130]. The above-mentioned attributes make PGC an ideal choice for HT-ILC applications. Most HT-ILC methods were applied for separating copolymers according to their CCD. Ethene and propene homopolymers or copolymers were the only polymers analyzed with HT-ILC, due to their insolubility in solvents at room temperature.

Another type of stationary phase used in ILC analysis is a monolithic disc. Maksimova *et al.* [131] used monolithic disks of different surface chemistries for the separation of PS, PTMBA and PMMA of different molecular weights. Three monolithic disks were studied: PSDVB, poly(glycidyl methacrylate-*co*-butyl methacrylate-*co*-ethylene dimethacrylate) (C4) and poly(glycidyl methacrylate-*co*-ethylene dimethacrylate) (GMA-EDMA). No distinction could be made between the separation retention mechanisms on the different monolithic disks, which were all based on both a combination of precipitation-redissolution effects and adsorptive interactions. The latter are enhanced with increasing monolith polarity. All studied monolithic disks were found to be suitable as stationary phases for ILC separations of polymers. The influence of monolith surface

chemistry on peak resolution showed that adsorption was a significant contributor to the retention mechanism.

The PSDVB monolithic disks were not the only PSDVB stationary phases studied. Cheng *et al.* [122] used PSDVB columns (called PLRP-S) for the separation of statistical poly(N-vinyl pyrrolidone-*co*-vinyl acetate) (PVPVA) polymers. According to the authors, columns with a nominal pore size of 1000 Å were selected to minimize SEC effects and maximize interactions between the copolymers and the stationary phase surface. A water/THF gradient was applied. For the water-soluble PVPVA copolymers, separation was thought to be mainly based on interactions between the hydrophobic vinyl acetate (VA) units and the stationary phase. As a result, separation was based on chemical composition. Indeed, an increase in retention was observed with an increase in VA content. However, in some cases samples with different VA content eluted at the same elution time. This was found to be due to differences in the MWD. Therefore, a calibration curve of copolymer standards with known chemical compositions could not be used for CCD determination. However, using the developed method, low-concentration (±1.0%) homo-PVP contaminants in the copolymers could be separated and quantified.

Finally, columns packed with glass beads were studied for polymer separation by Reingruber *et al.* [66]. This stationary phase was used for the separation of poly(ethyl diazoacetate) and poly(benzyl diazoacetate) homopolymers and copolymers based on the CCD. Separation was first attempted using conventional NP and RP columns, but due to different concurrent selectivity's, interpretation of chromatograms was not possible. The glass-bead column was used under the assumption that the adsorptive interactions would be minimized, but the samples were still retained on the glass beads. It was not understood which property dominated the retention. Interpretation of the chromatograms, however, was easy. The developed LC method could be used for screening purposes only, since the resolution power did not suffice to accurately quantify the CCD.

Most applications use a mobile phase consisting of only organic solvents. Several used water or a hydro-organic mixture as one of the mobile phase components [54, 92, 122, 132, 133] . Most of these methods used a HPLC or UHPLC ODS column for the analysis. Only in the application of Hilbert and Marcus [133], a custom polyethylene terephthalate (PET) capillary-channeled polymer fiber column was used. For compatibility reasons, no NP columns were used with aqueous mobile phase components.

At low or moderate temperatures, the most commonly used adsorption and/or precipitation promoting solvents in one- and two-dimensional gradient LC were found

to be methanol and acetonitrile. THF is the most popular solvent used as desorption and/or dissolution promoting agent, followed by chloroform. THF has a high elution strength and is capable of dissolving many polymers. Also, it is miscible with most solvents [134]. A gradient from methanol as adsorbent/precipitant to THF as desorbent/good solvent is most commonly described in the articles.

Thus far, only binary gradients have been discussed. However, sometimes application of a ternary gradient leads to better separations. Ternary gradient systems are applied when the analytes show significant solubility differences in different solvents [114]. Li *et al.* [135] used ILC for analysis of copolymers of the enantiomers poly(L-lactic acid) (PLLA) and poly(D-lactic acid) (PDLA). Pure PLLA and PDLA polymers show semicrystalline behavior. Poly(D,L-lactic acid) copolymers are known to be amorphous. Also, all semicrystalline PLAs cannot be dissolved in THF, while the amorphous PLAs can be dissolved. Chloroform is a good solvent for all samples, but a weak eluent when using a NP column. A gradient from chloroform to THF was studied, but separation was not successful due to additional adsorption effects. For this reason, a ternary solvent gradient was developed. n-Hexane was added to the gradient, which is a non-solvent for all copolymers. Samples were injected with chloroform as mobile phase, causing retention of all copolymers. Then, a gradient to n-hexane was applied, resulting in precipitation of all polymers. After that, the THF fraction was gradually increased, causing redissolution (and thus desorption) of the amorphous PLAs. Finally, the chloroform fraction was increased again, resulting in desorption of the semicrystalline PLAs. This led to elution at higher retention volumes for samples of higher stereochemical purity. All PLAs having an isomeric excess of less than 80% elute at the same retention volumes and could therefore not be separated.

In HT-ILC, high boiling point solvents must be used as mobile phase [39, 40, 45]. 1-Decanol was the most popular solvent used as adsorption/precipitation promoting agent in these publications. TCB was almost always used as desorbent/strong solvent. Sometimes, 2-ethyl-1-hexanol was used instead of 1-decanol [136-138]. Chitta *et al.* [136] concluded that both 1-decanol and 2-ethyl-1-hexanol as well as 2-octanol can be used as adsorbent/precipitant for polyethylene/1-alkene copolymers. Retention of the copolymers in 2-ethyl-1-hexanol and 2-octanol is similar and stronger than retention in 1-decanol. Also, it was concluded that both TCB and ODCB can be used as desorbent/strong solvent, with TCB being the strongest eluent. Macko *et al.* [137] tested 2-ethyl-1-hexanol and cyclohexanone as adsorbents/precipitants in combination with TCB as desorbent for separating poly(ethene-*co*-vinyl acetate) analysis. Similar dependences between elution volume at peak maximum and peak molecular weight were obtained

using both adsorption-promoting solvents. Molecular-weight independence was found for polymers above 20 kDa for both solvent gradients.

Like in SEC, additives can be added to the mobile phase. Wright *et al.* [82] added 1.2% methanol to DCM to improve the elution strength of the system. Hilbert and Marcus [133] added trifluoroacetic acid (TFA) because it had been shown to be an excellent ion-pairing agent. Simultaneously, the ionic nature of the stationary phase was decreased, since TFA capped the cationic sites on the fiber surface in this work.

By using a NP stationary phase, both chain-end functionalized PS and polybutadiene could be analyzed using an isocratic solvent composition. NP columns are often used for FTD determination, since the polar stationary phase interacts much more strongly to the functional groups than RP columns [124]. The research from Hutchings *et al.* featured two isocratic methods. An NP stationary phase was used for separation of PS with different chain-end functionalities, namely PS-OX where X is *tert*-butyl(dimethylsilyl), PS-OH and PS-Br. A 55/45 (v/v) isooctane/THF mixture was used as mobile phase. All three PS samples eluted at different retention volumes. In separate runs, a difference in retention times was observed between PS-Br and PS-OX. When analyzing a mixture, these two peaks overlap. PS-OH, however, was baseline separated from the other two samples. PS-OH exhibits hydrogen bonding with the NP stationary phase, causing the analyte to be retained the strongest, other analytes did not exhibit equally strong interactions.

Polybutadiene samples of different molecular weights with and without -OH chain-end functionality were analyzed using the same NP column. Again, an isocratic solvent composition was used, but the amount of THF was strongly decreased compared to the PS injections mentioned before. Polybutadiene is very non-polar, and therefore it requires only a small fraction of strong eluent to overcome the interactions between the polymer backbone and the stationary phase. A 96/4 (v/v) isooctane/THF mixture was used. The unfunctionalized polymers elute close to each other and close to the solvent injection peak. The functionalized polymers of different molecular weights, however, could be separated from each other.

Table 1.5. Selected ILC applications

Analyte	Column	Mobile phase components	Gradient	Ref
Glycolic acid ethoxylate 4-nonphenyl ether	Custom PET C-CP fiber	A: Water with 0.06% TFA B: MeCN with 0.06% TFA	A to B (lin)	[133]
Poly((2-dec-9-enyl)-2-oxazoline)	Eclipse DBX-C18	A: Water B: THF	A isocratic, A to B (lin), B isocratic	[54]
Poly(2-phenyl-2-oxazoline)	Eclipse DBX-C18	A: Water B: THF	A isocratic, A to B (lin), B isocratic	[54]
Poly((2-phenyl-2-oxazoline)-*co*-((2-dec-9-enyl)-2-oxazoline)	Eclipse DBX-C18	A: Water B: THF	A isocratic, A to B (lin), B isocratic	[54]
Poly(3-hydroxyvalerate-*co*-hydroxybutyrate)	Kromasil C18	A: Chloroform/EtOH 10/90 B: Chloroform	A to B	[58]
Poly(3-hydroxyvalerate-*co*-hydroxybutyrate)	Supelco silica gel NH2	A: Chloroform/EtOH 10/90 B: Chloroform	A to B	[58]
Poly(benzyl diazoacetate)	Custom non-porous glass beads column	A: Chloroform B: Methanol	2/98 A/B isocratic, 2% A to 100% A, A isocratic	[66]
Poly(t-butyl methacrylate)	Monolithic S-DVB disk	A: MeOH B: THF	A to B	[131]
PET	Nucleosil C18	A: Acetone/MeOH 75/25 B: Acetone/THF 75/25	A to B (lin)	[120]
Poly(ethyl diazoacetate)	Custom non-porous glass beads column	A: Chloroform B: Methanol	2/98 A/B isocratic, 2% A to 100% A, A isocratic	[66]
Poly(ethyl diazoacetate-co-benzyl diazoacetate)	Custom non-porous glass beads column	A: Chloroform B: Methanol	2/98 A/B isocratic, 2% A to 100% A, A isocratic	[66]
Poly(lactic acid)	Nucleosil silica	A: Chloroform B: Hexane C: THF	A to B (lin), B isocratic, B to C (lin), C isocratic, C to A (lin), A isocratic	[135]
PMMA	Hypersil Gold C18 aQ	A: MeOH B: THF	Saw tooth gradient	[73]
PMMA	Nucleosil silica	A: Chloroform B: THF	A to B (lin)	[123]
PMMA	Monolithic S-DVB disk	A: MeOH B: THF	A to B	[131]
PMMA	Accucore C18	A: MeOH B: THF	Saw tooth gradient	[139]

Table 1.5. Continued

Analyte	Column	Mobile phase components	Gradient	Ref
Poly(MMA-*graft*-S)	Nucleosil silica	A: Chloroform B: 30% THF in chloroform	95% A to 100% B (lin)	[75]
Poly(MMA-*block*-S)	Nucleosil silica	A: Chloroform B: THF	A to B (lin)	[123]
Poly(phenylene ether)	Hypercarb	A: MeCN B: Chloroform	A to B (lin), B isocratic	[48]
PS	Hypersil Gold C18 aQ	A: MeOH B: THF	Saw tooth gradient	[73]
PS	Nucleosil C18	A: MeCN B: DCM	50% A to 90% B (lin), 90% B isocratic	[80]
PS	Monolithic S-DVB disk	A: MeCN B: THF	A to B (lin)	[131]
PS	Monolithic poly(glycidyl methacrylate-*co*-butyl methacrylate-*co*-ethylene dimethacrylate) disk	A: MeCN B: THF	A to B (lin)	[131]
PS	Monolithic poly(glycidyl methacrylate-*co*-ethylene dimethacrylate)	A: MeCN B: THF	A to B (lin)	[131]
PS	Accucore C18	A: MeOH B: THF	Saw tooth gradient	[139]
Poly(S-*co*-butadiene)	Spherisorb S5 ODS	A: Hexane B: THF	A to B (lin)	[81]
Poly(S-*block*-n-butyl acrylate)	Nucleosil silica	A: Heptane B: DCM with 1.2% MeOH	A isocratic, A to B (lin), B isocratic	[82]
Poly(vinyl acetate)	PLRP-S	A: 5% THF in water B: 75% THF in water	A to B (lin), B isocratic	[122]
Poly(vinyl chloride)	Accucore C18	A: MeOH B: THF	Saw tooth gradient	[139]
Poly(vinyl pyrrolidone)	PLRP-S	A: 5% THF in water B: 75% THF in water	A to B (lin), B isocratic	[122]
Poly(vinyl pyrrolidone-*co*-vinyl acetate)	PLRP-S	A: 5% THF in water B: 75% THF in water	A to B (lin), B isocratic	[122]
Polybutadiene	Nucleosil silica	THF/isooctane 45/55	-	[124]
PS	Nucleosil silica	THF/isooctane 4/96	-	[124]

1.3.1 Ion-exchange chromatography (IEX)

A mode of "interactive" LC, in which analytes undergo active electrostatic interaction with functional groups on the stationary phase is ion-exchange chromatography. Stationary-phase functionalities and analyte functionalities carry opposite charges. Various modes of IEX are discerned, with main descriptors being the type of ions that can be separated (anionic or cationic) and the nature of the stationary phase. The functional group on the stationary phase may be charged irrespective of the pH of the eluent (such as quaternary ammonium or sulfonate groups), resulting in a "strong" ion exchanger. The stationary-phase groups may also be neutral or charged, depending on the eluent pH and the pK_a of the ionizable group. Ion exchangers which such functionalities are called "weak". The analytes characterized using IEX are almost exclusively water-soluble substances, such as proteins [140, 141] and amino-acids [142]. Synthetic polymers remain a class of analytes for which IEX is not applied, as it is very difficult to establish suitable conditions for elution and separation, if only for the fact that most water-borne resins are not water-soluble.

1.3.2 Liquid chromatography at critical conditions (LCCC)

When the elution behavior of polymers in a chromatographic system is based on exclusion, high-molecular-mass fractions/polymers are eluted first. When interaction occurs between polymer and stationary phase, chromatographic behavior is mainly based on adsorption. In this case, low-molar-mass fractions are eluted first. Somewhere in between, conditions may exist where the free energy of transfer between the mobile phase and the stationary phase becomes negligible for the polymer backbone, these conditions are called 'critical' [31, 38, 109]. LCCC is thus performed in an intermediate regime between adsorption chromatography and SEC, which is schematically depicted in Figure 1.11. Under critical conditions, the separation is molar-mass-independent, with chromatographic retention only based on small differences in chemical structure of the sample fractions such as the nature and number of functional groups, end-groups, and perhaps blockiness, grafts or branches. By definition, LCCC is an isocratic elution technique.

For separations based on functional groups- or end-groups, the critical conditions of the non-functionalized polymer are applied, so that retention is only based on polymer functionalities. For copolymer analysis in LCCC, the critical conditions for one of the homopolymers are used. Under the critical conditions for the A-block of an AB block copolymer, the separation will be based on the extent of exclusion of block B. The

length of the A-block does not affect the separation, since all A-homopolymers of different molecular weights elute at the same elution volume under critical conditions. The critical conditions are different for each polymer and may vary for different column packings, since these may give rise to different interactions [38]. The critical conditions also vary with temperature and possibly with pressure [143]. For functionality-based separations by LCCC, NP columns are mostly used [29, 116].

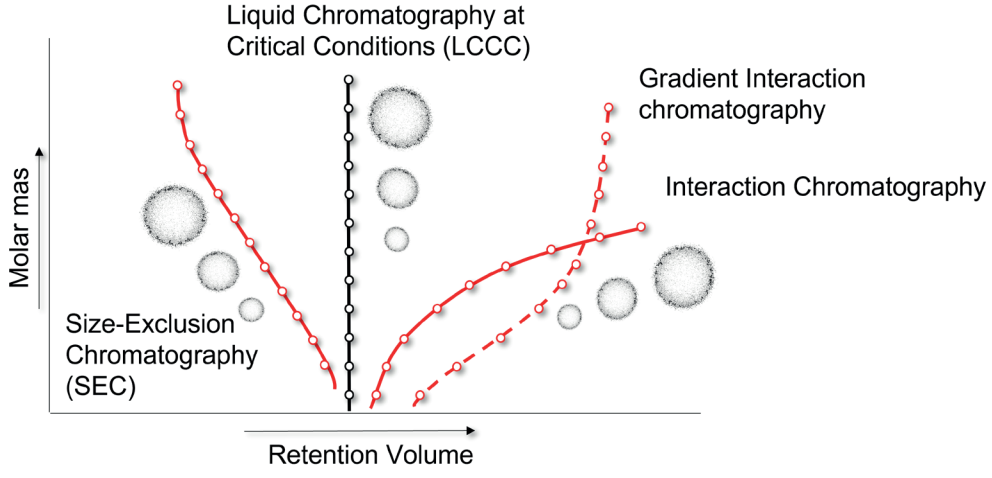

Figure 1.11. Dependence of the peak-average molar mass on the elution volume at peak maximum. The black line marks the LCCC conditions. The red lines describe elution in SEC- and liquid adsorption modes.

Although theoretically possible, perfect critical conditions are hard to establish and to maintain. Most LCCC analysis will therefore take place at near-critical conditions [38, 144]. Around the critical conditions, small changes in eluent composition or temperature can significantly affect the mode of polymer separation, causing it to alter from SEC to adsorption chromatography or vice versa. Polymer retention may vary more strongly for stationary phase materials with larger surface areas. This can possibly be circumvented by reducing the surface area. The use of stationary phase material with larger pores will, thus, eliminate this problem [38].

Although LCCC has numerous advantages for CCD and FTD determinations, achieving and maintaining the critical conditions can be difficult. Sometimes, the critical mobile phase composition and temperature must be regulated within 0.1%, or else the critical conditions are not maintained [145, 146]. Since LCCC is at the borderline between SEC and interaction chromatography, small changes in eluent composition can cause the

separation mode to alter. As is previously described, this leads to uncontrollable sample behavior [38, 147]. Eluents are sometimes pre-mixed in order to maintain a constant mobile phase composition [148]. In that case, however, temperature changes can still distort the critical conditions.

Also, determination of the critical conditions of one block in block copolymers is performed by determining the homopolymer critical conditions. The critical conditions of the blocks may, however, differ from those of the homopolymers [147]. Furthermore, high-molecular-weight polymers tend to precipitate as the critical conditions are approached. This limits the application range to low-molecular-weight polymers [148].

This approach was applied several times. Irfan *et al.* [68] developed two methods for poly(EO-*block*-ε-caprolactone) analysis. Both methods characterized di- and tri-block copolymers with regard to total relative molecular weight, chemical composition, molecular weight of the individual blocks and homopolymer content in block copolymer samples. Similar results were obtained by M.I. Malik [147] for poly(EO-*block*-MMA), Sinha *et al.* [148] for poly(EO-*block*-S), Lee *et al.* [108] for poly(S-*block*-butadiene and Schmid *et al.* [60] for poly(S-*block*-THF).

Apel *et al.* [149] also developed a gradient method, but for branching analysis of poly(bisphenol A carbonate). This gradient was applied in a narrow range around the critical conditions of poly(bisphenol A carbonate), meaning it is a solvent gradient at near-critical conditions (SG-NCC). The SC-NCC allowed separation of branched and linear poly(bisphenol A carbonate). The chromatographic separation was also influenced by molecular weight. Another LCCC branching analysis was performed using isocratic solvent compositions. Linear, partially branched and hyperbranched polyesters of similar molar masses were separated by Al Samman *et al.* [120] using acetone/THF as mobile phase composition on a C18 column.

Separation of poly(bisphenol A carbonate) according to hydroxyl end-groups was performed by Apel *et al.* [149]. Critical conditions of poly(bisphenol A carbonate) were used, so that end-group differences would govern the separation. A Hypercarb column was used as stationary phase. Separation of the analytes according to end-groups was successful, as confirmed by matrix assisted laser desorption/ionization – time of flight mass spectrometry (MALDI-TOF-MS) analysis. Wei *et al.* [150] developed three methods for the analysis of non-, mono- and bi-functional benzaldehyde-substituted PEGs. The three methods use different reversed-phase columns, being XB-C18, XB-Phenyl and UPLC BEH C18, each with a corresponding acetonitrile/water mixture to achieve

critical conditions. All three methods succeeded in separating the PEGs according to benzaldehyde end-groups.

Finally, Sinha *et al.* [151] applied LCCC for separation of polystyrene according to degree of deuteration. Blends of protonated and deuterated polystyrene were successfully separated. Depending on the molar masses of the blend components, baseline separation could be achieved. The LCCC method was coupled with SEC in the second dimension in order to improve the separation.

As previously mentioned, HT-LCCC was only applied for polyolefin analysis. Like in previously described HT-SEC and HT-ILC methods, Hypercarb columns are used. Mobile phases used are mixtures of TCB and *n*-decane, 2-ethyl-1-hexanol and ODCB and 2-octanol and ODCB. These solvents are often used in HT-analysis. Similarly, poly(ethylene-*block*-1-octene)s were separated according to block length by Mekap *et al.* [31].

1.3.3 Limitations of interaction chromatography for analysis of acid-functional polymers

Interaction chromatography is a versatile tool, which may separate a variety of polymers with high resolution. It is very useful to study differences in the chemical composition distribution of copolymers, but it must be stressed that separation in interaction chromatography is not strictly based on enthalpic effects. In these cases, separation is not performed on a single distribution but always on a mixture of chemical composition and molar mass – which both influence the polymer adsorption/desorption- and interaction or redissolution behavior. For polymers with similar molar mass, retention behavior of copolymers may be a descriptor of the chemical composition distribution. However, this approach requires preparation of carefully prepared model systems. A change in molar mass, polymer endgroup, or comonomer content will change the chromatographic behavior – which renders the use of model systems difficult to be applied in a general way. This also applies to acid-functional polymers. The incorporated acid groups will have an influence on the chemical composition distribution, as it is very hydrophilic. ILC-type of separations are not specifically tailored towards the analysis of acid-functional polymers, as adsorption/desorption and redissolution effects apply to the complete polymer chain. As the acid-functional polymers are typically applied in the lower percentile range, the relative influence of such functionalities on overall interaction in existing ILC methods is limited. Due to the different chemical nature of the acid-functional monomers compared to non-functional monomers, there is potential for developments using interaction chromatography but no developments have taken place in this direction.

Table 1.6. Selected LCCC applications

Analyte	Column	Mobile phase	Ref
Poly(bisphenol A carbonate)	Nucleosil silica	A: Chloroform with 0,002% 2-methyl-2-butene B: 97.5/2.5 MTBE/chloroform Gradient: A isocratic, A to B (lin)	[149]
Poly(bisphenol A carbonate)	Hypercarb™	95.5/4.5 Chloroform/TCB	[152]
Poly(caprolactone-*block*-EO)	PerfectSil NP	THF/DMF 97.5/2.5	[68]
Poly(caprolactone-*block*-EO)	Jupiter RP-C18	MeCN/THF/TEA 85/15/1	[68]
PEG, benzaldehyde-substituted	XB-C18	MeCN/water 40/60	[150]
PEG, benzaldehyde-substituted	UPLC BEH C18	MeCN/water 40/60	[150]
PEG, benzaldehyde-substituted	XB-Phenyl	MeCN/water 45/55	[150]
Poly(EO-*block*-MMA)	Jupiter RP-C18	MeCN/THF/TEA 90/9/1	[147]
Poly(EO-*block*-MMA)	Jupiter RP-C18	Acetone/water/TEA 85/14/1	[147]
Poly(EO-*block*-PO-*block*-EO)	Jupiter RP-C18	A: 37% acetone in water B: 87% methanol in water Gradient from 50 or 70% B to 100% B	[147]
Poly(EO-*block*-S)	Symmetry C18	THF/water 88.5/11.5	[148]
PET	Nucleosil C18	94/6 acetone/THF	[120]
PS, regular and deuterated	Nucleosil C18	THF/MeCN 47/53	[151]
Poly(S-*block*-butadiene)	Nucleosil silica	THF/*n*-hexane 42/58	[108]
Poly(S-*block*-butadiene)	Nucleosil C18	DCM/MeCN 78/22	[108]
Poly(S-*block*-THF)	YMC-ODSA	88.4/11.6 THF/water	[84]
Poly(E-*block*-1-octene)	Hypercarb™	TCB/*n*-decane 48.5/51.5	[152]

1.4 Two-dimensional liquid chromatography (2D-LC)

Most polymers do not consist of a single molecular or physical distribution, such as molecular weight distribution, chemical composition distribution, functionality type distribution etc., but a complex combination of these polymer distributions. To fully characterize such samples, comprehensive two-dimensional approaches using different separation mechanisms are very useful [37, 39, 153]. In addition to that, chromatographic resolution can be increased by applying two-dimensional liquid chromatography (2D-LC) [37]. For the first chromatographic dimension, highest selectivity and best adaptability is required, providing a high resolution. This ensures highest purity of the eluting fractions [37, 132]. The efficiency and flow rate of the second dimension are also of great importance. The speed of the second-dimension run determines the flow rate which can be applied in the first dimension. If the speed of the second-dimension analysis is high, first dimension flow rates can also be increased, ensuring the full first dimension eluent is injected onto the second dimension separation within acceptable analysis times [132].

For polymer analysis, ILC × SEC is the most commonly used 2D-LC approach, taking advantage of the high resolution of ILC in the first dimension and the universality of SEC in the second dimension [132, 154]. ILC shows better sensitivity on chemical nature than SEC, but cannot easily be used in the second dimension because gradients are applied. Also, many ILC conditions (mobile phase, stationary phase, temperature etc.) can be adjusted to improve separation, which is relatively easy and allows for more homogeneous fractions [37, 154]. Furthermore, solvents used in SEC are often strong eluents in ILC. If the eluent in the first dimension is stronger than the eluent in the second dimension, breakthrough peaks often appear: part of the sample elutes unretained in the second dimension due to insufficient mixing of the injection plug with the eluent [113, 154]. Another reason why SEC is primarily used in the second dimension, is because SEC runs can be fast, using short, wide-bore columns or core-shell columns [49] or by applying HT-SEC or UHP-SEC [132, 154]. Although SEC runs are fast, the flow rates in the first ILC dimension are often still below the optimum of the Van Deemter curve.

By coupling SEC to LCCC or TGIC, the relation between the CCD, FTD or other distributions and the molecular weight distribution can be obtained, which is similar to ILC × SEC. Like in ILC × SEC, SEC is used in the second dimension for the same reasons as previously mentioned [38]. By coupling LCCC to ILC or TGIC, the same information can be obtained, but with a better resolution [155]. Another advantage of TGIC × LCCC, is that similar

eluents are used in both dimensions, since near-critical solvent compositions are often used in TGIC. In some cases, it is possible to use the same solvent for both dimensions, eliminating problems such as the breakthrough effect [155]. Even though similar mobile phases are used, information on CCD, FTD and/or MWD can be obtained. This is possible because separation in LCCC is based on differences in chemical composition and functionality types, whereas TGIC is capable of separating according to MWD and/or CCD. Like ILC, TGIC is used in the first dimension because a gradient is applied [154].

Two-dimensional separation techniques with HDC as one of the dimensions is not commonly applied. HDC can be applied instead of SEC, with its high speed as an important advantage [156]. Also, HDC is employed to study molecules that are too large or too fragile to be analyzed successfully by SEC, HDC can be applied in 2D-LC methods [157].

SEC is most commonly applied in the second dimension in ILC × SEC methods, as the possibility to perform overlapping injections and the lack of need for re-equilibration of the chromatographic system provide significant advantages to the speed of the (fast) ^{2}D separations. Yang *et al.*[92], however, used SEC in the first dimension and ILC in the second dimension for the analysis of water-soluble polymers. For these water-soluble polymers, the SEC × HPLC setup had some advantages. The first advantage is that refocusing of the first dimension effluent on top of the second dimension column can be easily achieved, which leads to improved second dimension separation. Also, SEC fractions with narrow MWD are transferred to the second dimension, resulting in better decoupling of MWD and CCD without the need to use LCCC [92, 158, 159].

Most ILC × SEC analyzes were performed to obtain the chemical composition in relation to the molecular weights of copolymers. This was successfully applied to random copolymers [54, 66], block copolymers [74, 82], star block copolymers [81] and graft copolymers [75]. Moyses [160] used narrow PS standards to optimize resolution in the SEC dimension. ILC separation was based on precipitation/redissolution, meaning elution is based on composition and molecular weight. For the polystyrene standards, which have the same chemical composition, retention was only affected by molecular weight.

In a publication by Uliyanchenko *et al.* [132], two UHP-ILC methods were described, which were both used in the first dimension of a 2D-LC analysis. For the second dimension, UHP-SEC was used. The advantages of UHP-SEC over SEC are faster analysis and higher separation efficiency. The UHP-ILC × UHP-SEC approach can therefore, as

confirmed in a theoretical study, provide higher separation power than LC × LC, LC × UHPLC or UHPLC × LC. One method was developed for the analysis of PMMA/PBMA homo- and copolymers. In both dimensions, UPLC BEH C18 columns were used, applying a MeCN/THF gradient in the first dimension and using THF as mobile phase in the second dimension. During the first five minutes, the mobile phase was kept at (near) critical conditions for PMMA, resulting in a molecular weight-independent elution. Only a slight molecular weight dependence for elution was found for the copolymers and PBMA homopolymers, meaning separation was almost exclusively based on chemical composition. In the second dimension, polymers with similar chemical composition were efficiently separated by size in the second dimension. The resulting UHP-GPEC × UHP-SEC plot provided information on CCD, the MWD and their mutual dependence. Such detailed information cannot be obtained from one-dimensional experiments. Also, the analysis time was decreased significantly from 4 hours to 22 minutes.

A second method, which was described in the same publication, is a UHP-ILC × UHP-SEC method for polyurethanes. This is one of few articles published on the analysis of polyurethanes. The polyurethane prepolymers were synthesized with poly(propylene glycol) (PPG 2000) and toluene diisocyanate (TDI), with some samples containing dimethylolpropionic acid (DMPA). In the first dimension, a UPLC BEH C18 column was used with a gradient from water with 0.1% formic acid to THF. The eluting fractions contained significant amounts of water and as a result, adsorptive interactions prevented SEC analysis on the same BEH C18 columns. Separations strictly based on size could only be performed using a UPLC BEH HILIC column. The mobile phase used in the second dimension was a 80/20 (v/v) THF/water mixture. With the developed method, an estimate could be obtained of the ratio of polymers containing an acid functionality and polymers without acid groups. Also, information on both low-molecular-weight components (excess TDI) and the polymeric fractions could be obtained, all in a single analysis with an analysis time of 60 min. Again, this information could not be provided by one-dimensional experiments.

LCCC × SEC and TGIC × SEC have the same aim as ILC × SEC, *i.e.* obtaining information on the relation between MWD and another type of distribution . LCCC × SEC was applied for analyzing block copolymers [60], and branching [149] and for the separation of regular and deuterated polystyrene [151]. The LCCC separation in the latter analysis is performed at the critical conditions of deuterated polystyrene (d-PS), at which regular polystyrene (h-PS) shows SEC behavior. Separation of the polystyrenes could be improved by slightly modifying the column temperature. An increase in temperature caused d-PS to show SEC

behavior, whereas h-PS showed LAC behavior. Using the 2D-LC method, a blend of two h-PS and two d-PS standards of different molar masses could be well-separated. TGIC × SEC was applied for branching analysis of star-shaped polystyrenes [78, 80] and for the analysis of polystyrene/polybutadiene block copolymers [108]. In the latter study, Lee *et al*. analyzed poly(styrene-*block*-butadiene) using both NP and reversed-phase stationary phases. The analyzed copolymer samples were polystyrene/polybutadiene star-shaped block copolymers synthesized using polystyrene/polybutadiene block precursors with short and long styrene chains. Star block copolymers with different number of arms and polystyrene chain lengths were the products of the synthesis.

TGIC was chosen for the first dimension because polymers with various molecular weights and compositions had to be analyzed. LCCC separated according to the size of the 'visible block'. The different block copolymers were successfully separated according to the number of arms and polystyrene chain lengths. Retention time in LCCC increased as the number of arms decreased. A clear relation between arm length and retention time was observed, independent of polystyrene chain lengths. In TGIC the copolymers with only short polystyrene chains eluted first. Retention time increased according to increasing number of long chains. Using the 2D-LC method, the various copolymer species could be located in the chromatogram. TGIC × LCCC was said to be easy to perform, since TGIC conditions were near the critical conditions used in LCCC.

Pirok *et al*. [61, 102] published two applications for the characterization of polymer latexes using HDC × SEC. 2D-LC is not often applied for nanoparticle analysis. Nanoparticles are conventionally analyzed using one-dimensional HDC or asymmetrical field field-flow fractionation (AF_4) methods [161-163]. Both techniques provide a very similar, size-based selectivity [61]. No other LC mechanism can be coupled with HDC or AF_4 to provide meaningful information on the intact particles, since these are too large to fully or partly enter pores. HDC × SEC, however, can be applied by performing HDC in the first dimension on the intact particles and SEC in the second dimension on dissolved polymer particles.

In the first publication on HDC × SEC [61], polyacrylate and polystyrene latexes were the analytes of interest. HDC was performed using an aqueous surfactant solution as mobile phase, THF was added to the eluting fractions, which is a good solvent for the polymer nanoparticles. The presence of water in the resulting solutions, however, caused significant adverse adsorption effects in SEC. Also, these sample solutions were quite dilute. Therefore, two stationary-phase-containing cartridges ('traps') were

installed in the valve used for modulation. Most of the water could be removed, while the analyte polymers were retained on the traps. The developed 2D-LC method allowed relating the size distribution of the intact particles to the molecular-weight distribution of the constituting polymers. The application of stationary-phase materials instead of sample loops in two-dimensional LC, commonly referred to as stationary-phase-assisted modulation (SPAM), has lately gained interest [153, 164]. The application of SPAM may circumvent several inherent problems in conventional loop-based 2D-LC, such as breakthrough effects, excessive dilution or incompatibility issues between LC dimensions. As an alternative to SPAM, which may suffer from poor physical stability of the trapping columns, active solvent modulation (ASM) was developed by Stoll *et al*. [165]. With specially designed modulation valves and an extra pump system, refocusing of the 1D-analytes can be performed with all the advantages of SPAM but without the disadvantages associated with the column trapping material [166] .

In another article, Pirok *et al.* [102] described a method for on-line comprehensive HDC × SEC with automated data processing. Charged MMA/BA/MAA latexes were used as analytes. THF was again used as mobile phase in SEC. Again, the eluting aqueous HDC fractions were mixed with THF by the use of traps in the modulation valves. An algorithm was developed to correct for band broadening in HDC. The corrected data were used to obtain the two-dimensional relation between particle size and polymer molecular weight. This relation can be used to study particle formation during emulsion polymerization.

The development and combination of various types of chromatographic separations potentially unlocks a whole new level of detail in which complex matrices, such as polymers, can be studied. Specifically, when life can be made significantly easier by alleviating the aforementioned limitations (breakthrough, dilution, incompatibility between dimensions), the application of two-dimensional LC will increasingly expand from the traditional academic setting to many industrial laboratories.

Table 1.7. Selected 2D-LC applications

	Analyte	Column	Mobile phase	Ref
ILC × SEC	Poly((2-dec-9-enyl)-2-oxazoline)	1st dim: Eclipse DBX-C18 RP 2nd dim: 2x PLgel Mixed-D	1st dim: H_2O/THF gradient 2nd dim: THF with BHT	[66]
ILC × SEC	Poly(2-phenyl-2-oxazoline)	1st dim: Eclipse DBX-C18 RP 2nd dim: 2x PLgel Mixed-D	1st dim: H_2O/THF gradient 2nd dim: THF with BHT	[66]
ILC × SEC	Poly((2-phenyl-2-oxazoline)-*co*-((2-dec-9-enyl)-2-oxazoline)	1st dim: Eclipse DBX-C18 RP 2nd dim: 2x PLgel Mixed-D	1st dim: H_2O/THF gradient 2nd dim: THF with BHT	[66]
SEC × ILC	PAA copolymers and PEA copolymers	1st dim: Shodex OH pak SB-804Q 2nd dim: Zorbax Eclipse C18	1st dim: 20 mM ammonium acetate 2nd dim: 100 mM ammonium formate/MeCN gradient	[92]
ILC × SEC	PETs, silylated	1st dim: Nucleosil C18 2nd dim: 2x PSS SDV	1st dim: acetone/MeOH to acetone/THF gradient 2nd dim: THF	[121]
ILC × SEC	Poly(ethyl diazoacetate-*co*-benzyl diazoacetate)	1st dim: Custom glass bead 2nd dim: PLgel Mixed-C	1st dim: MeOH/chloroform gradient 2nd dim: chloroform	[66]
ILC × SEC	Poly(MAA-*graft*-S)	1st dim: Nucleosil Silica 2nd dim: PSS linear M	1st dim: chloroform/THF gradient 2nd dim: THF	[75]
ILC × SEC	Poly(MMA-*co*-BA)	1st dim: Spherisorb grafted silica 2nd dim: PSS High-Speed linear M	1st dim: hexane/THF gradient 2nd dim: THF	[74]
ILC × SEC	PS	1st dim: Spherisorb S5CN 2nd dim: 2x PLgel Mixed-B	1st dim: MeOH/THF gradient 2nd dim: THF	[160]
ILC × SEC	Poly(styrene-*co*-butadiene)	1st dim: Spherisorb S5 2nd dim: PSS SDV High-Speed linear M	1st dim: hexane/THF gradient 2nd dim: THF	[81]
ILC × SEC	Poly(styrene-*block*-n-BA)	1st dim: Nucleosil Si 2nd dim: PSS SDV	1st dim: DCM + 1.2% MeOH / heptane gradient 2nd dim: THF	[82]
HT-ILC × SEC	Polyethene	1st dim: Hypercarb™ 2nd dim: PL Rapide	1st dim: 1-decanol/TCB gradient 2nd dim: TCB with BHT	[167]
HT-ILC × HT-SEC	Poly(ethene-*co*-1-octene)	1st dim: Hypercarb™ 2nd dim: PL Rapide H	1st dim: 1-decanol/TCB gradient 2nd dim: TCB	[168]

Table 1.7. Continued

	Analyte	Column	Mobile phase	Ref
HT-ILC × HT-SEC	Poly(ethene-*co*-octene)	1st dim: Hypercarb™ 2nd dim: PL Minimix-B	1st dim: 2-butoxyethanol/TCB gradient 2nd dim: TCB	[169]
HT-ILC × HT-SEC	Poly(ethene-*co*-propene)	1st dim: Hypercarb™ 2nd dim: PL Rapide H	1st dim: 1-decanol/TCB gradient 2nd dim: TCB	[170]
HT-ILC × HT-SEC	Poly(ethene-*co*-propene)	1st dim: Hypercarb™ 2nd dim: PL Rapide M	1st dim: decane/TCB gradient 2nd dim: TCB with 200 ppm BHT	[171]
HT-ILC × HT-SEC	Polyolefin blends	1st dim: Hypercarb™ 2nd dim: PL Rapide H	Both dim: 1-decanol/TCB gradient	[172]
HT-ILC × HT-SEC	Polyolefin blends	1st dim: Hypercarb™ 2nd dim: PL Rapide H	1st dim: decane/TCB gradient 2nd dim: TCB with 200 ppm BHT	[173]
UHP-ILC × UHP-SEC	PMMA and PBMA copolymers	1st dim: 3x Acquity UPLC BEH C18 2nd dim: Acquity UPLC BEH C18	1st dim: MeCN/THF gradient 2nd dim: THF	[132]
UHP-ILC × UHP-SEC	PUR and PUR copolymers	1st dim: 3x Acquity UPLC BEH C18 2nd dim: Acquity UPLC BEH HILIC	1st dim: H_2O + 0.1% formic acid/THF gradient 2nd dim: 80/20 THF/H_2O	[132]
LCCC × SEC	Poly(ε-caprolactone-*block*-PS)	1st dim: PL RP-S 2nd dim: PSS SDV-gel	1st dim: THF/MeOH gradient 2nd dim: THF	[60]
LCCC × SEC	Poly(bisphenol A carbonate)	1st dim: Nucleosil NP 2nd dim: PSS SDV	1st dim: chloroform + 0.002% 2-methyl-2-butene / MTBE/chloroform 97.5/2.5 gradient 2nd dim: chloroform	[149]
LCCC × SEC	PS, regular and deuterated	1st dim: Nucleosil C18 2nd dim: PSS Linear M SDV	1st dim: THF/MeCN 47/53 2nd dim: THF	[151]
TGIC × LCCC	Poly(styrene-*block*-butadiene)	1st dim: Nucleosil NP 2nd dim: Nucleosil NP	1st dim: THF/*n*-hexane 38/62; 5 to 78 °C 2nd dim: THF/*n*-hexane 42/58	[108]
TGIC × LCCC	Poly(styrene-*block*-butadiene)	1st dim: Nucleosil C18 2nd dim: Nucleosil C18	1st dim: DCM/MeCN 64/36; 21 to 65 °C 2nd dim: DCM/MeCN 78/22	[108]
TGIC × SEC	PS	1st dim: Nucleosil C18 2nd dim: PLgel Mixed-C	1st dim: DCM/MeCN 57/43; 2 to 35 °C 2nd dim: THF	[78]

Table 1.7. Continued

	Analyte	Column	Mobile phase	Ref
TGIC × SEC	PS	1st dim: Nucleosil C18 2nd dim: SDVB	1st dim: DCM/MeCN 57/43; 5 to 40°C 2nd dim: THF	[80]
TGIC × SEC	Poly(styrene-*block*-butadiene)	1st dim: Nucleosil NP 2nd dim: Shodex & Polyphore	1st dim: THF/n-hexane 38/62; 5 to 78°C 2nd dim: THF	[108]
TGIC × SEC	Poly(styrene-*block*-butadiene)	1st dim: Nucleosil C18 2nd dim: Shodex & Polyphore	1st dim: DCM/MeCN 64/36; 21 to 65°C 2nd dim: THF	[108]
TGIC × LCCC	Poly(styrene-*block*-butadiene)	1st dim: Nucleosil NP 2nd dim: Nucleosil NP	1st dim: THF/*n*-hexane 38/62; 5 to 78°C 2nd dim: THF/*n*-hexane 42/58	[108]
TGIC × LCCC	Poly(styrene-*block*-butadiene)	1st dim: Nucleosil C18 2nd dim: Nucleosil C18	1st dim: DCM/MeCN 64/36; 21 to 65°C 2nd dim: DCM/MeCN 78/22	[108]
HDC × SEC	Polyacrylate latexes	1st dim: PL-PSDA cartridge type-2 2nd dim: 3x Phenomenex experimental core-shell	1st dim: disodium dihydrogen orthophosphate/SLS/Brij L23/sodium azide in MilliQ 2nd dim: THF	[61]
HDC × SEC	Poly(MMA-*co*-BA-*co*-MAA) latexes	1st dim: PL-PSDA cartridge type-1 2nd dim: PLgel Mixed-C	1st dim: disodium dihydrogen orthophosphate/SLS/Brij L23/sodium azide in MilliQ 2nd dim: THF with 0.1% TFA	[102]

1.5 Capillary electrophoresis (CE)

A technique less intensively used for the characterization of polymers is capillary electrophoresis (CE). CE is an analytical technique which separates charged analytes in a narrow-bore (25-100 µm ID) capillary filled with electrolytes. Separation is obtained by the application of a high electric field across the capillary. Positively charged analytes will be attracted towards the end of the capillary where the negatively charged electrode is present (cathode), and negatively charged analytes will be attracted towards the positively charged electrode (anode). Meanwhile, neutral species are not affected by the electrical charge. Due to the described electrostatic attraction, the charged analytes start to migrate. This driving force is described by

$$F_d = q * E \tag{16}$$

In the above equation, F_d equals the driving force (Jm^{-1}), q is the charge of the analyte (C) and E is the applied field strength (Vm^{-1}).

Next to the driving force, there is also a friction force present which counteracts the driving force

$$F_f = 6\pi * \eta * r_H * V_e \tag{17}$$

In this equation, F_f depicts the friction force (Jm^{-1}), η the mobile phase viscosity (Pa.s), r_H the analyte radius (m) and v_e the electrophoretic migration velocity (ms^{-1}).

Within milliseconds after a voltage is applied, an equilibrium is reached in which the friction force (F_f) becomes equal to the driving force (F_d). Thus, a constant or maximum electrophoretic mobility is obtained. By rewriting the formulas in the equilibrium, it is possible to obtain an equation for the electrophoretic migration velocity:

$$V_e = \frac{q * E}{6\pi * \eta * r_H} \tag{18}$$

More commonly used is the electrophoretic mobility independent of the field strength, known as μ_e. This can be easily obtained by dividing the equation for the electrophoretic migration velocity (ms^{-1}) by the field strength E.

$$\mu_e = \frac{V_e}{E} = \frac{q}{6\pi * \eta * r_H} \tag{19}$$

From this equation, the parameters which influence the electrophoretic mobility can be derived. Both q and r_H are compound-specific parameters while η is a mobile-phase parameter. Even though charge and hydrodynamic radius are compound specific, they partly depend on the mobile phase composition. The charge of the analyte will change depending on the pH of the mobile phase, and the analyte radius will depend on the solvation characteristics of the solvent. μ_e Is constant (after a few milliseconds) and characteristic for a given charged analyte in the specific medium.

Apart from the electrophoretic mobility another type of "mobility" is often influencing the separation, *i.e.* electro-osmosis. The origin of electro-osmosis is found in the bare fused-silica capillaries, which are commonly used in CE. At the wall of the capillary silanol groups are present, which have a pK_a value of about 6 (in aqueous solutions). Thus, depending on the pH of the buffer, the silanol groups can be negatively charged. If cations are present in the buffer they are attracted to the negatively charged wall of the capillary, which results in the formation of an electrical double layer, composed of a Stern layer and a diffuse layer. When a voltage is applied, the cations in the diffuse layer will start to migrate towards the cathode. The entire bulk liquid is dragged along creating an electro-osmotic flow (EOF) towards the cathode. An advantage of the EOF compared to a pressure driven flow is the (almost) flat flow profile, whereas a pressure driven flow shows a parabolic ("Poiseuille") flow profile. The flat flow profile does not induce additional peak broadening, so that resolution is maintained. However, the presence of the EOF influences analyte mobilities. The mobilities that are measured during an analysis are the apparent mobilities, μ_a, which defined as

$$\mu_a = \mu_{EOF} + \mu_e \tag{20}$$

)From this equation it can be derived that neutrals will move at a velocity equal to the EOF. Cations, which move in the same direction as the EOF by definition, will elute before the neutrals and anions will elute after the neutrals. The latter is only true if

$$-\mu_{e,anion} < \mu_{EOF} \tag{21}$$

If not, the anion will move towards the inlet vial, where commonly no detectors are located. These anions can still be measured by simply reversing the polarity of the power source. Alternatively, an additional pressure can be applied to force the anionic species towards the detectors. This will affect the shape of the flow profile, and introduce additional band broadening. An overview of the electrophoretic process is depicted in Figure 1.12:

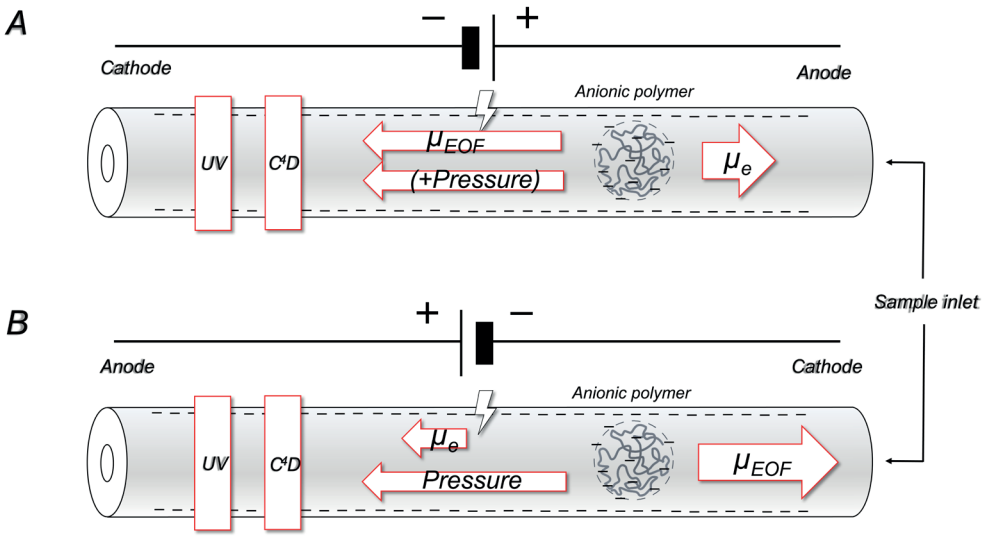

Figure 1.12. Schematic representation of the possible mobilities (electrophoretic, electro-osmosis and external pressure) during electrophoresis. Top: conditions with a positive voltage. Bottom: conditions with a negative voltage.

A CE-separation is based on (constant) velocity differences between the analytes. The EOF can have both a positive as well as a negative influence on the separation. For the analysis of cations, the EOF would have a negative influence on the relative differences in apparent mobilities of the cations. The opposite is true for anions. However, if anions have a mobility close to the EOF, the migration times increase dramatically. Still, the EOF can offer some advantages. Both cations and anions can be measured in one analysis and the analysis times can be reduced in some instances.

Polymer latexes and other nanoparticles have been analyzed by capillary electrophoresis. CE was performed for polystyrene nanosphere analysis by Van Orman and McIntire [174]. The analyzed nanospheres possessed sulfate or carboxyl surface groups, and were thus negatively charged. The fused-silica capillaries were pretreated with a cationic surfactant, cetyltrimethylammoniumbromide (CTAB), followed by flushing with KOH and then with the background electrolyte (BGE). The BGE was either 1 mM *N*-[2-acetamido]-2-aminoethane sulfonic acid pH 5.80 or 6.46 or 10 mM boric acid solution adjusted to pH 7.5. No correlation was found between the migration velocities and surface charge or charge-to-mass ratio. In contrast, a good correlation was found between migration time and particle size.

In another publication by Van Orman Huff and McIntire [175], the electrophoretic mobilities of carboxy modified, sulfonated and amine latexes were determined by CE. In this study, the capillary was not pretreated, but only flushed with NaOH in between runs. The BGE was a 10 mM phosphate buffer, pH 7.4. Again, a size-related increase in electrophoretic mobility magnitude was observed.

Jones and Ballou [176] applied CE for separating particles with different numbers of attached carboxylate or sulfate groups. The number of functional groups per particle increased with increasing particle diameter. Surface charge densities were, however, not the same and also increased with increasing particle diameter. Fused-silica capillaries were used without dynamic coating, contrary to the research of Van Orman and McIntire [174]. Particles of different sizes with the same functional groups eluted from small to large. Electrophoretic behavior depended on both the size and the chemical composition of the particle surface, as also observed by Anik *et al.* [177]

The electrophoretic mobilities of 0.6 μm amidine-modified and 0.22 μm carboxylate-modified polystyrene latex microspheres and 0.24 μm PMMA microspheres were determined using CE by Glynn *et al.* [178]. In accordance with Jones and Bailou [176], they found that the type of functional group at the surface of the particles affected particle migration. However, since only one size of each type of microsphere was analyzed, nothing could be said about the relation between particle size and number of functional groups per particle on the electrophoretic mobilities.

Vanhoenacker *et al.* [179] analyzed acrylic-styrene-copolymer emulsion particles of the same size, but with difference in chemical composition and particles of the same chemistry, but with different sizes. A fused-silica capillary without coating was used for analysis. The particles studied were styrene/2-ethyl-hexyl acrylate/acrylic acid and styrene/2-ethyl-hexyl acrylate/methacrylic acid copolymers. Also, a styrene/2-ethyl-hexyl acrylate polymer was studied. The values obtained for the zeta potentials in separate measurements were in accordance with the observed electrophoretic mobilities. For particles of the same chemistry, but with different sizes, the migration order correlated with the measured zeta potentials, but no linear relationship was observed. The use of a high electric field and a low ionic strength BGE led to a relaxation effect, *i.e.* the electric double layer around the particles was thought to be deformed and moving towards the electrode of opposite charge. The analyte particle would then be dragged with the deformed double layer. At low ionic strength, the thickness of the electric double layer is maximized, and therefore the relaxation effect is strongest at

low ionic strengths [180]. The relaxation effect increases with increasing particle size, which is why larger particles migrate faster than smaller ones if this effect occurs [179, 181].

A similar study was performed by Hwang *et al.* [182], but with polystyrene and gold nanoparticles. An uncoated fused-silica capillary was used with 50 mM Tris buffer at pH 9.2 as BGE. Polystyrene standards with diameters of 20, 50, 155 and 300 nm were successfully separated. Also, gold and polystyrene nanoparticles of the same size were separated. Like in the previously mentioned studies, these particles were again separated based on particle surface chemistry.

Anik *et al.* [177] separated latexes containing a polystyrene core and poly-ethyl acrylate-acrylic acid shell. The particles were stabilized with sodium lauryl sulphate (SLS). Acrylic acid functionality in the polymer was obtained by partial hydrolysis of polyethyl-acrylate. The polymers were separated according to the rate of hydrolysis. A fused-silica capillary was used in combination with a 53 mM borate buffer with 10 mM Brij 78. Addition of the latter constituent resulted in reduced electrophoretic mobilities, most likely due to replacement of SLS molecules on the particle surface by the non-ionic surfactant. Copolymer particles with hydrolysis rates between 40 and 90 percent were successfully separated.

Oukacine *et al.* [183] analyzed polystyrene/poly methacrylic acid (MAA) latexes of similar sizes, but with different acid contents. Similar to the work of Anik *et al.* [177] the latexes were stabilized with SLS. Uncoated fused-silica capillaries were used. The nonionic surfactant (Brij 35) was found to replace the anionic surfactant adsorbed on the particle surface. This resulted in an increase of the surface-charge density with increasing MAA content, opposite to when no surfactant was added to the electrolyte. A change in surface charge density is observed above and below the critical micelle concentration (CMC) of Brij 35. The electrophoretic mobilities of the Brij 35-modified latexes were measured using CE, and were found to increase with increasing MAA content. Finally, Riley *et al.* [184] reported a method for size-based separation of polystyrene particles with various surface modifications. Carboxylate particles of 0.2, 0.5, 1.0 and 3.0 μm were baseline separated. Also, 1.0 μm sized amino, carboxylate and sulfate modifications could be separated, but electrostatic interactions between the carboxylate-functionalized and amino-functionalized particles were observed.

Table 1.8: Selected CE applications

Analyte	Capillary	Background electrolyte	Detection	Ref
Polystyrene nanoparticles	Fused silica, 50 µm	5.0 mM Na2HPO4, 1 mM NaOH, pH 10.7	UV @ 225 / 254 nm	[174]
Functionalized polystyrene particles	Fused silica, 50 µm	10 mM phosphate buffer, pH 7.4	UV @ 225 nm	[175]
Carboxylate / sulfate modified polystyrene nanoparticles	Fused silica, 75 µm	5-12 mM phosphate buffer, pH 6.6,7.2, 8.5, and 10.7	UV @ 254 nm	[176]
Amidine particles	Fused silica, 75 µm	2 / 100 mM borate buffer, pH 8.4	UV @ 214 nm	[178]
Carboxylate-modified polystyrene particles,	Fused silica, 75 µm	2 / 100 mM borate buffer, pH 8.4	UV @ 214 nm	[178]
PMMA microspheres	Fused silica, 75 µm	2 mM borate buffer, pH 8.4	UV @ 214 nm	[178]
Acrylic-styrene copolymer latexes	Fused silica, 75 µm	5 mM phosphate buffer, pH 9.0	UV @ 214 nm	[179]
Polystyrene nanoparticles	Fused silica, 50 µm	50 mM tris buffer, pH 9.2	UV @ 254 / 520 nm	[182]
Gold nanoparticles	Fused silica, 50 µm	50 mM tris buffer, pH 9.2	UV @ 254 / 520 nm	[182]
Core-shell styrene-acrylic particles (PS-co-PEA/AA)	Fused silica, 100 µm	5-50 mM borate buffer, pH 6.0 – 10.1	UV @ 194 nm	[177]
Polystyrene-methacrylic acid copolymer latexes	Fused silica, 50 µm	5-50 mM borate buffer pH 9.2, brij 35 (0-0.22 mM)	UV @ 193 nm	[183]
Functionalized polystyrene particles	Fused silica, 75 µm	5 mM tris, 50 mM glycine, pH 7.75	UV @ 214 nm	[184]

1.6 Scope of the thesis

The research chapters in this thesis deal with various chromatographic methods which have been developed for the separation- and detection of acid-functional polymers. As adding acid functionality is the most frequently used mechanism to stabilize water-borne polymers, understanding of the polymer microstructure with respect to such functional groups is critical. The possibilities for polymer characterization techniques that are specifically tailored towards this functionality are limited. The approaches developed and described in this thesis expand the possibilities for the characterization of acid-functional polymers, providing an alternative to conventional polymer-characterization techniques. These characterization approaches are new and they provide unique information on the incorporation of acid-functional monomers in complex polymers.

Pyrolysis of polymers bearing functionalities with active hydrogens (such as carboxylic acids) results in thermal rearrangements of these functional groups. Essentially all information regarding these groups is lost in the pyrolysis process. Chapter 2 describes the selective derivatization of carboxylic-acid groups in water-borne polymer systems, based on a reaction with phenacylbromide. The resulting derivatized polymers could be characterized by pyrolysis-gas chromatography (PyGC), and the presence of the derivatized acid monomer could be clearly established.

In Chapter 3, the derivatization protocol established in Chapter 2 was applied to determine the heterogeneity of carboxylic-acid functionalization of polymers as a function of molecular weight. This analysis was performed using size-exclusion chromatography coupled with both refractive-index detection and ultraviolet-absorbance detection. The latter was used as a concentration detector for the UV-active phenacyl groups bonded to the carboxylic acid functionalities.

Specific chromatographic separation of carboxylic acid-functional polymers is described in Chapter 4. This separation was established by employing non-aqueous ion-exchange chromatography with N-methylpyrrolidone as mobile phase. This is a polar aprotic solvent capable of dissolving polymers, while still enabling ion dissociation. The latter aspect is essential to perform ion-exchange chromatography. The developed approach showed specific separation based solely on the number of incorporated acid groups. The retention behavior was compared to that of traditional interaction-LC approaches.

An alternative separation method was established using capillary electrophoresis (Chapter 5), separating analytes based on charge/size ratio. High-pH background

electrolytes were shown to yield a separation based on acid content for polymers with comparable molar mass. However, these conditions were found to be detrimental to the fused-silica capillary. Carboxylate anions in the background electrolyte were shown to specifically coordinate with the carboxylic-acid functionality in the polymers. It was shown that both background electrolytes yielded essentially the same information on the polymer microstructure from a carboxylic-acid point of view.

Chapter 6 describes the coupling of the non-aqueous ion-exchange chromatography approach developed in Chapter 4 with size exclusion chromatography in on-line two-dimensional liquid chromatography. The coupling of these orthogonal separation methods provided more detailed information regarding the polymer microstructure and several stages of the polymerization process could be identified with the obtained information.

References

1. C. Jiao, L. Sun, Q. Shao, J. Song, Q. Hu, N. Naik, Z. Guo, Advances in Waterborne Acrylic Resins: Synthesis Principle, Modification Strategies, and Their Applications, ACS Omega 6(4) (2021) 2443-2449. https://doi.org/10.1021/acsomega.0c05593.
2. M.L. Nobel, E. Mendes, S.J. Picken, Acrylic-based nanocomposite resins for coating applications, Journal of Applied Polymer Science 104(4) (2007) 2146-2156. https://doi.org/10.1002/app.24318.
3. P.A. Gupta, H. Bhayani, S.K. Pramanik, A.C. Rao, S.P. Deshmukh, Cost effective approach of acrylic resin based flooring applications, Construction and Building Materials 79 (2015) 48-55. https://doi.org/10.1016/j.conbuildmat.2014.12.047.
4. F.E. Golling, R. Pires, A. Hecking, J. Weikard, F. Richter, K. Danielmeier, D. Dijkstra, Polyurethanes for coatings and adhesives – chemistry and applications, Polymer International 68(5) (2018) 848-855. https://doi.org/10.1002/pi.5665.
5. Y. Liu, F. Li, I. van Casteren, R. Tennebroe, P.R. Lang, Self-, co-organisation behaviour and encapsulation efficiency of waterborne polyurethane pre-polymers, Colloids and Surfaces A: Physicochemical and Engineering Aspects 544 (2018) 165-171. https://doi.org/10.1016/j.colsurfa.2018.01.052.
6. A. Noreen, K.M. Zia, M. Zuber, S. Tabasum, M.J. Saif, Recent trends in environmentally friendly water-borne polyurethane coatings: A review, Korean Journal of Chemical Engineering 33(2) (2015) 388-400. https://doi.org/10.1007/s11814-015-0241-5.
7. K.L. A.M. van Herk, Advances in Polymer Science, Hybrid Latex Particles, Springer, 2010. https://doi.org/ 10.1007/978-3-642-16060-8.
8. O. Bayer, Das Di-lsocyanat-Polyadditionsverfahren (Polyurethane), ANGEWANDTE CHEMIE 9(59) (1947) 257-288.
9. L. Ugarte, A. Saralegi, R. Fernández, L. Martín, M.A. Corcuera, A. Eceiza, Flexible polyurethane foams based on 100% renewably sourced polyols, Industrial Crops and Products 62 (2014) 545-551. https://doi.org/10.1016/j.indcrop.2014.09.028.
10. J. Saunders, S. Steingiser, P. Gemeinhardt, A. Morecroft, E. Hardy, Properties of Flexible Urethane Foams, Industrial & Engineering Chemistry Chemical & Engineering Data Series 3(1) (2002) 153-161. https://doi.org/10.1021/i460003a030.
11. S. El Khezraji, S. Thakur, M. Raihane, M.A. Lopez-Manchado, L. Belachemi, R. Verdejo, M. Lahcini, Use of Novel Non-Toxic Bismuth Catalyst for the Preparation of Flexible Polyurethane Foam, Polymers (Basel) 13(24) (2021). https://doi.org/10.3390/polym13244460.
12. R. Tennebroek, I. van der Hoeven-van Casteren, R. Swaans, S. van der Slot, P.J.M. Stals, B. Tuijtelaars, C. Koning, Water-based polyurethane dispersions, Polymer International 68(5) (2018) 832-842. https://doi.org/10.1002/pi.5627.
13. A. Overbeek, Polymer heterogeneity in waterborne coatings, Journal of Coatings Technology and Research 7(1) (2009) 1-21. https://doi.org/10.1007/s11998-009-9201-5.
14. F. Xu, B. Qian, Z. Hu, W. Chen, Z. Zhuang, B. Zhu, H. Zhang, K. Zhu, A Novel Route to Emulsifier-free, Waterborne Hydroxyl Functional Polyacrylate with Low VOC Level and its Application in 2K-WPU Coatings, Journal of Macromolecular Science, Part A 50(5) (2013) 555-561. https://doi.org/10.1080/10601325.2013.781465.

15. J. Xu, Y. Jiang, T. Zhang, Y. Dai, D. Yang, F. Qiu, Z. Yu, P. Yang, Synthesis of UV-curing waterborne polyurethane-acrylate coating and its photopolymerization kinetics using FT-IR and photo-DSC methods, Progress in Organic Coatings 122 (2018) 10-18. https://doi.org/10.1016/j.porgcoat.2018.05.008.

16. C.G. Koukiotis, M.M. Karabela, I.D. Sideridou, Mechanical properties of films of latexes based on copolymers BA/MMA/DAAM and BA/MMA/VEOVA-10/DAAM and the corresponding self-crosslinked copolymers using the adipic acid dihydrazide as crosslinking agent, Progress in Organic Coatings 75(1-2) (2012) 106-115. https://doi.org/10.1016/j.porgcoat.2012.04.004.

17. R.S. Gurney, A. Morse, E. Siband, D. Dupin, S.P. Armes, J.L. Keddie, Mechanical properties of a waterborne pressure-sensitive adhesive with a percolating poly(acrylic acid)-based diblock copolymer network: effect of pH, J Colloid Interface Sci 448 (2015) 8-16. https://doi.org/10.1016/j.jcis.2015.01.074.

18. J. Richard, J. Maquet, Dynamic micromechanical investigations into particle/particle interfaces in latex films, Polymer 33(19) (1992) 4164-4173. https://doi.org/10.1016/0032-3861(92)90622-4.

19. J. Bullermann, S. Friebel, T. Salthammer, R. Spohnholz, Novel polyurethane dispersions based on renewable raw materials—Stability studies by variations of DMPA content and degree of neutralisation, Progress in Organic Coatings 76(4) (2013) 609-615. https://doi.org/10.1016/j.porgcoat.2012.11.011.

20. G.N. Manvi, R.N. Jagtap, Effect of DMPA Content of Polyurethane Dispersion on Coating Properties, Journal of Dispersion Science and Technology 31(10) (2010) 1376-1382. https://doi.org/10.1080/01932690903269776.

21. K.R.M. Vidts, B. Dervaux, F.E. Du Prez, Block, blocky gradient and random copolymers of 2-ethylhexyl acrylate and acrylic acid by atom transfer radical polymerization, Polymer 47(17) (2006) 6028-6037. https://doi.org/10.1016/j.polymer.2006.06.044.

22. C.A. Sanders, S.R. George, G.A. Deeter, J.D. Campbell, B. Reck, M.F. Cunningham, Amphiphilic Block-Random Copolymers: Self-Folding Behavior and Stabilizers in Emulsion Polymerization, Macromolecules 52(12) (2019) 4510-4519. https://doi.org/10.1021/acs.macromol.9b00519.

23. N. Zoco, L.L.d. Arbina, J.R. Leiza, J.M. Asua, G. Arzamendi, Molecular Weight Development in EmulsionCopolymerization ofn-Butyl Acrylate and Styrene, Journal of Applied Polymer Science 87 (2003) 1918-1926. https://doi.org/10.1002/app.11521.

24. I. Marquez, F. Alarcia, J.I. Velasco, Synthesis and Properties of Water-Based Acrylic Adhesives with a Variable Ratio of 2-Ethylhexyl Acrylate and n-Butyl Acrylate for Application in Glass Bottle Labels, Polymers (Basel) 12(2) (2020). https://doi.org/10.3390/polym12020428.

25. S. Upadhyaya, A. Konwar, D. Chowdhury, N.S. Sarma, High-performance water-borne fluorescent acrylic-based adhesive: synthesis and application, RSC Advances 10(43) (2020) 25408-25417. https://doi.org/10.1039/d0ra03782f.

26. Z. Peng, Z. Zhou, Q. Feng, Y. Zheng, Q. Yang, X. Liu, Synthesis and performance application of self-crosslinking water-borne epoxy resin for cementing, Journal of Applied Polymer Science 138(45) (2021) 51351. https://doi.org/10.1002/app.51351.

27. L. Yang, Z. Xie, Z. Li, Studies on acrylate copolymer soap-free waterborne coatings crosslinked by metal ions, Journal of Applied Polymer Science 74 (1999) 91-96. https://doi.org/10.1002/(SICI)1097-4628(19991003)74:1<91::AID-APP10>3.0.CO;2-Q.

28. F. Malz, J.H. Arndt, J. Balko, B. Barton, T. Busse, D. Imhof, R. Pfaendner, K. Rode, R. Brull, Analysis of the molecular heterogeneity of poly(lactic acid)/poly(butylene succinate-co-adipate) blends by hyphenating size exclusion chromatography with nuclear magnetic resonance and infrared spectroscopy,J Chromatogr A 1638 (2021) 461819.https://doi.org/10.1016/j.chroma.2020.461819.
29. P.J.C.H. Cools, F. Maesen, B. Klumperman, A.M. van Herk, A.L. German, Determination of the chemical composition distribution of copolymers of styrene and butadiene by gradient polymer elution chromatography, Journal of Chromatography A 736(1-2) (1996) 125-130. https://doi.org/10.1016/0021-9673(95)01369-5.
30. F. Fitzpatrick, B. Staal, P. Schoenmakers, Molar mass distributions by gradient liquid chromatography: predicting and tailoring selectivity, J Chromatogr A 1065(2) (2005) 219-29. https://doi.org/10.1016/j.chroma.2004.12.030.
31. D. Mekap, T. Macko, R. Brüll, R. Cong, A.W. deGroot, A. Parrott, P.J.C.H. Cools, W. Yau, Liquid chromatography at critical conditions of polyethylene, Polymer 54(21) (2013) 5518-5524. https://doi.org/10.1016/j.polymer.2013.08.040.
32. A.M. Caltabiano, J.P. Foley, H.G. Barth, Size exclusion chromatography of synthetic polymers and biopolymers on common reversed phase and hydrophilic interaction chromatography columns, J Chromatogr A 1437 (2016) 74-87. https://doi.org/10.1016/j.chroma.2016.01.055.
33. E.S.P. Bouvier, S.M. Koza, Advances in size-exclusion separations of proteins and polymers by UHPLC, TrAC Trends in Analytical Chemistry 63 (2014) 85-94. https://doi.org/10.1016/j.trac.2014.08.002.
34. H.G. Barth, C. Jackson, B.E. Boyes, Size Exclusion Chromatography, Analytical Chemistry 66(12) (2002) 595-620. https://doi.org/10.1021/ac00084a022.
35. R.R. Burgess, A brief practical review of size exclusion chromatography: Rules of thumb, limitations, and troubleshooting, Protein Expr Purif 150 (2018) 81-85. https://doi.org/10.1016/j.pep.2018.05.007.
36. D.C. Harris, Quantitative Chemical Analysis, 9th Edition ed., Macmillan Learning2015.
37. D. Held, P. Kilz, Size-exclusion chromatography as a useful tool for the assessment of polymer quality and determination of macromolecular properties, Chemistry Teacher International 3(2) (2021) 77-103. https://doi.org/10.1515/cti-2020-0024.
38. H.J.A. Philipsen, B. Klumperman, A.M. van Herk, A.L. German, Critical retention behaviour of polymers a study on the influence of some practical parameters, Journal of Chromatography A 727(1) (1996) 13-25. https://doi.org/10.1016/0021-9673(95)01074-2.
39. E. Uliyanchenko, S. van der Wal, P.J. Schoenmakers, Challenges in polymer analysis by liquid chromatography, Polymer Chemistry 3(9) (2012) 2313. https://doi.org/10.1039/c2py20274c.
40. H.G.B. Sadao Mori, Size Exclusion Chromatography, Springer laboratories2010.
41. M. Potschka, Universal Calibration of Gel Permeation Chromatography and Determination of Molecular Shape in Solution Analytical Biochemistry 162 (1986) 47-64. https://doi.org/doi:10.1016/0003-2697(87)90009-1.
42. T.C. Ward, Molecular Weight and Molecular Weight Distributions in Synthetic Polymers, Journal of Chemical Education 58(11) (1981) 867-879. https://doi.org/10.1021/ed058p867,.
43. J.E. Puskas, Y. Chen, K. Kulbaba, G. Kaszas, Comparison of the molecular weight and size measurement of polyisobutylenes by size exclusion chromatography/multi-angle laser light scattering and viscometry, Journal of Polymer Science Part A: Polymer Chemistry 44(5) (2006) 1777-1783. https://doi.org/10.1002/pola.21272.

44. A.M. Striegel, Longitudinal diffusion in size-exclusion chromatography: a stop-flow size-exclusion chromatography study, J Chromatogr A 932(1-2) (2001) 21-31. https://doi.org/10.1016/s0021-9673(01)01214-6.

45. H. Pasch, M.I. Malik, Advanced Separation Techniques for Polyolefins, Springer2014.

46. D.A. Skoog, F.J. Holler, S.R. Crouch, Principles of Instrumental Analysis, 7 ed., Cengage Learning, Inc2017.

47. N.D. Hann, Effects of Lithium Bromide on the Gel-Permeation Chromatography of Polyester-Based Polyurethanes in Dimethylformamide, Journal of Polymer Science 15 (1977) 1331-1339. https://doi.org/10.1002/pol.1977.170150604.

48. S.Moyses,A.Ginzburg,The chromatography of poly(phenylene ether) on a porous graphitic carbon sorbent, J Chromatogr A 1468 (2016) 136-142. https://doi.org/10.1016/j.chroma.2016.09.034.

49. B.W. Pirok, P. Breuer, S.J. Hoppe, M. Chitty, E. Welch, T. Farkas, S. van der Wal, R. Peters, P.J. Schoenmakers, Size-exclusion chromatography using core-shell particles, J Chromatogr A 1486 (2017) 96-102. https://doi.org/10.1016/j.chroma.2016.12.015.

50. R. Hayes, A. Ahmed, T. Edge, H. Zhang, Core-shell particles: preparation, fundamentals and applications in high performance liquid chromatography, J Chromatogr A 1357 (2014) 36-52. https://doi.org/10.1016/j.chroma.2014.05.010.

51. M.R. Schure, R.E. Moran, Size exclusion chromatography with superficially porous particles, J Chromatogr A 1480 (2017) 11-19. https://doi.org/10.1016/j.chroma.2016.12.016.

52. A. Kurganov, E. Victorova, A. Kanateva, Monolithic capillary columns based on pentaerythritol acrylates for molecular-size-based separations of synthetic polymers, J Sep Sci 38(13) (2015) 2223-8. https://doi.org/10.1002/jssc.201500211.

53. F. Svec, Y. Lv, Advances and recent trends in the field of monolithic columns for chromatography, Anal Chem 87(1) (2015) 250-73. https://doi.org/10.1021/ac504059c.

54. A. Chojnacka, K. Kempe, H.C. van de Ven, C. Englert, R. Hoogenboom, U.S. Schubert, H.G. Janssen, P. Schoenmakers, Molar mass, chemical-composition, and functionality-type distributions of poly(2-oxazoline)s revealed by a variety of separation techniques, J Chromatogr A 1265 (2012) 123-32. https://doi.org/10.1016/j.chroma.2012.09.080.

55. E. Uliyanchenko, P.J. Schoenmakers, S. van der Wal, Fast and efficient size-based separations of polymers using ultra-high-pressure liquid chromatography, J Chromatogr A 1218(11) (2011) 1509-18. https://doi.org/10.1016/j.chroma.2011.01.053.

56. E. Uliyanchenko, S. van der Wal, P.J. Schoenmakers, Deformation and degradation of polymers in ultra-high-pressure liquid chromatography, J Chromatogr A 1218(39) (2011) 6930-42. https://doi.org/10.1016/j.chroma.2011.08.014.

57. A. Agirre, J.I. Santos, J.R. Leiza, Toward Understanding the Architecture (Branching and MWD) of Crosslinked Acrylic Latexes, Macromolecular Chemistry and Physics 214(5) (2013) 589-598. https://doi.org/10.1002/macp.201200482.

58. C.N. Pomeranz, S.V. Olesik, Separation of poly-3-hydroxyvalerate-co-3-hydroxybutyrate through gradient polymer elution chromatography, J Chromatogr A 1218(44) (2011) 7943-7. https://doi.org/10.1016/j.chroma.2011.08.065.

59. K.A. Barrera-Rivera, R. Vera-Graziano, E. López-Sánchez, A. Martinez-Richa, Characterization of chain dimensions of poly(ε-caprolactone) diols in THF by size-exclusion chromatography coupled with multi-angle light scattering (SEC-MALS), Journal of Polymer Research 22(3) (2015). https://doi.org/10.1007/s10965-015-0672-z.

60. C. Schmid, S. Weidner, J. Falkenhagen, C. Barner-Kowollik, In-Depth LCCC-(GELC)-SEC Characterization of ABA Block Copolymers Generated by a Mechanistic Switch from RAFT to ROP, Macromolecules 45(1) (2011) 87-99. https://doi.org/10.1021/ma2022452.

61. B.W.J. Pirok, N. Abdulhussain, T. Aalbers, B. Wouters, R.A.H. Peters, P.J. Schoenmakers, Nanoparticle Analysis by Online Comprehensive Two-Dimensional Liquid Chromatography combining Hydrodynamic Chromatography and Size-Exclusion Chromatography with Intermediate Sample Transformation, Anal Chem 89(17) (2017) 9167-9174. https://doi.org/10.1021/acs.analchem.7b01906.

62. S.W. Li, H.E. Park, J.M. Dealy, M. Maric, H. Lee, K. Im, H. Choi, T. Chang, M.S. Rahman, J. Mays, Detecting Structural Polydispersity in Branched Polybutadienes, Macromolecules 44(2) (2010) 208-214. https://doi.org/10.1021/ma101803h.

63. H. Maier, F. Malz, W. Radke, Characterization of the Chemical Composition Distribution of Poly(n-butyl acrylate-stat-acrylic acid)s, Macromolecular Chemistry and Physics 216(2) (2015) 228-234. https://doi.org/10.1002/macp.201400399.

64. F. Samperi, S. Battiato, C. Puglisi, A. Scamporrino, V. Ambrogi, L. Ascione, C. Carfagna, Combined techniques for the characterization of linear-hyperbranched hybrid poly(butylene adipate) copolymers, Journal of Polymer Science Part A: Polymer Chemistry 49(16) (2011) 3615-3630. https://doi.org/10.1002/pola.24800.

65. T. Masuda, Y. Matsuki, T. Shimoda, Characterization of polydihydrosilane by SEC-MALLS and viscometry, Polymer 53(14) (2012) 2973-2978. https://doi.org/10.1016/j.polymer.2012.04.046.

66. E.M. Reingruber, A. Chojnacka, E. Jellema, B. de Bruin, W. Buchberger, P.J. Schoenmakers, Chromatographic examination of the chemical composition and sequence distribution of copolymers from ethyl and benzyl diazoacetate, J Chromatogr A 1255 (2012) 259-66. https://doi.org/10.1016/j.chroma.2012.02.059.

67. T.H. Mourey, L.A. Slater, R.C. Galipo, D.L. Janes, R.E. Moody, Size-exclusion chromatography of poly(ethylene 2,6-naphthalate), J Chromatogr A 1256 (2012) 129-35. https://doi.org/10.1016/j.chroma.2012.07.067.

68. M. Irfan, A.M. Bhayo, S.G. Musharraf, M.I. Malik, Chromatographic characterization of amphiphilic di- and tri-block copolymers of poly(ethylene oxide) and poly(epsilon-caprolactone), J Sep Sci 41(17) (2018) 3352-3359. https://doi.org/10.1002/jssc.201800465.

69. G. Liu, X. Qiu, S. Bo, X. Ji, Chain Conformation and Local Rigidity of Isomerized Polyimides in Dimethyl Formamide by Size Exclusion Chromatography Coupled with Multi-Detectors, Chromatographia 75(1-2) (2011) 7-15. https://doi.org/10.1007/s10337-011-2159-3.

70. J.E. Puskas, W. Burchard, A.J. Heidenreich, L.D. Santos, Analysis of branched polymers by high resolution multidetector size exclusion chromatography: Separation of the effects of branching and molecular weight distribution, Journal of Polymer Science Part A: Polymer Chemistry 50(1) (2012) 70-79. https://doi.org/10.1002/pola.24982.

71. A.M. Artem Badasyan, Irena Kralj Cigić, Tim Bencik, Matjaz Valant Polymer nanoparticle sizes from dynamic light scattering and size exclusion chromatography: the case study of polysilanes, Soft Matter 14 (2018) 4735--4740. https://doi.org/doi:10.1039/c8sm00780b.

72. R.S. Braido, L.E.P. Borges, J.C. Pinto, Chemical recycling of crosslinked poly(methyl methacrylate) and characterization of polymers produced with the recycled monomer, Journal of Analytical and Applied Pyrolysis 132 (2018) 47-55. https://doi.org/10.1016/j.jaap.2018.03.017.

73. B. Durner, T. Ehmann, F.-M. Matysik, High-resolution polymer high performance liquid chromatography: optimization of the saw tooth gradient profile for various stationary phases and separations on preparative scale, Analytical Methods 11(39) (2019) 4960-4968. https://doi.org/10.1039/c9ay00689c.

74. S. Moyses, J. Ness, G. Papakonstantopoulos, 2-D chromatography applied to the study of block copolymers synthesized by nitroxide-mediated controlled free-radical seeded emulsion polymerization, J Sep Sci 33(22) (2010) 3511-8. https://doi.org/10.1002/jssc.201000524.

75. R. Leinweber, P. Montag, J. Preis, W. Radke, Characterization of poly(methyl methacrylate)-graft-poly(styrene)s using various chromatographic techniques, J Chromatogr A 1473 (2016) 76-82. https://doi.org/10.1016/j.chroma.2016.10.046.

76. R.A. García, B. Coto, M.-T. Expósito, I. Suarez, A. Fernández-Fernández, S. Caveda, Molecular characterization of polypropylene heterophasic copolymers by fractionation techniques, Macromolecular Research 19(8) (2011) 778-788. https://doi.org/10.1007/s13233-011-0811-2.

77. S.V. Orski, L.A. Kassekert, W.S. Farrell, G.A. Kenlaw, M.A. Hillmyer, K.L. Beers, Design and Characterization of Model Linear Low-Density Polyethylenes (LLDPEs) by Multidetector Size Exclusion Chromatography, Macromolecules 53(7) (2020) 2344-2353. https://doi.org/10.1021/acs.macromol.9b02623.

78. S. Ahn, H. Lee, S. Lee, T. Chang, Characterization of Branched Polymers by Comprehensive Two-Dimensional Liquid Chromatography with Triple Detection, Macromolecules 45(8) (2012) 3550-3556. https://doi.org/10.1021/ma2021985.

79. A. Korolev, E. Victorova, T. Ibragimov, A. Kanatyeva, A. Kurganov, Monolithic columns with optimized pore structure for molecular size-based separations of synthetic polymers, J Sep Sci 35(8) (2012) 957-63. https://doi.org/10.1002/jssc.201101042.

80. D. Murima, H. Pasch, Comprehensive branching analysis of star-shaped polystyrenes using a liquid chromatography-based approach, Anal Bioanal Chem 411(20) (2019) 5063-5078. https://doi.org/10.1007/s00216-019-01846-7.

81. S. Moyses, Two-dimensional chromatography applied to the study of the thermo-oxidative degradation of poly(styrene-b-butadiene) star block copolymers, J Sep Sci 35(14) (2012) 1741-7. https://doi.org/10.1002/jssc.201200174.

82. T.G. Wright, H. Pfukwa, H. Pasch, Advanced analytical methods for the structure elucidation of polystyrene-b-poly(n-butyl acrylate) block copolymers prepared by reverse iodine transfer polymerisation, Anal Chim Acta 892 (2015) 183-94. https://doi.org/10.1016/j.aca.2015.08.005.

83. S. Krüger, F. Krahl, K.-F. Arndt, Random cross-linked poly(styrene-co-maleic anhydride): Characterization of cross-linking intermediates by size exclusion chromatography, European Polymer Journal 46(5) (2010) 1040-1048. https://doi.org/10.1016/j.eurpolymj.2010.01.024.

84. C. Schmid, J. Falkenhagen, T.F. Beskers, L.-T.T. Nguyen, M. Wilhelm, F.E. Du Prez, C. Barner-Kowollik, Multi-Block Polyurethanes via RAFT End-Group Switching and Their Characterization by Advanced Hyphenated Techniques, Macromolecules 45(16) (2012) 6353-6362. https://doi.org/10.1021/ma301117k.

85. G. Vancoillie, M. Vergaelen, R. Hoogenboom, Ultra-high performance size-exclusion chromatography in polar solvents, J Chromatogr A 1478 (2016) 43-49. https://doi.org/10.1016/j.chroma.2016.11.034.

86. M. Janco, J.N.t. Alexander, E.S. Bouvier, D. Morrison, Ultra-high performance size-exclusion chromatography of synthetic polymers: demonstration of capability, J Sep Sci 36(17) (2013) 2718-27. https://doi.org/10.1002/jssc.201300444.

87. A.M. Caltabiano, J.P. Foley, A.M. Striegel, Aqueous size-exclusion chromatography of polyelectrolytes on reversed-phase and hydrophilic interaction chromatography columns, J Chromatogr A 1532 (2018) 161-174. https://doi.org/10.1016/j.chroma.2017.12.007.

88. S.M. Rowland, A.M. Striegel, Characterization of copolymers and blends by quintuple-detector size-exclusion chromatography, Anal Chem 84(11) (2012) 4812-20. https://doi.org/10.1021/ac3003775.

89. J. Zataray, A. Agirre, P. Carretero, L. Meabe, J.C. de la Cal, J.R. Leiza, Characterization of poly (N-vinyl formamide) by size exclusion chromatography-multiangle light scattering and asymmetric-flow field-flow fractionation-multiangle light scattering, Journal of Applied Polymer Science 132(34) (2015) n/a-n/a. https://doi.org/10.1002/app.42434.

90. V.D. Krasikov, N.I. Gorshkov, I.I. Malakhova, O.S. Egorova, Y.V. Pokhvoshchev, Size-exclusion liquid chromatography of poly(N-vinylformamide)s in aqueous solutions, Journal of Analytical Chemistry 72(4) (2017) 460-467. https://doi.org/10.1134/s1061934817040050.

91. I. Lacík, M. Stach, P. Kasák, V. Semak, L. Uhelská, A. Chovancová, G. Reinhold, P. Kilz, G. Delaittre, B. Charleux, I. Chaduc, F. D'Agosto, M. Lansalot, M. Gaborieau, P. Castignolles, R.G. Gilbert, Z. Szablan, C. Barner-Kowollik, P. Hesse, M. Buback, SEC Analysis of Poly(Acrylic Acid) and Poly(Methacrylic Acid), Macromolecular Chemistry and Physics 216(1) (2015) 23-37. https://doi.org/10.1002/macp.201400339.

92. P. Yang, W. Gao, J.E. Shulman, Y. Chen, Separation and identification of polymeric dispersants in detergents by two-dimensional liquid chromatography, J Chromatogr A 1566 (2018) 111-117. https://doi.org/10.1016/j.chroma.2018.06.063.

93. A.B. Jean-François Cotte, Agathe Sordoillet, Isabelle Jaudinaud, Véronique Chambon, Philippe Talaga, Determination of molecular size parameters and quantification of polyacrylic acid by high performance size-exclusion chromatography with triple detection, Anal Bioanal Chem. 409 (2017) 2083–2092. https://doi.org/DOI 10.1007/s00216-016-0155-z.

94. Z. Zhao, Q. Li, X. Ji, R. Dimova, R. Lipowsky, Y. Liu, Molar mass fractionation in aqueous two-phase polymer solutions of dextran and poly(ethylene glycol), J Chromatogr A 1452 (2016) 107-15. https://doi.org/10.1016/j.chroma.2016.04.075.

95. M. Schollenberger, W. Radke, SEC-Gradients, an alternative approach to polymer gradient chromatography: 1. Proof of the concept, Polymer 52(15) (2011) 3259-3262. https://doi.org/10.1016/j.polymer.2011.05.047.

96. M. Schollenberger, W. Radke, Size exclusion chromatography-gradients, an alternative approach to polymer gradient chromatography: 2. Separation of poly(meth)acrylates using a size exclusion chromatography-solvent/non-solvent gradient, J Chromatogr A 1218(43) (2011) 7828-31. https://doi.org/10.1016/j.chroma.2011.08.090.

97. H. Maier, F. Malz, G. Reinhold, W. Radke, SEC Gradients: An Alternative Approach to Polymer Gradient Chromatography. Separation of Poly(methyl methacrylate-stat-methacrylic acid) by Chemical Composition, Macromolecules 46(3) (2013) 1119-1123. https://doi.org/10.1021/ma3023553.

98. A.M. Striegel, W.W. Yau, J.J. Kirkland, D.D. Bly, Modern Size Exclusion Liquid Chromatography - Practice of Gel Permeation and Gel Filtration Chromatography, 2 ed., Wiley2009.

99. A.M. Striegel, A.K. Brewer, Hydrodynamic chromatography, Annu Rev Anal Chem (Palo Alto Calif) 5 (2012) 15-34. https://doi.org/10.1146/annurev-anchem-062011-143107.

100. R.P. Dias, Size Fractionation by Slalom Chromatography and Hydrodynamic Chromatography, Recent Patents on Engineering 2 (2009) 95-103.https://doi.org/10.2174/187221208784705251.

101. H. Small, F.L. Saunders, J. Solc, Hydrodynamic chromatography A new approach to particle size analysis, Advances in Colloid and Interface Science 6(4) (1976) 237-266. https://doi.org/10.1016/0001-8686(76)85004-x.

102. B.W.J. Pirok, N. Abdulhussain, T. Brooijmans, T. Nabuurs, J. de Bont, M.A.J. Schellekens, R.A.H. Peters, P.J. Schoenmakers, Analysis of charged acrylic particles by on-line comprehensive two-dimensional liquid chromatography and automated data-processing, Anal Chim Acta 1054 (2019) 184-192. https://doi.org/10.1016/j.aca.2018.12.059.

103. A.K. Brewer, A.M. Striegel, Hydrodynamic chromatography of latex blends, Journal of Separation Science 33(22) (2010) 3555-3563. https://doi.org/10.1002/jssc.201000565.

104. J. Op de Beeck, W. De Malsche, J. Vangelooven, H. Gardeniers, G. Desmet, Hydrodynamic chromatography of polystyrene microparticles in micropillar array columns, J Chromatogr A 1217(39) (2010) 6077-84. https://doi.org/10.1016/j.chroma.2010.07.031.

105. R. Edam, S. Eeltink, D.J. Vanhoutte, W.T. Kok, P.J. Schoenmakers, Hydrodynamic chromatography of macromolecules using polymer monolithic columns, J Chromatogr A 1218(48) (2011) 8638-45. https://doi.org/10.1016/j.chroma.2011.10.006.

106. A.A. Korolev, E.N. Viktorova, V.A. Orekhov, A.A. Kurganov, Unusually high efficiency of the separation of polymers by hydrodynamic chromatography on hollow capillary columns, Russian Journal of Physical Chemistry A 86(7) (2012) 1161-1164. https://doi.org/10.1134/s0036024412070096.

107. A.A. Korolev, E.N. Viktorova, A.A. Kurganov, Hydrodynamic Chromatography of Polystyrenes on Hollow Capillary Columns, Russian Journal of Physical Chemistry A 92(11) (2018) 2320-2324. https://doi.org/10.1134/s0036024418110195.

108. S. Lee, H. Choi, T. Chang, B. Staal, Two-Dimensional Liquid Chromatography Analysis of Polystyrene/Polybutadiene Block Copolymers, Anal Chem 90(10) (2018) 6259-6266. https://doi.org/10.1021/acs.analchem.8b00913.

109. P.C. Bert Klumperman, Harry Philipsen, Wim Staal, A qualitative study to the influence of molar mass on retention in gradient polymer elution chromatography (GPEC), Macromol. Symp. 110 (1996) 1-13. https://doi.org/DOI: 10.1002/MASY.19961100102.

110. W.J. Staal, P. Cools, A.M. Van Herk, A.L. German, Monitoring of Originated Polymer in Pure Monomer with Gradient Polymer Elution Chromatography (GPEC)®, Journal of Liquid Chromatography 17(14-15) (1994) 3191-3199. https://doi.org/10.1080/10826079408013198.

111. H.J.A. Philipsen, M.R. de Cooker, H.A. Claessens, B. Klumperman, A.L. German, Characterization of low-molar-mass polymers by gradient polymer elution chromatography II. Solubility effects in the analysis of polyester resins under reversed-phase conditions, Journal of Chromatography A 761(1-2) (1997) 147-162. https://doi.org/10.1016/s0021-9673(96)00807-2.

112. A.M. Striegel, Method development in interaction polymer chromatography, Trends Analyt Chem 130 (2020). https://doi.org/10.1016/j.trac.2020.115990.

113. H.J.A. Philipsen, B. Klumperman, A.L. German, Characterization of low-molar-mass polymers by gradient polymer elution chromatography I. Practical parameters and applications of the analysis of polyester resins under reversed phase conditions, Journal of Chromatography A 746 (1996) 211-224. https://doi.org/10.1016/S0021-9673(96)00807-2.

114. H.J.A. Philipsen, B. Klumperman, F.A.M. Leerrnakers, F.P.C. Wubb, A.L. German, Molar Mass Effects in Reversed-Phase Gradient Polymer-Elution Chromatography of Oligomers, Chromatographia 55 (2002) 533-540. https://doi.org/10.1007/BF02492898.

115. H.J.A. Philipsen, Determination of chemical composition distributions in synthetic polymers, Journal of Chromatography A 1037 (2003) 329-350. https://doi.org/10.1016/j.chroma.2003.12.047.

116. H.J.A. Philipsen, H.A. Claessens, M. Bosman, B. Klumperman, A.L. German, Normal phase gradient polymer elution chromatography of polyester resins, Chromatographia 48(9-10) (1998) 623-630. https://doi.org/10.1007/bf02467591.

117. X. Jiang, A.v.d. Horst, P.J. Schoenmakers, Breakthrough of polymers in interactive liquid chromatography, Journal of Chromatography A 982 (2002) 55-68. https://doi.org/10.1016/S0021-9673(02)01483-8.

118. X. Jiang, A. van der Horst, V. Lima, P.J. Schoenmakers, Comprehensive two-dimensional liquid chromatography for the characterization of functional acrylate polymers, J Chromatogr A 1076(1-2) (2005) 51-61. https://doi.org/10.1016/j.chroma.2005.03.135.

119. B. Durner, B. Scherer, T. Ehmann, F.-M. Matysik, Comparison of Molar Mass Determination of Poly(dimethylsiloxanes) by Size Exclusion Chromatography and High-Resolution Polymer High Performance Liquid Chromatography Based on a Sawtooth Gradient, ACS Applied Polymer Materials 1(9) (2019) 2388-2397. https://doi.org/10.1021/acsapm.9b00483.

120. M. Al Samman, W. Radke, A. Khalyavina, A. Lederer, Retention Behavior of Linear, Branched, and Hyperbranched Polyesters in Interaction Liquid Chromatography, Macromolecules 43(7) (2010) 3215-3220. https://doi.org/10.1021/ma902537e.

121. M. Al Samman, W. Radke, Two-dimensional chromatographic separation of branched polyesters according to degree of branching and molar mass, Polymer 99 (2016) 734-740. https://doi.org/10.1016/j.polymer.2016.07.077.

122. G. Cheng, J. Cullen, C.S. Wu, Separation of statistical poly[(N-vinyl pyrrolidone)-co-(vinyl acetate)]s by reversed-phase gradient liquid chromatography, J Chromatogr A 1218(2) (2011) 237-41. https://doi.org/10.1016/j.chroma.2010.11.017.

123. W. Radke, The retention behavior of diblock copolymers in gradient chromatography; Similarities of diblock copolymers and homopolymers, J Chromatogr A 1593 (2019) 17-23. https://doi.org/10.1016/j.chroma.2019.01.043.

124. L.R. Hutchings, S. Agostini, M.E. Oti, J. Keth, Normal-phase (temperature gradient) interaction chromatography – A powerful tool for the characterisation of high molecular weight chain-end functionalised polymers, European Polymer Journal 73 (2015) 105-115. https://doi.org/10.1016/j.eurpolymj.2015.10.010.

125. C.I. De Matteis, D.A. Simpson, M.R. Euerby, P.N. Shaw, D.A. Barrett, Chromatographic retention behaviour of monosubstituted benzene derivatives on porous graphitic carbon and octadecyl-bonded silica studied using molecular modelling and quantitative structure-retention relationships, J Chromatogr A 1229 (2012) 95-106. https://doi.org/10.1016/j.chroma.2011.12.090.

126. C. West, C. Elfakir, M. Lafosse, Porous graphitic carbon: a versatile stationary phase for liquid chromatography, J Chromatogr A 1217(19) (2010) 3201-16. https://doi.org/10.1016/j.chroma.2009.09.052.

127. T.E. Bapiro, F.M. Richards, D.I. Jodrell, Understanding the Complexity of Porous Graphitic Carbon (PGC) Chromatography: Modulation of Mobile-Stationary Phase Interactions Overcomes Loss of Retention and Reduces Variability, Anal Chem 88(12) (2016) 6190-4. https://doi.org/10.1021/acs.analchem.6b01167.

128. J. Crazes, Encyclopedia of Chromatography Third edition, ed., CRC Press, 2009.

129. R. kaliszan, Structure and Retention in Chromatography (Chromatography: Principles & Practice Series), 1st edition ed.1997.

130. T. Teutenberg, K. Hollebekkers, S. Wiese, A. Boergers, Temperature and pH-stability of commercial stationary phases, J Sep Sci 32(9) (2009) 1262-74. https://doi.org/10.1002/jssc.200800712.

131. E. Maksimova, E. Vlakh, E. Sinitsyna, T. Tennikova, HPLC analysis of synthetic polymers on short monolithic columns, J Sep Sci 36(23) (2013) 3741-9. https://doi.org/10.1002/jssc.201300852.

132. E. Uliyanchenko, P.J. Cools, S. van der Wal, P.J. Schoenmakers, Comprehensive two-dimensional ultrahigh-pressure liquid chromatography for separations of polymers, Anal Chem 84(18) (2012) 7802-9. https://doi.org/10.1021/ac3011582.

133. K.J. Hilbert, R.K. Marcus, Separation of water-soluble polymers using capillary-channeled polymer fiber stationary phases, J Sep Sci 33(22) (2010) 3571-7. https://doi.org/10.1002/jssc.201000519.

134. G. Ramis-Ramos, M.C. García-Álvarez-Coque, Liquid Chromatography: Chapter 10. Solvent Selection in Liquid Chromatography, Elsevier Science2013.

135. T. Li, S. Strunz, W. Radke, R. Klein, T. Hofe, Chromatographic separation of polylactides by stereochemical composition, Polymer 52(1) (2011) 40-45. https://doi.org/10.1016/j.polymer.2010.10.056.

136. R. Chitta, T. Macko, R. Brüll, C. Boisson, E. Cossoul, O. Boyron, Characterization of the Chemical Composition Distribution of Ethylene/1-Alkene Copolymers with HPLC and CRYSTAF-Comparison of Results, Macromolecular Chemistry and Physics 216(7) (2015) 721-732. https://doi.org/10.1002/macp.201400490.

137. T. Macko, J.-H. Arndt, R. Brüll, HPLC Separation of Ethylene–Vinyl Acetate Copolymers According to Chemical Composition, Chromatographia 82(4) (2019) 725-732. https://doi.org/10.1007/s10337-019-03697-x.

138. T. Macko, R. Brüll, Y. Wang, B. Coto, I. Suarez, Characterization of ethylene-propylene copolymers with high-temperature gradient adsorption liquid chromatography and CRYSTAF, Journal of Applied Polymer Science 122(5) (2011) 3211-3217. https://doi.org/10.1002/app.34432.

139. B. Durner, T. Ehmann, F.M. Matysik, High-resolution polymer high performance liquid chromatography: Application of a saw tooth gradient for the separation of various polymers, J Chromatogr A 1587 (2019) 88-100. https://doi.org/10.1016/j.chroma.2018.11.075.

140. H.M. Rakotondravao, N. Ishizuka, K. Sakakibara, R. Wada, E. Ichihashi, R. Takahashi, T. Takai, J.I. Horiuchi, Y. Kumada, Characterization of a macroporous epoxy-polymer based resin for the ion-exchange chromatography of therapeutic proteins, J Chromatogr A 1656 (2021) 462503. https://doi.org/10.1016/j.chroma.2021.462503.

141. J. Liang, G. Fieg, S. Jakobtorweihen, Ion-Exchange Adsorption of Proteins: Experiments and Molecular Dynamics Simulations, Chemie Ingenieur Technik 87(7) (2015) 903-909. https://doi.org/10.1002/cite.201400095.

142. J.A. Hogenboom, P. D'Incecco, F. Fuselli, L. Pellegrino, Ion-Exchange Chromatographic Method for the Determination of the Free Amino Acid Composition of Cheese and Other Dairy Products: an Inter-Laboratory Validation Study, Food Analytical Methods 10(9) (2017) 3137-3148. https://doi.org/10.1007/s12161-017-0876-4.

143. Y. Mengerink, R. Peters, S. van der Wal, H.A. Claessens, C.A. Cramers, Endgroup-based separation and quantitation of polyamide-6,6 by means of critical chromatography, J Chromatogr A 949(1-2) (2002) 337-49. https://doi.org/10.1016/s0021-9673(02)00030-4.

144. A.I. Abdulahad, C.Y. Ryu, Liquid chromatography at the critical condition: Thermodynamic significance and influence of pore size, Journal of Polymer Science Part B: Polymer Physics 47(24) (2009) 2533-2540. https://doi.org/10.1002/polb.21862.

145. D. Berek, Critical assessment of "critical" liquid chromatography of block copolymers, J Sep Sci 39(1) (2016) 93-101. https://doi.org/10.1002/jssc.201500956.

146. S.V. Olesik, Liquid chromatography at the critical condition, Anal Bioanal Chem (378) (2004) 43-45. https://doi.org/DOI 10.1007/s00216-003-2319-x.

147. M.I. Malik, Critical parameters of liquid chromatography at critical conditions in context of poloxamers: Pore diameter, mobile phase composition, temperature and gradients, J Chromatogr A 1609 (2020) 460440. https://doi.org/10.1016/j.chroma.2019.460440.

148. P. Sinha, M. Grabowsky, M.I. Malik, G.W. Harding, H. Pasch, Characterization of Polystyrene-block-Polyethylene Oxide Diblock Copolymers and Blends of Homopolymers by Liquid Chromatography at Critical Conditions (LCCC), Macromolecular Symposia 313-314(1) (2012) 162-169. https://doi.org/10.1002/masy.201250318.

149. N. Apel, E. Uliyanchenko, S. Moyses, S. Rommens, C. Wold, T. Macko, R. Brull, Separation of Branched Poly(bisphenol A carbonate) Structures by Solvent Gradient at Near-Critical Conditions and Two-Dimensional Liquid Chromatography, Anal Chem 90(8) (2018) 5422-5429. https://doi.org/10.1021/acs.analchem.8b00618.

150. Y.Z. Wei, Y.F. Chu, E. Uliyanchenko, P.J. Schoenmakers, R.X. Zhuo, X.L. Jiang, Separation and characterization of benzaldehyde-functional polyethylene glycols by liquid chromatography under critical conditions, Polymer Chemistry 7(48) (2016) 7506-7513. https://doi.org/10.1039/c6py01653g.

151. P. Sinha, G.W. Harding, K. Maiko, W. Hiller, H. Pasch, Comprehensive two-dimensional liquid chromatography for the separation of protonated and deuterated polystyrene, J Chromatogr A 1265 (2012) 95-104. https://doi.org/10.1016/j.chroma.2012.09.088.

152. N. Apel, E. Uliyanchenko, S. Moyses, S. Rommens, C. Wold, T. Macko, K. Rode, R. Brull, Selective chromatographic separation of polycarbonate according to hydroxyl end-groups using a porous graphitic carbon column, J Chromatogr A 1488 (2017) 77-84. https://doi.org/10.1016/j.chroma.2017.01.075.

153. B.W.J. Pirok, D.R. Stoll, P.J. Schoenmakers, Recent Developments in Two-Dimensional Liquid Chromatography: Fundamental Improvements for Practical Applications, Anal Chem 91(1) (2019) 240-263. https://doi.org/10.1021/acs.analchem.8b04841.

154. K. Im, H.-w. Park, S. Lee, T. Chang, Two-dimensional liquid chromatography analysis of synthetic polymers using fast size exclusion chromatography at high column temperature, Journal of Chromatography A 1216(21) (2009) 4606-4610. https://doi.org/10.1016/j.chroma.2009.03.072.

155. K. Im, Y. Kim, T. Chang, K. Lee, N. Choi, Separation of branched polystyrene by comprehensive two-dimensional liquid chromatography, J Chromatogr A 1103(2) (2006) 235-42. https://doi.org/10.1016/j.chroma.2005.11.050.

156. E. Venema, P.d. Leeuw, J.C. Kraak, H. Poppe, R. Tijssen, Polymer characterization using on-line coupling of thermal field flow fractionation and hydrodynamic chromatography, Journal of Chromatography A 765 (1997) 135-144. https://doi.org/10.1016/S0021-9673(96)00924-7.

157. S. Fanali, P.R. Haddad, C.F. Poole, M.-L. Riekkola, Liquid Chromatography: Fundamentals and Instrumentation, 2 ed.2017. https://doi.org/10.1016/b978-0-12-805393-5.09996-6.

158. F. Bedani, P.J. Schoenmakers, H.G. Janssen, Theories to support method development in comprehensive two-dimensional liquid chromatography--a review, J Sep Sci 35(14) (2012) 1697-711. https://doi.org/10.1002/jssc.201200070.

159. J.A. Raust, A. Brull, C. Moire, C. Farcet, H. Pasch, Two-dimensional chromatography of complex polymers 6. Method development for (meth)acrylate-based copolymers, J Chromatogr A 1203(2) (2008) 207-16. https://doi.org/10.1016/j.chroma.2008.07.067.

160. S. Moyses, 2-D chromatography with optimized size exclusion chromatography resolution and multi-angle light scattering coupling, J Sep Sci 33(10) (2010) 1480-6. https://doi.org/10.1002/jssc.201000009.

161. I.K. Ventouri, S. Loeber, G.W. Somsen, P.J. Schoenmakers, A. Astefanei, Field-flow fractionation for molecular-interaction studies of labile and complex systems: A critical review, Anal Chim Acta 1193 (2022) 339396. https://doi.org/10.1016/j.aca.2021.339396.

162. A.M. Striegel, Multi-detector hydrodynamic chromatography of colloids: following in Hamish Small's footsteps, Heliyon 7(4) (2021) e06691. https://doi.org/10.1016/j.heliyon.2021.e06691.

163. A. Barquero, A. Agirre, J.R. Leiza, Asymmetric-Flow Field-Flow Fractionation of complex waterborne polymer dispersions: Effect of the concentration of water in the measurement of molar mass distributions, J Chromatogr A 1652 (2021) 462363. https://doi.org/10.1016/j.chroma.2021.462363.

164. R.J. Vonk, A.F. Gargano, E. Davydova, H.L. Dekker, S. Eeltink, L.J. de Koning, P.J. Schoenmakers, Comprehensive Two-Dimensional Liquid Chromatography with Stationary-Phase-Assisted Modulation Coupled to High-Resolution Mass Spectrometry Applied to Proteome Analysis of Saccharomyces cerevisiae, Anal Chem 87(10) (2015) 5387-94. https://doi.org/10.1021/acs.analchem.5b00708.

165. D.R. Stoll, K. Shoykhet, P. Petersson, S. Buckenmaier, Active Solvent Modulation: A Valve-Based Approach To Improve Separation Compatibility in Two-Dimensional Liquid Chromatography, Anal Chem 89(17) (2017) 9260-9267. https://doi.org/10.1021/acs.analchem.7b02046.

166. M. Pursch, A. Wegener, S. Buckenmaier, Evaluation of active solvent modulation to enhance two-dimensional liquid chromatography for target analysis in polymeric matrices, J Chromatogr A 1562 (2018) 78-86. https://doi.org/10.1016/j.chroma.2018.05.059.

167. P.S. Eselem Bungu, K. Pflug, H. Pasch, Combination of preparative and two-dimensional chromatographic fractionation with thermal analysis for the branching analysis of polyethylene, Polymer Chemistry 9(22) (2018) 3142-3157. https://doi.org/10.1039/c8py00522b.

168. D. Mekap, T. Macko, R. Brüll, R. Cong, W. deGroot, A. Parrott, W. Yau, Multiple-Injection Method in High-Temperature Two-Dimensional Liquid Chromatography (2D HT-LC), Macromolecular Chemistry and Physics 215(4) (2014) 314-319. https://doi.org/10.1002/macp.201300649.

169. A. Roy, M.D. Miller, D.M. Meunier, A.W. deGroot, W.L. Winniford, F.A. Van Damme, R.J. Pell, J.W. Lyons, Development of Comprehensive Two-Dimensional High Temperature Liquid Chromatography × Gel Permeation Chromatography for Characterization of Polyolefins, Macromolecules 43(8) (2010) 3710-3720. https://doi.org/10.1021/ma100010e.

170. T.M. Sampat Singh Bhati, Robert Brüll Quantification of identical and unique segments in ethylene-propylene copolymers using two dimensional liquid chromatography with infra-red detection, Polyolefins Journal 3(2) (2016) 119-133. https://doi.org/10.22063/poj.2016.1323.

171. D. Lee, C.L. Shan, D.M. Meunier, J.W. Lyons, R. Cong, A.W. deGroot, Toward absolute chemical composition distribution measurement of polyolefins by high-temperature liquid chromatography hyphenated with infrared absorbance and light scattering detectors, Anal Chem 86(17) (2014) 8649-56. https://doi.org/10.1021/ac501477a.

172. A. Ginzburg, T. Macko, V. Dolle, R. Brüll, Characterization of polyolefins by comprehensive high-temperature two-dimensional liquid chromatography (HT 2D-LC), European Polymer Journal 47(3) (2011) 319-329. https://doi.org/10.1016/j.eurpolymj.2010.11.016.

173. D. Lee, M.D. Miller, D.M. Meunier, J.W. Lyons, J.M. Bonner, R.J. Pell, C.L. Shan, T. Huang, Development of high temperature comprehensive two-dimensional liquid chromatography hyphenated with infrared and light scattering detectors for characterization of chemical composition and molecular weight heterogeneities in polyolefin copolymers, J Chromatogr A 1218(40) (2011) 7173-9. https://doi.org/10.1016/j.chroma.2011.08.036.

174. B.B. VanOrman, G.L. McIntire, Analytical separation of polystyrene nanospheres by capillary electrophoresis, Journal of Microcolumn Separations 1(6) (1989) 289-293. https://doi.org/10.1002/mcs.1220010607.

175. B.B. VanOrman, G.L. McIntire, Determination of the Electrophoretic Mobility of Polystyrene Particles by Capillary Electrophoresis, Journal of Microcolumn separations 6 (1994) 591-594. https://doi.org/10.1002/mcs.1220060610.

176. H.K. Jones, N.E. Ballou, Separations of Chemicafly Different Particles by Capillary Electrophoresis, Analytical Chemistry 62 (1990) 2484-2490. https://doi.org/10.1021/ac00221a014.

177. N. Anik, M. Airiau, M.P. Labeau, W. Bzducha, H. Cottet, Characterization of copolymer latexes by capillary electrophoresis, Langmuir 26(3) (2010) 1700-6. https://doi.org/10.1021/la902661m.

178. J. J. R. Glynn, B.M. Belongia, R.G. Arnold, K. L. Ogden, J.C. Baygents, Capillary Electrophoresis Measurements of Electrophoretic Mobility for Colloidal Particles of Biological Interest, Applied and Environmental Biology (1998) 2572-2577. https://doi.org/10.1128/aem.64.7.2572-2577.1998.

179. G. Vanhoenacker, L. Goris, P. Sandra, Capillary zone electrophoresis for the characterization of latex particles, Electrophoresis 22 (2001) 2490-2494. https://doi.org/10.1002/1522-2683(200107)22:12<2490::AID-ELPS2490>3.0.CO;2-B.

180. M.S. Sergey P. Radko, Andreas Chrambach, Size-Dependent Electrophoretic Migration and Separation of Liposomes by Capillary Zone Electrophoresis in Electrolyte Solutions of Various Ionic Strengths, Anal. Chem 72 (2000) 5955-5960. https://doi.org/doi:10.1021/ac000661e.

181. A. Fichtner, A. Jalil, U. Pyell, Determination of the Exact Particle Radius Distribution for Silica Nanoparticles via Capillary Electrophoresis and Modeling the Electrophoretic Mobility with a Modified Analytic Approximation, Langmuir 33(9) (2017) 2325-2339. https://doi.org/10.1021/acs.langmuir.6b04543.

182. W.-M. Hwang, C.-Y. Lee, D.W. Boo, J.-G. Choi, Separation of Nanoparticles in Different Sizes and Compositions by Capillary Electrophoresis, Bull. Korean Chem. Soc. 24(5) (2003). https://doi.org/10.5012/bkcs.2003.24.5.684.

183. F. Oukacine, A. Morel, H. Cottet, Characterization of carboxylated nanolatexes by capillary electrophoresis, Langmuir 27(7) (2011) 4040-7. https://doi.org/10.1021/la1048562.

184. K.R. Riley, S. Liu, G. Yu, K. Libby, R. Cubicciotti, C.L. Colyer, Using capillary electrophoresis to characterize polymeric particles, J Chromatogr A 1463 (2016) 169-75. https://doi.org/10.1016/j.chroma.2016.08.017.

CHAPTER 2

Acid monomer analysis in waterborne polymer systems by targeted labeling of carboxylic acid functionality, followed by pyrolysis – gas chromatography

Ton Brooijmans, Remco Okhuijsen, Ingrid Burggraaf-Oerlemans, Peter Schoenmakers, Ron Peters

J. Chromatogr. A (2018), https://doi.org/10.1016/j.chroma.2018.05.024.

Abstract

Pyrolysis – gas chromatography – (PyGC) is a common method to analyze the composition of natural and synthetic resins. The analysis of acid functionality in, for example, waterborne polyacrylates and polyurethanes polymers has proven to be difficult due to solubility issues, inter- and intramolecular interaction effects, lack of detectability in chromatographic analysis, and lack of thermal stability. Conventional analytical techniques, such as PyGC, cannot be used for the direct detection and identification of acidic monomers, due to thermal rearrangements that take place during pyrolysis. To circumvent this, the carboxylic acid groups are protected prior to thermal treatment by reaction with 2-bromoacetophenone. Reaction conditions are investigated and optimized wrt. conversion measurements. The approach is applied to waterborne polyacryalates and the results are discussed. This approach enables identification and (semi)quantitative analysis of different acid functionalities in waterborne polymers by PyGC.

2.1 Introduction

The variety of applications of waterborne polymeric dispersions is broad and ranges from uses in paints, adhesives, paper coatings, floor polishes, printing inks and textile finishes to pharmaceuticals, including sustained- and controlled-release formulations. The application range for these waterborne polymers will continue to expand, due to stricter requirements for emissions of organic compounds, such as used in traditional solvent-borne coating systems.

The variation in the chemical composition of synthetic resins can be very large, with combinations of monomers tailored to specific application needs. Most often resins are prepared using functional monomers, such as hydroxy-, ketone- and carboxylic-acid-functional groups. These monomers allow specific applications, such as cross-linking in two-component systems or stabilization of polymer particles in aqueous environments. In waterborne polyacrylate dispersions, the two most common acidic compounds that are incorporated in the acrylic polymer backbone are acrylic acid (AA) and methacrylic acid (MAA), while waterborne polyurethane dispersions are created using dimethylolpropanoic acid (DMPA) monomer.

To determine the overall chemical polymer composition, several approaches can be used. Nuclear-magnetic-resonance (NMR) spectroscopy and Fourier-transform infrared (FTIR) spectroscopy are frequently used to obtain an average composition of the polymer. FTIR is not applicable to detect acid content in polymers, because the sensitivity is limited and because the technique cannot discern between acrylic and methacrylic acids. NMR may in principle be used, but it is a complex technique that requires significant expertise to obtain the required information.

Besides NMR and FT-IR, a common way to determine the average chemical composition is pyrolysis gas chromatography (PyGC). With this technique the polymer is heated to elevated temperatures (500-1400°C) in the presence of an inert gas, which results in thermal decomposition of the polymer chains [1-5]. Performing pyrolysis on polymers results in the formation of reproducible decomposition products, which are characteristic for the original (co)polymer composition. The volatile fraction of these decomposition products are chromatographically separated by gas chromatography (GC) and detected by mass spectrometry (MS) and/or flame-ionization detection (FID). PyGC-FID/MS analysis of polyacrylates allows determination of the original starting monomeric units as decomposition products. Especially, non-functional (meth)acrylic ester groups show reproducible thermal decomposition to their original monomeric structures [3], such

as methyl-methacrylate (MMA), methyl acrylate (MA), butyl methacrylate (BMA), butyl acrylate (BA), 2-ethylhexyl acrylate (2-EHA) and 2-ethylhexyl methacrylate (2-EHMA). In general, due to inter- and intramolecular thermal rearrangements, the polymer composition has an influence on the nature of the observed thermal decomposition products. Specifically, in the case of (meth)acrylic esters it is known that side products (alcohol and alkene degradation products) are formed during pyrolysis (Figure 2.1). The resulting volatile products of the pyrolysis of (meth)acrylic esters can be identified and quantified with reasonable accuracy, due to the high precision of the analysis.

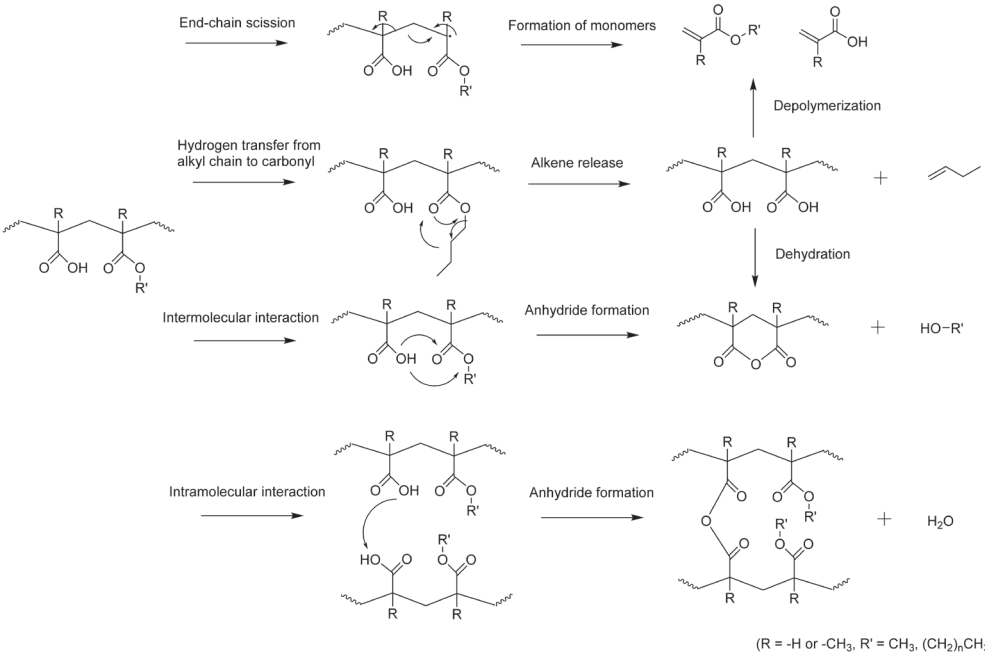

Figure 2.1. Schematic pyrolysis reaction pathway for a copolymer of (meth)acrylic acid and alkyl (meth) acrylate. Alkene release was exemplified using R'= $(CH_2)_3CH_3$.

However, in PyGC analysis of polyacrylates containing acid-functional acrylic monomers, the accuracy (recovery) and precision (repeatability) of the acid-functional monomers are often not satisfactory [6]. Moreover, it is not possible to distinguish between the presence of incorporated acrylic- or methacrylic acid in acrylic copolymers, because thermal decomposition of other (meth)acrylic monomer esters (such as BA or BMA) results in the formation of (meth)acrylic acid [5]. The selectivity of direct pyrolysis of (meth)acrylates is, therefore, limited.

At pyrolysis temperatures, acrylic acid monomers segments may rearrange to anhydrides with the loss of water (Figure 2.1). The anhydrides formed are thermally unstable, undergoing decarboxylation and subsequent reactions [6]. The resulting compounds are commonly non-volatile and cannot easily be related to the starting (meth)acrylic monomer.

Direct analysis of acid functionality with PyGC is, therefore, generally problematic to perform. Even if the incorporated (meth)acrylic acid is thermally decomposed to the intact monomer, difficulties will be encountered with both separation and detection. Common GC columns used in PyGC are not suitable for the analysis of carboxylic acids, as broad and asymmetrical peaks are typically observed. Due to the relatively low amount of carbon present in (meth)acrylic acid compared to other (meth)acrylic monomers, there is also a relatively low sensitivity in FID detection. The poor separation and detection of the (meth) acrylic acid monomers can be negated using pyrolysis-liquid chromatography (PyLC) as described by Van der Horst *et al.* [7]. Collecting the (meth)acrylate pyrolyzate in a cryogenic trap enables analysis with liquid chromatography (LC) combined with photodiode-array detection (PDA). The main advantage of using this type of setup is that detection is based on the molar response of the C=C carbon unsaturations in (meth)acrylic monomers. Another approach to improve the separation and detection of acrylic acids, has been described by Osete-Cortina *et al.* [8] and Van der Peyl *et al.* [9]. They show that the (meth)acrylic-acid degradation products from (meth)acrylic-ester monomers in pyrolysis can be reacted with a trimethylsilyl reagent to obtain better peak shapes for (meth)acrylic acid. Due to the fact that (meth)acrylic acid can also be present as a degradation product of (meth)acrylic esters, the direct pyrolysis in the presence of silylation reagents (or any other derivatization reagent used) is not representative for the acid type or total concentration of incorporated acid.

Both approaches described [7-9], focus on improvement of the separation and detection of (meth)acrylic pyrolyzates using direct pyrolysis of the sample, while the main problem in the pyrolytic characterization of (meth)acrylic resins is the formation of rearrangement products during the pyrolysis. A double-shot pyrolysis method, in which the reagent and solvent are evaporated first, followed by a pyrolysis step of the derivatized polymer residue deposited in the liner, yields a better representation of the type and amount of acid present, since no side reaction of pyrolytically degraded (meth) acrylic acid with derivatization reagent can occur.

Apart from trimethylsilylation using reagents such as BSTFA (N,O-bis(trimethylsilyl) acetamide) or MSTFA (N-methyl-N-(trimethylsilyl)trifluoroacetamide), other common derivatization reagents used in the small molecule analysis of carboxylic acids are chloroformates [10, 11] and bromo-acetophenone compounds [12, 13].

Derivatization of polymers prior to analysis may be a useful tool to obtain information which is not readily obtainable in another way, such as the incorporation of acid functionalities in acrylic polymers. Specifically, applying derivatization of specific functional groups in combination with chromatography and selective detection techniques, such as ultraviolet (UV) or fluorescence spectroscopy or MS, may yield valuable information on molecular architecture. The challenges for the derivatization of polymers include their limited solubility, possible steric hindrance and inter- and intramolecular hydrogen bonding. All these factors reduce the derivatization efficiency. Nevertheless, several approaches to derivatize polymer functionalities have been described. For instance, Thompson et al. derivatized polyacrylic acid with amines using 4-(4,6-dimethoxy-1,3,5-triazin-2-yl)-4-methylmorpholinium chloride (DMTMM) as the reagent [14]. This condensing agent was reported to efficiently activate carboxylic-acid groups [15, 16]. The resulting activated acid group can be displaced by using alcohols or amines, resulting in the formation of esters or amides, respectively. Broersen *et al*. described the analysis of primary-amine containing functional polymers by a pre-column derivatization with o-phthalic aldehyde in combination with SEC and fluorescence/UV detection [17]. The work done by Borisov *et al*. [18] focuses on MS applications using derivatization of polymers, including acylation of hydroxy-functional ethoxylates with phthalic anhydrides or 2-fluoro-1-methylpyridinium p-toluenesulfonate. Techniques used to characterize the materials were fast-atom-bombardment MS (FAB-MS), matrix-assisted laser-desorption/ionization MS (MALDI-MS) and time-of-flight secondary-ion MS (TOF-SIMS). Straessler *et al*. [19] described the determination of the carboxylic-end-group distribution of polybutadiene polymers based on activation of carboxylic acids with oxalyl chloride. The obtained acid chloride is very reactive towards alcohols and amines, resulting in ester or amide groups, respectively. Drawback of this reaction is the water-sensitivity of oxalyl chloride, which might hamper analysis of waterborne polymer systems. Similar water sensitivity is observed when using dimethylformamide dipropyl acetal as a propylation agent [20] and extensive drying of the sample is required prior to analysis. Flash pyrolyzation using tetramethylammonium hydroxide or tetramethylammonium acetate [21] is also a viable way of derivatizing polymers. However, products of the reaction of (meth)acrylic acid with tetramethyl ammonium hydroxide are methyl acrylate and methyl methacrylate, which are also common monomers encountered in acrylic polymers. Identical reasoning applies for the alternative reagent tetraethylammonium hydroxide, which would provide ethyl esters after reaction with (meth)acrylic acid. As (meth)acrylic acid and its methyl- or ethyl ester may both be used in the same polymer, the (m)ethylation reaction of (meth)acrylic acid with tetramethylammonium hydroxide is not selective.

In the present study, we have established a sample-preparation method, which – in combination with PyGC - is able to identify unambiguously the acid (as phenacyl ester) incorporated in the polymer backbone, without time-consuming sample-preparation steps, such as freeze-drying. (Meth)acrylate-ester degradation, yielding (meth)acrylic acid, was clearly discerned from the incorporated acid.

2.2 Experimental

2.2.1 Materials

Model acrylate emulsion polymers were synthesized using radical emulsion polymerization of methyl methacrylate (MMA, Sigma Aldrich), n-butyl acrylate (BA, Sigma Aldrich), n-butyl methacrylate (BMA, Sigma Aldrich) and acrylic or methacrylic acid (AA or MAA, Sigma Aldrich), as outlined in Table 2.1. Sodium lauryl sulphate (32% in water, VWR, Amsterdam, The Netherlands) was used as emulsifier and ammonium persulphate (Evonik, Marl, Germany) as initiator. The samples are dispersed in water to approximately 30% by weight. Ammonia (25% in water, VWR) was used in a stoichiometric equivalent of 0.7 to partly neutralize the acid groups.

Table 2.1. Model acrylate emulsion polymer compositions. Acid content is measured using titration with KOH (see Experimental section).

Polymer	Acrylic acid [%w/w]	Methacrylic acid [%w/w]	Methyl Methacrylate [%w/w]	Butyl Acrylate [%w/w]	Butyl Methacrylate [%w/w]	Solids [%w/w in H_2O]
MP1	2.7	-	48	25	25	29.6
MP2	11	-	40	25	25	28.9
MP3	21	-	30	25	25	28.1
MP4	-	2.9	48	25	25	29.7
MP5	-	12	40	25	25	29.4
MP6	-	22	30	25	25	28.7

N-Methylpyrrolidone (NMP, peptide synthesis grade) and tetrahydrofuran (THF, uLCMS grade) were purchased from Biosolve (Valkenswaard, The Netherlands). Triethylamine (TEA, 99.5%), hydrochloric acid (HCl, 37%), N-methylmorpholine (NMM, >99%), chloro-dimethoxytriazine (CDMT, >98%), ethyl chloroformate (ECF, >99%), propyl chloroformate (PCF, >99%), 3-nitrobenzyl chloroformate (NBCF, >96%), p-bromophenacyl bromide (pBPB, 99.8%), p-nitrophenacyl bromide (pNPB, >98%) and 2-bromoacetophenone (PB, 99%) were purchased from Sigma-Aldrich (Zwijndrecht, The Netherlands).

2.2.2 Instrumentation

PyGCMS analyzes were performed on a Thermo2000 GC equipped with a DSQ-I MS detector and a TraceGC FID (Interscience, Breda, The Netherlands). The system uses a Combipal autosampler (Interscience) and an OPTIC-4 GC injector (ATAS GL, Veldhoven, The Netherlands) to enable so-called "double-shot" pyrolysis analysis. The SGE column used was 30 m × 0.25 mm i.d., with a 5% phenyl/95% dimethylpolysiloxane stationary phase of 0.25 µm film thickness (VWR).

To determine volatiles in the "double-shot" analysis, 1 µl of sample was injected at 50°C into the GC injector, which was subsequently heated to 172°C at a rate of 20°C s-1. After reaching this temperature, the GC inlet was cooled down to 50°C in 8 min. The carrier-gas flow was 2 mL/min helium, while the split flow was kept at 15 mL/min. The oven was kept at 50°C for 0.5 min and then heated to 100°C at a rate of 5°C/min. After this step, the oven temperature was increased to 300°C at a rate of 22°C/min and kept at 300°C for 2 min. To protect the MS filament, the current was disabled for 3.5 minutes after injection. After determining the volatiles, the polymer has remained in the GC liner. The second shot was started by heating the OPTIC GC injector from 50°C to 550°C at a rate of 50°C s-1. This temperature was kept constant for 2 minutes, after which the injector was cooled down to 50°C. The column flow for the second shot was also 2 mL/min helium. The initial split flow was 50 mL/min, which was increased to 100 mL/min when the pyrolysis temperature of 550°C was reached. The oven-temperature program for the second shot was identical to that for the first shot.

Fast size-exclusion chromatography (SEC) was performed on a Waters (Etten-Leur, The Netherlands) Alliance 2695 system with a W410 differential-refractive-index (dRI) detector and a W2998 photo-diode-array (PDA) detector. The eluent was NMP with 0.01 M LiBr at 1 mL/min and a column temperature of 70°C. A 300 mm × 8 mm i.d. GRAM column (PSS, Mainz, Germany) was used, with 10 µm particle diameter and 100 Å pore diameter. A 50 mm × 8 mm i.d. GRAM guard column was used (10 µm particle diameter).

Acid titrations were performed using a Titrino instrument from Metrohm (Schiedam, The Netherlands). Samples were dissolved in THF (uLCMS grade, Biosolve), in a ratio of 1 to 50 by volume. The titration solvent is 0.1 M potassium hydroxide in methanol (VWR).

2.2.3 Procedures

DMTMM was prepared by reacting 1 equivalent of CDMT with 1.1 equivalent of NMM in THF, as described by Kunushima et al. CDMT and NMM are both soluble in THF, whereas

DMTMM forms a white precipitate, which is filtrated and dried under nitrogen flow prior to use in acid-activation experiments.

Acid-activation experiments using DMTMM were performed by diluting 200 mg of acid-functional polymer, with a known amount of incorporated acid, in 8 mL NMP. After dissolving the polymer, DMTMM was added to the solution in varying stoichiometric amounts). After 1 h at room temperature, benzylamine was added to the solution (also in varying stoichiometric amounts). Samples were precipitated through the addition of 8 mL H_2O. The precipitate was separated from the liquid phase, washed with water and dried in an oven at 70°C.

When using chloroformates as activating agents, the following procedure was used: 200 mg of acid-functional polymer, with a known amount of incorporated acid, was dissolved in 8 mL of THF. A catalyst was added (100 µL of TEA, NMM or pyridine in varying stoichiometric amounts) and alkylchloroformate was added. The reaction mixture was stirred for 1 h at room temperature prior to the addition of 1 mL of displacing alcohol.

Derivatization with phenacyl bromides was performed by dissolving 200 mg of acid-functional polymer, with a known amount of incorporated acid, in 8 mL NMP. Varying stoichiometric amounts of TEA were added to the solution as catalyst. Phenacyl bromide in varying stoichiometric amounts was dissolved in NMP and this solution was added to the polymer mixture. After reacting for 30 minutes, polymer was precipitated by the addition of 5 mL solution of 1% HCl in H_2O. Polymers were washed with water and methanol and dried in an oven at 70°C. Dried sample was redissolved in THF prior to PyGCMS analysis.

2.2.4 Quantification of monomers using the effective carbon number (ECN)

The area (A) of each component is divided by its theoretical ECN. Values are normalized to 100% by obtaining the sum of all corrected monomer areas , components which originate from the same base component (*e.g.* 1-butene from butyl acrylate) are summed to yield a single content value (φ_w). General formula of φ_w calculation is displayed below:

$$\varphi_w\, Monomer\ 1 = \frac{A_{Monomer\ 1} / ECN_{Monomer\ 1}}{\sum \left(\left(\frac{A_{Monomer\ 1}}{ECN_{Monomer\ 1}} \right) + \left(\frac{A_{Monomer\ 2}}{ECN_{Monomer\ 2}} \right) + \cdots \right)}$$

Methacrylic-acid content is calculated by dividing the observed FID area % of phenacyl methacrylate by the ECN of phenacyl methacrylate and multiplying this with the ECN of methacrylic acid. This is based on the assumption that 1-butene and 1-butanol are formed through thermal rearrangements from butyl acrylate (as depicted in Figure 2.1).

2.3 Results and discussion

PyGC analysis of underivatized polyacrylates provides information on the monomer composition. In the PyGCMS chromatograms (Figure 2.2) the non-acid functional monomers MMA, BA and BMA are clearly visible. No (meth)acrylic acid could be identified in both model polymeric systems MP2 and MP5 (compositions are depicted in Table 2.1). Due to the thermal rearrangements of other (meth)acrylic ester monomers outlined in the introduction in Figure 2.1, methacrylic acid is visible in the pyrogram in MP 2 (Table 2.1). Since there is no methacrylic acid used in the polymerization process of this sample, this could result in false positive identification of the acid type in a polymer. Furthermore, apart from a very minor difference in the intensity of the methacrylic-acid peak, no significant difference is observed between the pyrograms of MP 2 and 5.

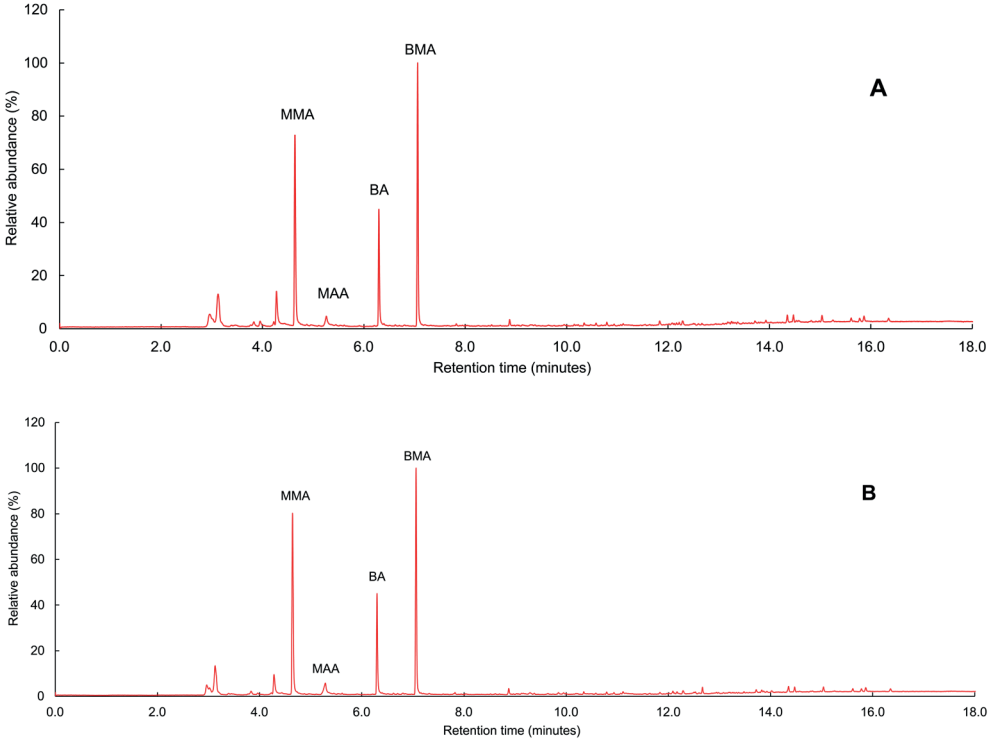

Figure 2.2. PyGCMS chromatograms of model polymers MP2, with an overall chemical composition of AA/MMA/BA/BMA (A) and MP5, with an overall chemical composition of MAA/MMA/BA/BMA (B) without sample derivatization.

2.3.1 DMTMM protocol

Functionalization of acid-functionality in acrylic copolymers was studied with several derivatization reagents. First, the model polyacrylate samples (Table 2.1) were derivatized using DMTMM activation. The transamidation of the activated ester was achieved with primary and secondary amines, according to the reaction scheme outlined in Figure 2.3. Several amines were used as transamidation reagents, including propylamine, butylamine and N,N-methylbenzylamine. Conversion was determined using acid titration. By measuring the acid number of derivatized polymers and dividing this by the starting acid number, conversion of acid can be calculated. After derivatization with the various amines, all samples showed a significant reduction of the acid functionality (as shown in Table 2.2 for benzylamine) by approximately 90%. PyGCMS analysis of the derivatized samples showed that only transamidation with benzylamine resulted in an additional peak in PyGCMS chromatograms (see Figure 2.4). Therefore, benzylamine was chosen for further research.

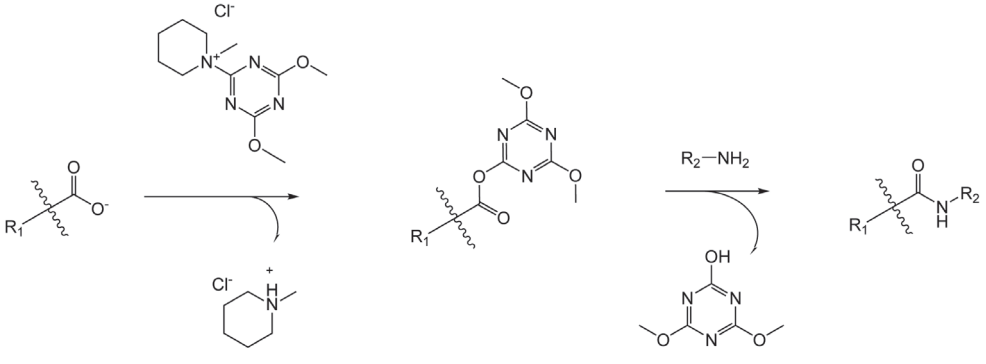

Figure 2.3. Activation of carboxylic-acid groups by DMTMM followed by amine displacement.

The above reaction protocol was performed with different equivalents of DMTMM and benzylamine. MP 2 (composed of 10% AA, 40% MMA, 25% BA, 25% BMA by weight) was used for these experiments. Based on titration, model polymer 2 has an acid number of 84 mg KOH/g sample, which corresponds with 11% (w/w) of AA. The acid conversions using different equivalents of DMTMM and benzylamine are given in Table 2.2.

Table 2.2. Conversion of acid-derivatization reaction with DMTMM activation.

Experiment	Equivalents DMTMM	Equivalents Benzylamine	Conversion [%]
1.	3	3	89.0
2. duplicate of 1.	3	3	88.5
3.	5	5	90.8
4. duplicate of 3.	5	5	91.0
5.	7	7	92.4
6. duplicate of 5.	7	7	90.5
7. triplo of 5.	7	7	91.5
8.	9	9	92.2
9. duplicate of 8.	9	9	91.2
10.	11	11	92.6
11. duplicate of 10.	11	11	91.4

Different amounts of reagent and displacing benzylamine were used. The use of higher relative ratios of reagents appeared to have a small positive effect on the conversion. In all cases approximately 90% the acid is converted to the benzylacrylamide derivate. If triazine-activated acid groups are still present in the titration mixture, the OH- ions in the methanolic KOH are likely to act as a nucleophilic agent, which results in the starting acid being re-formed (see Figure 2.4). This may explain the remaining carboxylic acid functionality.

Using the DMTMM/benzylamine derivatization protocol, it appears to be possible to discern the acid type in acrylate polymers by PyGCMS analysis. However, peak areas of the benzyl(meth)acrylamide are lower compared to the other acrylester monomers. Figure 2.4 shows pyrograms of model polymers after DMTMM activation and subsequent amine derivatization.

MMA, BA and BMA are detectable after pyrolysis, along with a not entirely convincing peak for N-benzylacrylamide or benzylmethacrylamide, indicated with an asterisk in Figure 2.4. There is a difference in the intensity of 1-butanol (pyrolysis reaction product of BA) in the two samples, which could not be explained. Several other peaks are visible at higher retention times, which were identified as dimeric structures from the acrylate monomers, and several components, which strongly resemble triazine derivatives, such as trimethoxytriazine. The presence of these components suggests that side products are not removed efficiently from the polymer precipitate or that transamidation of the triazine activation group by the amine is incomplete. Apart from these side products, the polymer bound N-benzyl(meth)acrylamide is also prone to dehydration and

cyclisation reactions, due to the presence of an active hydrogen on the amide bond. The use of alcohols to displace the triazine activating group did not result in detectable ester formation. Since quantitative conversion of carboxylic-acid functional groups and subsequent pyrolysis are likely not feasible using this method, activation with DMTMM was abandoned.

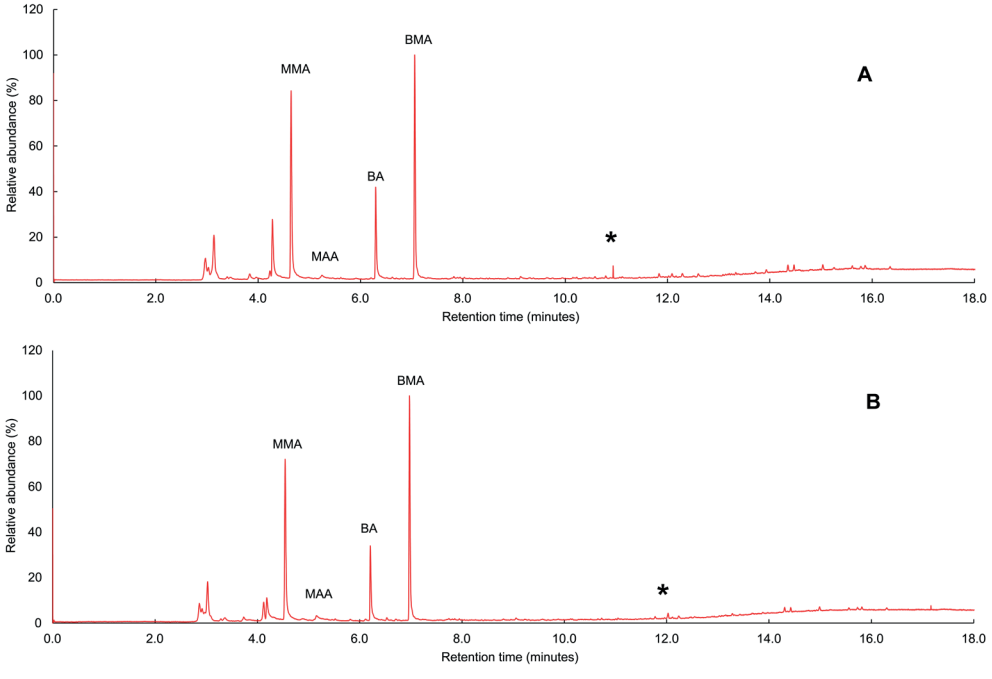

Figure 2.4. PyGCMS chromatograms of model polymer MP2, with an overall chemical composition of AA/MMA/BA/BMA polymer (A) and MP5, with an overall chemcial composition of MAA/MMA/BA/BMA (B) after activation with DMTMM and reaction with benzylamine. The benzyl(meth)acrylamide (derivate of acrylic and methacrylic acid) is indicated with an asterisk.

2.3.2 Chloroformate procedure

Polyacrylate samples were derivatized using chloroformate activation followed by reaction of the formed anhydride with alcohol (see Figure 2.5). The esters created from (meth)acrylic acid do not have an active proton and will behave similarly in PyGCMS to the already present (meth)acrylic esters such as MMA and BA.

A common side reaction is the decarboxylation of the mixed anhydride. This results in formation of an ester with the alkyl group from the chloroformate and the release of

carbon dioxide. In the experiments with polymeric carboxylic acids it was found that very small amounts of such esters are formed.

A limited conversion of carboxylic acids to esters was found for all variations tested. These variations included the use of different solvents (NMP, THF, acetonitrile, dimethylsulfoxide), different basic catalysts (TEA, tris-2-ethylhexylamine, pyridine), different chloroformates (ethyl chloroformate, propyl chloroformate), different reaction temperatures (0, 25, 50°C), different alcohol reactants (methanol, ethanol, n-propanol) and reaction protocols (adding sample to chloroformate reagent or adding chloroformate reagent to the sample).

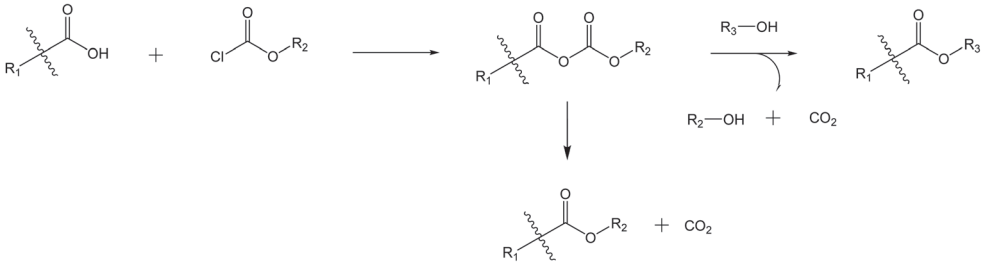

Figure 2.5. Reaction of carboxylic acid with chloroformate. The mixed anhydride that results from this reaction can be displaced by alcohols, forming esters with the release of carbon dioxide and an alcohol corresponding to the alkyl group from the chloroformate.

As with the DMTMM procedure, it was possible to discern between the acid type in polymers, but quantitative analysis was not possible. Possible causes of this limited reactivity are the steric hindrance of the active center of the mixed anhydride and stabilization of the mixed anhydride by the attached polymer chain.

2.3.3 Phenacylbromide procedure

Functionalization of acid-functionality in acrylic copolymers was focused on the use of several acetophenone-type molecules. The reagents used were phenacyl bromide, *p*-bromophenacyl bromide and *p*-nitrophenacyl bromide. These phenacyl bromide compounds were chosen so as to provide sufficient volatility of the monomer-acid reaction products. The reaction of acetophenone reagents with polymer bound (meth) acrylic acid molecules is shown in Figure 2.6.

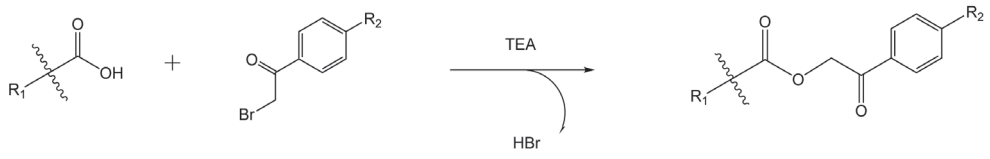

Figure 2.6. Reaction of carboxylic acid with acetophenone reagent. TEA is used as catalyst / neutralizing agent.

The chosen acetophenone reagents have different side groups (R_2). The PyGC-MS chromatograms of the derivatized model polymers MP2 and MP5 are shown in Figure 2.7 (TEA and acetophenone used in 10-fold excess).

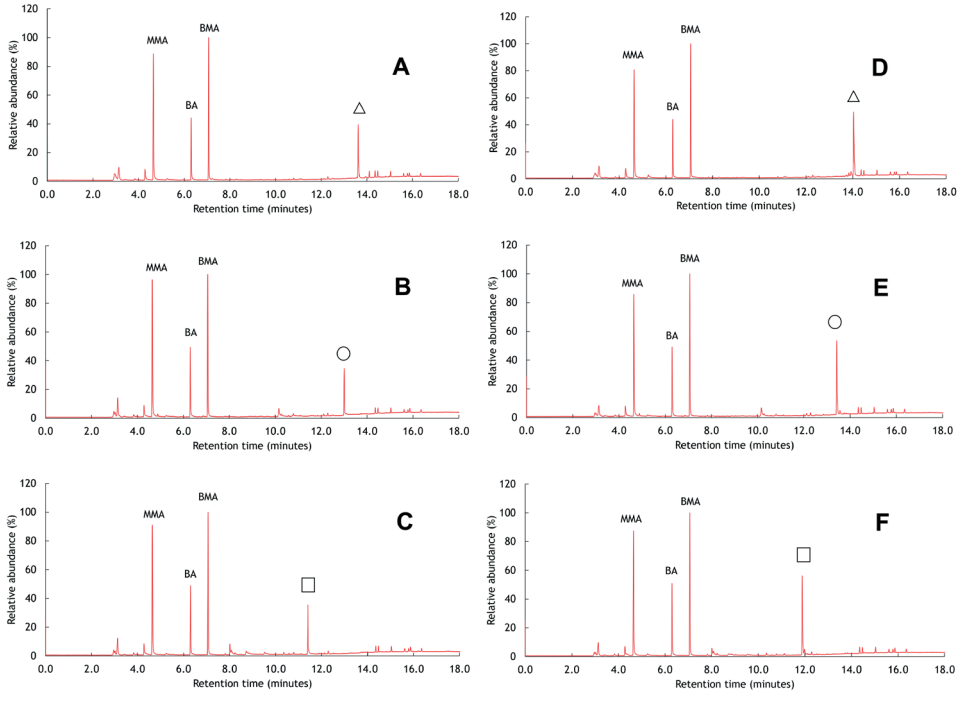

Figure 2.7. PyGC-MS chromatograms of AA model polymer MP2 (A, B, C) and MAA model polymer MP5 (D, E, F). Chromatograms A and D correspond to p-nitrophenacyl bromide as reagent (reaction products indicated by Δ), chromatograms B and E correspond to p-bromophenacylbromide (reaction products indicated by o, chromatograms C and F correspond to phenacyl bromide (reaction products indicated by □).

The (meth)acrylic esters MMA, BA and BMA present in the model polymers elutes between 3 to 8 minutes. All samples show extra peaks at retention times above 8 minutes (the

higher boiling point region). In the case of chromatogram 2.7A, 2 extra peaks are formed. The largest peak was found to be *p*-nitrophenacylacrylate, while the minor peak is the alcohol pyrolysis degradation product of *p*-nitrophenacylacrylate, *i.e.* *p*-nitrophenacyl alcohol. This component is also present in chromatogram D, but in significantly smaller concentrations. As described by Özlem *et al.* [22], alcohol by-products from pyrolysis are more abundant in case of acrylic components than for methacrylic components, which explains the presence of this peak in chromatogram A (polymer MP2). A similar pattern is observed in chromatograms B and E, with the peaks of interest shifted to slightly lower boiling points. This is expected, since *p*-bromophenacyl esters formed in these samples contain a Br atom instead of the p-nitro group in *p*-nitrophenacyl esters, which decreases the boiling point of the reaction products. Chromatograms 2.7C and 2.7F show two peaks in the region of interest, which were identified as phenacyl(meth)acrylate and phenacyl alcohol. The choice was made to continue optimization experiments with phenacyl bromide, as the formed phenacyl esters are more volatile than p-bromophenacyl esters and do not suffer from chromatographic interferences from higher-boiling dimeric structures (Figure 2.1), which result from the pyrolysis of (meth)acrylic ester copolymers.

In Figure 2.8, the mass spectra of the observed reaction products of the carboxylic acid functionality with phenacyl bromide (phenacyl acrylate and phenacyl methacrylate) are shown. Typical masses for acrylate- and methacrylate monomers are *m/z* 55 and 69, respectively, which is in agreement with the observed mass spectra for phenacyl acrylate and phenacyl methacrylate.

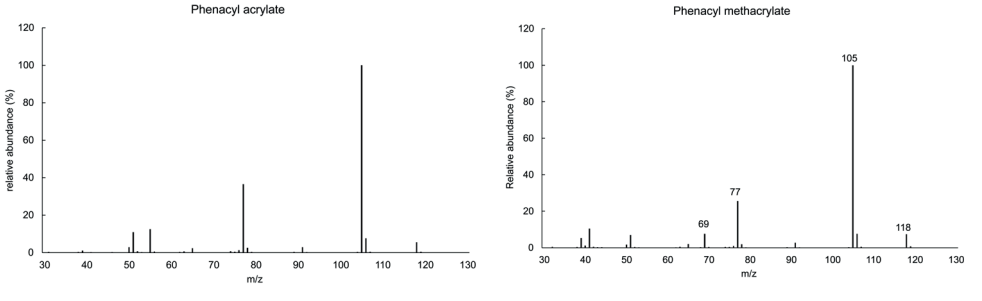

Figure 2.8. Observed mass spectra of phenacyl acrylate (Figure 2.7c, retention time 11.1 min) and phenacyl methacrylate (Figure 2.7f, retention time 12.2 min).

Acrylic-copolymer solubility varies strongly between solvents. A common solvent used for these types of copolymers is THF. Sample solubility in THF decreases with increasing

molecular weight and increasing acid content. For functional polymers, a factor complicating our understanding of the solubility is inter- and intramolecular hydrogen bonding. When the acid content in the polymer increases, solubility will decrease. It is of importance to select a solvent which is able to dissolve the polymers, so that selective solubilization and functionalization of carboxylic groups is avoided. The solvent should also be non-reactive towards the polymer/functional groups and should also be a good reaction medium for the preparation of phenacyl esters.

To determine the influence of the solvent (THF and NMP, which are both regarded as good solvents for acrylate polymers) on the derivatization reaction, SEC analyzes were performed (Figure 2.9). The eluted polymers were detected using UV absorption at 280 nm for both THF and NMP, using MP2 with phenacyl bromide and TEA as reaction system (both added at room temperature in 8-fold excess with respect to acid content):

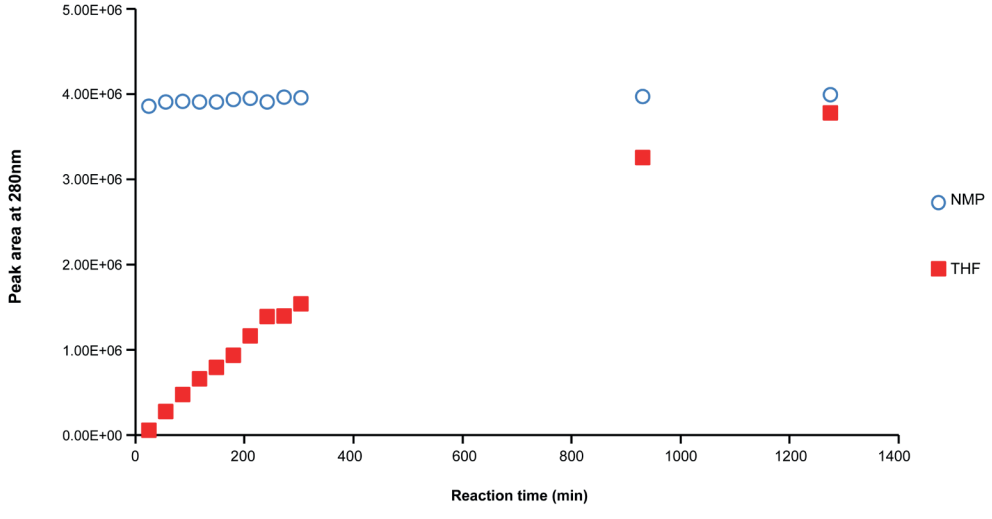

Figure 2.9. Peak area (UV absorption at 280 nm) of MP2 in THF and NMP as solvent systems.

NMP appears to be the more suitable reaction medium, since the polymer peak area is already at its maximum at the first measurement (within 30 min), which is shown in Figure 2.9. The reaction in THF needs at least 20 hours at room temperature to reach a comparable level of UV absorption. NMP, however, is difficult to remove from a GC injector, even at high temperatures and split flows. For this reason, THF is more favorable, even though phenacyl ester formation rate is significantly slower.

To quantify the concentration of derivatized carboxylic acid groups, the UV absorption of the polymeric part of the fast-SEC separation was compared to the molar response curve of acetoxyacetophenone. To this end, an external-standard calibration curve of acetoxyacetophenone was constructed (linear fit, y = 5267.3 x + 128428; R^2 = 0.9993). It was assumed that the UV absorbance of polymers, after reaction of carboxylic acid functionalities, is solely dependent on the concentration of phenacyl groups. Model copolymers MP2 and MP5 (Table 2.1) were subjected to this analysis and showed conversion degrees of 85% MP2) and 88% (MP5). It proved not possible to increase the conversion degree significantly by increasing the reaction temperature (60-80°C), the reaction time (4 hours) or the amount of reagent added.

Table 2.3. PyGC-FID area percentages of phenacyl esters of acrylic MP2 (Table 2.1) with variation in equivalents of TEA and phenacyl bromide reagent.

	Equivalents of base				
Equivalents phenacylbromide	**2**	**4**	**6**	**8**	**10**
2	6.62	9.12	9.25	10.81	10.94
4	8.22	12.39	13.03	13.93	13.28
6	10.24	12.19	13.75	14.09	13.69
8	11.42	13.53	14.12	14.14	14.25
10	12.69	13.97	13.84	14.14	13.76

Table 2.4. Pyr-GC-FID area percentages of phenacyl esters of acrylic model polymer 5 with variation in equivalents of TEA and phenacyl bromide reagent.

	Equivalents of base				
Equivalents phenacylbromide	**2**	**4**	**6**	**8**	**10**
2	8.83	8.00	8.74	9.63	10.51
4	14.2	17.90	17.56	19.29	18.44
6	15.86	21.10	21.65	21.26	21.96
8	19.39	20.78	22.2	21.77	21.41
10	18.78	22.50	22.53	22.05	21.42

A possible explanation for the high, but not complete conversion could be the presence of homo-(M)AA segments within the polymers. In emulsion polymerization, the initiation reaction is typically performed in the water phase, using water-soluble redox or radical initiators, such as hydrogen peroxide or ammonium persulphate. When radicals form in the water phase, rapid reaction with (meth)acrylic monomers can take place. The monomers most likely to react first with the water-soluble initiator clearly are the most

polar (most water soluble) monomers, in this case (M)AA [23]. Other, less polar monomers will be present almost exclusively in the emulsifier-stabilized monomer droplets. When the initiation and propagation phases have resulted in a sufficiently large oligomer, the growing radical chain will enter the monomer droplets, where it will react further with the monomers present there. It is, therefore, likely that multiple carboxylic acid groups will be adjacent at the initiator end of the polymer chain. If one of these carboxylic acid groups is functionalized with phenacyl bromide, a significant degree of steric hindrance will hamper the reaction of the adjacent carboxylic acid groups with phenacyl bromide.

Acrylic model copolymers MP2 and MP5 (containing 11%(*w/w*) acid) were subjected to reaction with phenacyl bromide with TEA as catalyst and THF as solvent. Between two- and ten-fold the stoichiometric amounts (reagent to acid) were used. Samples were reacted for 20 h prior to analysis with PyGC-MS/FID.

Based on the data as outlined in Tables 2.3 and 2.4, the largest area percentages of derivatized acid are obtained at higher stoichiometric amounts of phenacyl bromide and TEA (6 and higher). However, the observed percentages are based on phenacyl esters, not on the originally present (meth)acrylic acid. To convert relative FID areas to acid content effective carbon numbers (ECN) can be used [24]. In PyGC-FID the conversion can be performed in two ways, viz. (i) addition of a reference component, which only volatilizes during the pyrolysis run (ii) comparing the individual pyrolyzed components using relative peak areas and their individual ECN values. For these experiments, monomer contents were calculated through the latter option, as described in the Procedures section.

Table 2.5. Main components detected in the pyrolysis of model polymers MP4, MP5 and MP6 together with theoretical ECN values, FID areas, experimental monomer content (φw) and theoretical monomer content (φc).

		FID area %			Experimental content (φ_w)			Theoretical content (φ_c)		
Component	**Theoretical ECN**	**MP4**	**MP5**	**MP6**	**MP4**	**MP5**	**MP6**	**MP4**	**MP5**	**MP6**
Methyl methacrylate	3.9	43.1	31.0	20.1	52.9	43.4	31.7	48.0	40.0	30.0
1-Butene	3.9	8.3	6.0	4.9						
1-Butanol	3.5	2.1	1.4	1.3	26.6	24.1	23.2	25.0	25.0	25.0
Butyl acrylate	5.9	16.7	14.6	12.6						
Butyl methacrylate	6.9	28.3	24.8	21.5	19.6	19.6	19.2	25.0	25.0	25.0
Phenacyl alcohol	6.5	0.2	2.5	3.7	0.8	12.9	25.9	2.0	10.0	20.0
Phenacyl methacrylate	9.9	1.3	19.7	35.9						

Several conclusions can be drawn from the data as outlined in Table 2.5. The weight fraction of butyl methacrylate in the polymer is systematically underestimated, which may be explained by the formation of 1-butene and 1-butanol from both butyl acrylate and butyl methacrylate. There is a significant difference between calculated and theoretical methacrylic acid content. However, it was shown to be possible to determine the approximate composition of polyacrylates, even when acid-functionalities were present. The fraction of acid monomer can be estimated using the developed derivatization method. The accuracy of the analysis may yet be improved by determining pyrolysis response factors, but this is considered to be beyond the scope of the present research.

2.4 Conclusions

A specific derivatization protocol was developed for the characterization of carboxylic-acid functional copolymers, based on TEA and phenacyl-bromide reagent. One of the main advantages of this approach is that the phenacyl esters produced during the precolumn-derivatization protocol do not give rise to the dehydration and decarboxylation effects, which are common if (meth)acrylic-acid containing polymers are subjected directly to pyrolysis. Reasonable estimate of the polymer composition can be obtained, which is typically within ten percentage points. Although calculated acid content shows more deviation compared to the underivatized monomers, confirmation of the presence and identification of the type of acid can be achieved rapidly and easily.

Acknowledgement

The authors would like to thank Laura Soeterboek and Linda van den Broek for their work on this project. Kristel de Vos is acknowledged for the preparation of the waterborne acrylic model polymers.

References

1. F. Bertini, G. Audisio, V.V. Zuev, Investigation on the thermal degradation of poly-n-alkyl acrylates and poly-n-alkyl methacrylates (C1–C12), Polymer Degradation and Stability 89(2) (2005) 233-239. https://doi.org/10.1016/j.polymdegradstab.2004.11.023.
2. J.K. Haken, L. Tan, Mechanism of Thermal Degradation of Poly(Alkyl Acrylate) s Using Pyrolysis Gas Chromatography Mass Spectrometry, Journal of Polymer Science Part A: Polymer Chemistry 26 (1988) 1315-1322. https://doi.org/10.1002/pola.1988.080260506.
3. R. Rial-Otero, M. Galesio, J.-L. Capelo, J. Simal-Gándara, A Review of Synthetic Polymer Characterization by Pyrolysis–GC–MS, Chromatographia 70(3-4) (2009) 339-348. https://doi.org/10.1365/s10337-009-1254-1.
4. M. Ferriola, A. Gentilhomme, M. Cochez, N. Oget, J.L. Mieloszynski, Thermal degradation of poly(methyl methacrylate) (PMMA): modelling of DTG and TG curves, Polymer Degradation and Stability 79 (2003) 271-281. https://doi.org/10.1016/S0141-3910(02)00291-4.
5. Z. Czech, R. Pełech, Use of pyrolysis and gas chromatography for the determination of acrylic acid concentration in acrylic copolymers containing carboxylic groups, Polymer Testing 27(7) (2008) 870-872. https://doi.org/10.1016/j.polymertesting.2008.06.009.
6. R.P. Lattimer, Pyrolysis mass spectrometry of acrylic acid polymers, Journal of Analytical and Applied Pyrolysis 68-69 (2003) 3-14. https://doi.org/10.1016/s0165-2370(03)00080-9.
7. A.v.d. Horst, Y.v. Hooijdonk, A. Kroes, Pyrolysis-Liquid Chromatography for the Analysis of Acrylic Resins LCGC Europe 29(9) (2016) 488-796.
8. L. Osete-Cortina, M.T. Domenech-Carbo, Characterization of acrylic resins used for restoration of artworks by pyrolysis-silylation-gas chromatography/mass spectrometry with hexamethyldisilazane, J Chromatogr A 1127(1-2) (2006) 228-36. https://doi.org/10.1016/j.chroma.2006.05.081.
9. G.J.Q.v.d. Peyl, T.C.T. Linnartz, C.A.J.J.v. Rossum, M. Zeelenberg, Identification of polar monomers in poly acrylate dispersions with pyrolysis-gas chromatography / mass spectrometry, Journal of Analytical and Applied Pyrolysis 19 (1991) 279-283. https://doi.org/10.1016/0165-2370(91)80049-E.
10. P. Husek, Chloroformates in gas chromatography as general purpose derivatizing agents, Journal of Chromatography B 717 (1998) 57-91. https://doi.org/10.1016/S0378-4347(98)00136-4.
11. P.S. P. Husek, P. Matucha, Smooth Esterification of Di- and Tricarboxylic Acids with Methyl and Ethyl Chloroformates in Gas Chromatographic Profiling of Urinary Acidic Metabolites, 58(9/10) (2003) 623-630. https://doi.org/10.1365/s10337-003-0078-7.
12. Y.A. Bailey-Shaw, K.D. Golden, A.G. Pearson, R.B. Porter, Characterization of Jamaican agro-industrial wastes. Part II, fatty acid profiling using HPLC: precolumn derivatization with phenacyl bromide, J Chromatogr Sci 50(8) (2012) 666-72. https://doi.org/10.1093/chromsci/bms061.
13. R.L. Merker, M.J. Scott, The Reaction of Alkyl Halides with Carboxylic Acids and Phenols in the Presence of Tertiary Amines, The Journal of Organic Chemistry 26(12) (2002) 5180-5182. https://doi.org/10.1021/jo01070a095.
14. K. Thompson, S. Michielsen, Novel synthesis of N-substituted polyacrylamides: Derivatization of poly(acrylic acid) with amines using a triazine-based condensing reagent, Journal of Polymer Science Part A: Polymer Chemistry 44(1) (2006) 126-136. https://doi.org/10.1002/pola.21042.

15. M. Kunishima, C. Kawachi, K. Hioki, K. Terao, S. Tani, Formation of carboxamides by direct condensation of carboxylic acids and amines in alcohols using a new alcohol- and water soluble condensing agent: DMT-MM, Tetrahedron 57 (2001) 1551-1558. https://doi.org/10.1016/S0040-4020(00)01137-6.

16. C.E. Garrett, X. Jiang, K. Prasad, O. Repic, New observations on peptide bond formation using CDMT, Tetrahedron Letters 43 (2002) 4161-4165. https://doi.org/10.1016/S0040-4039(02)00754-2.

17. J.J.Broersen, H.Jansen, C.D. Ruiter, U.A.Th.Brinkman, R.W.Frei, F. A.Buijtenhuijs, F.P.B.v.d. Maeden, Derivatization of some polymers with o-phthalaldehyde prior to high-performance size-exclusion chromatography, Journal of Chromatography A 436 (1988) 39-46. https://doi.org/10.1016/S0021-9673(00)94562-X.

18. R.S. Borisov, V.G. Zaikin, Derivatization of synthetic polymers in mass spectrometric studies, Journal of Analytical Chemistry 65(14) (2010) 1423-1435. https://doi.org/10.1134/s1061934810140017.

19. N.A. Straessler, P. Li, S.A. Parry, D.W. Coleman, M.O. Killpack, M.E. Wright, Derivatization of carboxyl-terminated polybutadiene for determining relative functionality distribution, Journal of Applied Polymer Science 123 (2012) 691-698. https://doi.org/10.1002/app.34581.

20. J.L. Sharp, G. Paterson, Identification of Small Amounts of Copolymerised Unsaturated Carboxylic Acid in Acrylic Polymers byan Alkylation - Pyrolysis - Gas Chromatographic -Mass Spectrometric Procedure, Analyst 105 (1980) 517-520. https://doi.org/10.1039/AN9800500517.

21. K. Takeuchi, H. Aoi, H. Ohtani, Precise compositional analysis of styrene/butyl acrylate/methacrylic acid terpolymer by two-step reactive pyrolysis–gas chromatography with tetramethylammonium acetate, Journal of Analytical and Applied Pyrolysis 113 (2015) 22-26. https://doi.org/10.1016/j.jaap.2014.09.018.

22. S. Özlem, J. Hacaloglu, Thermal degradation of poly(n-butyl methacrylate), poly(n-butyl acrylate) and poly(t-butyl acrylate), Journal of Analytical and Applied Pyrolysis 104 (2013) 161-169. https://doi.org/10.1016/j.jaap.2013.08.008.

23. R.M. Fitch, L. Shih, Emulsion polymerization: Kinetics of radical capture by the particles., Interface Chemistry. Progress in Colloid & Polymer Science 56 (1975) 1-11. https://doi.org/10.1007/BFb0117110.

24. J.T. Scanlon, D.E. Willis, Calculation of Flame Ionization Detector Relative Response Factors Using the Effective Carbon Number Concept, Journal of Chromatographic Science 23 (1985) 333-340. https://doi.org/10.1093/chromsci/23.8.333.

CHAPTER 3

Heterogeneity analysis of polymeric carboxylic acid functionality by selective derivatization followed by size exclusion chromatography

Ton Brooijmans, Remco Okhuijsen, Ingrid Burggraaf-Oerlemans, Bob Pirok, Peter Schoenmakers, Ron Peters

Anal.Chim.Acta.1072, 87–94 (2019). doi: 10.1016/j.aca.2019.04.051

Abstract

Water-borne polymers are increasingly applied in our society, replacing traditional solvent-borne coatings and thus reducing environmental impact of coatings. The majority of waterborne dispersions are stabilized by the incorporation of neutralizable carboxylic acid functionality. The characterization of synthetic waterborne polymer systems can be performed by a wide variety of chromatographic and spectroscopic techniques. However, none of these approaches is able to determine the acid functionality distribution over the molecular-weight distribution directly. In this research, an innovative approach is developed which enables this analysis. The approach is based on the specific and complete derivatization of carboxylic acid functionality with phenacylbromide. Size exclusion chromatography (SEC) analysis of the derivatized polymers is performed followed by ultraviolet- (UV) and refractive index (RI) detection, enabling the quantitative determination of the acid content per molecular weight fraction. The applicability of the developed protocol is shown for various polymer systems.

3.1. Introduction

Waterborne polymer systems are sustainable alternatives to solvent-borne polymers and thus are becoming increasingly more important. Their use results in a significantly decreased release of volatile organic compounds to the atmosphere. Waterborne polymers are used for a wide variety of applications, such as coatings for packaging, printing, decorative and industrial use. These polymers can be synthesized using different polymerization methods, including emulsion radical polymerization [1-7], step-growth polyurethane polymerization [8-10] or hybrids of these mechanisms [11-15]. The obtained polymers are dispersed in water and yield particles of nanometer to micrometer size. The most common method to achieve aqueous dispersibility of these non-water-soluble polymers is incorporation of acidic groups, such as (meth)acrylic acid in the case of polyacrylic emulsion polymers or dimethylolpropanoic acid (DMPA) in waterborne polyurethanes. These acidic groups may be neutralized by the addition of water-soluble base, such as ammonia, triethylamine (TEA) or potassium hydroxide which results in water-soluble ionic domains within a polymer chain thus stabilizing the polymer particles in aqueous environments.

The distribution of these incorporated hydrophilic acidic monomers over the molecular-weight distribution (MWD) plays a crucial role in polymer particle formation and colloidal stability. Presence of hydrophilic domains in a coating however may severely impact coating application properties, such as durability and adhesion [7, 16, 17]. To ensure that the coating properties meet the application-specific requirements, it is important that the acid distribution throughout the MWD can be determined [18]. The analysis of ionic groups in synthetic polymers is complicated, as commercial polymer systems are comprised from a large number and variety of comonomers [19]. Also, the presence of multiple distributions, such as molecular-weight, end-group, sequence and/or functionality-type distributions complicate the chemical characterization of these polymers. Established techniques such as gradient size-exclusion chromatography [20, 21] and gradient polymer-elution chromatography [22-27] are valuable for the analysis of ionic groups in simple acid-functionalized copolymers. However, application of these techniques to contemporary, highly complex polymers, which often contain many different comonomers next to the acid monomer, is less suitable as retention and elution behavior are strongly related to the overall polymer composition. From a synthesis-, application- and commercial perspective, there is a strong need to obtain more information about the incorporation of these ionic groups over the molecular-weight distribution.

In our previous study (Chapter 2 of this thesis, [28]), we have demonstrated the applicability of a carboxylic-acid selective derivatization protocol for the unambiguous identification of the type of acid used during the synthesis of waterborne acrylic polymers. This derivatization protocol may be further exploited to investigate the heterogenic incorporation of the anionic groups over the MWD. By selectively reacting the anionic groups with a UV-absorbing group, the acid distribution can be made visible by employing UV detection.

In this work, an analysis method for the rapid quantification and characterization of acidic monomer groups in synthetic polymers by SEC-dRI-UV is described. Quantitative aspects of the protocol are investigated, as well as the application of the developed method to characterize commercial waterborne polymer types.

3.2.Experimental

3.2.1 Materials

N-Methylpyrrolidone (NMP, peptide synthesis grade), triethylamine (≥99.5%), phenacylbromide (PB, ≥99%), phenacyl acetate (PA, ≥98%), lithium bromide (LiBr, ≥99%), butyl methacrylate (BMA, >99%), methyl methacrylate (MMA, >99%), methacrylic acid (MAA, >99%), sodium lauryl sulfonate (32% (w/w) in water) and ammonia (25% in water) were purchased from VWR (Amsterdam, The Netherlands). 1-Dodecane thiol (≤100%), ammonium persulphate (≥98%) were purchased from Merck (Amsterdam, The Netherlands).

3.2.2 Synthesis of waterborne polymers

Copolymers were synthesized by reacting butyl methacrylate, methyl methacrylate and methacrylic acid in various weight ratios (φ, see Table 3.1) using emulsion polymerization. Water containing 2.3% (w/w) sodium lauryl sulfonate was heated to 80°C prior to addition of the monomer seed, which consists of 5% (w/w) of the total monomer feed. Targeted total concentration of polymer is 30% (w/w) in water, further to be named solid content. Directly after addition of the monomer feed, 0.5% (on monomer) of ammonium persulphate was added to the mixture over 3 minutes to initiate the reaction. Remaining monomer feed (containing 0.5% (w/w) of 1-dodecane thiol as chain transfer agent) was added for 90 minutes while maintaining reaction temperature at 85°C. Reaction temperature was kept at 85°C for 60 minutes after completion of the monomer feed, after this time the batch is cooled to 30°C. At this stage, the neutralizing agent (ammonia) is added until a pH between 7.5 and 8.5 is obtained. Solid content

was measured by making a mass balance of 1 g of polymer before and after drying in a 120°C oven for 2 hours.

3.2.3 Instrumentation

Size-exclusion chromatography (SEC) was performed on a modular Agilent 1260 HPLC system, equipped with autosampler, pump, column compartment, multi wavelength UV detector and a 1260 multi-detector system (Amstelveen, The Netherlands) consisting of a RI detector, viscosity detector and 2 light scattering detectors which utilize different angles. The eluent was N-methylpyrrolidone with 0.01 M lithium bromide at 0.75 mL·min^{-1} and a column temperature of 60°C. Three 300 mm × 7.5 mm i.d. PLgel Mixed-B columns packed with 10 µm particles (Agilent, Amstelveen, The Netherlands) were used in series. A 50 mm × 7.5 mm i.d. PLgel guard column was used (packed with 5-µm particles). The injection volume was 100 µL. The UV wavelength used for selective detection of functionalized acid groups was 280 nm. System control was performed using Agilent GPC/SEC software, version A.02.01, data processing was performed using home-built macros in Microsoft Excel (2016 Edition).

3.2.4 Procedures

Derivatization of acid-functional polymers with phenacylbromide was performed by dissolving 200 mg of acid-functionalized polymer, with a known fraction of incorporated acid and solid content, in 8 mL NMP, thus resulting in a known dilution factor. TEA was added in 4-fold stoichiometric excess with respect to absolute acid amount. After 1 hour of stirring, a similar stoichiometric excess of phenacyl bromide was added to the mixture and mixed for 10 minutes. This solution was used for SEC analysis without any further sample preparation. For samples with an unknown acid content, 100 mg of phenacylbromide and 100 µL of TEA were added using the described procedure. A schematic of this reaction is shown in Figure 3.1.

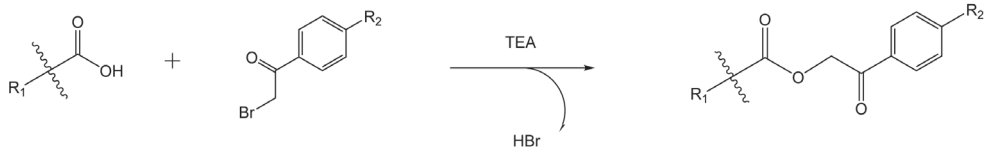

Figure 3.1. Reaction of carboxylic acid with acetophenone reagent. TEA is used as catalyst / neutralizing agent.

Calculation of incorporated-acid content by selective derivatization of the acid functionality was performed by preparing a stock solution of PA in NMP. A 10-point calibration curve (concentration range 14 mg·kg^{-1} to 600 mg·kg^{-1}) was prepared from this stock solution. To obtain the acid concentration from the PA calibration curve, the PA concentrations were corrected for molar mass:

$$Conc_{\text{Target acid}} = \frac{MW_{\text{Target acid}}}{MW_{\text{pa}}} * Conc_{\text{PA}}$$

In this equation, $Conc_{\text{Target acid}}$ is the calculated concentration of target acid present in the calibration point, $MW_{\text{Target acid}}$ is the molecular weight of the acid (72.1 g/mol for acrylic acid, 86.1 g/mol for methacrylic acid and 134.1 g/mol for DMPA), MW_{pa} is the molecular weight of phenacylacetate (178.2 g/mol) and $Conc_{\text{PA}}$ is the calculated phenacylacetate concentration in the calibration point.

These standards are analyzed using the described SEC setup, integrating the low molecular weight PA peak in the UV trace. The UV peak area of the polymeric fraction (see Figure 1b, dotted line between t_r 23-32 minutes) was integrated and corrected for the solids content and the dilution factor which was calculated for each polymer.

3.3.Results and discussion

3.3.1 Total acid content determination by SEC-UV-RI

To detect the presence of acids in a polymer, the phenacyl bromide functionalization protocol will result in a distinct UV signal at 280 nm which is visible during elution of the polymer. This is illustrated in Figure 3.2. Figure 3.2A shows the chromatograms of both refractive index- and UV 280 nm trace of sample MMA 2 without derivatization, while Figure 3.2B is the same sample after derivatization with phenacylbromide.

The polymer sample without derivatization shows no significant UV absorbance at polymer elution times (*tr*24-32 min), whereas a clear elution band can be observed for the derivatized polymer. Remaining derivatization agent and catalyst elute around t_0 and are shown as positive peaks on both RI- and UV traces. It can also be noted that the elution time, and thus the hydrodynamic volume, of the polymer (refractive index signal) did not change significantly as a result of the derivatization. Peak intensity in refractive index signal was found to increase, which can be explained by the more favourable detector response increment (*dn/dc*) of the aromatic functionality compared to the bare incorporated carboxylic acid monomer [29].

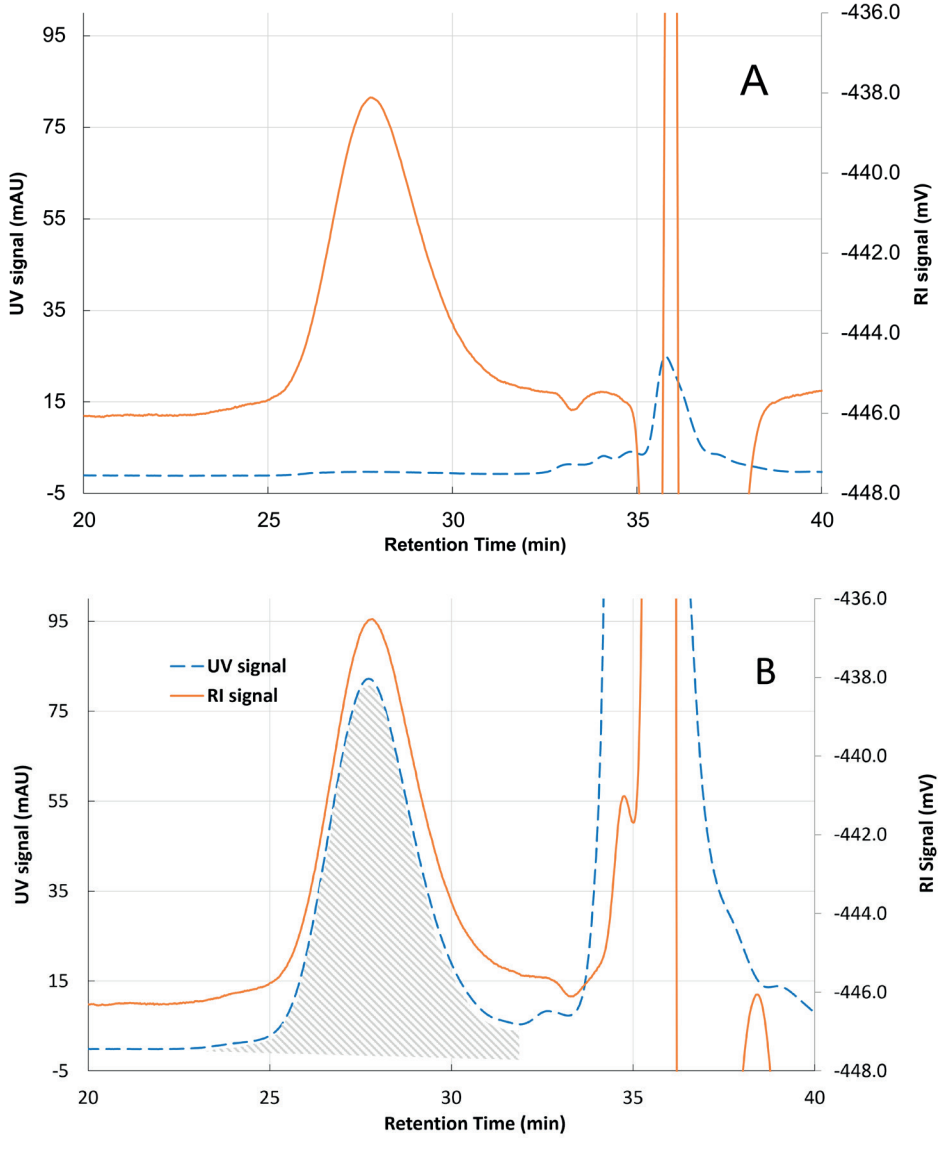

Figure 3.2. Refractive index- and UV chromatograms at 280 nm of model polymer MMA 2 (2% (w/w) MAA). a) sample MMA 2 without derivatization, and b) sample MMA 2 after derivatization.

The UV peak of the polymer was integrated (as shown in Figure 3.2b) and compared to the phenacyl acetate calibration curve (linear fit, R^2= 0.99998, y=104.11x+470.28), as described in the Procedures section 3.2.4. In Table 3.1, results from the SEC-dRI-UV analysis are displayed.

Table 3.1. Acid content (weight fractions) in model polymer systems. Theoretical values compared with the SEC protocol.

MMA-MAA copolymers			BMA-MAA copolymers		
Sample	**φ MAA Synthesis %(w/w)**	**Average φ MAA SEC %(w/w)[a]**	**Sample**	**φ MAA Synthesis %(w/w)**	**Average φ MAA SEC %(w/w)[a]**
MMA 1	0.0	-	BMA 1	0.0	-
MMA 2	2.0	1.9	BMA 2	2.0	2.0
MMA 3	4.0	4.0	BMA 3	4.0	3.7
MMA 4	6.0	6.1	BMA 4	6.0	5.5
MMA 5	8.0	8.5	BMA 5	8.0	8.1
MMA 6	10.0	10.3	BMA 6	10.0	10.0

[a] *Samples are analyzed in 6-fold, relative standard deviations below 2%.*

From the obtained results, it can be concluded that the derivatization protocol performs well for the detection and quantification of acid functionality. Results using this protocol are in good agreement with the theoretical acid content values (which are established gravimetrically during the synthesis of the polymers) with a relative deviation between 0 and 10%. We did not find significant reactivity of phenacylbromide with other possible functional groups in waterborne polymers (e.g. hydroxyl, amine, urethane, urea and sulfonic acid), but as this is considered out of scope of this study it should be investigated in more detail in further research.

3.3.2 Acid distribution analysis

Additional information about distribution of carboxylic acid groups from SEC analysis may be obtained by the addition of an additional concentration detector next to the UV detector. In this research, a refractive index detector was used to detect the polymer concentration. The assumption is made that refractive-index response for a single polymer across the polymer molecular weight is constant. Significant deviations of the refractive index of a certain polymer fraction slice compared to the polymer bulk are only expected in the low molecular weight region [30], as molecular weight build-up will rapidly average out the composition and thus the polymer refractive index. More generic SEC solvents with lower refractive indices, such as tetrahydrofuran (THF) may be used in the derivatization protocol, yet would be accompanied by drastically different reaction kinetics of anionic groups [28], easily requiring several days before complete derivatization is obtained. For practical reasons, the decision was made to perform the derivatization and analysis in NMP.

Both RI and UV signals are aligned by correcting the elution time for the interdetector delay, after which the peak area under the polymer is determined for both detectors. For every fraction of the molecular weight distribution, the area of the UV signal is divided by the total UV peak area, which in turn in divided by the area of the RI signal divided by the total RI peak area. The result is multiplied by the acid content (φ_{total}) as determined by the external standard UV calibration using phenacylacetate (see section 3.1).

$$\varphi_{slice} = \frac{A_{280\ nm} \Big/ \sum A_{280\ nm}}{A_{RI} \Big/ \sum A_{RI}} * \varphi_{total}$$

The output for this calculation is the acid content per data slice, an example of this output is shown in Figure 3.3.

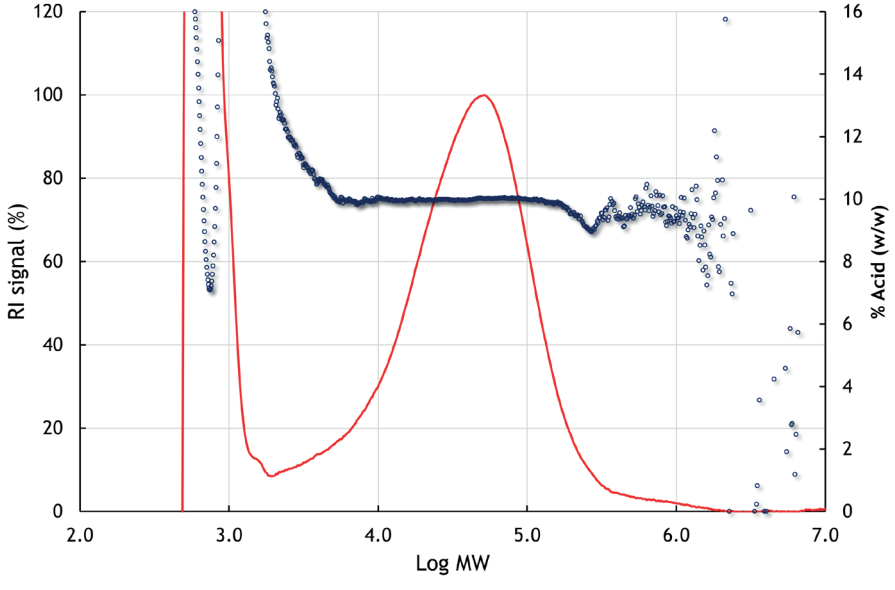

Figure 3.3. Acid distribution as a function of molecular weight of model polymer BMA6 (10 % w/w acid monomer. Refractive index signal (blue trace) is displayed to show polymer elution profile.

The polymer appears to contain an evenly distributed acid content over the molecular weight, which means that every polymer chain contains the same relative concentration of acid. There is an increase in apparent acid content visible in the low molecular weight (M_w ~2000 kDa), which is mainly caused by the presence of excess derivatization agent.

This could be counteracted by using an optimized SEC column setup for increased low molecular weight resolution between reagent and polymer or by sample clean-up prior to SEC analysis. It must be mentioned that also the non-derivatized sample (Figure 3.2a) displays some UV absorption in the low molecular weight region. Towards the higher molecular weight region, scattering of data points is observed. This indicates that accuracy of the acid content determination is lower compared to the bulk of the polymer. This is caused by the relatively low signals for both RI and UV detectors in this molecular weight region.

All model systems were analyzed using the derivatization protocol and SEC-dRI-UV, resulting in the acid distribution plots shown in Figure 3.4 (MMA-MAA copolymers) and Figure 3.5 (BMA-MAA copolymers). All polymers show a homogeneous acid distribution over the molecular weight with the clear difference of a different acid content.

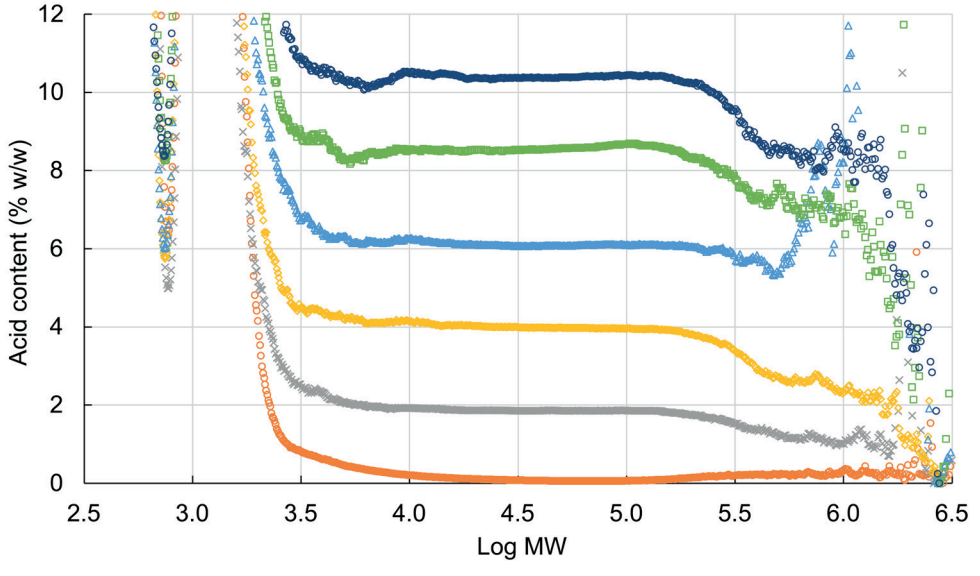

Figure 3.4. Acid distribution overlay of model polymers MMA 1 to 6.

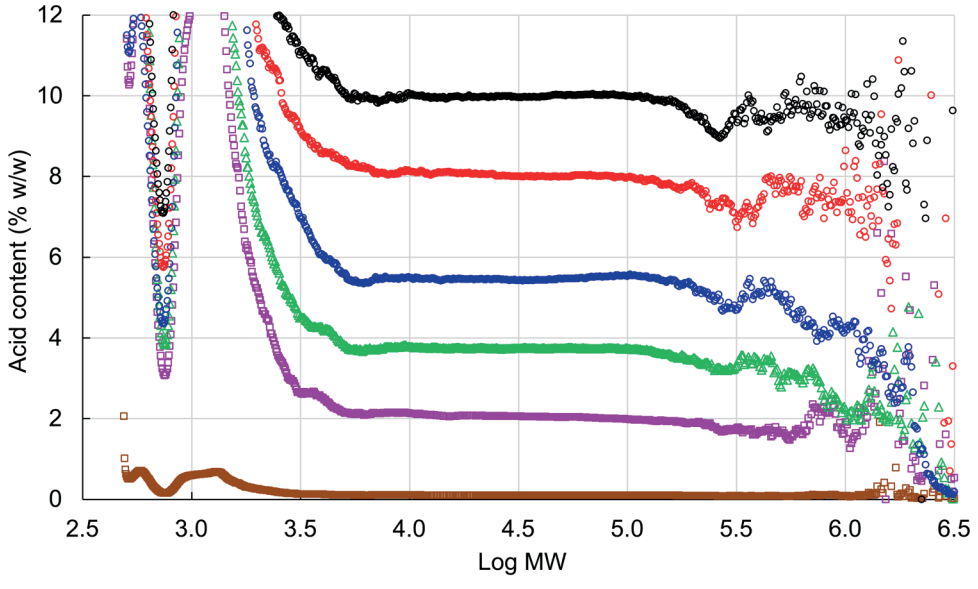

Figure 3.5. Acid distribution overlay of model polymers BMA 1 to 6.

3.3.3 Industrial sample analysis

Using the developed protocol, an unidentified commercially available resin and a polyurethane prepolymer were analyzed. Results for the commercially available resin are shown in Figure 3.6, which shows the sample being based on the oligomer-polymer concept [18] with respective molecular weights of the oligomer and polymer of approximately 10 kDa and 100 kDa . Using the UV-signal and the phenacyl acetate calibration together with confirmed acid identity (acrylic acid) from our previously published pyrolysis method [28], the total polymer acid content was calculated to be 6.7% (w/w). Calculation of the acid distribution shows a relatively acid-rich oligomer containing roughly 9% (w/w) of acrylic acid, and a polymer which also contains acrylic acid in approximately 4.5% (w/w) content. Presence of an acid-rich oligomer is common for oligomer-polymer systems, but the presence of acid in the polymer is encountered less often. This crucial information about polymer architecture helps explain polymer properties and performance, and would not be available without the developed protocol.

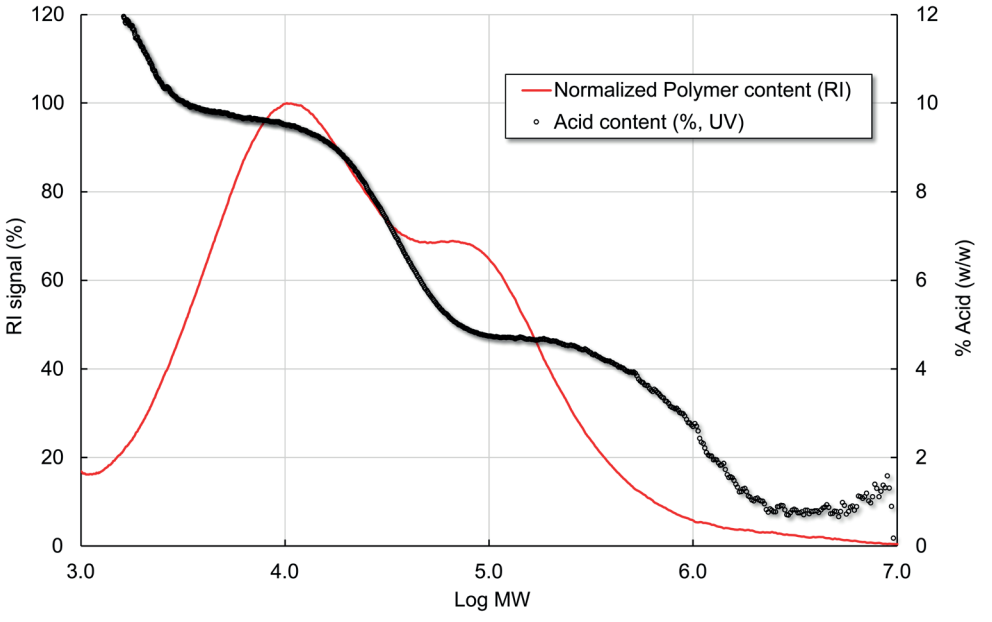

Figure 3.6. Acid distribution of commercial resin A. Bimodal molecular weight distribution with an acid-rich oligomer indicates an oligomer-polymer system.

Applicability of the developed protocol is not limited to acrylate polymers, but may also be used for the characterization of other carboxylic acid-containing polymers. An example is shown in Figure 3.7 which shows the analysis of a polyurethane prepolymer. This prepolymer was prepared in-house and consists of the reaction product of isophorone diisocyanate, polytetrahydrofuran (pTHF) 1000 and DMPA. The UV trace shows acid content to be approximately 2% (w/w), which was consistent with the polymerization recipe. Also, a homogeneous incorporation of acid with respect to molecular weight was observed.

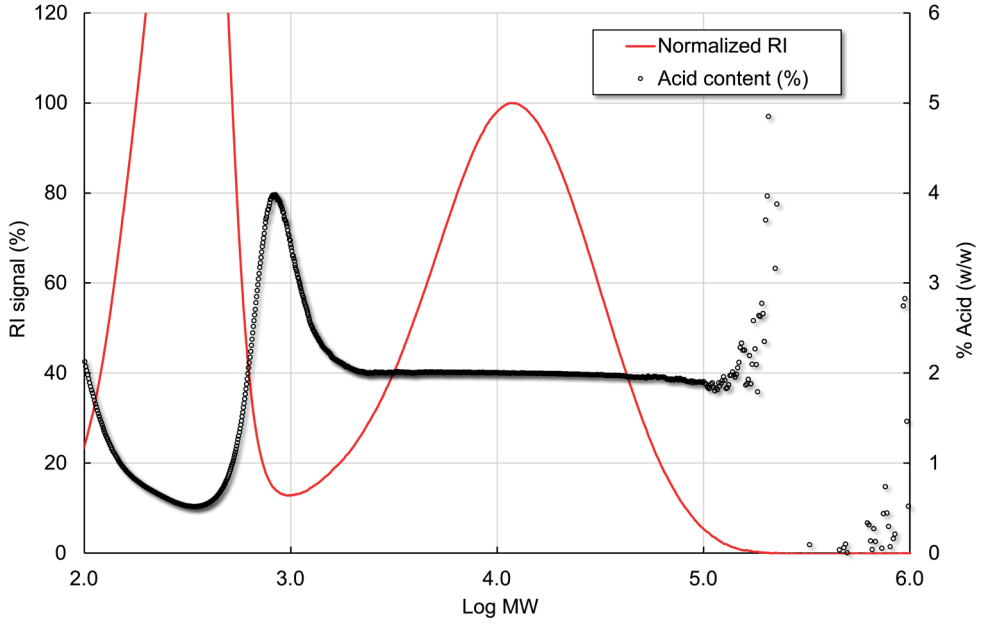

Figure 3.7. Acid distribution of a polyurethane prepolymer, consisting of Isophorone diisocyanate, pTHF1000 and DMPA.

3.4. Discussion and conclusion

A specific derivatization protocol was established and used for the quantitative determination of acid content in waterborne polymers. Obtained results correspond well to the theoretical acid content of the polymers. Sample preparation is simple and yields quantitative information, and only requires addition of reagent and catalyst to the dissolved polymer in excess amounts. A possible drawback could be that the SEC analysis requires the polymer sample to be fully soluble to obtain repeatable and accurate results whereas titration requires at least swelling of the polymer. The SEC analysis cannot be applied for (pre)crosslinked polymers as these will not dissolve in any solvent.

By incorporation of a concentration detector such as a RI next to a UV detector which specifically detects presence of acid, the acid distribution across the molecular weight can be determined. The compositional influence on RI signal is a drawback of the use of RI in combination with high-refractive index solvents such as NMP. The model polymer systems used in this research were prepared in such a way, that a homogeneous composition over molecular weight is obtained. Polymers prepared in a different way,

may exhibit a variation in acid distribution and/or a compositional variation of the comonomers. This will have an effect on both RI- and UV detector signals, but it must be noted that UV-signal differences between derivatized and non-derivatized acid functionality will be significantly larger than any difference in refractive index caused by compositional drift. Detection techniques such as high-temperature evaporative light scattering detection (HT-ELSD) are theoretically better suited as concentration detector compared to RI detection, as there is no significant influence of polymer composition on the detector signal [31, 32] and detector signal can be linearized.

The described protocol is able to provide molecular weight, acid content and acid distribution of a polymer sample in a single analysis run. This combined information is not readily obtainable using other methods of instrumental analysis. The reported protocol provides more information on the chemical heterogeneity of the incorporated acid monomers, and may be utilized regardless of type, number and polarity of comonomers which makes it a valuable addition to polymer analysis laboratories.

Acknowledgements

Jens de Bont, Lisette Konings and Yvonne Brandsma-Vromans are acknowledged for the preparation of polyurethane- and polyacrylic model polymer systems used in this study.

References

1. C. Li, H. Xiao, X. Wang, T. Zhao, Development of green waterborne UV-curable vegetable oil-based urethane acrylate pigment prints adhesive: Preparation and application, Journal of Cleaner Production 180 (2018) 272-279. https://doi.org/10.1016/j.jclepro.2018.01.193.
2. S.H. Park, T.H. Lee, Y.I. Park, S.M. Noh, J.C. Kim, Effect of the n-butyl acrylate/2-ethylhexyl acrylate weight ratio on the performances of waterborne core–shell PSAs, Journal of Industrial and Engineering Chemistry 53 (2017) 111-118. https://doi.org/10.1016/j.jiec.2017.04.010.
3. H. Liu, J. Bian, Z. Wang, C.J. Hou, Synthesis and Characterization of Waterborne Fluoropolymers Prepared by the One-Step Semi-Continuous Emulsion Polymerization of Chlorotrifluoroethylene, Vinyl Acetate, Butyl Acrylate, Veova 10 and Acrylic Acid, Molecules 22(1) (2017). https://doi.org/10.3390/molecules22010184.
4. J. Tan, W. Liu, H. Wang, Y. Sun, S. Wang, Preparation and properties of UV-curable waterborne comb-like (meth)acrylate copolymers with long fluorinated side chains, Progress in Organic Coatings 94 (2016) 62-72. https://doi.org/10.1016/j.porgcoat.2016.01.027.
5. J. Scheerder, R. Dollekens, H. Langermans, The colloidal properties of alkaline-soluble waterborne polymers, Journal of Applied Polymer Science 135(17) (2018) 46168. https://doi.org/10.1002/app.46168.
6. M.L. Picchio, M.C.G. Passeggi, M.J. Barandiaran, L.M. Gugliotta, R.J. Minari, Waterborne acrylic–casein latexes as eco-friendly binders for coatings, Progress in Organic Coatings 88 (2015) 8-16. https://doi.org/10.1016/j.porgcoat.2015.06.012.
7. Z. Aguirreurreta, J.C. de la Cal, J.R. Leiza, Preparation of high solids content waterborne acrylic coatings using polymerizable surfactants to improve water sensitivity, Progress in Organic Coatings 112 (2017) 200-209. https://doi.org/10.1016/j.porgcoat.2017.06.028.
8. I. Jiménez-Pardo, P. Sun, R.A.T.M. van Benthem, A.C.C. Esteves, Design of self-dispersible charged-polymer building blocks for waterborne polyurethane dispersions, European Polymer Journal 101 (2018) 324-331. https://doi.org/10.1016/j.eurpolymj.2018.02.026.
9. J. Wu, D. Chen, Synthesis and characterization of waterborne polyurethane based on covalently bound dimethylol propionic acid to e-caprolactone based polyester polyol, Progress in Organic Coatings 97 (2016) 203-209. https://doi.org/10.1016/j.porgcoat.2016.04.033.
10. M.E.V. Hormaiztegui, M.I. Aranguren, V.L. Mucci, Synthesis and characterization of a waterborne polyurethane made from castor oil and tartaric acid, European Polymer Journal 102 (2018) 151-160. https://doi.org/10.1016/j.eurpolymj.2018.03.020.
11. H. Wang, S. Qin, X. Yang, G. Fei, M. Tian, Y. Shao, K. Zhu, A waterborne uniform graphene-poly(urethane-acrylate) complex with enhanced anticorrosive properties enabled by ionic interaction, Chemical Engineering Journal 351 (2018) 939-951. https://doi.org/10.1016/j.cej.2018.06.151.
12. G.A. Alvarez, M. Fuensanta, V.H. Orozco, L.F. Giraldo, J.M. Martín-Martínez, Hybrid waterborne polyurethane/acrylate dispersion synthesized with bisphenol A-glicidylmethacrylate (Bis-GMA) grafting agent, Progress in Organic Coatings 118 (2018) 30-39. https://doi.org/10.1016/j.porgcoat.2018.01.016.
13. Q. Yong, H. Pang, B. Liao, W. Mo, F. Huang, H. Huang, Y. Zhao, Preparation and characterization of low gloss aqueous coating via forming self-roughed surface based on waterborne polyurethane acrylate hybrid emulsion, Progress in Organic Coatings 115 (2018) 18-26. https://doi.org/10.1016/j.porgcoat.2017.10.024.

14. X. Zhang, M. Zhu, W. Wang, D. Yu, Silver/waterborne polyurethane-acrylate's antibacterial coating on cotton fabric based on click reaction via ultraviolet radiation, Progress in Organic Coatings 120 (2018) 10-18. https://doi.org/10.1016/j.porgcoat.2018.03.004.

15. J. Xu, Y. Jiang, T. Zhang, Y. Dai, D. Yang, F. Qiu, Z. Yu, P. Yang, Synthesis of UV-curing waterborne polyurethane-acrylate coating and its photopolymerization kinetics using FT-IR and photo-DSC methods, Progress in Organic Coatings 122 (2018) 10-18. https://doi.org/10.1016/j.porgcoat.2018.05.008.

16. J. Machotová, E. Černošková, J. Honzíček, J. Šňupárek, Water sensitivity of fluorine-containing polyacrylate latex coatings: Effects of crosslinking and ambient drying conditions, Progress in Organic Coatings 120 (2018) 266-273. https://doi.org/10.1016/j.porgcoat.2018.03.016.

17. N. Agarwal, R.J. Farris, Water Absorption by Acrylic-Based Latex Blend Films and Its Effect on Their Properties, Journal of Applied Polymer Science 72 (1999) 1407-1419. https://doi.org/10.1002/(SICI)1097-4628(19990613)72:11<1407::AID-APP4>3.0.CO;2-5.

18. A. Overbeek, Polymer heterogeneity in waterborne coatings, Journal of Coatings Technology and Research 7(1) (2009) 1-21. https://doi.org/10.1007/s11998-009-9201-5.

19. H.S.A. Bauer, H. Leander, S.-J. Raymond, V. Stanislawczyk, W. Fish, Waterborne polymers for heat seal adhesive, United States, 2019.

20. M. Schollenberger, W. Radke, Size exclusion chromatography-gradients, an alternative approach to polymer gradient chromatography: 2. Separation of poly(meth)acrylates using a size exclusion chromatography-solvent/non-solvent gradient, J Chromatogr A 1218(43) (2011) 7828-31. https://doi.org/10.1016/j.chroma.2011.08.090.

21. M. Schollenberger, W. Radke, SEC-Gradients, an alternative approach to polymer gradient chromatography: 1. Proof of the concept, Polymer 52(15) (2011) 3259-3262. https://doi.org/10.1016/j.polymer.2011.05.047.

22. P.J.C.H. Cools, F. Maesen, B. Klumperman, A.M. van Herk, A.L. German, Determination of the chemical composition distribution of copolymers of styrene and butadiene by gradient polymer elution chromatography, Journal of Chromatography A 736(1-2) (1996) 125-130. https://doi.org/10.1016/0021-9673(95)01369-5.

23. P.J.Schoenmakers, P. Aarnoutse, Chemical Analysis for Polymer Engineers, in: J.K. T. Meyer (Ed.), Handbook of Polymer Reaction Engineering, Wiley2005.

24. A. Snijder, B. Klumperman, R. Van Der Linde, End-group modification of poly(butyl acrylate) prepared by atom transfer radical polymerization: Mechanistic study using gradient polymer elution chromatography, Journal of Polymer Science Part A: Polymer Chemistry 40(14) (2002) 2350-2359. https://doi.org/10.1002/pola.10321.

25. C.N. Pomeranz, S.V. Olesik, Separation of poly-3-hydroxyvalerate-co-3-hydroxybutyrate through gradient polymer elution chromatography, J Chromatogr A 1218(44) (2011) 7943-7. https://doi.org/10.1016/j.chroma.2011.08.065.

26. H.J.A. Philipsen, B. Klumperman, F.A.M. Leerrnakers, F.P.C. Wubb, A.L. German, Molar Mass Effects in Reversed-Phase Gradient Polymer-Elution Chromatography of Oligomers, Chromatographia 55 (2002) 533-540. https://doi.org/10.1007/BF02492898.

27. H.J.A. Philipsen, M.R. de Cooker, H.A. Claessens, B. Klumperman, A.L. German, Characterization of low-molar-mass polymers by gradient polymer elution chromatography II. Solubility effects in the analysis of polyester resins under reversed-phase conditions, Journal of Chromatography A 761(1-2) (1997) 147-162. https://doi.org/10.1016/s0021-9673(96)00807-2.

28. T. Brooijmans, R. Okhuijsen, I. Oerlemans, PJ. Schoenmakers, R. Peters, Acid monomer analysis in waterborne polymer systems by targeted labeling of carboxylic acid functionality, followed by pyrolysis - gas chromatography, J Chromatogr A 1560 (2018) 63-70. https://doi.org/10.1016/j.chroma.2018.05.024.

29. J.F. Knill, C.J. Kennedy, Polymer Handbook 4ed.2004. https://doi.org/10.1002/1097-0126(200007)49:7<807::AID-PI436>3.0.CO;2-1.

30. A.M. Striegel, W.W. Yau, J.J. Kirkland, D.D. Bly, Modern Size Exclusion Liquid Chromatography - Practice of Gel Permeation and Gel Filtration Chromatography, 2 ed., Wiley2009.

31. A. Boborodea, S. O'Donohue, Linearization of evaporative light scattering detector signal, International Journal of Polymer Analysis and Characterization 22(8) (2017) 685-691. https://doi.org/10.1080/1023666x.2017.1367066.

32. A. Boborodea, S. O'Donohue, New evaporative light scattering detector for high temperature gel permeation chromatography, International Journal of Polymer Analysis and Characterization 22(7) (2017) 631-638. https://doi.org/10.1080/1023666x.2017.1358835.

CHAPTER 4

Charge-based separation of synthetic macromolecules by non-aqueous ion exchange chromatography

Ton Brooijmans, Pascal Breuer, Peter Schoenmakers, Ron Peters

J. Chrom. A 2020, 1626, 461351.https://doi.org/10.1016/j.chroma.2020.461351.

Abstract

Traditional polymer-separation methods, such as size-exclusion chromatography and (gradient) liquid adsorption chromatography, cannot provide separations exclusively based on the number of deprotonated carboxylic-acid groups along the backbone chain of polymers. A novel separation method, based on non-aqueous ion-exchange chromatography (NAIEX), was developed, which allows such a separation of acid-functional polymers that are soluble in organic solvents. The polar, aprotic N-methylpyrrolidone was found to be a suitable solvent. It features a high relative permittivity (favoring dissociation of ion pairs into free ions) and it is a good solvent for polymers and organic salts, such as triethyl-ammonium formate. A negative charge is established on these polymers by deprotonation of the carboxylic-acid groups in the presence of an organic superbase (tetramethyl guanidine). Traditional potent organic bases, such as triethylamine, do not possess the base strength to compensate for the increase in pKa of polymeric carboxylic acid groups in non-aqueous conditions. Triethyl-ammonium formate is proposed as an alternative to traditional salts used for elution in aqueous ion-exchange chromatography. Separation was performed on an industry-standard strong-anion-exchange column and (near-)universal detection of the polymers was performed by high-temperature evaporative-light-scattering detection. The NAIEX method yielded a separation based on the acid-functionality distribution of the polymer. NAIEX was compared with traditional normal- and reversed-phase liquid-chromatography approaches for the separation of acid-functional copolymers.

4.1. Introduction

Certain synthetic macromolecules resemble biological polymers, as these are comprised of a wide variety of monomeric units, and, depending on their environment, will assume a three-dimensional structure. The incorporation of polar monomers in synthetic macromolecules may induce dispersibility of polymers in water in the form of nano-sized particles. The most-commonly applied polar monomers are acrylic acid or methacrylic acid in acrylic polymers and dimethylol-propanoic acid (DMPA) in polyurethane polymers. These acidic monomers are incorporated in a polymer backbone and may be neutralized by a wide variety of bases (*e.g.* ammonia, triethylamine, alkali hydroxides), resulting in a water-soluble acid salt, which provides stability for the polymer particle in aqueous environments. This route is commonly followed in many industrial production processes for water-borne resins, enabling the production of environmentally friendly water-based coatings.

To monitor and improve the industrial processes as well as improving end-product properties, there is a need for characterization of the acid incorporation in polymers, as is it responsible for the stabilization of the polymer particles. Analysis of the average-acid content in copolymers can be performed with titration [1], nuclear-magnetic-resonance (NMR) spectroscopy, liquid-chromatographic (LC) separation techniques in either reversed- or normal-phase modes [2-7] and gradient-size-exclusion chromatography (gradient-SEC) [8-11]. Although the described separation methodologies have a broad application window, specifically for copolymers, the currently available separation methodologies yield no direct correlation between retention behaviour and presence or distribution of acid groups for samples with compositional differences, because retention also depends on the overall polymer polarity. Unravelling the composition distribution becomes increasingly complex when three or more types of monomers are used within a polymer, creating an enormous number of possible copolymers.

Ion-exchange chromatography (IEX) is a well-established liquid-chromatographic technique for the separation of ions according to their charge-to-size ratio. IEX is often used to separate water-soluble ions, such as peptides and proteins [12]. One of the advantages of this technique is that separation occurs under non-denaturation conditions, so as to keep biological molecules in their native state. Proteins are composed of a number of amino acids and they have a specific charge at a certain pH due to the presence of many different carboxylic acid, amide, amine, and other functionalities. Separation in IEX can be established by applying a pH gradient or a salt gradient. By altering the pH of the eluent, the surface charge of the molecule may be changed to the point where there is no interaction with the IEX stationary phase [13]. Alternatively, a

salt gradient can be used to compete for available sites on the stationary-phase surface for interaction with the ionogenic analytes, which effectively negates analyte/column interactions [14-16].

In principle, IEX is a viable approach for the separation of synthetic polymers solely based on their charge. Yet, to our knowledge, such separations of water-borne polyacrylates have not been reported to date. Important considerations in developing such single-parameter separations are (*i*) the selected solvent, which should be capable of dissolving neutral and charged polymers, as well as salts, (*ii*) the neutralizing agent, which should be capable of causing deprotonation in non-aqueous environments, and (*iii*) the desorption of the adsorbed polymer from the stationary phase. If the carboxylic-acid moieties in the polymers are deprotonated using (in)organic bases, water-borne polymers may be regarded as charged species, which could render them suitable for analysis with IEX and, thus, for separation exclusively based on the number of deprotonated carboxylic-acid groups of the polymer. Contrary to common analytes studied with IEX, such as inorganic ions, peptides, *etc*., most industrial polymers do not dissolve in water. Instead, they may be dissolved in (often exotic) organic solvents. However, the presence of organic solvents has a strong effect on the dissociation constant (p*k*a) of acids (A), as the activity (*a)* of the proton changes dramatically upon the use of a different solvent (s) compared to water [17-19]:

$$pK_a = - log \frac{a(SH^+) * a(A-)}{a(HA)}$$

Based on the above literature, the p*k*a of carboxylic acids can be 6 or 7 units higher in an organic solvent than their p*k*a in water. Consequently, the organic bases that are commonly used to deprotonate the acid groups in aqueous dispersions (triethylamine, ammonia) are often not strong enough to provide deprotonation in non-aqueous environments. Moreover, certain bases, such as alkali hydroxides, are not soluble in non-aqueous environments. Traditional IEX methods also employ a salt gradient to compete for active ion-exchange sites with analyte species adsorbed on the stationary phase. Solubility of traditional salts (such as sodium chloride) in organic media is limited, which limits their applicability in non-aqueous IEX.

In this research, we have developed a separation of non-water soluble, carboxylic-acid-containing polymers based solely on their charge. Charge is obtained by deprotonating the acid functionalities of the polymer using an organic superbase, 1,1,3,3-tetramethyl

guanidine (TMG), the conjugated acid of which has a high enough p*k*a to achieve deprotonation of the carboxylic-acid functionalities in non-aqueous conditions [20]. The chosen solvent is N-methylpyrrolidone (NMP), as it is capable of dissolving a wide range of polymers. NMP also has a relative permittivity (or dielectric constant, ε) of 32.0, which is high in comparison with common organic solvents, such as hexafluoro isopropanol (ε = 15.7) and tetrahydrofuran (ε = 7.6), thus favouring the dissociation of ion pairs into free (solvated) ions [17]. The developed non-aqueous IEX (NAIEX) separation is compared to more traditional reversed- and normal-phase LC approaches, and NAIEX is shown to have outstanding potential for separating acid-functional polymers based solely on the number of carboxylic-acid groups in the polymer.

4.2 Experimental

4.2.1 Materials

All material purity percentages are by weight, except when otherwise indicated. N-Methylpyrrolidone (NMP, peptide-synthesis grade), triethylamine (≥99.5%), butyl acrylate (BA, >99%), methyl methacrylate (MMA >99%), ethyl acrylate (EA, >99%), ethyl methacrylate (EMA, >99%) methacrylic acid (MAA, >99%), acrylic acid (AA, >99%), 2,2,4-trimethylpentane (>99.5%), sodium lauryl sulfonate (32% in water) and ammonia (25% in water) were purchased from VWR (Amsterdam, The Netherlands). 1-Dodecane thiol (99.8%), ammonium persulphate (≥98%) were purchased from Merck (Amsterdam, The Netherlands). 1,1,3,3-tetramethylguanidine (99%), N-methyl-d_3-2-pyrrolidinone-d_6 and formic acid (98-100%) were purchased from Sigma-Aldrich (Zwijndrecht, The Netherlands). Triethylammonium formate was synthesized in-house from formic acid and triethylamine according to the procedure of Attri *et al*. [21].

4.2.2 Synthesis of model polymers

Copolymers were synthesized by reacting either BA, MMA, EA or EMA, with AA or MAA in various weight ratios (φ, see Table 4.1) using emulsion polymerization [22, 23]. Water containing 2.3% by weight sodium lauryl sulfonate was heated to 80°C prior to addition of the monomer seed (*i.e.* a preformed polymer dispersion), which contains 5% by weight of total monomer. The targeted total concentration of polymer is 30% by weight in water. Directly after addition of the monomer feed, 0.5% (based on the weight of monomer) of ammonium persulphate was slowly added to the mixture during three minutes to initiate the reaction. The remaining 95% of the monomer feed (containing 0.5 % by weight of 1-dodecane thiol as chain transfer agent) was added during 90 minutes, while maintaining

the reaction temperature at 85°C. The same temperature was maintained for 60 minutes after completion of the monomer feed. Thereafter, the batch was cooled to 30°C. At this stage, neutralizing agent (25% by weight of ammonia in water) was added until a pH between 7.5-8.5 was obtained. Model polymers MMA 7-12 were synthesized by preparing a stock solution of MMA (20.6 g) and MAA (1.2 g) which was mixed well. 2.5 mL of this mixture was transferred into a 20 mL headspace tube, after which 10.0 mL butylglycol was added. Reaction was initiated by the addition of 0.5 – 8.0 % (w/w) of 2,2'-Azodi-2-methylbutyronitrile (AMBN). Vials were tightly capped, and placed in a 6-position headspace GC agitator, which was operated at 75° C using consecutive 500 rpm mixing for 5 seconds and a stop time of 2 seconds. The mixtures were reacted for 18 hours.

Table 4.1. Overall theoretical composition of model polymer systems.

Sample	**φ_{EA} % (w/w)**	**φ_{AA} % (w/w)**	**M_n(kDa)[a]**	**M_w(kDa)[a]**	**#acids/chain[b]**
EA 1	100.0	0.0	31	81	0.0
EA 2	97.7	2.3	30	77	9.7
EA 3	95.4	4.6	30	78	19.1
EA 4	92.0	8.0	32	86	35.5
EA 5	89.6	10.4	31	83	45.0
EA 6	87.5	12.5	34	84	59.1
Sample	**φ_{MMA} % (w/w)**	**φ_{MAA} % (w/w)**	**M_n(kDa)[a]**	**M_w(kDa)[a]**	**#acids/chain[b]**
MMA 1	100.0	0.0	26	44	0.0
MMA 2	98.1	1.9	27	50	7.1
MMA 3	96.0	4.0	29	59	16.1
MMA 4	93.9	6.1	27	49	22.9
MMA 5	91.5	8.5	27	50	31.9
MMA 6	89.7	10.3	25	60	35.8
MMA 7	94.5	5.5	40	93	30.3
MMA 8	94.5	5.5	25	65	19.4
MMA 9	94.5	5.5	15	45	114
MMA 10	94.5	5.5	11	33	8.4
MMA 11	94.5	5.5	8.3	26	6.4
MMA 12	94.5	5.5	7.1	22	5.5
Sample	**φ_{BA} % (w/w)**	**φ_{AA} % (w/w)**	**M_n(kDa)[a]**	**M_w(kDa)[a]**	**#acids/chain[b]**
BA 1	100.0	0.0	29	75	0.0
BA 2	97.8	2.2	29	72	8.9
BA 3	95.3	4.7	30	69	19.6
BA 4	93.0	7.0	27	65	26.2
BA 5	90.8	9.2	26	72	33.1
BA 6	87.8	12.2	28	82	45.6

Table 4.1. Continued

Sample	φ_{EMA} % (w/w)	φ_{MAA} % (w/w)	M_n(kDa)[a]	M_w(kDa)[a]	#acids/chain[b]
EMA 1	100.0	0	47	89	0.0
EMA 2	98.0	0.99	46	90	5.3
EMA 3	95.8	2.11	48	93	11.8
EMA 4	93.5	3.26	46	89	17.4
EMA 5	92.0	3.99	48	95	22.3
EMA 6	89.2	5.40	50	92	31.4

[a] Molecular weight determined by SEC (see Section 4.2.3.2 for conditions).
[b] Determined by multiplying M_n with φ, and divide by molecular weight of the acid used.

Samples were prepared for chromatographic injection by dissolving 50 mg of polymer dispersion (approximately 30% by weight polymer in water) in 1.5 mL of NMP. These samples were dissolved at ambient temperature for one hour using a vial shaker (VWR, Amsterdam, The Netherlands) operated at 1000 *rpm*, prior to injection onto the chromatographic systems.

4.2.3 Instrumentation

4.2.3.1 Reversed-phase and normal-phase liquid chromatography

Separations were performed on an Acquity H-Class separation system (Waters, Milford, MA, USA) using an Acquity ELSD (Waters) for detection purposes. In the case of reversed-phase (RP) LC, the column used was a BEH Shield C18, 100×2.1mm i.d., 1.8-µm particles RPLC column (Waters). Column temperature was kept at 40°C throughout the analysis. Injection volume of the prepared samples (see paragraph 2.3) was 2 µL. Flow rate was 0.4 mL·min^{-1}. Starting mobile phase (A) was 70% (v/v) acetonitrile and 30% (v/v) water containing 0.1% (v/v) trifluoroacetic acid, which was held constant for 0.2 min. A linear 10-minute gradient was applied to mobile phase B, which was 100% tetrahydrofuran. The final composition was maintained for an additional two minutes. A 2-min linear gradient brought the mobile-phase composition back to initial conditions, which were maintained for two minutes before the next injection.

In case of normal-phase (NP) LC, two Xselect Cyano columns, 100×2.1mm i.d., 2.5-µm particles (Waters) were used, connected in series. Column temperature was kept at 40°C throughout the analysis. Injection volume of the prepared sample (see paragraph 2.3) was 2 µL. Flow rate was 0.5 mL·min^{-1}. Starting mobile phase (A) was 100% (v/v) 2,2,4-trimethylpentane, which was held for 0.2 minutes. A linear gradient was applied to mobile phase B, which was 100% (v/v) tetrahydrofuran, in ten minutes. This

composition was maintained for two minutes, before a gradient returned the mobile-phase composition to the initial conditions in two minutes. The initial conditions were maintained for two minutes before the next injection.

4.2.3.2 Size exclusion chromatography

SEC measurements involving the 1260 HT-ELSD G7826A (Agilent technologies) were performed on a LC Waters Alliance 2695 separations module using a column set consisting of three PL gel Mixed-B styrene-divinylbenzene columns. Eluent was NMP, containing 10 mM ammonium acetate, flow rate is 1 $mL \cdot min^{-1}$ and injection volume was 100 µL. This setup was also used for the molecular weight determination of the model polymers used in this research, but by using a Waters 2410 refractive index detector instead of the HT-ELSD module. Narrow polystyrene standards ranging from 400 Da – 1 MDa were used to construct a conventional calibration curve.

4.2.3.3 Ion-exchange chromatography

Separations were performed on a 2695 Alliance separation system (Waters), using an Agilent 1260 HT-ELSD (Agilent, Waldbronn, Germany) for detection. A 150×2.1mm i.d., 8-µm particles, PL-SAX strong-anion-exchange column (Agilent, Waldbronn, Germany) was used, which contained styrene-divinylbenzene-based particles with a quaternized polyethyleneimine coating. The column temperature was kept at 40°C throughout the experiments. Initial column equilibration from aqueous conditions to non-aqueous conditions was performed by running a linear gradient from 1% (v/v) methanol in water to 100% methanol in 60 minutes. A second equilibration step was performed by running a 60-minute gradient from methanol to pure NMP. Injection volume of the prepared sample (see paragraph 2.3) was 5 µL. Depending on the experiment, the starting mobile phase (A) was 50 mM tetramethyl guanidine in NMP and the eluting mobile phase (B) was 200 mM triethylammonium formate in NMP, containing 50 mM tetramethyl guanidine. Starting conditions for IEX gradient elution were 100% A at a flow rate of 0.3 $mL \cdot min^{-1}$. The eluent composition was maintained at 100% A for 1 minute, after which the composition was changed linearly to 100% B in 20 minutes. This final composition was maintained for 1 minute, after which the initial conditions (100% A) were re-established in 2 minutes using a linear gradient. To fully re-equilibrate the system, the composition was held at 100% A for 5 minutes prior to the following injection. The ELSD was operated at 110°C for transfer line, evaporator and nebulizer. Detector gas flow was set to 0.5 standard L N_2/min with a lamp power of 100%.

4.2.4 Data processing

The detector signal was imported into Waters Empower 3 software using an SATIN A/D convertor (Waters) with a sampling rate of 5 Hz. The recorded raw data were processed using the solver function in a home-built Microsoft Excel program to obtain the solvent-specific linearization factor [24, 25], which was established at 1.75 (*corrected output* = *(elsdsignal - baselinesignal*)$^{0.571}$). Linear and uniform detector response was validated using homopolymers of polyethylene glycol, polystyrene, poly(methyl methacrylate) and poly(ethyl methacrylate).

4.2.5 Nuclear magnetic resonance spectroscopy

^{1}H-NMR spectra are recorded on a Bruker 400 MHz (Bruker, Rheinstetten, Germany) using a 30° pulse width and relaxation delay d1 of 2 seconds at 25°C. Acrylic acid was dissolved in NMP (containing 5% by volume of NMP-d9 (N-methyl-d_3-2-pyrrolidinone-d_6) for locking) to a concentration of approximately 0.6% by weight. Samples were prepared with an increasing molar ratio of TMG/AA ranging from 0,12 to 10. ^{1}H-shift of the double-bond *trans*-proton was used for assessing the degree of deprotonation of the carboxylic acid group.

4.3 Results and discussion

4.3.1 Reversed-phase liquid chromatography

The samples described in the experimental section were analyzed by RPLC. The prepared polymers showed expected elution behaviour, a decrease of retention is observed upon an increase of the acid content in the polymer samples. An example of these elution profiles (EA-AA copolymers) is shown in Figure 4.1.

Similar behaviour is observed for all polymer systems. The most-polar copolymer (MMA-MAA) eluted first (Figure 4.2). When the length of the acrylate alkyl chain increases or when an acrylic backbone is replaced for a methacrylic one, the retention increases. In all cases, the incorporation of increasing concentrations of (meth)acrylic acid resulted in shorter retention times. Incorporation of multiple comonomers next to the (meth) acrylic acid monomers complicates this picture. Retention in this chromatographic mode is sensitive to changes in acid incorporation, but is not otherwise selective for the acid functionality itself, as various copolymers with varying concentrations of acid co-elute. As expected, the polarity of the comonomer also plays a significant role in retention behaviour. This can be seen in Figure 4.2 (compare, for example, EA with 12% AA and MMA without acid or EMA with 11% methacrylic acid and EA without acid).

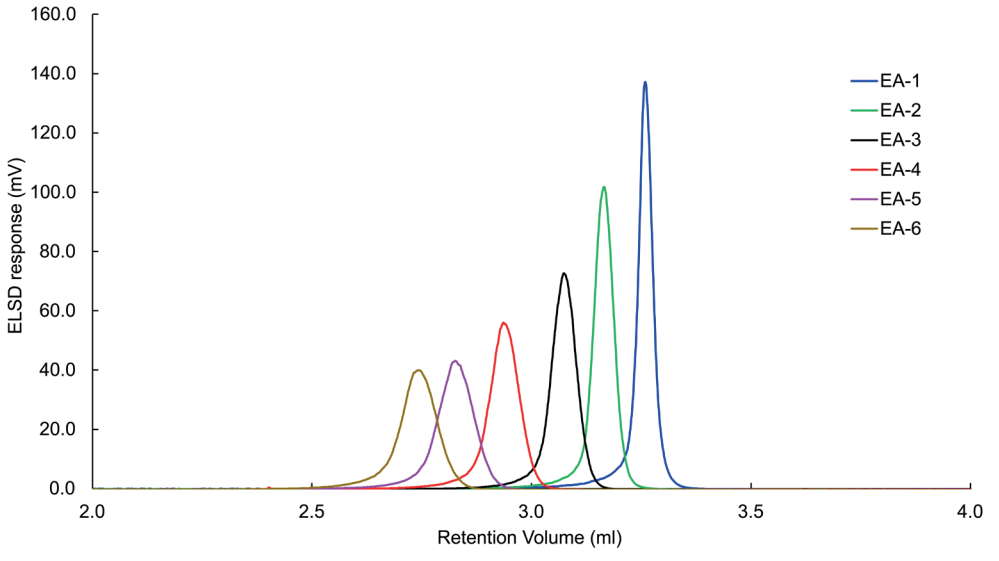

Figure 4.1. Reversed-phase elution profile of copolymers of acrylic acid with ethyl acrylate. Retention decreases upon increase of acrylic acid content. Gradient-elution conditions as specified in section 4.2.3.1.

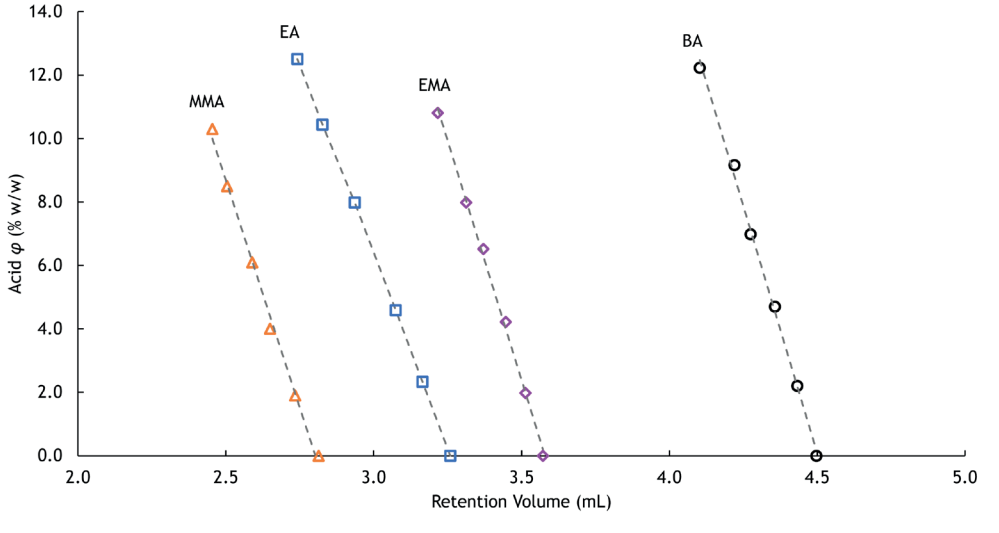

Figure 4.2. Reversed-phase retention volumes of copolymers of (meth)acrylic acid with comonomers varying in polarity. Retention increases in the order MMA < EA < EMA < BA. Gradient-elution conditions as specified in section 4.2.3.1.

4.3.2 Normal-phase liquid chromatography

As expected, in comparison with the RPLC retention patterns, NPLC yields opposite retention behaviour (see Figure 4.3 and Figure 4.4).

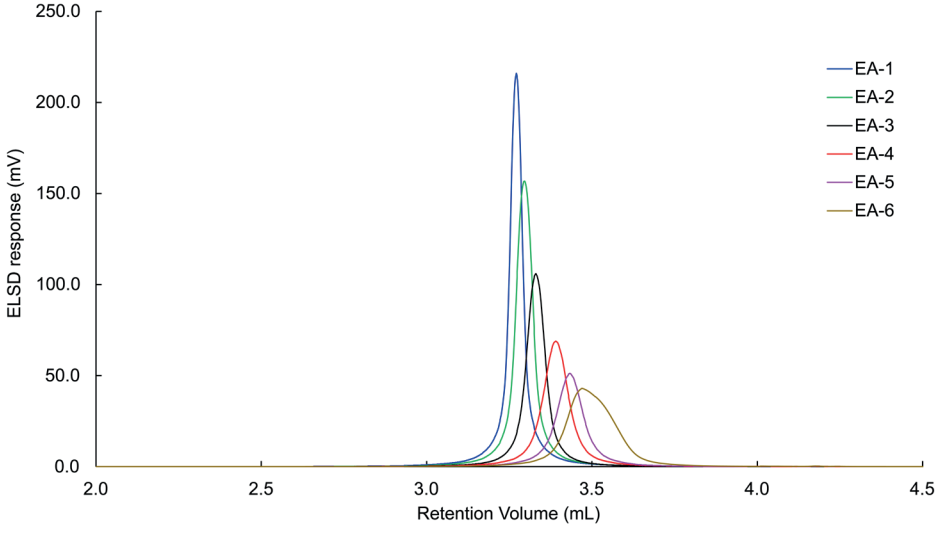

Figure 4.3. Normal-phase elution profile of copolymers of acrylic acid with ethyl acrylate. Retention increases upon increase of acrylic acid content. Gradient-elution conditions as specified in section 4.2.3.1.

In this case, the least-polar copolymer (with BA as comonomer) eluted first, followed by increasingly polar copolymers (elution order BA < EMA < EA < MMA). An increasing fraction of (meth)acrylic acid incorporated in the copolymers now resulted in an increase in retention, as expected due to the increased interaction of these polar monomers with the stationary phase. While, as in RPLC, retention was influenced by the presence of acidic monomers, the polarity of the polymer backbone was found to play a comparable role in the retention behaviour.

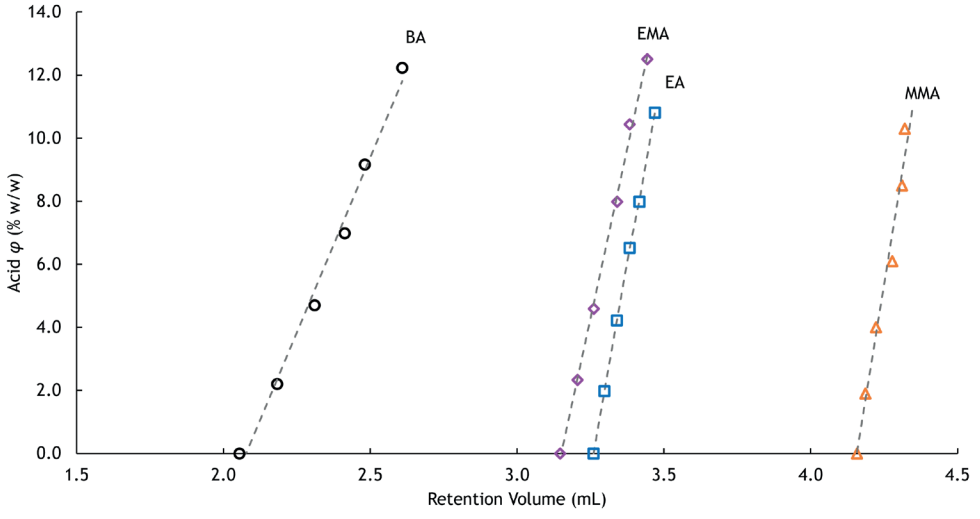

Figure 4.4. Normal-phase elution behavior of copolymers of (meth)acrylic acid with comonomers varying in polarity. Retention increases in the order BA < EMA < EA < MMA. Gradient-elution conditions as specified in section 4.2.3.1.

4.3.3 Nuclear magnetic resonance spectroscopy

Titration-NMR is a common way to measure pKa values in aqueous and non-aqueous conditions [26, 27]. To verify the dissociation of the carboxylic acids in NMP by the TMG base, ^{1}H-NMR experiments were performed using AA monomer as a model compound. Chemical shift of the *trans*-proton (average of two doublets) of the double bond without added base was 6.0 ppm (spectrum shown in Figure 4.5), this clearly shifted to lower chemical shifts upon addition of TMG in increasing molar ratios. A peak with a broad chemical shift was also observed in the ^{1}H-NMR region of interest, which is an interference from the protonated TMG.

Using the Henderson-Hasselbalch equation [28] together with the known pK_a of TMG (12.8, [20]), the molar ratio of TMG/acid could be translated to a non-aqueous pH, which is commonly noted as pH*. A clear sigmoidal curve of the selected proton chemical shift is obtained upon increase of the TMG/AA ratio, which shows an equivalence point around a pH* of 12.4. This approximation for the pK_a of AA in NMP corresponds very well with pK_a values of other, similar acids in NMP [20]. The obtained data shows that intended mobile phase conditions for NAIEX (50 mM TMG in NMP, which is a significant molar excess (>100) even for polymers with a high acid content) are more than sufficient to provide full dissociation (>99%) of the carboxylic-acid functional polymers in NMP.

We have assumed that any changes in acid pK_a due to radical polymerization of the acid monomer or the influence of neighbouring acid-groups in the polymer are negligable.

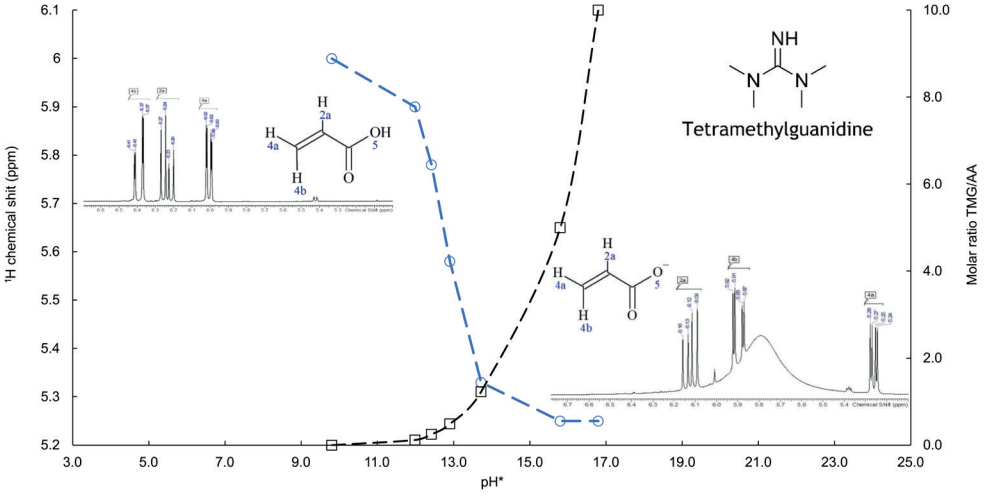

Figure 4.5. ^{1}H-NMR chemical shift of the trans-proton of AA (4a as indicated in the Figure inset) as a function of pH. Molar ratio of TMG to acid is shown on the right axis. Chemical shift indicated in blue circles, molar ratio in black squares. Figure insert shows the chemical structure of tetramethylguanidine.*

4.3.4 High-Temperature ELSD optimization

The ELSD peak areas of the polymer peaks were corrected by linearization of each data point using the following formula:

$$Corrected\ Output = (ELSD_{signal} - Baseline_{signal})^{1/a}$$

In which *a* is the power factor which can be approximated by optimizing the R^2 value of a linear correlation of the concentration-peak area calibration curves of several polymer concentrations. Key aspect in this calculation is that each point in the chromatogram is corrected for the power dependency, followed by peak area determination rather than direct peak area correction. The solver function in excel may be used to vary the *a* factor so that an optimally approximated linear calibration curve is obtained (Figure 4.6A through 4.6D).

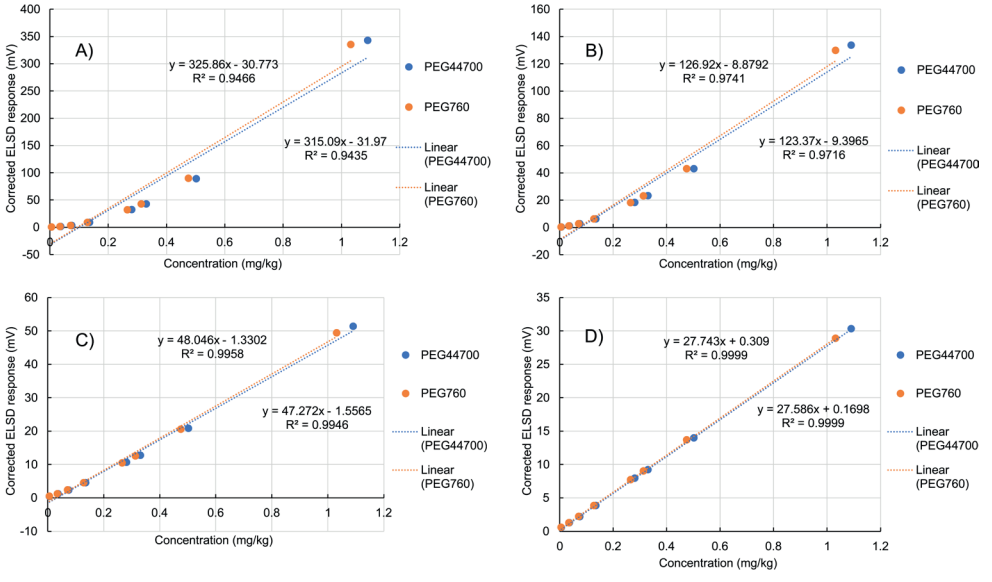

Figure 4.6. Linear approximation of PEG 760 Da+PEG 44700 Da peak areas. Power factor 1 (raw data, a), 1.2 (b), 1.5 (c) and 1.75 (d).

Supplier data, stating that the power factor is solely dependent on solvent composition, appears to be true as different types of polymers all show a near-linear response using a power factor of 1.75 (Figure 4.7). The only deviating polymer is pMMA 645 Da, which shows approximately 50% peak area compared to higher molecular weight polymers at comparable concentrations. This is likely due to the relatively volatile nature of this material when using the applied ELSD temperature settings (110°C). Although this is a limitation of the instrument, for materials >800 Da the linear approximation of the detector signal provides a (near) universal detector signal for any kind of eluted polymer, regardless of *dn/dc*. Obviously, this is assuming complete elution of the polymers.

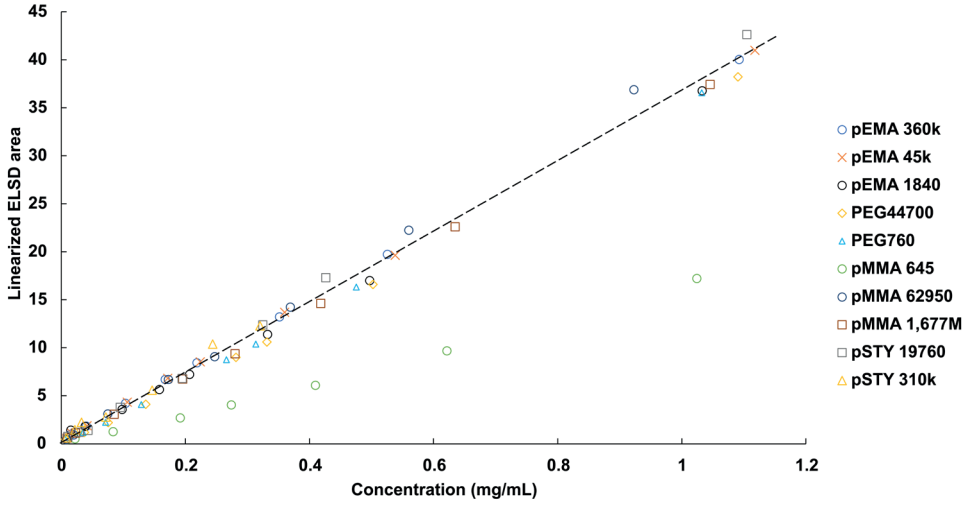

Figure 4.7. Corrected (linearized) ELSD peak area as function of concentration of various polymer types and molecular weights using ELSD power factor of 1.75.

4.3.5 Non-aqueous ion-exchange chromatography

There are various scenarios to affect retention in ion exchange chromatography. These are schematically represented in Figure 4.8.

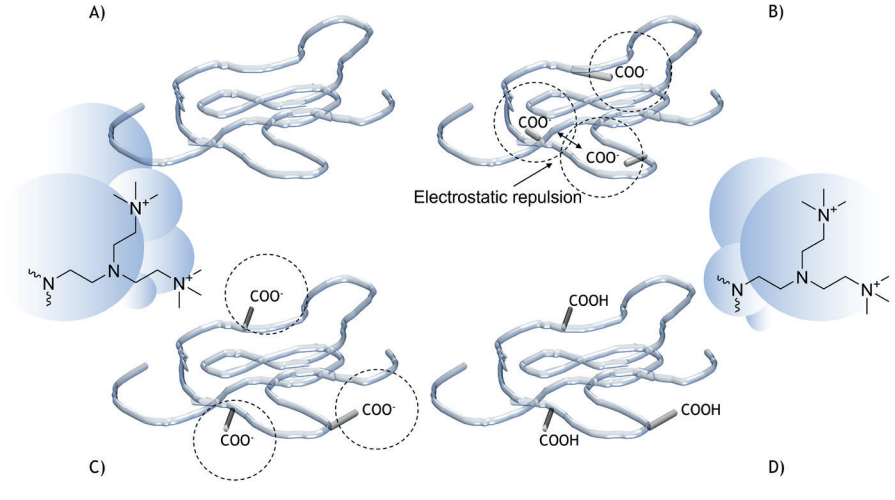

Figure 4.8. Schematic representation of random polymer coils in solution. A) polymer without anionic groups, B) polymer containing deprotonated carboxylic-acid moieties unavailable for interaction with quaternary ethyleneimine stationary phase, C) polymer featuring deprotonated carboxylic acid functionalities, D) polymer featuring neutral carboxylic acid functionalities. Dashed circles indicate charged moieties.

Figure 4.8A represents a polymer without acid functionalities, which cannot undergo ion-exchange interactions and will elute unretained. This is in agreement with the observed elution volume (around 0.6 mL) of the polymers without acid functionalities (EA-1) seen in Figure 4.9. Indeed, the elution volume of these polymers corresponds to the dead volume of the column (vo).

Polymers bearing deprotonated carboxylic acid groups are depicted in Figure 4.8C, the anionic polymer can undergo IEX interaction with the charged moieties of the stationary-phase surface and will be retained. However, it is possible that a fraction of the molecules of the acid-containing copolymer sample contain no acid groups. That would result in a fraction of the polymer eluting unretained. Moreover, the possibility of buried charges should be considered, as depicted in Figure 4.8B. As the polymer-bound anionic groups should be physically near the stationary-phase ion exchange sites, any deprotonated acid functionality that is not able to come into contact with the stationary phase can also limit retention. This effect is known as charge shielding [29, 30]. As these ionic groups are all negatively charged, one could expect an inter- or intramolecular electrostatic repulsion between these groups, which would be beneficial for the intended ion-exchange interaction with the stationary phase in the sense that the carboxylate groups are available for interaction. The degree to which these groups are actually available for interaction is difficult to quantify. Lastly, polymers which do feature carboxylic acid functionality but are not deprotonated will also elute unretained (Figure 4.8D). Since all experimental conditions employ a constant concentration of base, the existence of permanently non-deprotonated species is unlikely. Rather a dynamic equilibrium takes places between both neutral- and deprotonated states but, based on the NMR experiments shown in paragraph 4.3.3, dissociation of the acid monomers is largely complete. This makes the state as depicted in Figure 4.8D (which would occur in absence of base) unlikely.

As expected (and desired), all (meth)acrylic (co-)polymers without acid functionality were unretained in NAIEX analysis, regardless of polarity and alkyl length (V_0, Figures 4.9 and 4.10).

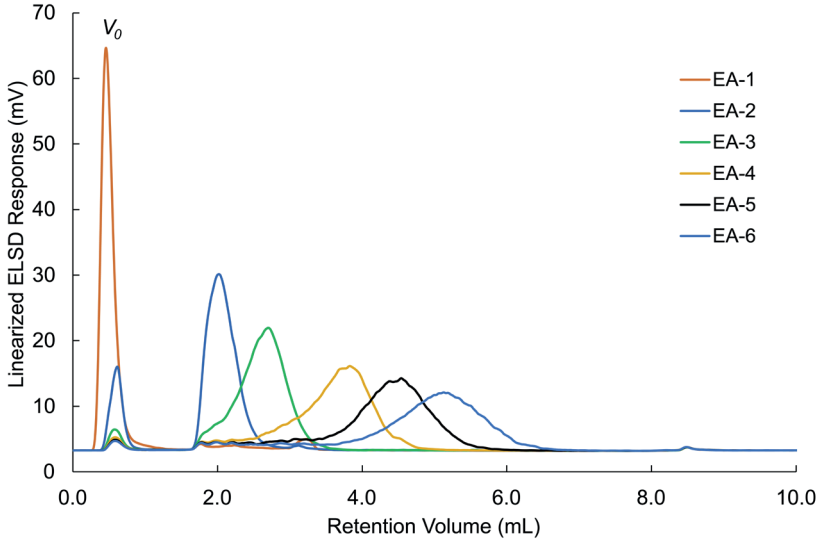

Figure 4.9. Overlay of ion-exchange chromatography separations of EA-AA copolymers EA-1 through EA-6 (see Table 4.1 for details). Base concentration 50 mM, further gradient-elution conditions as specified in section 4.2.4.2.

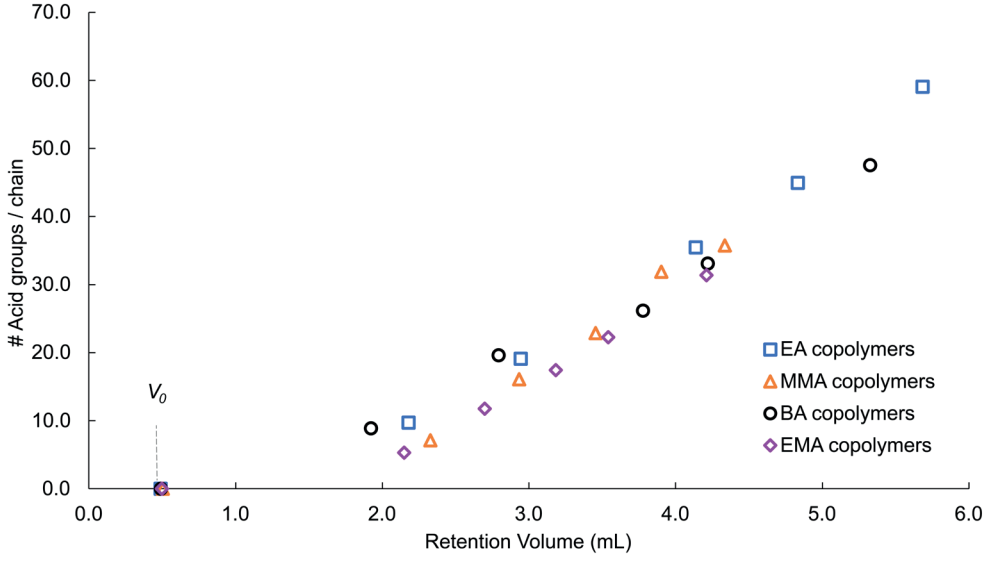

Figure 4.10. Retention of (meth)acrylic acid copolymers composed of various comonomers in non-aqueous ion-exchange chromatography. Base concentration 50mM, further gradient-elution conditions as specified in section 4.2.3.3.

Retention of the copolymers increased with increasing acid content. This indicated that the carboxylic acids of the polymers were deprotonated by the TMG, resulting in polymers with an increasing anionic charge – and thus retention. Addition of TMG to the starting mobile phase appeared critical for initial adsorption of the polymers to the stationary phase. Initial mobile-phase compositions without the TMG base result in elution of the acid-functionalized polymers at V_0. To elute copolymers with anionic moieties, the presence of organic salts in the mobile phase is necessary, indicating that the main retention mechanism is ion exchange.

The copolymers containing anionic functionality start to elute at a retention volume of 1.8 mL. The polymer distribution containing 2% by weight of AA (EA-2) shows, contrary to other (fronting/tailing) distributions, only a distinct tailing. This indicates that at this retention volume there is a rapid desorption of all adsorbed polymers (probably related to the non-linear adsorption isotherm as a result of limited ion-exchange capacity). Also, polymers with a higher average acid content start eluting around the retention volume of 1.8 mL, which indicates that also in these samples there is a fraction of low acid content. Minor disturbances in the baseline are observed between a retention volume of 1.8 mL and 4.0 mL (Figure 4.7), also in blank injections.

A correlation was observed between the retention volume and theoretical number of acid groups per chain in the polymers (Figure 4.10), with an increasing number of acid groups per chain resulting in an increase in retention volume irrespective of comonomer polarity. Also, we have found that an increase in molar mass using the same polymer composition results in an increased retention volume (Figure 4.11 and Figure 4.12). As an example: an increase in M_w from 22 kDa to 93 kDa (polymers MMA-7 through 12) results in an ion exchange retention volume increase of 0.9 mL.

This can be explained by the fact that polymers with a higher molar mass also contain a higher absolute number of acid-monomer units that can undergo interaction with the IEX stationary phase.

The above effects are significantly different from the retention behaviour in normal- and reversed-phase chromatography, where retention was found to depend on the overall polarity of the copolymer backbone, with only a minor effect acid content on retention. In contrast, retention in IEX appeared to be dominated by the number of acid groups incorporated in the copolymers, regardless of the polarity of the copolymer backbone.

As can be seen in Figure 4.9, a small fraction of the copolymers with high concentrations of incorporated acid was found to elute unretained (V_0). Possibly, there are no acid

groups in these chains – or an insufficient number of deprotonated acid groups that can interact with the stationary phase.

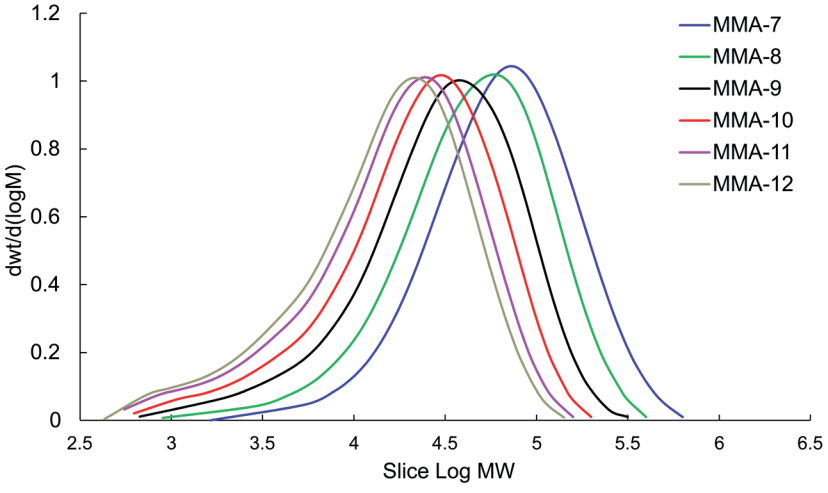

Figure 4.11. Molecular weight distribution profiles of pMMA-co-MAA resins of similar composition but difference in molar mass.

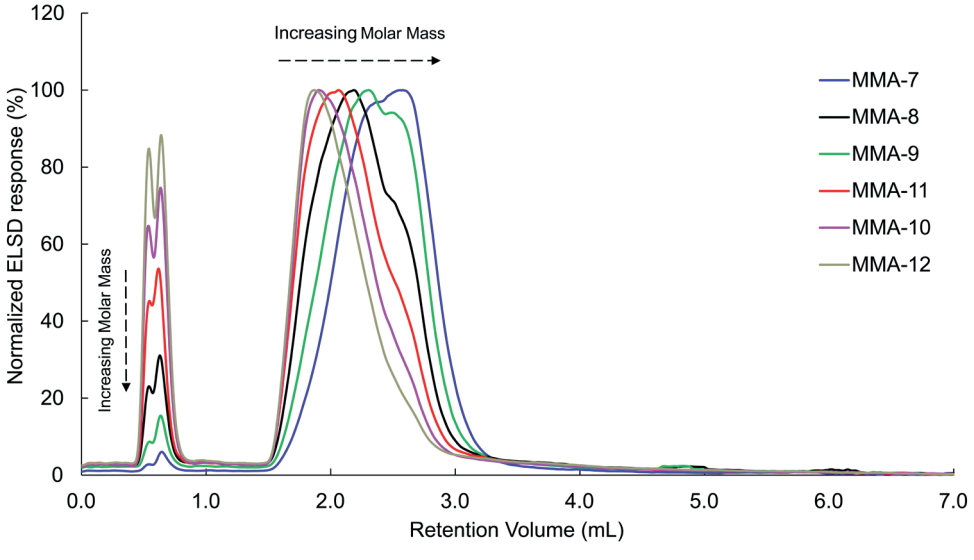

Figure 4.12. Ion Exchange elution profiles of MMA-7-12 resins of similar composition but difference in molar mass.

The insert in Figure 4.13 illustrates the relationship between retention volume and number of acid groups per chain in the copolymers. Using this correlation the retention-volume axis in Figure 4.10 can be translated into a compositional axis, with the curves describing the acid-functionality distribution (AFD) of the copolymers (Figure 4.13). The distributions were found to broaden roughly proportionally with the increase in number of acid groups per chain of the copolymer, in agreement with the notion that the number of statistical possibilities of acid incorporation increases with increasing acid content. Calculated peak apex of earliest-eluting (retained) copolymers is at 4-5 acid groups, which indicates that copolymers with a lesser number of acid-groups per chain will elute unretained. This would explain the unretained polymer fractions observed in Figure 4.9.

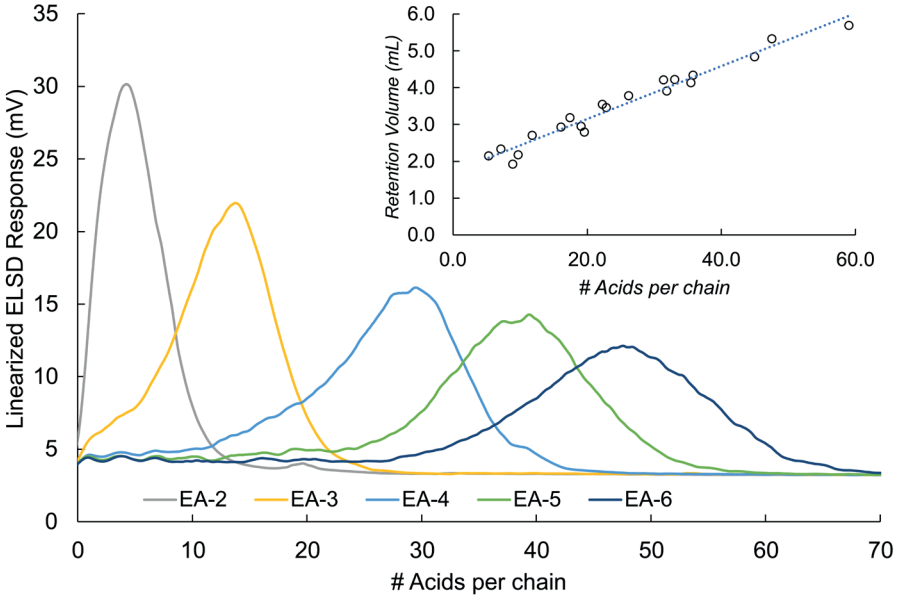

Figure 4.13. Acid functionality distribution based on NIEX chromatography for EA-2 through EA-6 copolymers with increasing number of incorporated acid groups. For conditions see section 4.2.4.2.

To investigate polymer elution and response in NAIEX-ELSD, injections of different concentrations of model polymer EMA-3 (containing 2.1% by weight of methacrylic acid, Table 4.1) were performed using the developed ion-exchange method. Absolute quantities of polymer injected ranged between 2 and 30 µg. The results of the injections of EMA-3 are shown in Figure 4.14.

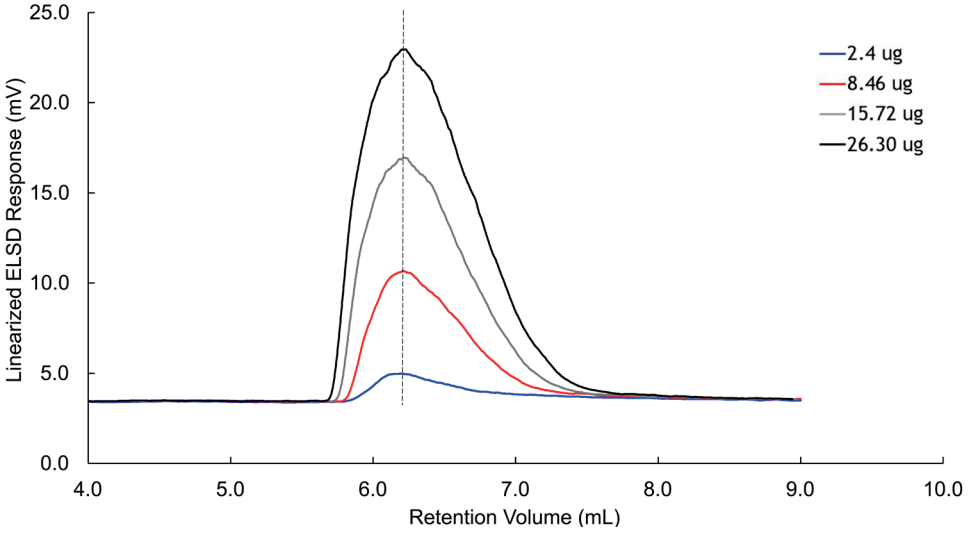

Figure 4.14. Peak-shape comparison of EMA-3 samples analyzed by NAIEX (t_r = 6.3 minutes).

A linear trend between peak area and injected concentration was observed (data not shown). This was consistent with the SEC-ELSD results from the detector-linearization protocol as described in the paragraph 4.3.4. The linear response curve that is obtained together with the observed peak shapes (without excessive peak tailing) suggest that elution is complete. We have no indication of significant irreversible adsorption of the polymer on the stationary phase. Moreover, chromatograms of the injected polymer samples show that the top does not shift when the injected concentration increase, indicating that the capacity of the stationary phase to interact with sample ions is not exceeded. This may not hold true for polymer samples with a lower number of acid groups, as already described in this paragraph for the elution of sample EA-2 (Figure 4.9).

Although the applied LC conditions were relatively harsh, we have not observed appreciable degradation in column performance over the course of several weeks. After approximately two months of prolonged exposure to the applied mobile phase (including storage), a decrease in retention volume is observed of roughly 10%. This indicates a slight loss in ion exchange capacity, most likely due to a degradation of the stationary phase ionic moieties. It is recommended to gradually re-equilibrate the IEX column back to aqueous conditions for storage purposes.

4.4. Conclusions

We have demonstrated non-aqueous ion-exchange chromatography of carboxylic-acid functional copolymers by after deprotonation using the organic superbase 1,1,3,3-tetramethylguanidine. An increase in the number of (meth)acrylic acid groups in a copolymer resulted in an increase in retention. Uncharged polymers (without carboxylic-acid groups) eluted unretained, regardless of the polarity of the polymer. Also for charged polymers the influence of the polarity of the comonomer was found to be very limited, indicating little or no or hydrophobic interactions. The necessity of adding organic base to the starting mobile phase for deprotonation of the polymers and of organic acid salt to the eluting mobile phase offer strong indications that ion-exchange is the prevailing retention mechanism. The proposed mode of polymer chromatography is an interesting alternative to conventional normal-phase and reversed-phase separations and it is thought to be particularly useful for obtaining acid-functionality distributions of complex copolymers. Ultimately, as in most cases dealing with complex polymers, two-dimensional LC approaches should be applied to obtain detailed insights in polymer heterogeneity. The developed NAIEX approach is expected to be well-suited for incorporation in such systems, we intend to explore the possibilities of such two-dimensional-setups in further research.

Acknowledgements

Lisette Konings and Jens de Bont from Covestro are acknowledged for the preparation of the model polymer systems. We would like to thank Agilent Technologies for the possibility to apply the HT-ELSD in this research and Wessel Jagers for his work on the optimization of HT-ELSD parameters. The authors thank Dr. Bob Pirok for the insightful discussions and constructive comments regarding this research. Finally, Dr. Jan Herrema and Evelien Pannekoek are acknowledged for their assistance in the ^{1}H-NMR experiments.

References

1. H. Morawetz, Y. Wang, Titration o Poly(acrylic acid) and Poly(methacrylic acid) in Methanol, Macromolecules 20 (1987) 94-95. https://doi.org/10.1021/ma00167a034.
2. P.J.C.H. Cools, F. Maesen, B. Klumperman, A.M. van Herk, A.L. German, Determination of the chemical composition distribution of copolymers of styrene and butadiene by gradient polymer elution chromatography, Journal of Chromatography A 736(1-2) (1996) 125-130. https://doi.org/10.1016/0021-9673(95)01369-5.
3. H.J.A. Philipsen, M.R. de Cooker, H.A. Claessens, B. Klumperman, A.L. German, Characterization of low-molar-mass polymers by gradient polymer elution chromatography II. Solubility effects in the analysis of polyester resins under reversed-phase conditions, Journal of Chromatography A 761(1-2) (1997) 147-162. https://doi.org/10.1016/s0021-9673(96)00807-2.
4. H.J.A. Philipsen, B. Klumperman, F.A.M. Leerrnakers, F.P.C. Wubb, A.L. German, Molar Mass Effects in Reversed-Phase Gradient Polymer-Elution Chromatography of Oligomers, Chromatographia 55 (2002) 533-540. https://doi.org/10.1007/BF02492898.
5. H. Gao, D.J. Siegwart, N. Jahed, T. Sarbu, K. Matyjaszewski, Characterization of α,ω-dihydroxypolystyrene by gradient polymer elution chromatography and two-dimensional liquid chromatography, Designed Monomers and Polymers 8(6) (2012) 533-546. https://doi.org/10.1163/156855505774597713.
6. C.N. Pomeranz, S.V. Olesik, Separation of poly-3-hydroxyvalerate-co-3-hydroxybutyrate through gradient polymer elution chromatography, J Chromatogr A 1218(44) (2011) 7943-7. https://doi.org/10.1016/j.chroma.2011.08.065.
7. A.M. Striegel, Determining the vinyl alcohol distribution in poly(vinyl butyral) using normal-phase gradient polymer elution chromatography, Journal of Chromatography A 971 (2002) 151-158. https://doi.org/10.1016/S0021-9673(02)00960-3.
8. M. Schollenberger, W. Radke, SEC-Gradients, an alternative approach to polymer gradient chromatography: 1. Proof of the concept, Polymer 52(15) (2011) 3259-3262. https://doi.org/10.1016/j.polymer.2011.05.047.
9. M. Schollenberger, W. Radke, Size exclusion chromatography-gradients, an alternative approach to polymer gradient chromatography: 2. Separation of poly(meth)acrylates using a size exclusion chromatography-solvent/non-solvent gradient, J Chromatogr A 1218(43) (2011) 7828-31. https://doi.org/10.1016/j.chroma.2011.08.090.
10. H. Maier, F. Malz, G. Reinhold, W. Radke, SEC Gradients: An Alternative Approach to Polymer Gradient Chromatography. Separation of Poly(methyl methacrylate-stat-methacrylic acid) by Chemical Composition, Macromolecules 46(3) (2013) 1119-1123. https://doi.org/10.1021/ma3023553.
11. H. Maier, F. Malz, W. Radke, Characterization of the Chemical Composition Distribution of Poly(n-butyl acrylate-stat-acrylic acid)s, Macromolecular Chemistry and Physics 216(2) (2015) 228-234. https://doi.org/10.1002/macp.201400399.
12. S. Fekete, A. Beck, J.L. Veuthey, D. Guillarme, Ion-exchange chromatography for the characterization of biopharmaceuticals, J Pharm Biomed Anal 113 (2015) 43-55. https://doi.org/10.1016/j.jpba.2015.02.037.

13. T. Ahamed, B.K. Nfor, P.D. Verhaert, G.W.v. Dedem, L.A.v.d. Wielen, M.H. Eppink, E.J.v.d. Sandt, M. Ottens, pH-gradient ion-exchange chromatography: an analytical tool for design and optimization of protein separations. , Journal of Chromatography A 1164 (2007) 181-188. https://doi.org/10.1016/j.chroma.2007.07.010.

14. Z. Kimia, S.N. Hosseini, S.S. Ashraf Talesh, M. Khatami, A. Kavianpour, A. Javidanbardan, A novel application of ion exchange chromatography in recombinant hepatitis B vaccine downstream processing: Improving recombinant HBsAg homogeneity by removing associated aggregates, J Chromatogr B Analyt Technol Biomed Life Sci 1113 (2019) 20-29. https://doi.org/10.1016/j.jchromb.2019.03.009.

15. A. Hirano, K. Iwashita, S. Sakuraba, K. Shiraki, T. Arakawa, T. Kameda, Salt-dependent elution of uncharged aromatic solutes in ion-exchange chromatography, J Chromatogr A 1546 (2018) 46-55. https://doi.org/10.1016/j.chroma.2018.02.049.

16. Y. Leblanc, N. Bihoreau, G. Chevreux, Characterization of Human Serum Albumin isoforms by ion exchange chromatography coupled on-line to native mass spectrometry, J Chromatogr B Analyt Technol Biomed Life Sci 1095 (2018) 87-93. https://doi.org/10.1016/j.jchromb.2018.07.014.

17. K. Sarmini, E. Kenndler, Ionization constants of weak acids and bases in organic solvents, J. Biochem. Biophys. Methods 38 (1999) 123-137. https://doi.org/10.1016/S0165-022X(98)00033-5.

18. K. Sarmini, E. Kenndler, Capillary zone electrophoresis in mixed aqueous–organic media: effect of organic solvents on actual ionic mobilities, acidity constants and separation selectivity of substituted aromatic acids. I. Methanol, Journal of Chromatography A 806 (1997) 325-335. https://doi.org/10.1016/S0021-9673(98)00060-0.

19. E. Rossini, A.D. Bochevarov, E.W. Knapp, Empirical Conversion of pK a Values between Different Solvents and Interpretation of the Parameters: Application to Water, Acetonitrile, Dimethyl Sulfoxide, and Methanol, ACS Omega 3(2) (2018) 1653-1662. https://doi.org/10.1021/acsomega.7b01895.

20. K. Izutsu, Electrochemistry in nonaqueous solutions, Wiley-VCH Verlag GmbH & Co.2002.

21. P. Attri, R. Bhatia, J. Gaur, B. Arora, A. Gupta, N. Kumar, E.H. Choi, Triethylammonium acetate ionic liquid assisted one-pot synthesis of dihydropyrimidinones and evaluation of their antioxidant and antibacterial activities, Arabian Journal of Chemistry 10(2) (2017) 206-214. https://doi.org/10.1016/j.arabjc.2014.05.007.

22. A.M.v. Herk, Chemistry and technology of emulsion polymerisation Blackwell Publishing2005.

23. J.C.d.l. Cal, J.R. Leiza, J.M. Asua, A. Butte, G. Storti, M. Morbidelli, Handbook of Polymer Reaction Engineering WILEY-VCH Verlag GmbH & Co2005.

24. A. Boborodea, S. O'Donohue, Linearization of evaporative light scattering detector signal, International Journal of Polymer Analysis and Characterization 22(8) (2017) 685-691. https://doi.org/10.1080/1023666x.2017.1367066.

25. A. Boborodea, S. O'Donohue, New evaporative light scattering detector for high temperature gel permeation chromatography, International Journal of Polymer Analysis and Characterization 22(7) (2017) 631-638. https://doi.org/10.1080/1023666x.2017.1358835.

26. J. Reijenga, A. van Hoof, A. van Loon, B. Teunissen, Development of Methods for the Determination of pKa Values, Anal Chem Insights 8 (2013) 53-71. https://doi.org/10.4137/ACI.S12304.

27. E.L. Ibarra-Montaño, N. Rodríguez-Laguna, A. Sánchez-Hernández, A. Rojas-Hernández, Determination of pKa Values for Acrylic, Methacrylic and Itaconic Acids by 1H and 13C NMR in Deuterated Water, Journal of Applied Solution Chemistry and Modeling 4 (2015) 7-18. https://doi.org/10.6000/1929-5030.2015.04.01.2.

28. R.d. Levie, The Henderson–Hasselbalch Equation: Its History and Limitations, Journal of Chemical Education 80 (2003) 146. https://doi.org/10.1021/ed080p146.

29. M. Abe, P. Akbarzaderaleh, M. Hamachi, N. Yoshimoto, S. Yamamoto, Interaction mechanism of mono-PEGylated proteins in electrostatic interaction chromatography, Biotechnol J 5(5) (2010) 477-83. https://doi.org/10.1002/biot.201000013.

30. J.E. Seely, C.W. Richey, Use of ion-exchange chromatography and hydrophobic interaction chromatography in the preparation and recovery of polyethylene glycol-linked proteins, Journal of Chromatography A 908 (2001) 235-241. https://doi.org/10.1016/S0021-9673(00)00739-1.

CHAPTER 5

Charge-based separation of acid-functional polymers using non-aqueous capillary electrophoresis employing deprotonation and heteroconjugation approaches

Ton Brooijmans, Pascal Breuer, Aniek Schreuders, Myrthe van Tilburg, Peter Schoenmakers, Ron Peters

Anal. Chem. 2021, 93, 14, 5924–5930, April 1, 2021,
https://doi.org/10.1021/acs.analchem.1c00311

Abstract

For selective analysis of the incorporated acidic monomers, a charge-based non-aqueous capillary electrophoresis (NACE) separation was developed. Two approaches were developed; i) deprotonation of the acid functionality with an organically-soluble strong base and ii) heteroconjugation of anions of carboxylic acids with incorporated acid functionality. In both approaches, N-methyl pyrrolidone, as a strong solvent for polymers with a favorable relative permittivity for presence of dissociated ionic species, was used for the separation. It was shown that anions of carboxylic acids specifically associate with the incorporated acid groups in the polymers, resulting in negatively charged complexes which could be separated based on charge-to-size ratio by NACE. Although both approaches give comparable results with respect to acid distribution for acid-functional polymers, the effective mobility of the deprotonated polymers is roughly double that obtained from the heteroconjugation approach. Unlike the heteroconjugation approach, deprotonation conditions were detrimental to the fused-silica capillary – limiting practical use. Polymers with different chemical composition, molecular weights and acid contents were subjected to the CE approaches developed; Polymers with varying molecular weight, but similar relative acid monomer content were shown to have similar migration times, which confirms that this approach separates polymers based on charge-to-size ratio.

5.1 Introduction

Water-borne polymers are an increasingly applied polymer class, which is used for various coating systems such as paints and inks. Contrary to traditional solvent-borne polymers, these polymers provide significantly reduced environmental- and workplace release of volatile organic compounds without sacrificing end product properties. Water-borne poly(meth)acrylics and polyurethanes are dispersed as small particles in water, stabilized by neutral or ionic surfactant species and/or the incorporation of polar/ionic monomers. To monitor and improve the industrial processes as well as to improve end-product properties, there is a strong need for methods allowing characterization of the acid incorporation in polymers. Recently, a non-aqueous ion-exchange chromatography approach was developed which could selectively separate polymers according to the content of incorporated carboxylic acid (Chapter 4 of this thesis [1]). Another interesting option to determine the acid distribution of these polymeric systems is capillary electrophoresis (CE), as it found numerous applications for the analysis of ionic analytes. In many cases, CE of ionogenic organic analytes is based on charging their acidic or basic moieties by selecting appropriate pH conditions. The application window of CE can be increased by using organic solvents, which potentially enables the analysis of non-water soluble materials, such as both natural and synthetic polymers. Various polymer applications have been described, such as capillary zone electrophoresis and non-aqueous capillary electrophoresis (NACE) using e.g. basic or acidic additives to (de) protonate the polymeric analytes [2-9]. To separate non-charged polymers to a specific property (size, degree of association with a charged species) various CE approaches have been developed such as capillary size-exclusion electrokinetic chromatography [10-12], or the addition of salts or surfactants to the background electrolyte (BGE) [13, 14].

As described above, various (NA)CE approaches have been developed and applied, but none of these approaches aimed for the selective separation based on the incorporated acid monomer in polyacrylate- and polyurethane polymers. To investigate the potential of NACE to determine the acid distribution in water-borne polymers, two strategies for achieving separation based on anionic polymeric charges under non-aqueous conditions were examined: i) deprotonation of the carboxylic acid moieties in the polymers and ii) heteroconjugation of anions with the polymer carboxylic acid moieties. Dissociation of carboxylic acids (HA) in a proton (H+) and conjugated base (A-) is a straightforward process, in which the degree of dissociation is dependent on the pH of the total system and the pK_a of the acid in question.

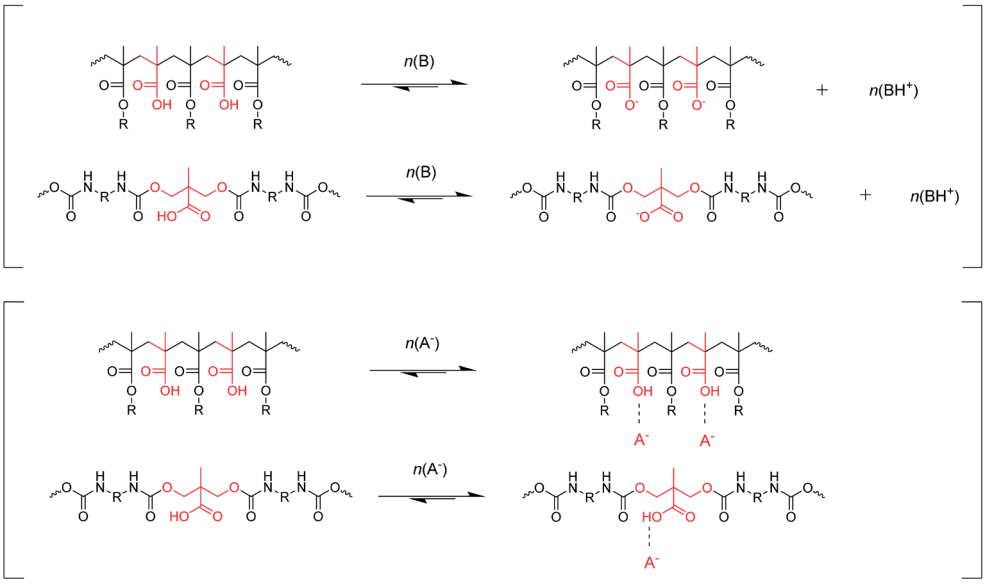

Figure 5.1. Schematic representation of the development of charge on acid-functional polyacrylate- and polyurethane polymers. Both high pH conditions (top) and heteroconjugation with anions (bottom), results in negatively charged polymers. Acidic sites are indicated in red.

Addition of a base (B) to an acid aids formation of a carboxylate (anion) functionality. A schematic representation of this process applied to polyacrylate and polyurethane polymers is shown in Figure 5.1. The actual number of induced charges in polymers by deprotonation is relevant, as there is a direct correlation of the number of charges per polymer chain with the electrophoretic mobility. As the studied polymers are not water-soluble, CE needs to be performed in an organic solvent (i.e. performing NACE). Previous research [1] revealed that N-methylpyrrolidone (NMP) is a good solvent for both the acid-functional polymers under study and the solubility of bases used for their deprotonation. However, under non-aqueous conditions, the pK_a of acids shifts to significantly higher values [15-17]. As a result, most organic bases do not have the base strength to dissociate these acids in non-aqueous conditions. A comparison of known pK_a values of acids in either water of NMP is shown in Figure 5.2.

Strong bases such as alkali-hydroxides have the base strength, but lack the solubility in organic solvents such as NMP. A base-type frequently used in non-aqueous titrations are the tetra-alkyl ammonium hydroxides. This compound class is soluble in most organic solvents due to the hydrophobic nature of the cation and consists of strong bases, capable of deprotonating carboxylic acids under non-aqueous conditions.

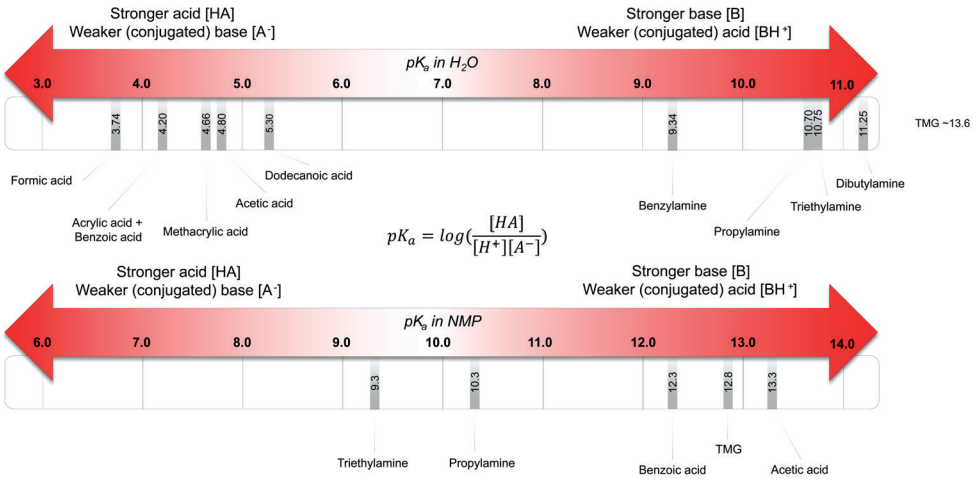

Figure 5.2. pK_a values of various acids in water (top arrow) and NMP (bottom arrow).

Charging of acidic polymers in dipolar aprotic solvents may also occur due to homo- or heteroconjugation [17]. Homoconjugation is the association of the acid anion (A-) with another acid molecule (HA), while heteroconjugation is the association of anion (A-) with a different acid type such as (meth)acrylic acid or dimethylol propionic acid in case of polyurethanes. This results in (A- * (meth)acrylic acid) complexes in the case of (meth) acrylic polymers or (A- * dimethylol propionic acid) complexes in the case of polyurethane polymers, as depicted in Figure 5.1. In this study, heteroconjugation is explored to provide charges to acidic polymers, making them suitable for characterization by CE [2, 18-25]. In the case of a polymer with a distribution in the number of incorporated acid groups, heteroconjugation may occur at multiple locations within the polymer which results in a poly-heteroconjugate. The process of heteroconjugation of carboxylic acid-containing polymers with anions (A-) is schematically represented in Figure 5.1, where n represents the number of charges (anionic heteroconjugation sites).

In this research, deprotonation- and heteroconjugation approaches for providing charges to acid-functional polymers were studied, using NMP as the solvent to establish BGE formulations. Model polymers of various composition and molecular weight are used. In the heteroconjugation approach, various organic anions are exploited to obtain charged polymers the effects of the type of anion are investigated. As the polymers of interest do not possess UV-absorbing functionalities, the detection is conducted using a contactless conductivity detector (C4D), as developed by Zemann *et al* [26].

5.2 Experimental

5.2.1 Materials

All material purity percentages are by weight, except when otherwise indicated. N-methylpyrrolidone (NMP, peptide-synthesis grade), tetrabutylammonium hydroxide (TBAH, 40% in methanol), formic acid (>99%), acetic acid (glacial), propionic acid (>99%), benzoic acid (>99.5%), hexanoic acid (>99.5%), lauric acid (>99%) and oleic acid (>98%) were purchased from VWR (Amsterdam, The Netherlands). 1,1,3,3-Tetramethylguanidine (TMG, 99%) and lithium bromide (>99% reagent plus grade) were purchased from Sigma-Aldrich (Zwijndrecht, The Nether-lands). Isophorone diisocyanate (Desmodur I, IPDI, >99.5%) and polypropylene glycol (PPG, average molar mass 2000 g/mol) were obtained from Covestro (Leverkusen, Germany). Dimethylol propionic acid (DMPA, >95%) was obtained from Perstorp (Arnsberg, Germany). Ultrapure water (18.2 $M\Omega.cm^{-1}$) was prepared using an ELGA Purelab Ultra water system (VWR). Methacrylic copolymers were synthesized by reacting methyl methacrylate (MMA) with methacrylic acid (MAA) in various molar ratios or molar masses using emulsion polymerization [27, 28], while the polyurethanes were prepared by reacting isophorone diisocyanate (IPDI) with a polyol mixture, consisting of PPG and DMPA. The composition (molar mass fraction of acid φ_m) is specified in Table 5.1).

5.2.2 Synthesis of water-borne methacrylic polymers

Methacrylic copolymers were synthesized by reacting MMA with MAA in various ratios (φ, see Table 5.1) using emulsion polymerization. Water containing 2.3% by weight sodium lauryl sulfonate was heated to 80°C prior to addition of the monomer seed (*i.e.* a pre-formed polymer dispersion), which contains 5% by weight of the total monomer feed. The targeted total concentration of polymer is 30% by weight in water. Directly after addition of the monomer feed, 0.5% (based on the weight of monomer) of ammonium persulphate was slowly added to the mixture during three minutes to initiate the reaction. The remaining 95% of the monomer feed (containing 0.5% by weight of 1-dodecane thiol as chain transfer agent) was added during 90 minutes, while increasing and maintaining the reaction temperature at 85°C. The same temperature was maintained for 60 minutes after completion of the monomer feed. Thereafter, the batch was cooled to 30°C. At this stage, neutralizing agent (25% by weight of ammonia in water) was added until a pH between 7.5-8.5 was obtained.

5.2.3 Synthesis of water-borne urethane polymers

Urethane polymers were prepared by reacting IPDI with a polyol mixture, consisting of PPG and DMPA (φ, displayed in Table 5.1). Synthesis was performed in two stages: prepolymer formation and dispersion/extension. An isocyanate-functional prepolymer was prepared by reacting the IPDI/PPG mixture using bismuth neodecanoate as catalyst. Reaction temperature was kept at 90°C for two hours, after which the temperature was decreased to 80°C for one hour. TEA was added to the prepolymer prior to dispersion stage. The prepolymer was gradually added to water in 45 minutes, keeping the sample temperature between 20-25°C. Urethane extension was performed by addition of N_2H_4, which resulted in a temperature increase of 5°C. Samples were mixed for one hour, after which the end samples were obtained (pH around 7.5, percentage of resin in water 18-20%).

Table 5.1. Characteristics of model polymer systems.

Sample	φ_m (%) [a]	M_n (kDa) [b]	M_w (kDa) [b]	Number of acids/chain [c]
pMMA-co-MAA-1	2.2	27	50	7.1
pMMA-co-MAA-2	4.7	29	59	16.1
pMMA-co-MAA-3	7.1	27	49	22.9
pMMA-co-MAA-4	9.9	27	50	31.9
pMMA-co-MAA-5	12.0	25	60	35.8
pMMA-co-MAA-6	6.4	37	93	23.7
pMMA-co-MAA-7	6.4	25	65	16.0
pMMA-co-MAA-8	6.4	15	45	9.6
pMMA-co-MAA-9	6.4	11	33	7.0
pMMA-co-MAA-10	6.4	8.3	26	5.3
pMMA-co-MAA-11	6.4	7.1	22	4.5
Polyurethane-1	3.0	40	380	11.9
Polyurethane-2	3.7	50	440	18.6
Polyurethane-3	4.5	52	400	23.3

[a] *Results from SEC-UV or titration.*
[b] *Molecular weight determined by SEC (see Experimental section for conditions).*
[c] *Determined by multiplying M_n with φ_m, and dividing by the molecular weight of the acid used.*

5.2.4 Size exclusion chromatography

Size-exclusion chromatography (SEC) was performed on a modular Agilent (Waldbronn, Germany) 1260 HPLC system, equipped with autosampler, pump, column compartment, multi wavelength UV detector and an 1260 multi-detector system consisting of a

refractive index detector, a viscosity detector and a light scattering detector. The eluent was NMP with 0.01 M lithium bromide at 0.75 mL·min^{-1} and a column temperature of 60°C. Three 300 mm × 7.5 mm i.d. PLgel Mixed-B columns packed with 10-µm particles (Agilent, Amstelveen, The Netherlands) were used in series. A 50 mm × 7.5 mm i.d. PLgel guard column was used (also packed with 10-µm particles). The injection volume was 100 µL. System control was performed using Agilent GPC/SEC software, version A.02.01.

5.2.5 Non-Aqueous Capillary Electrophoresis (NACE)

NACE was performed using a 7100 CE module, equipped with a PDA detector (Agilent, Waldbronn, Germany) and a TraceDec C4D (Innovative Sensor Technologies GmbH, Strasshof, Austria). Agilent standard fused-silica CE capillaries were used with an internal diameter of 50 or 75 µm, and a total length of 500 mm.

After installation of a new capillary, or at the start of a sequence (maximally 30 injections), a flushing sequence was performed with a series of liquids. Initially, 1 M sodium hydroxide was applied at 1000 mbar pressure for 5 min followed by 5 min rinsing with deionized water at 1000 mbar pressure and 2 min flushing with a hydro-organic mixture consisting of 20% (v/v) NMP in water. After this step, background electrolyte was run for 5 min. Samples were injected using pressure injection mode for 10 s at 50 or 25 mbar for 50 µm and 75 µm capillaries, respectively, followed by a background electrolyte dip for 2 s at the same pressure. The applied voltage was 30 kV, which was ramped up from 0 kV in 30 s.

Heteroconjugation conditions were achieved by using 20 mM TMG in NMP with 40 mM (formic, acetic, propionic, benzoic, hexanoic, lauric, oleic) acid as background electrolyte. The essentially neutral polymers are intended to be charged by the laurate anion, which is obtained from deprotonation by TMG. Analysis is performed using a 500 mm capillary with 75 µm i.d., with hydrodynamic injection (10 s, 25 mbar), 30 kV voltage, 60°C cassette temperature, and a positive pressure of 25 mbar applied on the sample inlet during analysis. Using standard formulas used in capillary electrophoresis the effective polymer mobilities can be determined:

$$\mu_{eff} = \frac{L_d * L_t}{V} \cdot \left(\frac{1}{t_m} - \frac{1}{t_{EOF}} \right)$$

In the equation above, L_d depicts the capillary length in m from CE inlet to the C4D, L_t the total capillary length in m, t_m the migration time of the polymers in s, t_{EOF} the migration time of the EOF marker in s and V the applied voltage.

5.3 Results and discussion

5.3.1 NACE using high pH conditions

The NACE separation of copolymers pMMA-co-MAA-1 to 5 (Table 5.1) employing deprotonation of polymer-incorporated acid functionalities using TBAH is shown in Figure 5.3. It clearly shows that the effective mobility of the polymers increases with increasing charge density. Some minor baseline disturbances are observed in all samples around an electrophoretic mobility of -1.0E^{-09} m^{2}V^{-1}s^{-1}, which slightly affected the migration profile of the 2.2% acid polymer (pMMA-co-MAA-1).

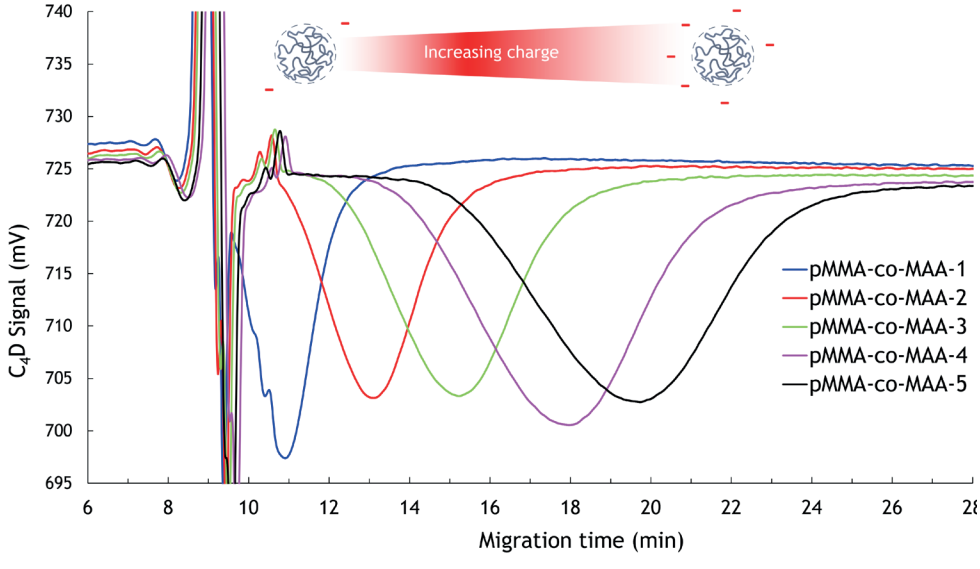

Figure 5.3. NACE of copolymers pMMA-co-MAA-1 to 5 (see Table 5.1 for the sample description) by deprotonation of polymer-incorporated acid functionality. Conditions used: 10 mM TBAH in NMP as background electrolyte, hydrodynamic injection (10 s, 50 mbar), 30 kV voltage, 60°C cassette temperature, 25 mbar pressure applied on sample inlet during analysis.

Addition of TBAH to NMP gives rise to a high background conductivity signal during CE, as well as relatively (for non-aqueous conditions) high currents. NACE of the model polymers clearly shows broad peaks of negatively charged species (based on the anodic directionality). These polymer are less conductive than the BGE, yielding relatively negative conductivity signals. An increase in the molar fraction of incorporated acid (φ_m) in the polymer results in higher migration times and thus larger polymer mobilities (more negative), which is expected due to the higher number of charges that can be present per polymer molecule. The sample without incorporated acid was not charged

and migrated with the EOF (not shown). The polymer containing 2.2% of MAA (sample pMMA-co-MAA 1) was, contrary to other the other samples, not baseline separated from the peak at 0 $m^2V^{-1}s^{-1}$. This suggests that this sample still contains a fraction of non-acid-containing polymer. Due to disruption by the EOF signal, complete characterization of this fraction is not possible. Increasing the TBAH base concentration from 10 to 20 or 50 mM induced an increase in effective polymer mobilities, as outlined in Figure 5.4. This indicates an increasing number of charged moieties on the polymer molecules with rising TBAH concentration. For the 20 and 50 mM TBAH it was observed that the polymer mobilities did not increase in direct proportion to the incorporated acid fraction. Polymers with higher acid fractions, as well as the polymer with the lowest fraction of incorporated acid show only a minimal increase in mobility, an effect that is not fully understood.

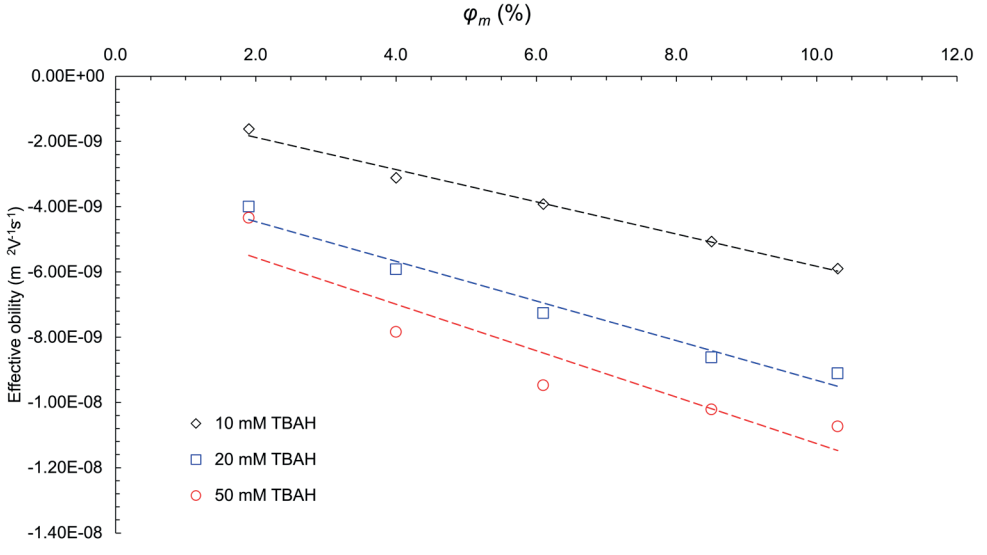

Figure 5.4. Effective mobilities of copolymers pMMA-co-MAA-1 to 5 as a function of TBAH concentration in the BGE.

After about 30 injections using the TBAH-containing BGE, significant deviations in migration times of both EOF and the polymers were observed. This effect persisted after rigorous capillary cleaning in between measurements and using fresh BGE. Replacement of the capillary resulted in the original separation profile and migration times. Cross-cuts of a used and an unused capillary were examined and compared by light microscopy (Figure 5.5).

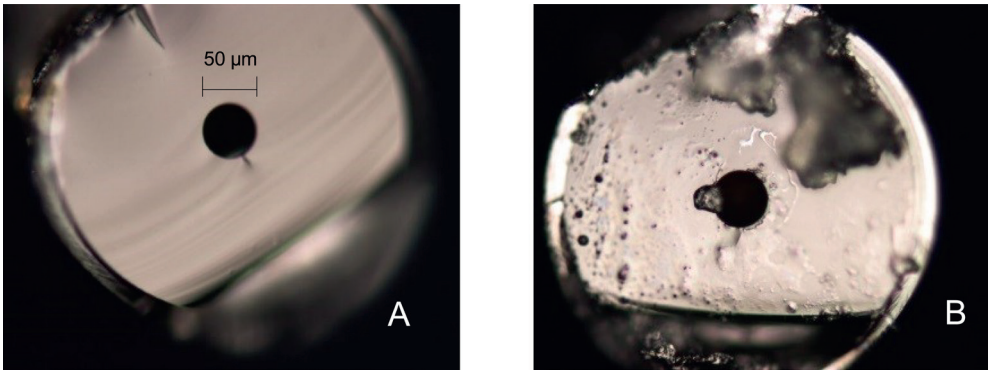

Figure 5.5. Cross-cut of a 50 µm fused-silica capillary. A: unused capillary. B: capillary after 30 injections of 50 mM TBAH in NMP.

These imaging investigations show that the fused silica capillary is severely corroded when applying the high pH BGE. Although aqueous high pH conditions are routinely used for capillary cleaning in CE, the combination of a strong base in NMP with high currents appear too harsh for standard fused-silica capillaries [29]. This could be a possible explanation for the inconsistent relation between electrophoretic mobilities and incorporated acid fractions as shown in Figure 5.4. Alternative capillary materials such as polyether ether ketone (PEEK) or polytetrafluoroethylene (PTFE) which are more resistant to high pH conditions might provide a possible solution, although the diminished EOF in these capillary types would require a whole new method to be developed. This is regarded as a topic for future investigation.

5.3.2 NACE using heteroconjugated anions

Addition of carboxylate anions to a NMP BGE for NACE analysis of carboxylic acid-containing polymers also shows broad electrophoretic peaks similar to profiles observed using NMP with TBAH to deprotonate the carboxylic acid moieties in the polymers. Figure 5.6 shows a typical electropherogram obtained using 20 mM TMG and 40 mM lauric acid in NMP to induce formation of heteroconjugated polymeric anions (using a mass-weighted distribution *P(µ)* in an effective-mobility scale as described by Cottet *et al*. [30]*)*. The migration profiles obtained for the different samples show that the added laurate ions specifically coordinate with the incorporated acid functionality. The non-acid containing polymers showed zero mobility (and as such migrate with the EOF - not shown in Figure 5.6), indicating that no association of the laurate anion occurs with polymers without acid functionality.

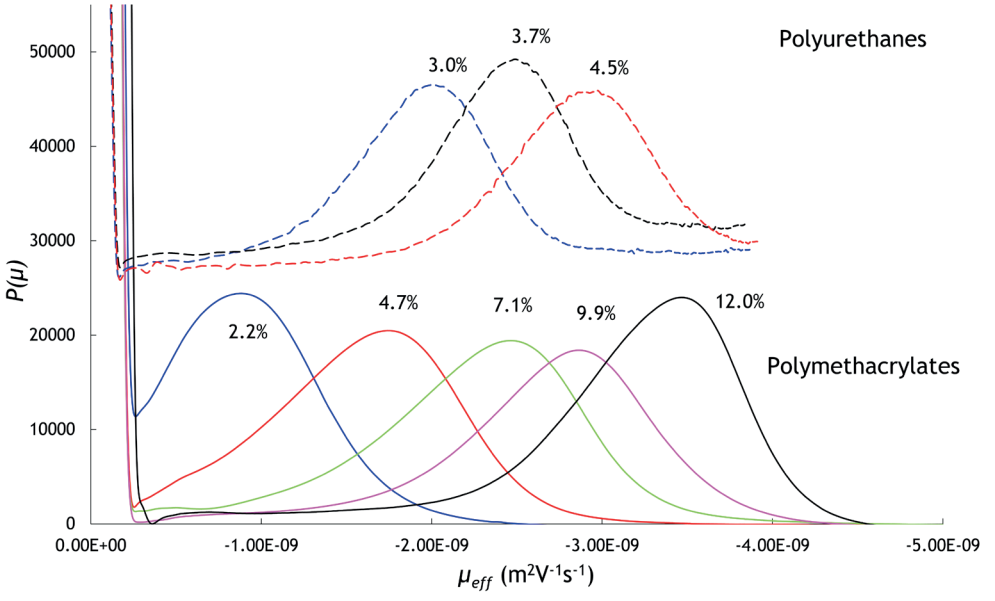

Figure 5.6. Mass-weighted effective mobility distribution of polyurethane-1 to 3 and methacrylic copolymers pMMA-co-MAA-1 through 5 (plotted on an effective mobility scale). BGE composition: 20 mM TMG and 40 mM lauric acid in NMP. Other conditions are described in the Experimental section.

The effective mobility of the heteroconjugated polymers increases with increasing acid content of the polymers (Figure 5.7). In general, there is also an enhancing effect on polymer-anion complex mobility from the use of anions with increasingly longer alkyl chains. As the association of anions with longer alkyl chains will likely result in polymer-anion complexes of a larger size, increase of mobility seems counter-intuitive, unless the overall charge increases when more apolar anions are used to generate heteroconjugated polymers. The acids that are applied and their pK_a; the acids which are used for anion formation vary in pK_a values, varying between 3.75-5.3 (under aqueous conditions), which can be above, equal or below the pK_a of polymer-incorporated methacrylic acid (4.8, aqueous). The acids with a pK_a equal to or lower than that of methacrylic acid (*i.e.* benzoic acid, formic acid) show a lower electrophoretic mobility of the polymer-anion complex as compared to acids with a pK_a higher than that of methacrylic acid. The assumption was made that, although absolute pK_a values in NMP differ significantly from pK_a values in water, the order of acid strength will not change significantly. Although the available pK_a values in NMP are limited, this appears to be valid [17]. A possible explanation may be that the conjugate base obtained from deprotonation by TMG (e.g. laurate) is a strong enough base to extract a proton from

the methacrylic acid incorporated in the polymer. The use of stronger acids (formic acid, benzoic acid) results in weaker conjugate bases (formate, benzoate), which are less capable of extracting a proton from the methacrylic acid. Increasing the anion concentration in the BGE from 10 mM to 20 mM yielded comparable electrophoretic behavior (see Figure 5.7). Overall, the effective mobilities of the polymer-anion complexes were slightly higher when an anion concentration of 20 mM is used.

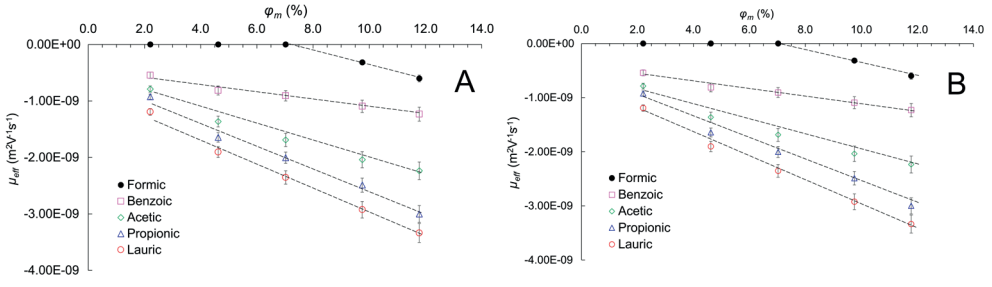

Figure 5.7. Plot of effective mobility vs. acid content φ_m of copolymers pMMA-co-MAA-1 to 5, using a NMP BGE containing different types of carboxylate ions (10 mM – A, and 20 mM -B). Displayed mobilities are average values of n=3. Conditions as defined in the Experimental section. The dashed lines are intended as a guide to the eye.

Although the exact mechanism of heteroconjugation in NMP appears to be complex, the process involving relatively large anions and the acid-functional polymers resulted in negatively charged polymers, with polymer mobilities reflecting the methacrylic acid content of the polymers.

The electropherograms obtained for acrylic- and urethane model systems were compared (Figure 5.6). Although the molecular weights of the polyurethanes are higher, effective mobilities and thus migration times are in a similar range as those of the polyacrylates. The polyurethanes appear to have a higher effective mobility than acrylic systems with a similar acid monomer content. Taking into account that the polymer mobilities are based exclusively on charge-to-size ratio, this indicates that the number of charges on the urethane polymers is larger (perhaps due to a lower pK_a of DMPA, *i.e.* 4.11), and/or that the size of the polyurethane molecules in solution is smaller than that of the polyacrylates. The latter is a well-known effect of polymer-solvent interactions. Another possible explanation is that, once some negatively charged complexes are formed on the polymer chain, the resulting anionic moiety exhibits a growing electrostatic repulsion towards further association of anionic species, especially when the unoccupied acidic

polymer functionality is in the vicinity of the occupied heteroconjugation sites. This would also explain why the urethane polymers appear to have higher effective mobilities than the methacrylic polymers, as neighboring acid groups in the polyurethane samples are always separated by at least one diisocyanate group. In acrylic polymers, the acid groups may be adjacent. Electrostatic repulsion would likely be lower when the distance between ionogenic moieties is larger, enabling a relatively greater number of charges to be present on a urethane polymer. Apparently, the difference in charge density between polymers of different chemistries can be significant.

The migration times of the model systems can be converted to an acid functionality scale using the compositional information from the model systems and the calculated effective electrophoretic mobilities (Figure 5.8). The calculated mass-weighted acid functionality distribution $P(\varphi_m)$ of the polyacrylates calculated from the results obtained with deprotonation- and heteroconjugation approaches is remarkably similar. This shows that, although not all polymeric acid groups are negatively charged, the obtained separation profile still accurately reflects the acid functionality distribution of these polymers. An important advantage of the heteroconjugation approach is that it does not have a detrimental effect on the fused silica capillary surface – enabling stable and reproducible analysis.

The main incentive to explore the potential of NACE for profiling acid functionality is that it separates analytes based on their charge-to-size ratio. Thus polymers which comprise distributions in both molecular weight and charge, but for which the charge-to-size ratio remains similar, will have similar effective mobilities. Model systems pMMA-co-MAA-6 to 11 (Table 5.1) were used to validate this feature, as these samples were prepared aiming at the same theoretical chemical composition, but with differences in molecular weight (see Table 5.1). The electropherograms of these samples are shown in Figure 5.9. Although the polymers with the lowest molecular weight have a slightly lower average mobility, overall, the apex mobilities of these polymer samples of varying molecular weight is very comparable. A possible explanation for the slightly fronting peaks in lower-molecular weight polymers could be that the polymer chain ends play a more significant role when polymers become shorter. In this case, presence of the non-charged chain stopper (dodecanethiol, which would logically be more pronounced in low molecular weight polymers), could have an influence in charge-to-size ratio for the smallest of polymers in this study, resulting in more peak fronting for low-molecular weight polymers.

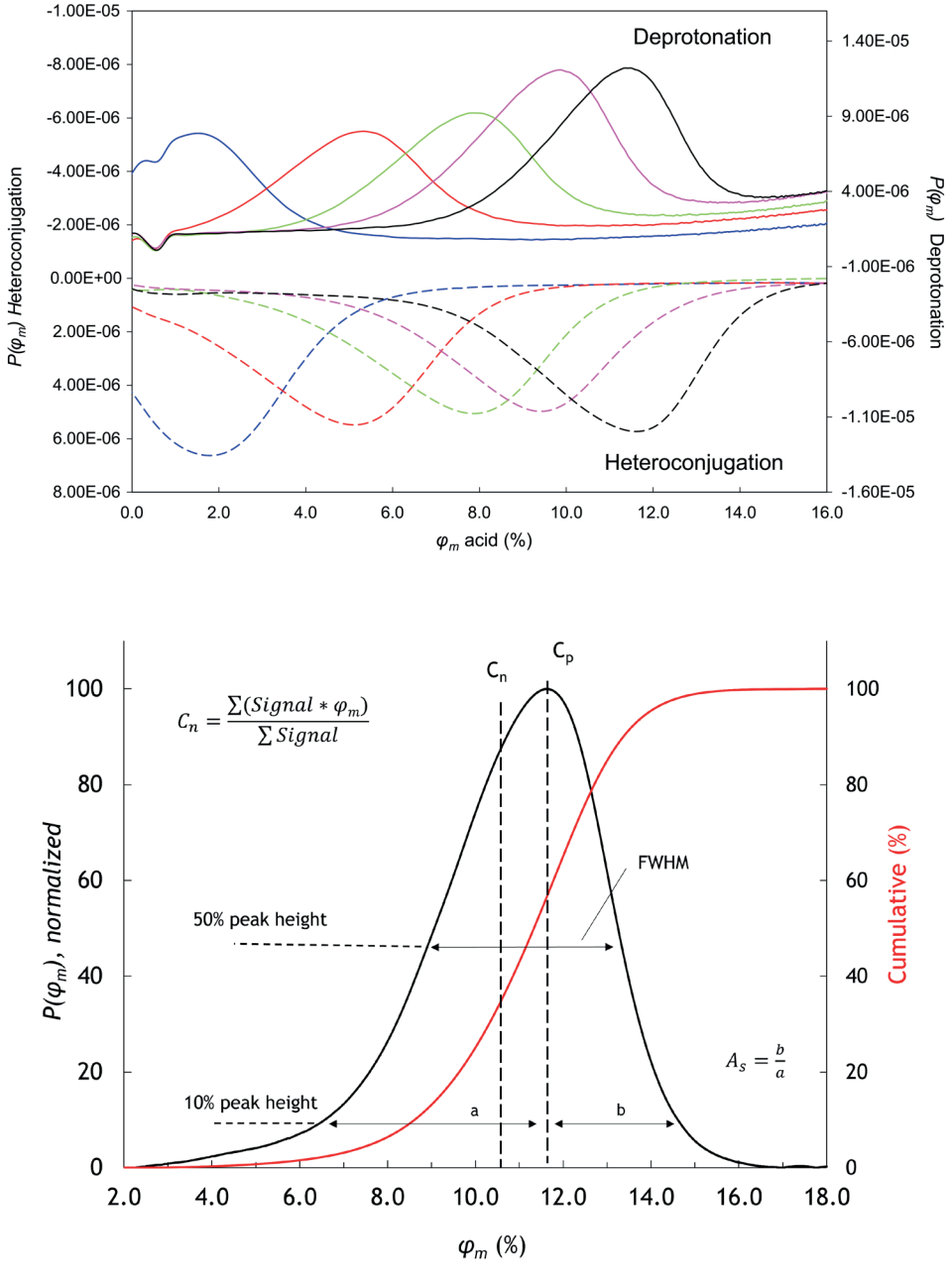

Figure 5.8. Top graph: Plot of acid functionality distributions of copolymers pMMA-co-MAA-1 through 5, measured by NACE under deprotonation- and heteroconjugation conditions (10 mM TBAH in NMP, and 20 mM TMG and 40 mM lauric acid in NMP, respectively). Further instrumental conditions as described in the Experimental section. Bottom graph: Description of the acid-functionality distribution of model polymer pMMA-co-MAA-5.

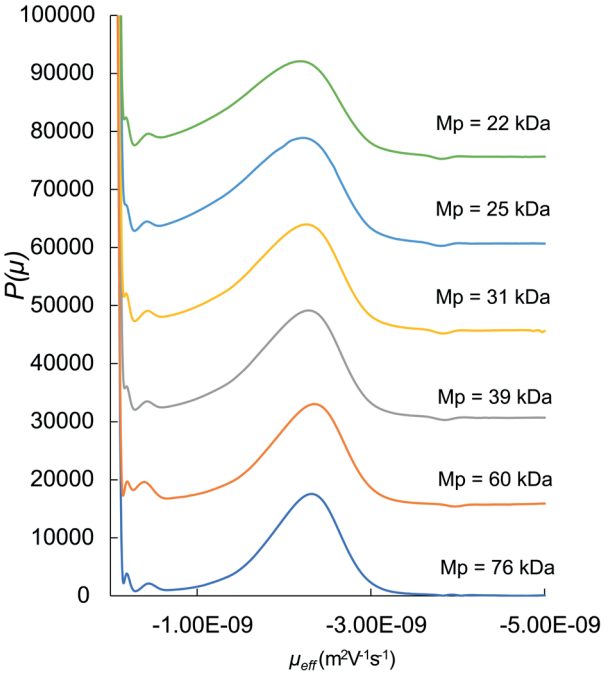

Figure 5.9. NACE of model polymers pMMA-co-MAA-6 to 11 with the same chemical composition but varying molecular weights. Conditions are described in the Experimental section.

The obtained acid-functionality distributions can be described by peak statistics. In Figure 5.8 (bottom), model polymer pMMA-co-MAA-5 is shown as an example for the determination of the number-average charge (C_n), the charge at peak top (C_p), the full width at half peak height (*FWHM*) and the asymmetry factor (*As*). All metrics of the methacrylic model system are further described in Table 5.2. Relevant metrics could not be obtained for sample pMMA-co-MAA-1 (Table 5.1) as it partly migrates with the EOF.

It is observed that all methacrylic polymer model systems show distribution asymmetry with distinct peak fronting. For the samples with a fixed chemical composition, but varying molecular weight there appears to be a trend of asymmetry increase upon decreasing molecular weight (also visualized in Figure 5.9). Similar effects are observed for the peak width (FWHM), with model systems pMMA-co-MAA-2 to 5 showing similar FWHM values. Polymers pMMA-co-MAA-6 to 11 (Table 5.1) show an increase in FWHM with decreasing molecular weight.

Table 5.2. Acid functionality distribution peak metrics

Sample	C_n [b]	C_p [b]	*FWHM* [b]	*As*
pMMA-co-MAA 1	-[a]	1.9	-[a]	-[a]
pMMA-co-MAA 2	3.2	5.1	4.0	0.71
pMMA-co-MAA 3	6.7	8.0	4.0	0.71
pMMA-co-MAA 4	9.4	9.8	3.7	0.63
pMMA-co-MAA 5	10.7	11.7	3.7	0.60
pMMA-co-MAA 6	4.70	6.6	2.7	0.69
pMMA-co-MAA 7	4.87	6.6	2.7	0.67
pMMA-co-MAA 8	4.53	6.5	3.2	0.59
pMMA-co-MAA 9	4.41	6.2	3.3	0.61
pMMA-co-MAA 10	4.19	6.0	3.6	0.54
pMMA-co-MAA 11	4.16	6.0	3.7	0.53

[a] *No data due to non-separated species from EOF.*
[b] C_n, C_p *and FWHM in* φ_m *acid (%).*

5.4 Conclusions

Acid-functional polymers, with methacrylic or urethane backbones, could be charged under non-aqueous conditions using either deprotonation or heteroconjugation approaches. Loci of charge in both approaches were shown to be the acidic monomer groups, which enabled a specific separation of these polymers according to the content of incorporated acid. Although the deprotonation approach was shown to be more efficient in terms of effective polymer mobility, the harsh BGE conditions resulted in less-robust separations due to severe degradation of the fused-silica separation capillary. Heteroconjugation was shown to be an alternative approach to obtain negatively charged polymers. Heteroconjugation did not require extreme-pH conditions, rendering this approach robust. The effective mobility of the anion-polymer complexes was shown be dependent on the type and/or the pK_a of the acid used for complexation, with medium- and long-chain acid anions, such as hexanoate and laurate, turning out to be preferred choices. Polymers with a variation in molar mass, but with the same theoretical composition, were shown to have similar effective mobilities. This confirms that the proposed separation was mainly based on charge-to-size ratio.

The heteroconjugation NACE approach was used to establish the acid-functionality distribution of several methacrylic model systems, which could be used to specifically characterize polymers by their incorporation of acidic monomers. Since acidic-monomer

incorporation is of vital importance in many water-borne-polymer systems, the characterization of this specific distribution is highly valuable to help design better, more efficient and more sustainable polymer systems.

Acknowledgements

Lisette Konings, Lex Donders and Jens de Bont are acknowledged for the preparation of the model polymer systems. Prof. Dr. Sjoerd van der Wal and Prof. Dr. Govert Somsen are acknowledged for their useful remarks and comments regarding this research.

References

1. T. Brooijmans, P. Breuer, P.J. Schoenmakers, R.A.H. Peters, Charge-based separation of synthetic macromolecules by non-aqueous ion exchange chromatography, J Chromatogr A 1626 (2020) 461351. https://doi.org/10.1016/j.chroma.2020.461351.
2. H. Cottet, M.P. Struijk, J.L.J. Van Dongen, H.A. Claessens, C.A. Cramers, Non-Aqueous Capillary Electrophoresis Using Non-Dissociating Solvents - Application to the Separation of Highly Hydrophobic Oligomers, Journal of Chromatography A 915 (2001) 241-251. https://doi.org/10.1016/S0021-9673(01)00643-4.
3. H. Cottet, W. Vayaboury, D. Kirby, O. Giani, J. Taillades, F. Schué, Nonaqueous Capillary Zone Electrophoresis of Synthetic Organic Polypeptides, Analytical Chemistry 75 (2003) 5554-5560. https://doi.org/10.1021/ac034526o.
4. H. Miramon, F. Cavelier, J. Martinez, H. Cottett, Highly Resolutive Separations of Hardly Soluble Synthetic Polypeptides by Capillary Electrophoresis., Analytical Chemistry 82 (2010) 394-399. https://doi.org/10.1021/ac902211f.
5. M.K. Menon, A.L. Zydney, Determination of Effective Protein Charge by Capillary Electrophoresis: Effects of Charge Regulation in the Analysis of Charge Ladders, Analytical Chemistry 72(22) (2000) 5714-5717. https://doi.org/10.1021/ac000752b.
6. K.H. Spriestersbach, F. Rittig, H. Pasch, Separation of non-UV-absorbing synthetic polyelectrolytes by CE with contactless conductivity detection, Electrophoresis 29(21) (2008) 4407-11. https://doi.org/10.1002/elps.200800248.
7. K.-H. Spriestersbach, F. Rittig, H. Pasch, Capillary Electrophoretic Analysis of Synthetic Copolymers with Indirect UV Detection and Contactless Conductivity Detection, International Journal of Polymer Analysis and Characterization 14(3) (2009) 196-209. https://doi.org/10.1080/10236660802673158.
8. P. Castignolles, M. Gaborieau, E.F. Hilder, E. Sprong, C.J. Ferguson, R.G. Gilbert, High-Resolution Separation of Oligo(acrylic acid) by Capillary Zone Electrophoresis, Macromolecular Rapid Communications 27(1) (2006) 42-46. https://doi.org/10.1002/marc.200500641.
9. J.J. Thevarajah, A.T. Sutton, A.R. Maniego, E.G. Whitty, S. Harrisson, H. Cottet, P. Castignolles, M. Gaborieau, Quantifying the Heterogeneity of Chemical Structures in Complex Charged Polymers through the Dispersity of Their Distributions of Electrophoretic Mobilities or of Compositions, Anal Chem 88(3) (2016) 1674-81. https://doi.org/10.1021/acs.analchem.5b03672.
10. G. Li, X. Zhou, Y. Wang, I.S. Krull, K. Mistry, N. Grinberg, H. Cortes, The Analysis of Synthetic Organic, Neutral Polymers Using Nonaqueous Capillary Gel Electrophoresis (NACGE), Journal of Liquid Chromatography & Related Technologies 27(6) (2007) 939-964. https://doi.org/10.1081/jlc-120030171.
11. K.A. Oudhoff, M. Macka, P.R. Haddad, P.J. Schoenmakers, W.T. Kok, Contactless conductivity detection of synthetic polymers in non-aqueous size-exclusion electrokinetic chromatography, J Chromatogr A 1068(1) (2005) 183-7. https://doi.org/10.1016/j.chroma.2004.11.081.
12. X. Leclercq, L. Leclercq, A. Guillard, L. Rodriguez, O. Braun, C. Favero, H. Cottet, Characterization of ultrahigh molar mass polyelectrolytes by capillary electrophoresis, J Chromatogr A 1631 (2020) 461536. https://doi.org/10.1016/j.chroma.2020.461536.

13. N. Fukai, S. Kitagawa, H. Ohtani, Effect of surfactant species and electrophoretic medium composition on the electrophoretic behavior of neutral and water-insoluble linear synthetic polymers in nonaqueous capillary zone electrophoresis, Electrophoresis 38(13-14) (2017) 1724-1729. https://doi.org/10.1002/elps.201700013.

14. K.A. Oudhoff, P.J. Schoenmakers, W.T. Kok, Characterization of Metallo Bis(terpyridine) Diblock Polymers by Nonaqueous Capillary Zone Electrophoresis, Chromatographia 60(7-8) (2004) 475-480. https://doi.org/10.1365/s10337-004-0390-x.

15. E. Kenndler, A critical overview of non-aqueous capillary electrophoresis. Part I: mobility and separation selectivity, J Chromatogr A 1335 (2014) 16-30. https://doi.org/10.1016/j.chroma.2014.01.010.

16. K. Sarmini, E. Kenndler, Ionization constants of weak acids and bases in organic solvents, J. Biochem. Biophys. Methods 38 (1999) 123-137. https://doi.org/10.1016/S0165-022X(98)00033-5.

17. K. Izutsu, Electrochemistry in nonaqueous solutions, Wiley-VCH Verlag GmbH & Co.2002.

18. J.L. Miller, D. Shea, M.G. Khaledi, Separation of acidic solutes by nonaqueous capillary electrophoresis in acetonitrile-based media: Combined effects of deprotonation and heteroconjugation, Journal of Chromatography A 888 (2000) 251-266. https://doi.org/10.1016/S0021-9673(00)00467-2.

19. R. Carabias-Martınez, E. Rodrıguez-Gonzalo, J. Domınguez-Alvarez, J. Hernandez-Mendez, Capillary Zone Electrophoresis in Nonaqueous Solvents in the Presence of Ionic Additives, 69 (1997) 4437-4444. https://doi.org/10.1021/ac9613038.

20. R. Kuldvee, M. Vaher, M. Koel, M. Kaljurand, Heteroconjugation-based capillary electrophoretic separation of phenolic compounds in acetonitrile and propylene carbonate, Electrophoresis 24(10) (2003) 1627-34. https://doi.org/10.1002/elps.200305378.

21. W. Vayaboury, D. Kirby, O. Giani, H. Cottet, Noncovalent coatings for the separation of synthetic polypeptides by nonaqueous capillary electrophoresis, Electrophoresis 26(11) (2005) 2187-97. https://doi.org/10.1002/elps.200410340.

22. M. Fillet, A.C. Servais, J. Crommen, Effects of background electrolyte composition and addition of selectors on separation selectivity in nonaqueous capillary electrophoresis, Electrophoresis 24(10) (2003) 1499-507. https://doi.org/10.1002/elps.200305412.

23. S.P. Porras, R. Kuldvee, S. Palonen, M.-L. Riekkola, Capillary electrophoresis of methyl-substituted phenols in acetonitrile, Journal of Chromatography A 990(1-2) (2003) 35-44. https://doi.org/10.1016/s0021-9673(02)01965-9.

24. J. Muzikár, T. Van De Goor, B. Gaš, E. Kenndler, Extension of the application range of UV-absorbing organic solvents in capillary electrophoresis by the use of a contactless conductivity detector, Journal of Chromatography A 924 (2001) 147-154. https://doi.org/10.1016/S0021-9673(01)00853-6.

25. T. Okada, Non-aqueous capillary electrophoretic separation of Bronsted acids as heteroconjugated anions, Journal of Chromatography A 771 (1997) 275-284. https://doi.org/10.1016/S0021-9673(97)00094-0.

26. A.J. Zemann, E. Schnell, D. Volgger, G.K. Bonn, Contactless Conductivity Detection for Capillary Electrophoresis, Analytical Chemistry 70(3) (1998) 563-567. https://doi.org/10.1021/ac9707592.

27. A.M.v. Herk, Chemistry and technology of emulsion polymerisation Blackwell Publishing2005.

28. J.C.d.l. Cal, J.R. Leiza, J.M. Asua, A. Butte, G. Storti, M. Morbidelli, Handbook of Polymer Reaction Engineering WILEY-VCH Verlag GmbH & Co2005.

29. H. Maraghechi, F. Rajabipour, C.G. Pantano, W.D. Burgos, Effect of calcium on dissolution and precipitation reactions of amorphous silica at high alkalinity, Cement and Concrete Research 87 (2016) 1-13. https://doi.org/10.1016/j.cemconres.2016.05.004.

30. J. Chamieh, M. Martin, H. Cottet, Quantitative analysis in capillary electrophoresis: transformation of raw electropherograms into continuous distributions, Anal Chem 87(2) (2015) 1050-7. https://doi.org/10.1021/ac503789s.

CHAPTER 6

Two-dimensional tools for analyzing polymer microstructure; coupling non-aqueous ion-exchange chromatography to size-exclusion chromatography

Ton Brooijmans, Pascal Camoiras Gonzalez, Bob Pirok, Peter Schoenmakers, Ron Peters

Submitted to Journal of Chromatography A.

Abstract

Traditional liquid-chromatographic techniques, such as size-exclusion chromatography, (critical) interaction chromatography, and hydrodynamic chromatography, can all reveal certain aspects of polymers and the underlying distributions. The distribution of incorporated acid groups present in polyacrylates can be determined by non-aqueous ion-exchange chromatography, independent of other distributions present. The microstructural details on how this number of acid groups is incorporated in the polymer remains unknown. A low-molecular-weight polymer molecule with high acid content and a high-molecular-weight polymer with a low acid content may have the exact same number of acid groups. To take a next step towards understanding the polymer microstructure of water-borne resins, the distribution of incorporated acid groups over the molar-mass distribution has been investigated.

For this purpose, an on-line coupling of non-aqueous ion-exchange chromatography (NAIEX) to size-exclusion chromatography (SEC) was established. Practical considerations regarding the system setup with respect to chromatography modes and column- and valve switching dimensionality are discussed. The orthogonality of NAIEX and SEC is demonstrated. Both liquid chromatography modes may be calibrated using polymer standards, yielding a calibrated separation plane. The value of the designed setup was demonstrated by the detailed characterization of the combined acid-group and molar-mass distribution in polymers with a low acid content, in the order of a few mass-%.

6.1 Introduction

Many industrial polymers have extremely complex microstructure. This arises from the many distributions that can be present in a single polymer system. Examples include the chemical-composition distribution (CCD), molar mass distribution (MMD), end-group distribution, branching distribution and a distribution in blockiness. To obtain insights in the polymer microstructure and to characterize these distributions, liquid chromatography (LC) separation techniques are required that are highly specific towards a certain polymer property.

Multi-dimensional LC is well-suited for the analysis of such complex materials, as the on-line coupling of orthogonal separation modes may drastically increase the peak capacity of the separation system and/or provide new insights in these materials due to separation of superimposed polymer distributions. Since the development of comprehensive two-dimensional liquid-chromatography (LC × LC) [1, 2], the technique has rapidly gained popularity in the 21st century for the analysis of polymers [3-8]. There have been significant recent technical advancements in this field related to the available LC hardware and increase in separation peak capacity [9-11], column hardware [11, 12], optimization software [13, 14] and fundamental understanding [6, 15], making LC × LC an established technique for the characterization of complex samples such as polymers. Peak capacity, however, is not the only important feature of 2D-polymer analysis, as the chromatographic selectivity determines which chemical information is obtained. In recent years, several novel developments were published in the field of two-dimensional polymer characterisation, such as a special coupling of size-exclusion chromatography (SEC) with hydrodynamic chromatography (HDC), enabling characterization of the molar mass distribution as function of the particle size distribution [7, 8]. The coupling of such so-called single-parameter separations, which are fully orthogonal, provides a more-detailed insight in the polymer microstructure. This insight can be used to design polymers with enhanced properties and/or more cost-effective processes. This is of specifically relevant for the development of high-performance water-based coating solutions. As water-borne polymers are environmentally more friendly than solvent-based alternatives, there is an ever-increasing demand for such polymer systems. Demands on the physical characteristics of such polymers (adhesion, durability) also increase, together with the need to better understand polymer heterogeneity [16, 17]. One of the critical types of monomer in water-borne polymers are the acid-functional monomers, as they determine particle stability. Recently, a technique has been developed that separates polymers solely according to the number of incorporated acid groups

(Chapter 4 of this thesis [18]). Despite the value of this single-parameter separation, insights into the exact build-up of acid-functional polymers is still missing. The developed approach can, for example, not discern between low-molar mass polymers with a high acid content and high-molar mass polymers with a low acid content, as the respective polymers may both contain the same number of acid groups/chain. This is also shown in equation 1:

$$n_{acid} = \frac{(M_n \cdot \varphi)}{M_{acid}} \quad (1)$$

in which n_{acid} is the absolute number of acid groups per molecule, M_n is the number-average molar mass in g/mol, φ is the weight fraction of acid groups and M_{acid} is the molar mass of the acid monomer in g/mol. As M_{acid} is constant, the number of acid groups depends solely on M_n and φ. A concomitant change in both these parameters may still yield the same outcome on the number of acid groups, while the polymer microstructure is different. In the present research we set out to obtain detailed information regarding the distribution of the acid groups in polymers as function of the molar mass, by coupling the recently developed non-aqueous ion-exchange-chromatography (NAIEX) approach with size-exclusion chromatography (SEC) in a two-dimensional liquid-chromatography system. The addition of the SEC separation could be beneficial by providing an indicative molar-mass distribution of each slice of the acid distribution. In this way we aimed to eliminate ambiguities around the polymer microstructure with respect to the number of acid groups incorporated. Our objective was to develop a system that would provide significant new insights in the microstructure of acid-functional polymers, above the information provided by the one-dimensional NAIEX approach and previously described analytical solutions [19].

6.2 Experimental

6.2.1 Materials

All material purity percentages are specified by weight, except when otherwise indicated. N-methylpyrrolidone (NMP, peptide-synthesis grade), triethylamine (≥99.5%), methyl methacrylate (MMA >99 %), methacrylic acid (MAA, >99%), sodium lauryl sulfonate (32 %(w/w) in water) and ammonia (25 %(w/w) in water) were purchased from VWR (Amsterdam, The Netherlands). 1-Dodecane thiol (99.8 %) and ammonium persulphate (≥98%) were purchased from Merck (Amsterdam, The Netherlands). 1,1,3,3-Tetramethylguanidine (99%) and formic acid (>98%) were purchased from Sigma-

Aldrich (Zwijndrecht, The Netherlands). Triethylammonium formate was synthesized in-house from formic acid and triethylamine according to the procedure of Attri *et al.* [20].

Water-borne copolymers were synthesized by reacting methyl methacrylate (MMA) and methacrylic acid (MAA) in various weight ratios (φ, see Table 6.1) using emulsion polymerization. Water containing 2.3% (w/w) sodium lauryl sulfonate was heated to 80°C prior to addition of the monomer seed, which consists of 5% (w/w) of the total monomer feed. The targeted total amount of polymer was 30% (w/w) in water. Directly after addition of the monomer feed, 0.5% (relative to the total amount of monomer) of ammonium persulphate was added to the mixture and 3 min were allowed to initiate the reaction. The remaining monomer feed (containing 0.5% (w/w) of 1-dodecanethiol as chain transfer agent) was added slowly during 90 min while maintaining reaction temperature at 85°C. The reaction temperature was kept at 85°C for 60 min after completion of the monomer feed, whereafter the batch was cooled to 30°C. At this stage, neutralizing agent (25% ammonia in water) was added until a pH between 7.5 and 8.5 was obtained.

Table 6.1. Overall composition of model polymer systems.

Sample	φ_{MMA} (% w/w)	φ_{MAA} (% w/w)	M_n (kDa)	M_w (kDa)	Average #Acids/chain[a]
MMA 1	98.0	2.0	27	50	6.3
MMA 2	96.0	4.0	29	59	13.5
MMA 3	94.0	6.0	27	49	18.8
MMA 4	92.0	8.0	27	50	25.1
MMA 5	90.0	10.0	25	60	29.1

[a] *Determined by multiplying* M_n *with* φ_{MAA}, *and divide this by the molecular weight of the acid monomer used (see eq 1).*

6.2.2 Instrumentation

Separations were performed on two 2695 Alliance separation modules (Waters, Milford, MA, USA), each consisting of an autosampler, a quaternary pump and a column oven. Column switching was performed with a 2-position 10-port dedicated 2DLC valve operated in comprehensive mode (PSS, Mainz, Germany) and a 1260 evaporative light scattering detector (ELSD; Agilent, Waldbronn, Germany) connected to the chromatography data system through an eSAT/IN convertor box. For the first-dimension (^{1}D) separation, an 150 × 2.1 mm i.d., 8 µm particle diameter, PL-SAX strong-anion-exchange column (Agilent) was used, which contained styrene-divinylbenzene-based particles with a quaternized polyethyleneimine coating. The ^{1}D column temperature

was kept at 50°C throughout the experiments. Initial column equilibration from aqueous conditions to non-aqueous conditions was performed by running a linear gradient from 1 % (v/v) methanol in water to 100 % (v/v) methanol in 60 min. A second equilibration step was performed by running a 60-min gradient from methanol to pure NMP. Starting mobile phase (A) was 50 mM tetramethyl guanidine in NMP and the eluting mobile phase (B) was 200 mM triethylammonium formate in NMP, containing 50 mM tetramethyl guanidine. Starting conditions for IEX gradient elution were 99 % (v/v) A, 1 % (v/v) B at a flow rate of 50 µL·min^{-1}. A gradient was applied from the initial conditions towards 100 % (v/v) B in 110 min. 100 % (v/v) B was maintained for 10 min, after which eluent composition was brought back to initial conditions in 1 min. The flow rate was maintained at 50 µL.min^{-1} throughout this program, but prior to injection of a next sample, re-equilibration of the ion-exchange column was performed by flushing the column for 20 min with the initial mobile phase at a flow rate of 300 µL·min^{-1}. The injection volume onto the ^{1}D system was 10 µL.

Size-exclusion chromatography was applied for the ^{2}D separation. A set of 50-µL 0.25 mm ID stainless steel loops were used for collecting fractions of the ^{1}D effluent. A 250 x 4.6 mm PLgel Minimix-C column was used, containing 5-µm styrene-divinylbenzene particles. The SEC flow rate was set to 1.5 mL·min^{-1} of THF (containing 0.5 %(v/v) formic acid). The column temperature was kept constant at 60°C. The ELSD detector was set to a nebulizer temperature of 90°C and an evaporator temperature of 120°C with a nitrogen flow of 2.7 standard litres per minute. Data were captured at 80 Hz, with a lamp (LED) intensity of 100% and a photomultiplier gain of 5. A schematic representation of the used setup is shown in Figure 6.1.

Chromatographic separations were controlled by Waters Empower 3 Waters software, Multidimensional graphical representations were prepared using MOREPEAKS version 1.00 [21].

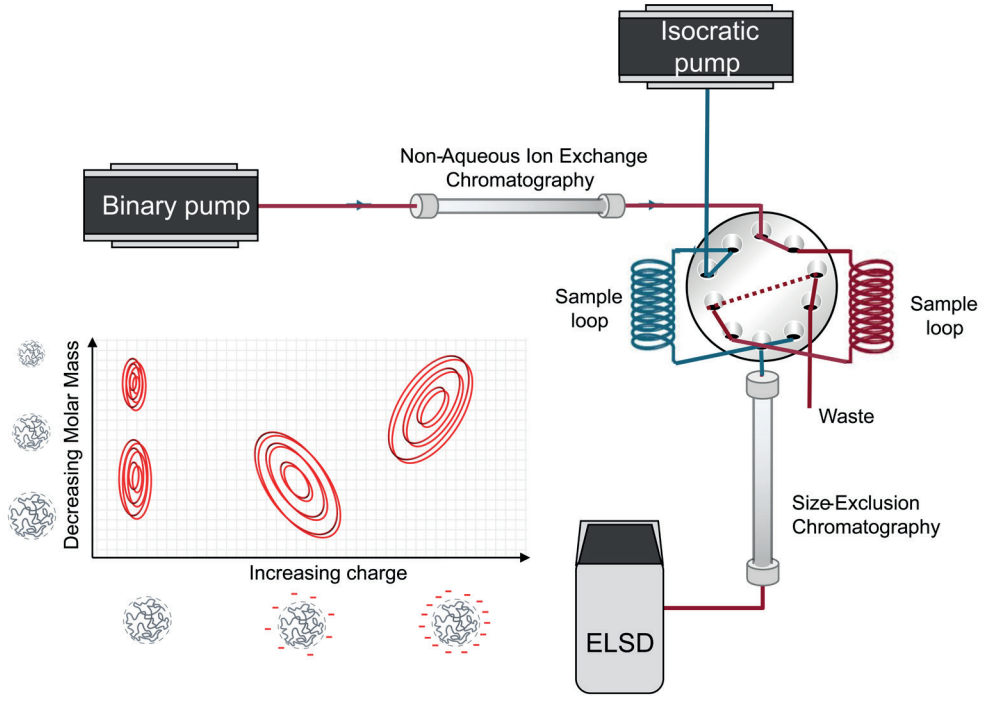

Figure 6.1. Schematic layout of the utilized LC x LC approach; ^{1}D NAIEX gradient (0.05 mL·min^{-1}) on a 150 x 2.1 mm PL-SAX column (50 µL.min^{-1}), 2-position 10-port switching valve and ^{2}D separation on a 250 × 4.6 mm PLgel Minimix-C SEC column (1.5 mL·min^{-1}).

6.3 Results and discussion

6.3.1 Coupling of non-aqueous ion-exchange chromatography to size-exclusion chromatography

Interaction chromatography as ^{1}D separation combined with SEC as ^{2}D mechanism is frequently applied for LC × LC [3, 6, 22]. The separation mode that yields the most chromatographic resolution is commonly used in the first dimension. Such an LC × LC setup has several advantages: The ^{2}D separation is isocratic which leads to a more uniform ELSD response (no eluent-composition dependency) and removes the need for equilibration that comes with eluent changes. Also, repeated injections in SEC can be optimized (overlapping injections). The optimal time between modulations equals (or only slightly exceeds) the duration of the SEC elution window (between total exclusion and total permeation). Separation parameters to optimize were ^{2}D SEC parameters, modulation time- and volume and ^{1}D gradient time, the choices made for these parameters are described below.

6.3.2 IEX x SEC modulation

To optimize the modulation time, the utilized ^{2}D column was evaluated in terms of dimensions and physical characteristics. Polymer-based columns are known to have a lower pressure resistance compared to silica-based columns [23], but the latter were discarded as possible ^{2}D columns due to the possible high pH of the 1D effluent.

The pressure resistance imposes a limit on the flow rate that can be applied for the ^{2}D separations. The PLgel column material used in this research has an upper pressure limit of 15 MPa. The linear flow rate at this pressure can be determined experimentally or estimated from Darcy's law, both indicate that the maximum flow rate for this column is around 2.2 mL.min^{-1}. In practice, pressure spikes are common during valve modulations and column lifetime is reduced when a column is operated close to its pressure limits. To keep the system functioning reliably, pressure (and thus flow rate) are usually kept well below the calculated maximum.

The exclusion volume of the ^{2}D column was measured by analysing a 2500 kDa polystyrene standard in SEC mode, and was established at 1.5 mL. The total permeation volume for this column was calculated as the volume of the column, corrected for the void volume:

$$V_0 = \varepsilon * \frac{\pi}{4000} * d^2 * L \qquad (2)$$

In the above equation, V_0 is the column void volume (mL), ε is the fractional pore volume (assumed to be 0.68), d is the diameter of the column in mm and L is the length of the column in mm. The calculated V_0 was slightly above 2.8 mL, which, together with the exclusion volume of 1.5 mL, leaves roughly 1.3 mL of effective separation volume. Combining the maximum flow rate (2.2 mL.min^{-1}) with the effective separation volume (1.3 mL) in SEC with overlapping injections shows that the minimal possible modulation time for this system is 0.6 min. However, this modulation time is calculated at the column pressure limits. It was desirable to reduce the pressure by reducing ^{2}D flow rate as mentioned above.

The ^{2}D column flow rate and injection volume were optimized by injecting varying volumes of a 1.0 mg.mL^{-1} polystyrene standard (316 kDa) on the PLgel Minimix-C SEC column. Results of these experiments are shown in Figure 6.2. It is observed that an increase of injection volume results in an increased peak width. Such an increase in peak width would invalidate SEC as a technique for measuring MMDs. The effects are likely

explained by volume overloading [23]. For all flow rates, the largest injection volume (100 µL) showed the largest peak width. The increase is also significantly impacted by the flow rate. At lower flow rates (1.0 – 1.25 mL.min^{-1}), increasing the injection volume from 50 µL to 100 µL results in significant confounding of the SEC selectivity. In this setup, an injection volume (=loop size) of 50 µL was chosen. To safely accommodate pressure spikes, we reduced the ^{2}D column flow rate from the maximum value of 2.2 mL.min^{-1} to 1.5 mL.min-^{1}. Accordingly, the modulation time was increased to 1 min, which resulted in a ^{1}D flowrate of 50 µL.min^{-1}.

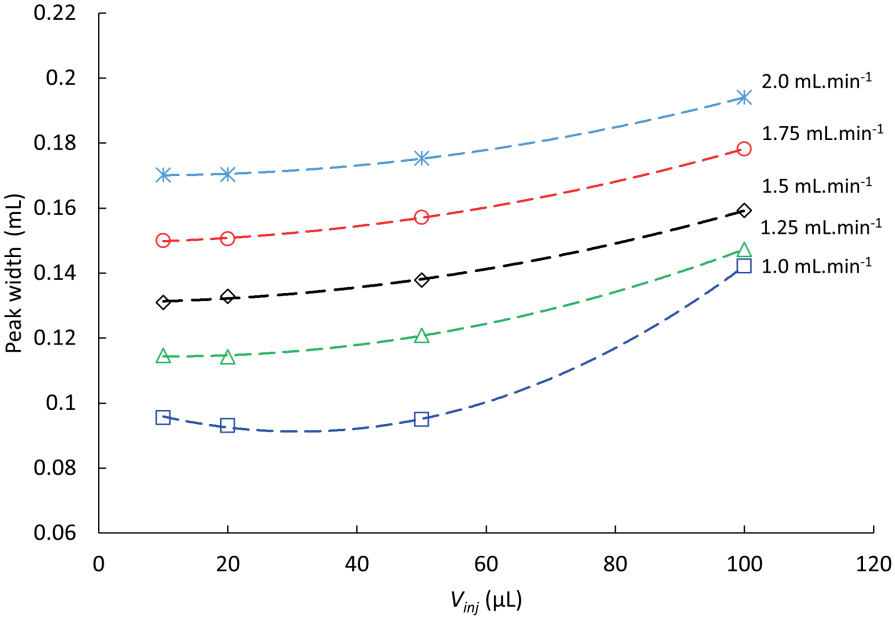

Figure 6.2. Dependence of observed ^{2}D SEC peak width on injection volume, measured at various flow rates. Column: PL gel Minimix-C, 250 x 4.6 mm, 5 µm particles, operated at 60°C. Eluent: tetrahydrofuran, 0.5% (v/v) formic acid. Sample: 1.0 mg·mL^{-1} polystyrene (316 kDa).

6.3.3 IEX gradient slope

The NAIEX approach that was developed in previous work [19] was adapted to serve as ^{1}D separation. As described above, the ^{1}D flow rate was reduced to 50 µL.min^{-1} to match the modulation time and loop volume. Gradient steepness was investigated for a mixture of a non-charged polymer (polystyrene), a polymer with medium charge density (MMA-2, Table 6.1) and a polymer with a high charge density (MMA-5, Table 6.1)). A linear gradient was applied from 1% B (200 mM triethylammonium formate, 50

mM tetramethylguanidine in NMP) to 100% B in 50, 70, 90, 110 or 150 min. The results are shown in Figure 6.3.

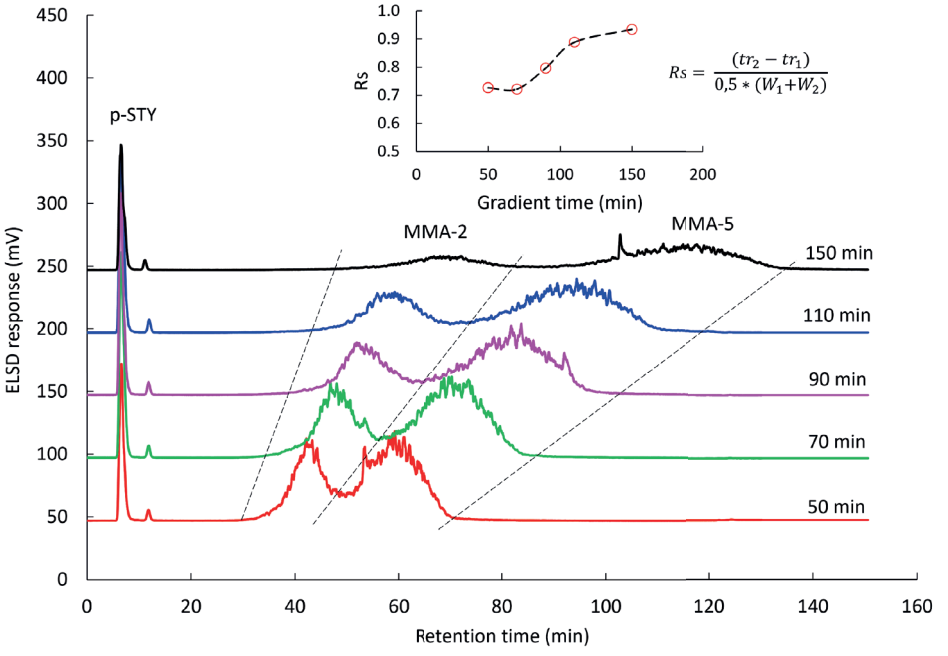

Figure 6.3. 1D chromatogram of a separation of a mixture of polystyrene (5 mg·mL^{-1}), MMA-2 (20 mg·mL^{-1}) and MMA-5 (50 mg·mL^{-1}). In the insert, the resolution between MMA-2 and MMA-5 (Table 6.1) is shown. Conditions: PL-SAX column, 150 x 2.1 mm, 8-µm particle size, operated at 50°C; Injection volume was 10 µL. Linear gradients of 99% A (50 mM tetramethylguanidine in NMP), 1% B (50 mM tetramethylguanidine, 200 mM triethylammoniumformate) towards 100% B in 50, 70, 90, 110 and 150 min using a flow rate of 50 µL.min^{-1}.

The elution behavior of polystyrene is unchanged between gradients, which (considering the absence of charge on this polymer) is expected. Polymers MMA-2 and MMA-5 are increasingly separated as the gradient steepness is reduced, although they do not become baseline separated. In the insert in Figure 6.3, the resolution between MMA-2 and MMA-5 was calculated for each gradient duration. A decrease in gradient steepness is seen to improve the resolution between the two charged species. The increase becomes smaller for very shallow gradients, at the cost of increasing ^{1}D analysis time. Increasing the gradient time from 110 to 150 min (36% increase) only yields an increase in resolution of 5%. Increasing the gradient time from 90 to 110 min (22% increase), led to an 11% increase in resolution. As a compromise between ^{1}D analysis time and 1D resolution, we chose a gradient time of 110 min for the two-dimensional approach.

Multivariate optimization of the two-dimensional polymer separation ("Blobtimization") to achieve optimal separation with respect to resolution is considered out of scope for this research, but could be a topic of further study.

Characterization of a mixture of calibration standards (PS) and polyacrylate polymers with various molar masses and acid contents (see Table 6.1) confirmed the intended separation based on acid-functionality and molar mass (see Figure 6.4).

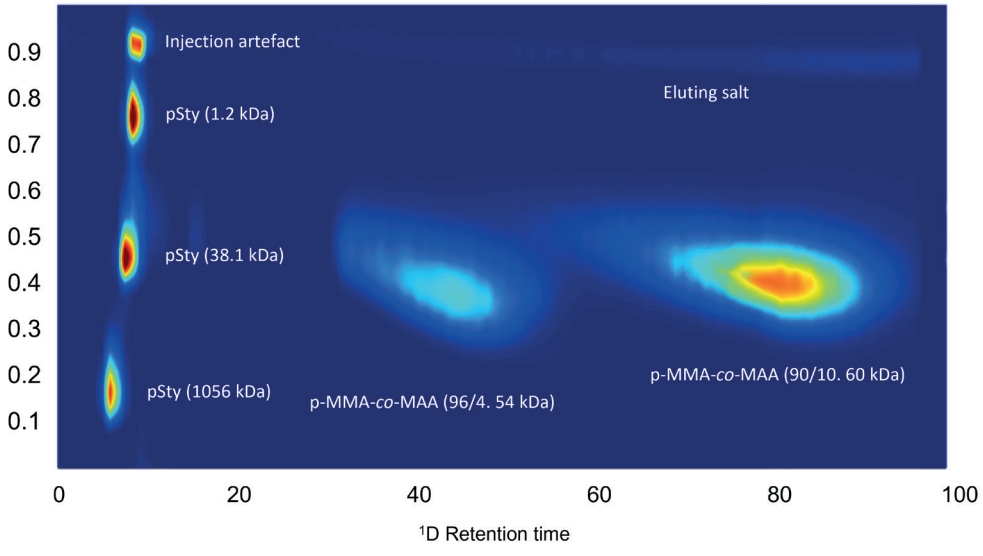

Figure 6.4. NAIEX x SEC of a mixture of polymers of various molar mass (polystyrene, 1056 kDa, 38.1 kDa, 1.2 kDa at 2 mg.mL^{-1} each) and acid contents (MMA-2 and MMA-5, 20 mg.mL^{-1} and 50 mg.mL^{-1}, respectively). Detailed system parameters are described in the Instrumentation section.

The polystyrene standards (which possess no acid and a narrow molar-mass distribution) elute approximately unretained from the ^{1}D column. There appears to be a slight dependence of the 1D elution volume on the polymer molar mass with a slight shift in elution times in the order of 1056 kDa > 38.1 kDa > 1.2 kDa. This can be explained by a SEC, *i.e.*, partial exclusion upon entropic elution of the polymers from the column with porous stationary phase particles. At the low end of the molar mass axis in the non-retained fraction (top left in Figure 6.4), a small peak is present. Although it is unknown what the identity of this component is, it was also found in blank injections and, therefore is not part of any polymer distribution. The p-MMA-co-MAA sample (96/4, M_w 54 kDa, see Table 6.1) shows ^{1}D elution around 50 min, with a ^{2}D retention time between 0.5 and 0.6 min. The acid-containing polymers (p-MMA-co-MAA 90/10, M_w 60

kDa and 96/4, M_w 54 kDa, see Table 6.1), appear to show a distribution directionality from the top left to bottom right. As polymer molar mass increases, the absolute number of acid groups present in the polymers also increases (assuming no change in polymer composition). Upon increasing the acid content in the polymer backbone, the shift in ^{1}D retention time is evident. A similar correlation between increasing molar mass and increasing number of acid groups was observed for all samples (Figure 6.5).

Visually, good orthogonality was obtained from the coupling of the two separation mechanisms, which resulted in a good coverage of the separation plane. As both NAIEX and SEC-separations were performed in strong solvents, breakthrough- or incompatibility effects were not expected and, indeed, not observed in the chromatograms.

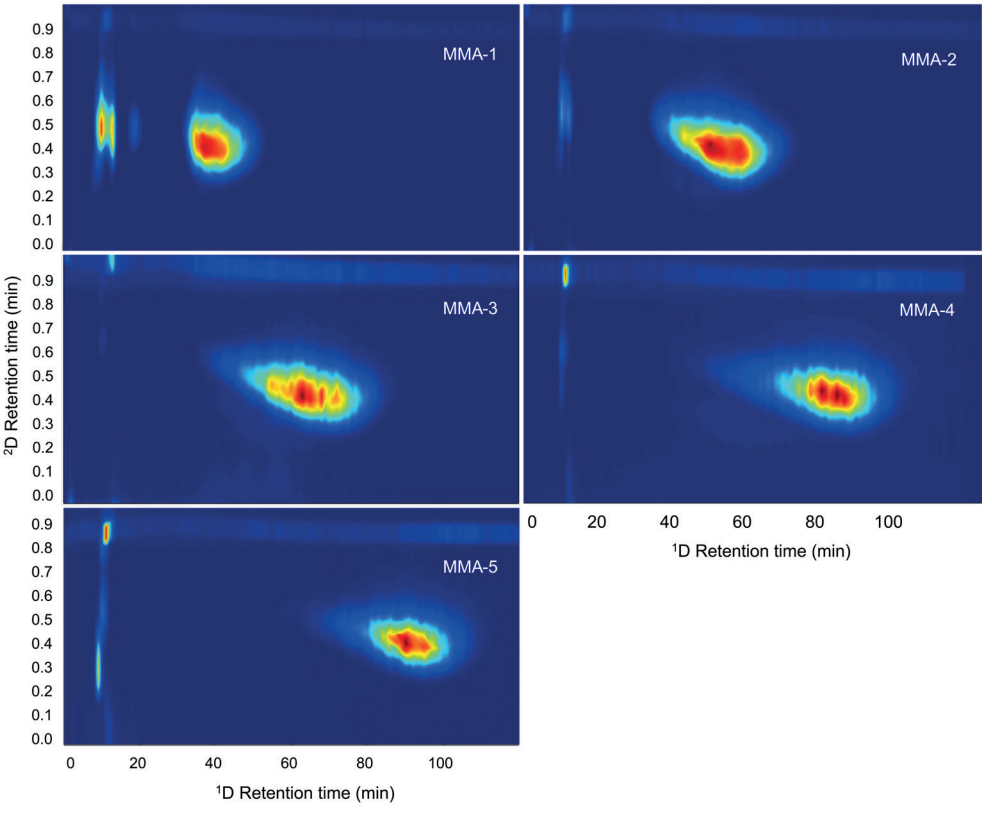

Figure 6.5. NAIEX x SEC of model polymers of various molar mass and acid content (MMA-1 through 5, Table 6.1). Detailed system parameters are described in the Instrumentation section.

6.3.4 Data evaluation

Both separation modes can be calibrated by the use of well-defined standards. For SEC, conventional calibration is a routinely performed task, in which narrowly distributed molar mass standards (most commonly polystyrene or poly-methyl methacrylate) are eluted according to their hydrodynamic volume, which is a measure for the molar mass. For NAIEX no such standards exist, but synthesis of model polymers with known molar mass and fractional acid content can overcome this limitation. The functionality number is obtained by the product of polymer number average molar mass (M_n) and the molar acid ratio (φ), while correcting for the molar mass of the acid monomer (see equation 1). Figure 6.6 shows the calibration of both separation axes, using the pMMA-co-MAA copolymers described in Table 6.1 for the ^{1}D separation (shown in red) and polystyrene standards for the ^{2}D separation (shown in black).

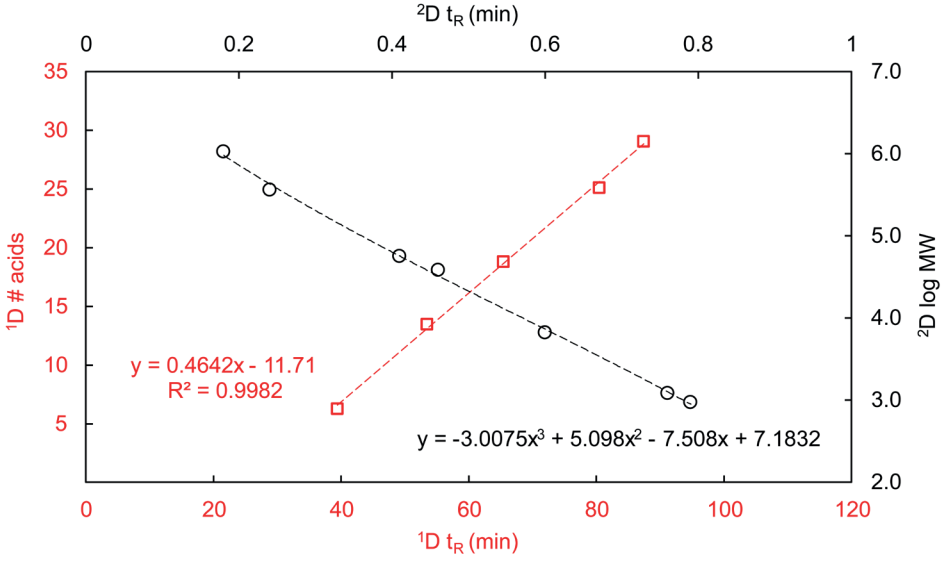

Figure 6.6. Calibration of ^{1}D and ^{2}D-axis. Separation of polystyrene standards in 1.5 mL.min^{-1} in THF containing 0.5% (v/v) formic acid on a 250 x 4.6 mm PLgel Minimix-C. ^{1}D conditions as in Figure 6.4 and 6.5.

The possibility to fully calibrate the separation plane enables the detailed characterization of any slice of the polymer distribution. An example of these calculations is shown in Figure 6.7. In this overview picture, it can be seen that the molar-mass cuts

of the distribution show distinctly different acid group distributions. In this particular polymer, the lower-molar-mass slice (log M_w = 4.0) shows a significantly broader acid-group distribution compared to a similar slice at log M_w = 5.0. Especially, the fraction of polymer chains with a low number of acid groups is significantly more pronounced in the log M_w = 4.0. Although it is difficult to quantitate the effect of this difference in the polymer distribution, it is possible that the polymer chains with low number of acid groups hardly contribute to the stabilization of polymer particles and, this, could be an important factor to monitor when stabilization problems occur.

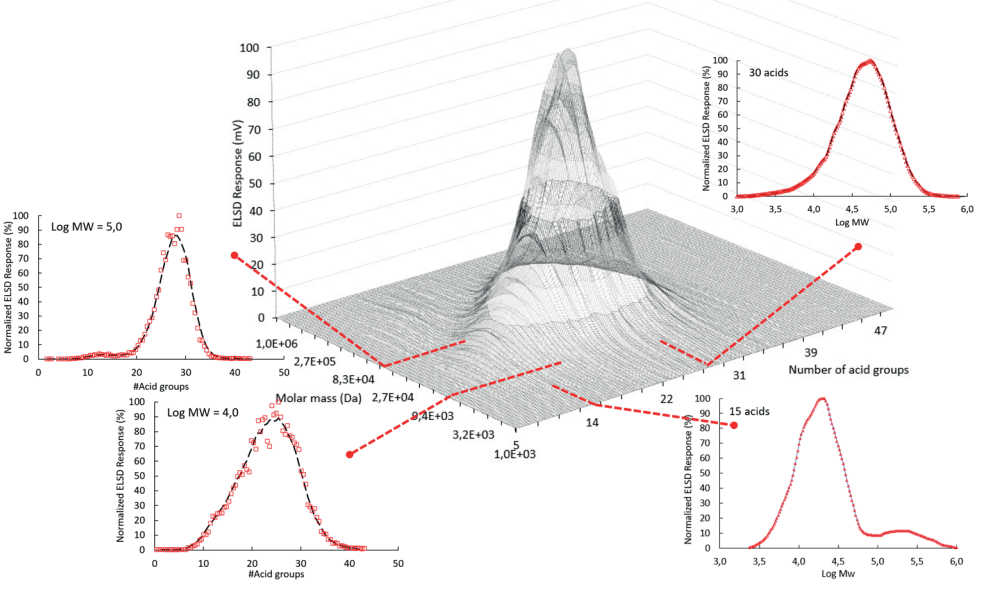

Figure 6.7. Reconstructed x,y traces from sample MMA-4 at four different regions of the two-dimensional distribution.

Similarly, the acid-number slices (depicting the molar mass distribution) at specific calculated numbers of acid groups also reveal a certain polymer microstructure. The expected Gaussian molar mass-distribution is only partly visible, and several distinct sections can be observed in the molar mass distributions (see Figure 6.5, right-hand side, molar-mass-extract traces). These sections could not be attributed to any chromatographic artefact and were perhaps related to the feed-stage conditions during the polymer synthesis. For instance, temperature changes, caused by radical reactions involving the monomeric units, may have triggered a difference in initiator dissociation, which in turn may result in slightly different monomer build-up in the polymer backbone.

This is a very interesting result from the NAIEX × SEC experiment, which may provide more insight in the procedures used in polymer synthesis.

The full calibration of the separation plane also enables us to characterize the distribution in terms of molar mass averages (for comparative use, because the ELSD signal is non-linear and not universal). The ^{1}D distribution cam be reconstructed by summing the SEC detector signal (Sum *N*i, red line, right-hand axis) in a certain modulation. An example of the result, with the calculated number-average and weight-average molecular weights for each SEC separation is shown in Figure 6.8 (images of the other samples can be found the Appendix).

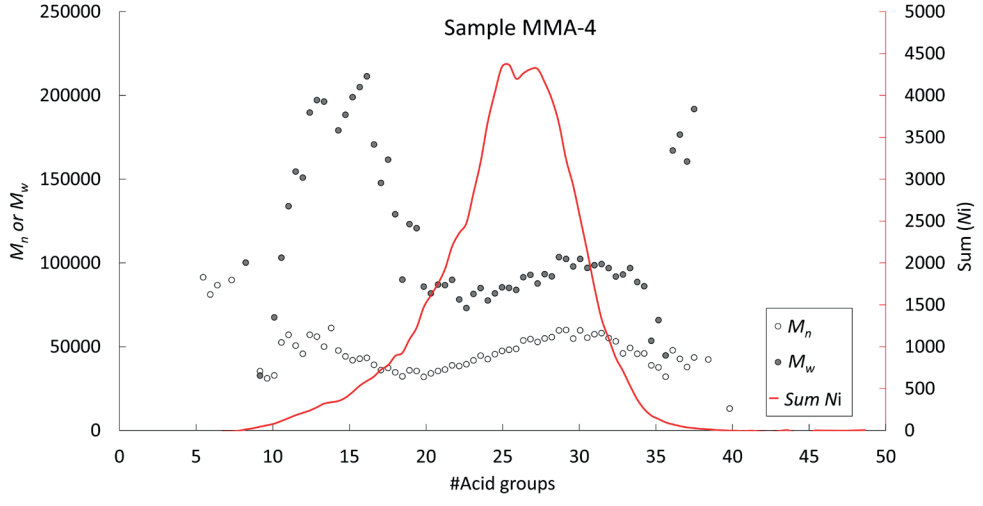

Figure 6.8: Reconstructed 1D chromatogram of sample MMA-4 plotted with calculated M_n and M_w for each modulation.

In the bulk of polymer (between about 20 and 30 min), a linear increase in both M_n and M_w is observed. At the high end of the distribution (higher numbers of acid groups) both molar-mass averages appear to decrease – an effect which is also visible from the original two-dimensional plot (Figure 6.5). Around the start of the distribution a clear upswing is observed for M_w. As shown in Figure 6.7 (log M_w = 5.0 slice), there is a low concentration of an additional polymer distribution with a high molar mass and a relatively low acid content. This is also visible in the low-acid containing slice, as a broad shoulder around log M_w 5.3. Presumably, this secondary distribution is formed during the seed stage of the polymerization where typically no chain transfer agent is present,

so that the resulting molar mass is expected to be high. This secondary distribution was also detected using other characterization techniques [20]. The decreasing molar mass averages observed at the acid-rich region (above 30 acid groups in Figure 6.8) also indicates a difference in polymer microstructure. This decrease in molar mass is visible in all samples (see Appendix A1 through A4), and appears to show a consistent effect related to the polymerization conditions. The observed effect may be evidence of a fraction of polymer formed by water-phase polymerization [24] or interfacial polymerization [25, 26], as both effects would typically result in polymers with a relatively high hydrophilicity (*i.e.* high acid-content in this case). These polymers would have a relatively low molar mass, due to radical termination caused by water-soluble initiator or monomer-initiator radicals, and they may play a role in the stabilization of the polymer particles. Although we do not have definitive proof that these types of species are formed in the present case, the consistence of the observations across all samples and the apparent molecular characteristics derived from the 2D-LC (NAIEX × SEC) combination are strong indications of their presence.

The ability to detect and characterize the fraction of seed-stage polymer, as well as the presumed water-phase (or interface) polymer species shows that the combination of NAIEX and SEC is highly advantageous compared to the use of these chromatographic approaches separately.

6.4 Conclusions

The newly developed non-aqueous-ion-exchange separation approach was successfully coupled to size-exclusion chromatography . The resulting comprehensive setup was used to establish the relation between molar mass and the number of incorporated acid groups in acid-functional polymers. The developed setup has the advantage that polymers with a large amount of acid groups can be divided into polymers with either a high fraction of acid groups incorporated and polymers which have a large absolute number of acid groups due their high molar mass. Good compatibility is observed between the two (organic-solvent-based) separation systems without any signs of breakthrough in the ^{2}D separation. By calibrating the entire separation plane, more-detailed polymer characterization (including molar mass averages) can be obtained than previously possible. The polymer microstructure can be revealed in terms of the number of stabilizing groups as function of the molar mass. The developed setup, combining two single-parameter polymer separations, is considered mature for utilization in industrial polymer characterization.

Acknowledgement

Lisette Konings and Jens de Bont are acknowledged for the preparation of the model polymer systems. Dr. Mike Schellekens is acknowledged for the very helpful discussions regarding emulsion polymerization processes in relation to the analytical developments.

Appendices

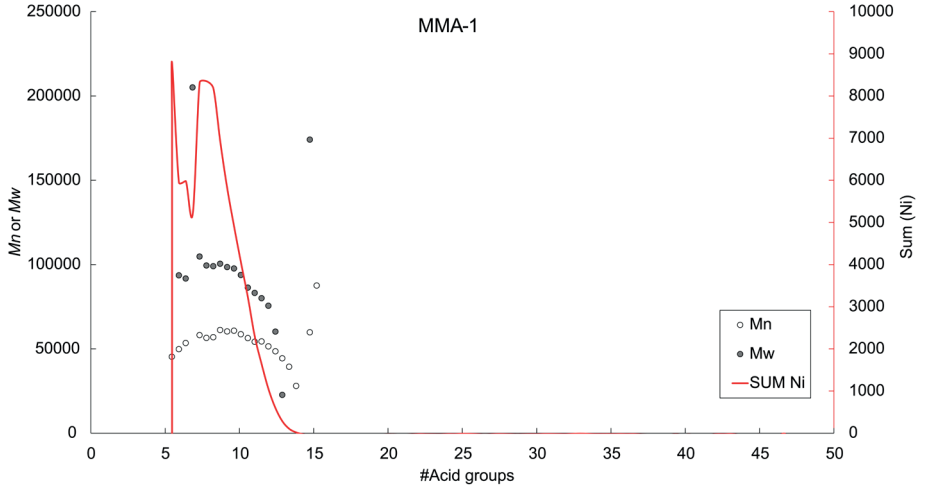

Appendix 6.1. Reconstructed 1D chromatogram of sample MMA-1 plotted with calculated M_n and M_w for each modulation.

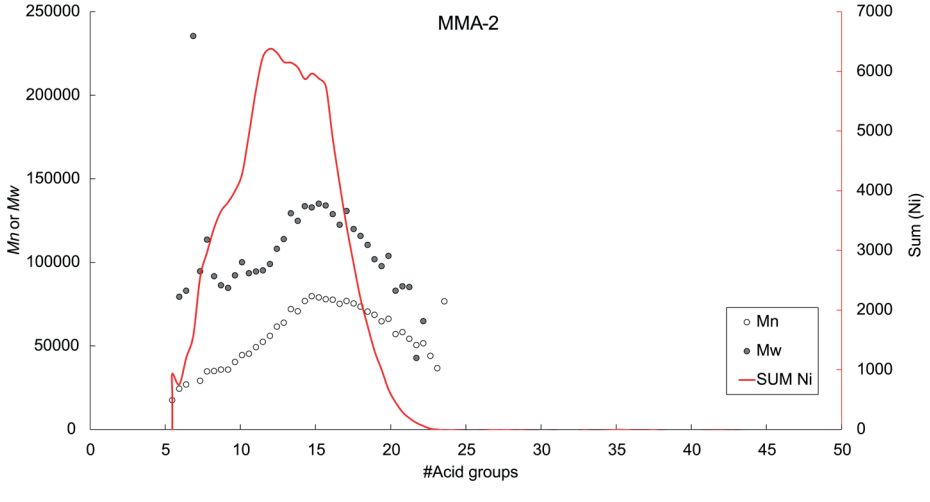

Appendix 6.2. Reconstructed 1D chromatogram of sample MMA-2 plotted with calculated M_n and M_w for each modulation.

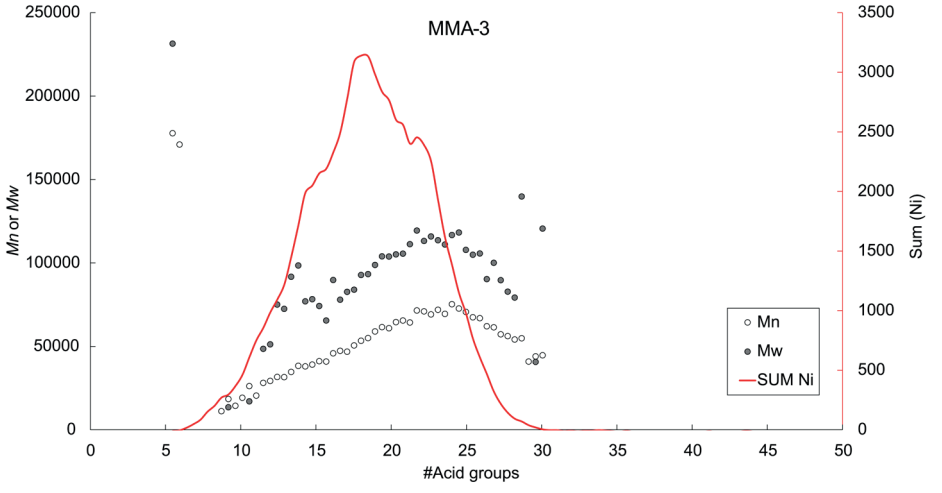

Appendix 6.3. Reconstructed 1D chromatogram of sample MMA-3 plotted with calculated M_n and M_w for each modulation.

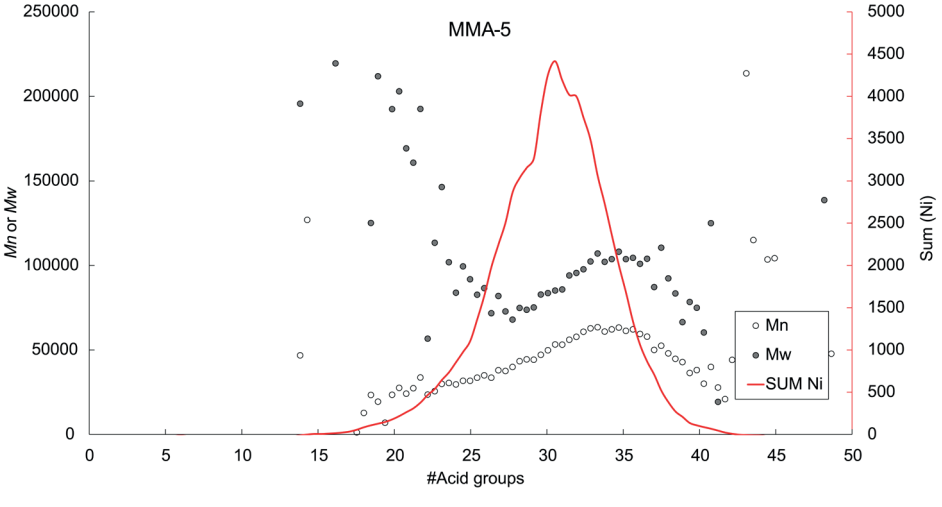

Appendix 6.4. Reconstructed 1D chromatogram of sample MMA-5 plotted with calculated M_n and M_w for each modulation.

References

1. F.Erni, R.W.Frei, Two-dimensional column liquid chromatographic technique for resolution of complex mixtures, Journal of Chromatography A 149 (1978) 561-569. https://doi.org/10.1016/S0021-9673(00)81011-0.
2. M.M. Bushey, J.W. Jorgenson, Automated instrumentation for comprehensive two-dimensional high-performance liquid chromatography of proteins, Analytical Chemistry 62(2) (2002) 161-167. https://doi.org/10.1021/ac00201a015.
3. P. Schoenmakers, P. Aarnoutse, Multi-dimensional separations of polymers, Anal Chem 86(13) (2014) 6172-9. https://doi.org/10.1021/ac301162b.
4. X. Jiang, A. van der Horst, V. Lima, P.J. Schoenmakers, Comprehensive two-dimensional liquid chromatography for the characterization of functional acrylate polymers, J Chromatogr A 1076(1-2) (2005) 51-61. https://doi.org/10.1016/j.chroma.2005.03.135.
5. I. Francois, K. Sandra, P. Sandra, Comprehensive liquid chromatography: fundamental aspects and practical considerations--a review, Anal Chim Acta 641(1-2) (2009) 14-31. https://doi.org/10.1016/j.aca.2009.03.041.
6. B.W.J. Pirok, D.R. Stoll, P.J. Schoenmakers, Recent Developments in Two-Dimensional Liquid Chromatography: Fundamental Improvements for Practical Applications, Anal Chem 91(1) (2019) 240-263. https://doi.org/10.1021/acs.analchem.8b04841.
7. B.W.J. Pirok, N. Abdulhussain, T. Aalbers, B. Wouters, R.A.H. Peters, P.J. Schoenmakers, Nanoparticle Analysis by Online Comprehensive Two-Dimensional Liquid Chromatography combining Hydrodynamic Chromatography and Size-Exclusion Chromatography with Intermediate Sample Transformation, Anal Chem 89(17) (2017) 9167-9174. https://doi.org/10.1021/acs.analchem.7b01906.
8. B.W.J. Pirok, N. Abdulhussain, T. Brooijmans, T. Nabuurs, J. de Bont, M.A.J. Schellekens, R.A.H. Peters, P.J. Schoenmakers, Analysis of charged acrylic particles by on-line comprehensive two-dimensional liquid chromatography and automated data-processing, Anal Chim Acta 1054 (2019) 184-192. https://doi.org/10.1016/j.aca.2018.12.059.
9. E. Uliyanchenko, P.J. Cools, S. van der Wal, P.J. Schoenmakers, Comprehensive two-dimensional ultrahigh-pressure liquid chromatography for separations of polymers, Anal Chem 84(18) (2012) 7802-9. https://doi.org/10.1021/ac3011582.
10. E. Uliyanchenko, P.J. Schoenmakers, S. van der Wal, Fast and efficient size-based separations of polymers using ultra-high-pressure liquid chromatography, J Chromatogr A 1218(11) (2011) 1509-18. https://doi.org/10.1016/j.chroma.2011.01.053.
11. E. Uliyanchenko, S. van der Wal, P.J. Schoenmakers, Deformation and degradation of polymers in ultra-high-pressure liquid chromatography, J Chromatogr A 1218(39) (2011) 6930-42. https://doi.org/10.1016/j.chroma.2011.08.014.
12. E. Uliyanchenko, S. van der Wal, P.J. Schoenmakers, Challenges in polymer analysis by liquid chromatography, Polymer Chemistry 3(9) (2012) 2313. https://doi.org/10.1039/c2py20274c.
13. B.W. Pirok, S. Pous-Torres, C. Ortiz-Bolsico, G. Vivo-Truyols, P.J. Schoenmakers, Program for the interpretive optimization of two-dimensional resolution, J Chromatogr A 1450 (2016) 29-37. https://doi.org/10.1016/j.chroma.2016.04.061.
14. T.S. Bos, L.E. Niezen, M.J. den Uijl, S.R.A. Molenaar, S. Lege, P.J. Schoenmakers, G.W. Somsen, B.W.J. Pirok, Reducing the influence of geometry-induced gradient deformation in liquid chromatographic retention modelling, J Chromatogr A 1635 (2021) 461714. https://doi.org/10.1016/j.chroma.2020.461714.

15. P.W. Carr, D.R. Stoll, Two-dimensional liquid chromatography: Principles, practical implementation and applications, Agilent, Waldbronn, Germany, 2015.

16. A. Overbeek, Polymer heterogeneity in waterborne coatings, Journal of Coatings Technology and Research 7(1) (2009) 1-21. https://doi.org/10.1007/s11998-009-9201-5.

17. J. Scheerder, R. Dollekens, H. Langermans, The colloidal properties of alkaline-soluble waterborne polymers, Journal of Applied Polymer Science 135(17) (2018) 46168. https://doi.org/10.1002/app.46168.

18. T. Brooijmans, P. Breuer, P.J. Schoenmakers, R.A.H. Peters, Charge-based separation of synthetic macromolecules by non-aqueous ion exchange chromatography, J Chromatogr A 1626 (2020) 461351. https://doi.org/10.1016/j.chroma.2020.461351.

19. T. Brooijmans, R.A. Okhuijsen, G.M.M. Oerlemans, B.W.J. Pirok, P.J. Schoenmakers, R.A.H. Peters, Heterogeneity analysis of polymeric carboxylic acid functionality by selective derivatization followed by size exclusion chromatography, Anal Chim Acta 1072 (2019) 87-94. https://doi.org/10.1016/j.aca.2019.04.051.

20. P. Attri, R. Bhatia, J. Gaur, B. Arora, A. Gupta, N. Kumar, E.H. Choi, Triethylammonium acetate ionic liquid assisted one-pot synthesis of dihydropyrimidinones and evaluation of their antioxidant and antibacterial activities, Arabian Journal of Chemistry 10(2) (2017) 206-214. https://doi.org/10.1016/j.arabjc.2014.05.007.

21. S.R.A. Molenaar, P.J. Schoenmakers, B.W.J. Pirok, Multivariate Optimization and Refinement Program for Efficient Analysis of Key Separations (MOREPEAKS), 2021.

22. E. Lubomirsky, A. Khodabandeh, J. Preis, M. Susewind, T. Hofe, E.F. Hilder, R.D. Arrua, Polymeric stationary phases for size exclusion chromatography: A review, Anal Chim Acta 1151 (2021) 338244. https://doi.org/10.1016/j.aca.2021.338244.

23. P. Hong, S. Koza, E.S. Bouvier, Size-Exclusion Chromatography for the Analysis of Protein Biotherapeutics and their Aggregates, J Liq Chromatogr Relat Technol 35(20) (2012) 2923-2950. https://doi.org/10.1080/10826076.2012.743724.

24. P.A. Lovell, F.J. Schork, Fundamentals of Emulsion Polymerization, Biomacromolecules 21(11) (2020) 4396-4441. https://doi.org/10.1021/acs.biomac.0c00769.

25. I. Schreur-Piet, J.P.A. Heuts, In situ stabilizer formation from methacrylic acid macromonomers in emulsion polymerization, Polymer Chemistry 8(43) (2017) 6654-6664. https://doi.org/10.1039/c7py01583f.

26. Y. Luo, F.J. Schork, Emulsion Copolymerization of Butyl Acrylate with Cationic Monomer Using Interfacial Redox Initiator System, Journal of Polymer Science 39 (2001) 2696-2709. https://doi.org/10.1002/pola.1247.

CHAPTER 7

Conclusions and recommendations

7.1 Water-borne resins

Reducing the impact of human life on our environment is one of the greatest challenges of modern time. The fundaments laid out in this generation will be decisive for the livability of the planet. Water-borne resins have a clear and ever-expanding role in this context, as almost all man-made surfaces (visible or not) are covered by one or more coatings. The use of water as the medium significantly reduces organic solvent-usage, which lessens the carbon footprint of resins tremendously. In addition, more and more biobased and/or biodegradable building blocks, such as itaconates, functional carbohydrates and/or terpenes, are commercialized for use in various types of polymerizations. At the time of writing, biobased resins do not yet enjoy the market-pull required for a major transition from oil-based resins to plant-based resins.

Water-borne resins are expected to continue to utilize carboxylic acid functionality as stabilization mechanism in favour of alternative stabilization mechanisms, such as non-ionic hydrophilic monomers, sulphonate-based monomers or cationic monomers, for several reasons:

i. Alternative stabilization mechanisms are considerably more expensive in use. Unless other clear advantages with respect to applications and/or properties outweigh the costs, large-scale use of these types of monomers will not occur.

ii. Cationic polymers harbour many of the traits of anionic polymers, but their production requires a strict separation from anionic polymers during the production process. Any small contamination of one resin type in the other will result in precipitation of the resin from the emulsion due to electrostatic interactions, negating the stabilization mechanisms of the polymer particles. Reserving a separate production line or applying extensive cleaning protocols during production switchover is possible, but this will result in additional operational effort (and costs) and reduced production flexibility.

iii. Acrylic and methacrylic acid from biobased sources are gaining interest. These monomers, which are chemically identical to their oil-based alternatives, can be a drop-in replacement, further reducing the carbon footprint of water-borne resins. Biobased alternatives for dimethylolpropanoic acid, such as reaction products of epoxidized soybean oil with glutaric acid are also under investigation. This may potentially also yield alternative possibilities for biobased stabilization of water-borne polyurethane coatings.

7.2 Resin characterization

As described above, water-borne resins are an essential ingredient of a more-sustainable future. This also causes a need for developments in resin-characterization techniques. Because insights must be gained in polymer distributions, separation methods are most essential, as described in this thesis. The advent of ultra-high-pressure liquid chromatography (UHPLC) and two-dimensional liquid chromatography (2DLC) has provided analytical scientists access to increasingly fast and efficient separations. However, due to the inherent nature of certain characterization techniques, more-efficient separations will only provide limited gains in information. For example, regardless of the efficiency of a reversed-phase or normal-phase separation, confounding polymer distributions (chemical composition distribution, molar mass distribution, end-group distribution) will confound the chromatogram and challenge the interpretation of the results. Size-exclusion chromatography (SEC) may be made highly efficient, but with the separation based on hydrodynamic volume, the results are influenced by the many distributions present in the polymers. To obtain fundamentally new insights, the coupling of these state-of-the-art separation techniques to novel, orthogonal, and preferably specific separations is key. Chapter 6 provides an example of such a combination, incorporating non-aqueous ion-exchange chromatography (NAIEX) and SEC in a two-dimensional setup. The level of detailed information provided on the polymer microstructure cannot be obtained from alternative, one-dimensional setups.

The work presented in this thesis implies several advancements in this field, which (after some modification, depending on the type of monomer) may be applied more generally. The developed approaches allow identification of the stabilizing acid monomers used in common water-borne polymers and provide insight in their incorporation in the polymer. These developments were all realized using generic reagents and commercial instrumentation. 2DLC was the notable exception at the time the research was conducted, but this technique is increasingly available and rapidly gaining ground in many research laboratories. Implementing the developed techniques in other laboratories should therefore be relatively straightforward.

The derivatization protocol for carboxylic-acid monomers was proven critical to prevent thermal side-reactions during characterization using pyrolysis. Similar thermal side-reactions are also expected for other monomers that contain active protons, such as amide-, amine- and hydroxy-functional monomers. Provided that suitable, selective derivatization approaches are available for these functional monomers, the described approaches (pyrolysis gas chromatography, PyGC, and SEC with differential-refractive-index and UV-absorbance detectors, SEC-RI-UV) can be made applicable for the characterization of other

types of functional monomers. Although the methods described in this thesis provide no information on the sequence distribution of functional monomers, an additional level of microstructural detail may be obtained when combining the derivatization approach with recent developments in sequence determination of acrylic polymers [1]. This would enable a qualitative and quantitative assessment of the distribution of stabilizing monomers along the main polymer chain. This can be particularly useful to properly describe and understand the stabilization mechanisms in water-borne polymers.

The application of capillary electrophoresis in polymer analysis opens up possibilities for miniaturization, for instance for multi-dimensional polymer separations in 3D-printed devices [2] . Buffer conditions are a source of concern, as the internal surface of such devices should be sufficiently stable if high pH values are needed. Fused silica was shown not to withstand the high-pH conditions set forth in Chapter 5. Alternative materials (*e.g.* polytetrafluoroethylene, PTFE, or polyether ether ketone, PEEK) may provide better pH resistance. The electro-osmotic flow will be completely different in such materials compared with that in fused silica, it is advised to first characterize such alternative materials in a standard capillary format.

Stability is also a source of concern in the described NAIEX setups. The high-pH conditions set forth in this thesis were shown to result in a reduction of the ion-exchange capacity of the stationary phase, likely due to elimination of quaternary ammonium functional groups from the polymer support. *In-situ* regeneration of these functional-group types is likely possible using di-epoxides and tertiary amines [3, 4], but the resulting quaternary polyethyleneimine-grafted coating on the polymer support will again experience degradation under the conditions of the experiment. The development of new, stable ion-exchange media based on polymer supports is a more-fundamental solution. Poly(meth)acrylates or silica-based particles as the polymer support do not meet the stability requirements. Alternatively, styrene-divinylbenzene (PSDVB) based resins may provide a suitable polymer support. New IEX stationary phases may also provide more flexibility in NAIEX analysis, either for use in UHPLC-type separations or in semi-preparative columns for isolation of specific polymer fractions.

Combining acid-specific separations with high-end detection techniques, such as quadrupole-time-of-flight mass spectrometry (q-TOF-MS) or high-field nuclear-magnetic-resonance spectroscopy (NMR) is particularly interesting to obtain more microstructural details of polymer architecture. Due to time restrictions (aggravated by the COVID pandemic) such advanced hyphenation techniques were not explored in this thesis. TThe hyphenation of high-performance, specific separation techniques with high end detection systems is a logical, but quite challenging next step in resin characterization.

References

1. W.C. Knol, S. Vos, T. Gruendling, B.W.J. Pirok, R.A.H. Peters, Expansion of the application range of pyrolysis-gas chromatography to copolymer sequence determination: Acrylate copolymers, Journal of Analytical and Applied Pyrolysis 165 (2022) 105578. https://doi.org/10.1016/j.jaap.2022.105578.
2. S.K. Anciaux, M. Geiger, M.T. Bowser, 3D Printed Micro Free-Flow Electrophoresis Device, Anal Chem 88(15) (2016) 7675-82. https://doi.org/10.1021/acs.analchem.6b01573.
3. O.I. Shchukina, A.V. Zatirakha, A.D. Smolenkov, P.N. Nesterenko, O.A. Shpigun, Anion exchangers with branched functional ion exchange layers of different hydrophilicity for ion chromatography, J Chromatogr A 1408 (2015) 78-86. https://doi.org/10.1016/j.chroma.2015.06.039.
4. O.I. Shchukina, A.V. Zatirakha, A.S. Uzhel, A.D. Smolenkov, O.A. Shpigun, Novel polymer-based anion-exchangers with covalently-bonded functional layers of quaternized polyethyleneimine for ion chromatography, Anal Chim Acta 964 (2017) 187-194. https://doi.org/10.1016/j.aca.2017.01.062.

SUMMARY

Summary

Complex systems, such as water-borne polymers, require increasingly sophisticated analytical techniques to understand the chemical or physical microstructure. Such understanding would enable scientists to optimize these systems for use in an a virtually endless array of applications. As concerns waterborne polymers, the way in which they are built directly influences the macroscopic properties of the coatings derived from such polymer systems. Common characteristics that are important for the application of coating materials include adhesion to a substrate, physical and chemical durability and, very practical for painters or printers, the applicability of the coating to a substrate which is determined by the rheological behavior of the colloidal polymer particles. Although many possibilities exist to tailor polymer functionalities, the influence of any change in chemical characteristics is still often determined empirically by applications tests. By far the most commonly used functionality in water-borne polymers is the acid group. The work covered in this thesis was aimed at developing tools to specifically separate and characterize complex polymer systems based on this acid functionality. Such tools will provide more insight in the chemical microstructure and distribution of stabilizing monomers in water-borne polymers. As the developed approaches specifically target the acid functionality, the chromatographic tools may be generically applied to other acid-functional materials.

As acid-functional monomers are being incorporated only in the low percentile range, spectroscopic techniques are often not sufficiently sensitive to discern the exact species that are used in a polymer system. In the work described in Chapter 2, a specific derivatization of the acid functionality in polymers was developed, using model polymers with varying type of acid and comonomer composition. A class of derivatization agents, phenacyl bromides, were shown to specifically react with acid functionalities. The derivatization yields determined by fast Size-Exclusion Chromatography (SEC) were found to be high. Pyrolysis of the derivatized polymers showed the existence of phenacyl esters, which could be clearly attributed to the specific acid monomer used with the aid of mass spectrometry (MS). As acidic monomers may also be created by intra- and/or intramolecular rearrangements under pyrolysis conditions, it is critical to remove excess derivatization agents to discern incorporated acid monomer from pyrolytically created acid monomer.

The specific derivatization protocol described in Chapter 2 was adopted for chemical-heterogeneity studies of polymers. The phenacyl functionality which is introduced by derivatizing acid-functional monomers can be specifically detected by ultraviolet (UV)

detection after SEC separation, under the assumption that no other UV-active species are present. In Chapter 3 a multi-detector SEC setup is described, consisting of at least a UV detector (measuring the concentration of acid monomer) and a refractive index (RI) detector (approximately measuring the total polymer concentration). This setup was then used to quantify the relative concentration of the acid monomer in each molecular-weight slice, enabling determination of the heterogeneity of the distribution of acid monomer as a function of the molar mass. The total surface area of the UV-active-polymer fraction could be quantified using a molar-response calibration curve of a commercial phenacyl ester. A very good agreement was observed between the theoretical acid content based on synthesis conditions and the acid content determined from the UV signal. As an added advantage of the derivatization, polymer solubility was increased. The refractive-index increment (*dn/dc*) of the polymer was also increased by the incorporation of the phenacyl side groups, which increased the sensitivity of the RI detector. The types of analysis as developed in Chapters 2 and 3 may be easily extended to other polymer functionalities, provided that a suitable derivatization approach is established.

A different development was a protocol to deprotonate the acid functionality in polymers in non-aqueous conditions. The acid-base equilibrium (pK_a) of the acid groups changes drastically in non-aqueous conditions compared to aqueous conditions, which poses challenges to the base strength that is required to achieve deprotonation of the acid groups. Chapter 4 describes that the combination of a polar solvent (N-methylpyrrolidone, NMP) and an organic superbase (tetramethylguanidine, TMG) yields complete deprotonation of the acid groups as determined by proton nuclear-magnetic-resonance spectroscopy (^{1}H-NMR). A good correlation was observed between the measured pK_a values of the acids in the NMP environment and available pK_a data in literature. The acid-functional polymers were subjected to non-aqueous ion-exchange chromatography (IEX). Initial conditions were chosen such that the polymers were deprotonated and thus negatively charged. These charged polymers interacted strongly with the quaternary-amine functionality of strong ion-exchange liquid chromatography (LC) columns, and thus are retained. Elution was performed by a gradient of triethylammonium formate, an organic-soluble salt (the most-common IEX salt is sodium chloride, which is insoluble in NMP and other organic solvents). The retention behavior of model systems under IEX conditions was compared to normal- and reversed phase polymer separations. Both the latter types of systems yielded a separation based on the overall polarity of the polymer, and not specifically on any

of the monomeric species present in the polymer. The IEX approach showed a very good correlation of the polymer retention behavior with the number of acid groups incorporated in the polymer, regardless of the other comonomers present.

Capillary electrophoresis (CE) may also be used for the separation of complex systems. It is a common tool in the fields of protein, virus, and antibody characterization. Chapter 5 presents an extension of the approach developed in Chapter 4. A direct translation of the IEX approach (NMP solvent and a strong, organic-soluble bases such as TMG and tetrabutylammonium hydroxide, in the background electrolyte) yielded good results, *i.e.* separation of polymers based on their charge-to-size ratio. However, this approach could only be applied for a few injections, as the high-pH conditions led to a rapid deterioration of the fused-silica electrophoresis capillary. Interestingly, changing the composition of the background electrolyte to an excess of acid also resulted in the formation of negatively charged polymer species. It was shown that so-called heteroconjugation, *i.e.* complexation of the polymer with the anionic species in the background electrolyte, had taken place. The effects of various types of acid in the background electrolyte were investigated, with acids having a higher pK_a proving more efficient in complexation of the acidic polymer. The acid distribution of various polymer species could be determined, with polyurethanes showing a different dependence of the elution time on the charge-to-size ratio. This could possibly be attributed to size differences in solution, but the absence of neighboring acids in the polyurethane structure may also have affected the CE behavior. The acid-functionality distribution could be constructed from the electrophoretic data, together with basic peak statistics. The influence of molar mass was shown to be very limited, as was expected for a separation based on charge-to-size ratio. Low molar-mass polymers did show peaks that were tailing towards the low-mobility part of the electropherogram, which could likely be explained by the increasing influence of non-charged polymer end-groups.

More insights into polymer microstructure may be obtained by the hyphenation of orthogonal separation principles. Multi-dimensional LC can drastically increase the peak capacity of a separation system and/or provide additional information on polymers based on the applied separation principles. Chapter 6 describes the on-line coupling of the ion exchange protocol from Chapter 4 in the 1st dimension, with SEC in the second dimension. An optimization was performed involving the dimensions of second-dimension column, the loop volume of the transfer valve, the first-dimension gradient slope, and the second-dimension flow rate. The observed two-dimensional IEX × SEC separation showed an orthogonal separation for a selection of polymers with

varying molar mass and acid content. Using calibration standards and model polymers, both IEX and SEC axes could be calibrated, yielding a calibrated separation plane. This enabled the quantitative evaluation of every point of the 2D-plane. When assessing the molar-mass averages across the acid distribution, clearly different stages in the acid distribution were discerned. These likely indicated a seed-stage polymer fraction, as well as acid-rich polymers, which could have originated from water-phase or interfacial polymerization. The combination of orthogonal separation modes in multidimensional LC offered clear advantages as compared to the application of the separation modes individually.

SAMENVATTING

S

Samenvatting

Complexe systemen, zoals watergedragen polymeren, vereisen een continue ontwikkeling in analytische technieken om de chemische or fysische microstructuur van deze systemen te begrijpen. Dit begrip stelt wetenschappers in staat om deze systemen te optimaliseren voor een eindeloze variatie aan toepassingen. In het geval van watergedragen polymeren is de manier waarop de polymeren samengesteld worden van directe invloed op de macroscopische eigenschappen van de coatings die gemaakt worden van deze polymeren. Karakteristieken die erg belangrijk zijn voor de applicatie van deze coatings zijn, onder andere, hechting aan het substraat, fysieke of chemische bestendigheden. Ook praktisch: bij gebruik van deze materialen door schilders en/of printers moet het reologisch gedrag van deze colloïdale systemen adequaat zijn voor de toepassing. Alhoewel er veel mogelijkheden zijn omtrent het specifiek synthetiseren van bepaalde chemische functionaliteiten, wordt het effect van de verandering in chemische structuur nog vaak empirisch bepaald door applicatietesten. Een van de meest voorkomende functionaliteiten in watergedragen polymeersystemen zijn de zuur-functionele monomeren. Het werk in dit proefschrift is erop gericht om chromatografische gereedschappen te ontwikkelen die deze complexe zuur-functionele polymeren specifiek scheidt op deze functionele groep, dan wel specifiek kan detecteren. Dit stelt men in staat om meer inzicht te verkrijgen in de chemische microstructuur en verdeling/inbouw van de stabiliserende groepen in watergedragen polymeersystemen. De ontwikkelde chromatografische gereedschappen gebruiken specifiek de zuur-functionele groepen om een scheiding of detectie te bewerkstelligen, en kunnen dus vrij generiek ingezet worden voor de karakterisatie van andere zuur-functionele polymeersystemen.

Aangezien zuur-functionele monomeren slechts in kleine hoeveelheden ingebouwd worden zijn spectroscopische technieken vaak niet gevoelig genoeg om exact te onderscheiden welke zuurtypes gebruikt zijn in een polymeersysteem. In Hoofdstuk 2 is een specifieke derivatisering ontwikkeld voor de zuur-functionele groepen in polymeersystemen. Hiervoor zijn modelsystemen gebruikt met een variatie in zuurtype en in monomeercompositie. Het is bewezen dat een bepaalde groep van derivatiseringsmaterialen, de phenacylbromides, specifiek met de polymere zuurgroepen reageerde onder vorming van phenacylesters. Derivatiseringsopbrengsten, bestudeerd met size-exclusie chromatografie (SEC), zijn hoog. Pyrolyse van de gederivatiseerde polymeersystemen liet zien dan phenacyl esters gevormd werden, het type phenacyl ester kon hierbij door middel van massaspectrometrie herleidt worden

naar het origineel gebruikte zuurmonomeer. Aangezien zuurmonomeren ook kunnen ontstaan tijdens een nevenreactie tijdens pyrolyse, wordt het als cruciaal gezien om een overmaat derivatiseringsreagens te verwijderen zodat ingebouwde zuurfunctionaliteit onderscheiden kan worden van pyrolytisch gecreëerd monomeer.

Het derivatiseringsprotocol zoals opgesteld in Hoofdstuk 2 is ook gebruikt voor de studie naar chemische heterogeniteit van polymeren. De phenacyl functionaliteit die geïntroduceerd wordt door de derivatisering van de zuurfunctionaliteit kan specifiek gedetecteerd worden door middel van ultraviolet (UV) detectie na scheiding door middel van SEC – aannemende dat er geen storende UV-actieve materialen aanwezig zijn in de polymeren. In Hoofdstuk 3 is een multi-detector SEC systeem beschreven, bestaande uit tenminste een UV detector (welke de concentratie van het zuurmonomeer meet in een molgewichtsfractie) en een brekingsindexdetector (RI, welke de totale polymeerconcentratie meet in dezelfde molgewichtsfractie). Deze setup kan gebruikt worden om de relatieve concentratie van de zuurmonomeren te berekenen in iedere molgewichtsfractie. Door deze informatie uit te zetten tegenover het molgewicht van het polymeer kan de heterogeniteit bepaald worden van het zuurmonomeer als functie van het molgewicht. Het totale piekoppervlak van de UV-actieve polymeerfractie kan berekend en vergeleken worden met de molaire response van een commercieel verkrijgbare phenacylester, waarbij de totale ingebouwde zuurhoeveelheid berekend kan worden. Een goede overeenkomst werd gevonden tussen de theoretische zuurhoeveelheid uit de synthese met de zuurhoeveelheid zoals berekend wordt uit de UV berekening. Een bijkomend voordeel van de derivatisering is dat de oplosbaarheid van de polymeren toeneemt, waarschijnlijk doordat er geen mogelijkheid meer is voor de zuurgroepen om inter- of intramoleculaire waterstofbruggen aan te gaan. Daarnaast wordt dn/dc verhoogd door inbouw van phenacyl zijgroepen, waardoor de gevoeligheid van RI detectie toeneemt. Het type analyse zoals beschreven is in Hoofdstuk 2 en 3 kan relatief makkelijk breder ingezet worden voor andere polymeer- of functionaliteitstypes, mits er een geschikt derivatiseringsprotocol toegepast wordt.

Een andere toepassing die is ontwikkeld, is om de zuurfunctionaliteit in polymeren te deprotoneren in niet-waterige condities. De zuurconstante (pK_a) van zuurgroepen verandert drastisch onder deze condities vergeleken met waterige condities. Dit zorgt voor uitdagingen om bases te vinden die sterk genoeg zijn om deprotonering te verkrijgen van zuurgroepen in niet-waterige condities. Hoofdstuk 4 beschrijft dat de combinatie van een polair aprotisch solvent (N-methylpyrrolidone, NMP) met een organische superbase (tetramethylguanidine, TMG) volledige deprotonering geeft

van de polymeergebonden zuurgroepen, zoals bepaald door middel van proton-NMR (^{1}H-NMR). Een goede correlatie is aangetoond tussen zuurconstantes van ingebouwde zuren in NMP met de zuurconstantes van vergelijkbare zuren uit de literatuur. Gebruik makend van deze condities zijn zuur-functionele polymeren zijn onderworpen aan niet-waterige ionenwisselingschromatigrafie (IEX). Initiële LC condities werd ingesteld zodat de zuur-functionele polymeren gedeprotoneerd waren en dus anionische groepen hadden. Deze geladen polymeren vertonen een sterke interactie met de quaternaire ammonium functionaliteit van de IEX stationaire fase en ondergaan dus adsorptie. Elutie van de geadsorbeerde polymeren werd bereikt door een gradiënt toe te passen met een toenemende concentratie aan triethylammonium formate, wat een organisch (oplosbaar) zout is (meest gebruikte zout in traditionele IEX is natriumchloride, welke onoplosbaar is in NMP en andere organische oplosmiddelen). Het retentiegedrag van modelsystemen onder IEX condities is vergeleken met traditionele normal- en reversed phase LC scheidingen. Beide traditionele methodieken resulteerden in een scheiding gerelateerd aan (hoofdzakelijk) de totale polariteit van de polymeren en geen specifieke scheiding op basis van aanwezigheid van een van de monomeertypes in deze modelsystemen. De IEX-aanpak vertoonde een goede correlatie tussen retentiegedrag en het nominale aantal zuurgroepen dat ingebouwd was in de polymeren – onafhankelijk van het type monomeer dat werd gebruikt naast het zuur-monomeer.

Een alternatieve aanpak is gerealiseerd door middel van capillaire elektroforese (CE). Deze techniek wordt zeer veel gebruikt voor de karakterisering van complexe systemen, zoals eiwitten, virusdeeltjes of antilichamen maar slechts zelden voor synthetische polymeren. Hoofdstuk 5 beschrijft een aanpak die gerelateerd is aan de ontwikkeling in Hoofdstuk 4, waarbij het gebruik van NMP en sterke organische bases zoals TMG en tetrabutylammonium hydroxide tot een duidelijke scheiding (gebaseerd op de verhouding lading/grootte) leidde tussen polymeren met een verschil in hoeveelheid ingebouwde zuurgroepen. Dit type scheiding kon echter slechts een beperkt aantal analyses aan, doordat de glazen CE capillairen sterk gecorrodeerd raakten door de hoge-pH condities in combinatie met hoge voltages en sterke solventen. Het veranderen van de compositie van het CE electroliet naar een overmaat zuur bleek ook te leiden tot het ontstaan van negatief geladen polymeren. Complexering van het polymeer met anionen uit het CE electroliet werd aangetoond – een proces wat bekend staat als heteroconjugatie. Het effect van verschillende zuren in het electroliet is onderzocht, waarbij zuren met een hogere pK_a dan het ingebouwde zuur aantoonbaar efficiënter waren in de complexering met het polymeer. De zuurverdeling van verschillende polymeren kon op deze manier

bepaald worden, waarbij polyurethanen een sterk afwijkend elektroforetisch gedrag vertoonden. Alhoewel dit toegeschreven kan worden aan grootte-verschillen in solutie, kan het gebrek aan direct naastgelegen zuren in urethaanchemie ook een effect hebben. De zuurverdeling kon aan de hand van elektroforetische data opgesteld worden, samen met een aantal fundamentele piek-statistieken die deze verdeling beschrijven. De invloed van molgewicht op het elektroforetische gedrag is onderzocht, en werd minimaal bevonden – iets dat verwacht werd voor een scheiding gebaseerd op lading/grootte-ratio's. Laag-moleculaire polymeren lieten hierbij een tailende piek zien richting het elektroforetische gebied met lage mobiliteit, wat verklaard worden door de toenemende relatieve invloed van de niet-geladen eindgroepen van het polymeer.

Additionele inzichten in de microstructuur van polymeren kan verkregen worden door de koppeling van orthogonale scheidingsprincipes. Multi-dimensionele LC kan de piekcapaciteit van een scheidingssysteem drastisch vergroten en/of andere informatie verschaffen aan de hand van de toegepaste scheidingsprincipes. Hoofdstuk 6 beschrijft de online koppeling van de IEX scheiding beschreven in Hoofdstuk 4, met SEC in de tweede dimensie. Een optimalisatie is uitgevoerd op dimensies van de ^{2}D kolom, loopvolume van de schakelkraan, ^{1}D gradiënt steilheid en ^{2}D flow rate. De verkregen IEX × SEC scheidingen laten een orthogonale scheiding zien voor een selectie aan polymeren met verschillen in molaire massa en zuurgehalte. Door gebruik te maken van kalibratiestandaarden en modelpolymeren konden beide LC dimensies gekalibreerd worden, wat geresulteerd heeft in een compleet gekalibreerd scheidingsvlak. Dit stelt men in staat tot karakterisering van ieder punt van het scheidingsvlak. Wanneer molecuulmassa-gemiddelden bepaald worden als functie van de zuurverdeling, worden verschillende stadia waargenomen in de zuurverdeling. Deze stadia zijn zeer waarschijnlijk indicaties voor het zogenaamde seed-stadium van de toegepaste emulsiepolymerisatie enerzijds, en anderzijds het bestaan van zeer zuurrijke polymeren die kunnen ontstaan als gevolg van waterfase- of scheidingsvlakpolymerisatie. De combinatie van orthogonale LC technieken in multidimensionale LC heeft een duidelijk voordeel over de toepassing van de individuele scheidingstechnieken.

0

OVERVIEW OF (CO)-AUTHORS' CONTRIBUTIONS

Overview of (co)-authors' contributions

Chapter 1: General introduction - Water-borne polymers and polymer separation techniques.

Ton Brooijmans:	Wrote the manuscript. Supervised involved student.
Aniek Schreuders:	Performed literature study. Assisted in writing the manuscript.

Chapter 2: Acid monomer analysis in waterborne polymer systems by targeted labeling of carboxylic acid functionality, followed by pyrolysis – gas chromatography.

Ton Brooijmans:	Developed the idea. Designed the experiments and identified possible routes for chemical modification of acid-functional polymers. Co-performed the experiments. Supervised involved students and experiments. Wrote the manuscript.
Remco Okhuijsen:	Co-performed the experiments. Reviewed the manuscript and made suggestions for improvements.
Ingrid Burggraaf-Oerlemans:	Co-performed the experiments. Reviewed the manuscript and made suggestions for improvements.
Peter Schoenmakers:	Overall supervisor of the project. Reviewed the manuscript and made suggestions for improvements.
Ron Peters:	Overall supervisor of the project. Reviewed the manuscript and made suggestions for improvements.

Chapter 3: Heterogeneity analysis of polymeric carboxylic acid functionality by selective derivatization followed by size exclusion chromatography.

Ton Brooijmans:	Developed the idea. Designed the experiments. Co-performed the experiments. Co-performed the experiments. Supervised involved students and experiments. Assisted in automation scripts for data processing. Wrote the manuscript.
Remco Okhuijsen:	Co-performed the experiments. Developed automation scripts for data processing. Reviewed the manuscript and made suggestions for improvements.

Ingrid Burggraaf-Oerlemans:	Co-performed the experiments. Reviewed the manuscript and made suggestions for improvements.
Bob Pirok:	Reviewed the manuscript and made suggestions for improvements.
Peter Schoenmakers:	Overall supervisor of the project. Reviewed the manuscript and made suggestions for improvements.
Ron Peters:	Overall supervisor of the project. Reviewed the manuscript and made suggestions for improvements.

Chapter 4: Charge-based separation of synthetic macromolecules by non-aqueous ion exchange chromatography.

Ton Brooijmans:	Co-developed the idea. Designed the experiments and instrumental setup. Co-performed the experiments. Supervised involved students and experiments. Wrote the manuscript.
Pascal Breuer:	Co-performed the experiments. Reviewed the manuscript and made suggestions for improvements.
Peter Schoenmakers:	Overall supervisor of the project. Reviewed the manuscript and made suggestions for improvements.
Ron Peters:	Overall supervisor of the project. Co-developed the idea. Reviewed the manuscript and made suggestions for improvements.

Chapter 5: Charge-based separation of acid-functional polymers using non-aqueous capillary electrophoresis employing deprotonation and heteroconjugation approaches.

Ton Brooijmans:	Developed the idea. Designed the experiments and instrumental setup. Co-performed the experiments. Supervised involved students and experiments. Wrote the manuscript.
Pascal Breuer:	Co-performed the experiments. Made suggestions to improve instrumental setup. Performed method optimizations. Reviewed the manuscript and made suggestions for improvements.

Aniek Schreuders:	Co-performed the experiments. Performed method optimizations. Reviewed the manuscript and made suggestions for improvements.
Myrthe van Tilburg:	Co-performed the experiments. Performed method optimizations. Reviewed the manuscript and made suggestions for improvements.
Peter Schoenmakers:	Overall supervisor of the project. Reviewed the manuscript and made suggestions for improvements.
Ron Peters:	Overall supervisor of the project. Reviewed the manuscript and made suggestions for improvements.

Chapter 6: Two-dimensional tools for analyzing polymer microstructure; coupling non-aqueous ion-exchange chromatography to size-exclusion chromatography.

Ton Brooijmans:	Developed the idea. Co-developed the instrumental setup and method optimizations. Co-performed the experiments. Wrote the manuscript.
Pascal Camoiras Gonzales:	Co-developed the instrumental setup and method optimizations. Co-performed the experiments. Reviewed the manuscript and made suggestions for improvements.
Bob Pirok:	Co-developed the instrumental setup and method optimizations. Reviewed the manuscript and made suggestions for improvements.
Peter Schoenmakers:	Overall supervisor of the project. Reviewed the manuscript and made suggestions for improvements.
Ron Peters:	Overall supervisor of the project. Reviewed the manuscript and made suggestions for improvements.

ABBREVIATIONS

A

Abbreviations

2D-LC	Two-dimensional Liquid Chromatography
2-EHA	2-Ethylhexylacrylate
2-EHMA	2-Ethylhexylmethacrylate
AA	Acrylic acid
BA	Butyl acrylate
BA	Butyl acrylate
BHT	Butylated hydroxytoluene
BMA	Butyl methacrylate
BSTFA	N,O-bis(trimethylsilyl)acetamide
CCD	Chemical Composition Distribution
CE	Capillary Electrophoresis
CHCl3	Chloroform
CMC	Critical Micelle Concentration
DCM	Dichloromethane
DMAc	Dimethylacetamide
DMF	Dimethylformamide
DMPA	Dimethylolpropionic acid
DMTMM	4-(4,6-dimethoxy-1,3,5-triazin-2-yl)-4-methylmorpholinium chloride
EA	Ethyl acrylate
EMA	Ethyl methacrylate
EtOH	Ethanol
FAB-MS	Fast-atom-bombardment MS
FID	Flame ionisation detector
FTD	Functional type distribution
GC	Gas chromatograhpy
GMA-EDMA	Glycidyl methacrylate - ethylene glycol dimethacrylate
GPC	Gel permeation chromatography
GPEC	Gradient polymer elution chromatography
HDC	Hydrodynamic chromatography
HILIC	Hydrophilic interaction chromatogrpahy
HPLC	High-performance liquid chromatography
(HT)-ELSD	(High Temperature) evaporative light scattering detector

(HT)-ILC	(High Temperature) interaction liquid chromatography
(HT)-SEC	(High-Temperature) size-exclusion chromatography
ILC	Interaction liquid chromatography
LCCC	Liquid chromatography under critical conditions
LiBr	Lithium bromide
LiCl	Lithium chloride
MA	Methyl acrylate
MAA	Methacrylic acid
MALDI-MS	Matrix-assisted laser-desorption/ionization MS
MeCN	Acetonitrile
MeOH	Methanol
MMA	Methyl methacrylate
MS	Mass spectrometry
MSTFA	N-methyl-N-(trimethylsilyl)trifluoroacetamide
MW	Molecular weight
MWD	Molecular weight distribution
NACE	Non-aqueous capillary electrophoresis
NAIEX	Non-aqueous ion exchange chromatography
NMM	N-methylmorpholine
NMP	N-methylpyrrolidone
NMR	Nuclear magnetic resonance
NPLC	Normal Phase Llquid chromatography
ODCB	o-Dichlorobenzene
ODS	Octadecylsilyl
pAA	Polyacrylic acid
PB	Phenacylbromide
PDLA	Poly(D-lactic acid)
PDMS	Polydimethylsiloxane
PE	Polyethylene
PEEK	Polyether ether ketone
PEG	Polyethylene glycol
PGC	Porous graphite column
PLLA	Poly(L-lactic acid)

PMMA	Polymethyl methacrylate
PP	Polypropylene
PPG	Polypropylene glycol
PSDVB	Polystyrene-divinylbenzene
PS	Polystyrene
PTHF	Polytetrahydrofuran
PVPVA	Poly(N-vinyl pyrrolidone-co-vinyl acetate)
PyGC	Pyrolysis-gas chromatography
PyLC	Pyrolysis-liuid chromatography
RPLC	Reversed phase liquid chromatography
SC	Slalom chromatography
SEC	Size-exclusion chromatography
SG-NCC	Solvent gradient at near critical conditions
SLS	Sodium lauryl sulfate
TCB	Trichlo robenzene
TEA	Triethylamine
TFA	Trifluoroacetic acid
TGIC	Temperature gradient interaction chromatography
THF	Tetrahydrofuran
TMG	Tetramethylguanidine
TOF-SIMS	Time-of-flight secondary-ion mass spectrometry
UHP-GPEC	Ultra-high performance gradient polymer elution chromatography
UHPLC	Ultra-high performance liquid chromatography
UHP-SEC	Ultra-high performance size-exclusion chromatography
UV	Ultraviolet
VOC	Volatile organic compound

SYMBOLS

S

Symbols

Vr	Retention/elution volume	mL
V_0	Column void volume	mL
V_i	Column packing pore volume	mL
K	Distribution constant	-
$[C]_s$	Concentration of analyte in pore volume	-
$[C]_m$	Concentration of analyte in mobile phase	-
M_n	Number-average molar mass	$g.mol^{-1}$
M_w	Weight-average molar mass	$g.mol^{-1}$
M_p	Molar mass at peak apex	$g.mol^{-1}$
$[\eta]$	Intrinsic viscosity	dL/g
M	Analyte molecular weight	$g.mol^{-1}$
R_θ	Rayleigh scattering factor	-
$P_{(\theta)}$	particle scattering function	-
Ai	Virial coefficient	-
n	Refractive index	-
λ_0	Incident light wavelength	nm
N	Avogadro's number	6.0221×10^{23} mol^{-1}
dn/dc	Refractive index increment of polymer solution	-
H	Plate height	mm
d_p	Stationary phase particle diameter	µm
D_m	Diffusion coefficient of analyte in mobile phase	
u	Flow	$m.s^{-1}$
W	Peak width at baseline	min
De	Deborah number	-
K_{pb}	Packed bed structure constant	-
η	Mobile phase viscosity	Pa.s
ϕ	Flory-Fox parameter	-
r_g	Radius of gyration	nm
R	Gas constant	$8,31446\ m3{\cdot}Pa{\cdot}K^{-1}{\cdot}mol^{-1}$
T	Temperature	º
ΔG_0	Gibbs free energy change	
ΔS_0	Entropic contribution to sorption process	

ΔH_0	Enthalpic contribution to sorption process	
λ	HDC aspect ratio	-
r_a / r_h	Analyte radius	nm
r_c	Flow channel radius	nm
F_d	Driving force	Jm^{-1}
q	Charge of the analyte	C
E	Electric field strength	Vm^{-1}
F_f	Friction force	Jm^{-1}
V_e	Electrophoretic mobility	ms^{-1}
μ_a	Apparant mobility	
μ_{EOF}	Electro-osmotic flow	
μ_e	Electrophoretic mobility, independent of field strength	
ε	Dielectric constant	Fm^{-1}
ζ	Zeta-potential	V
φ_w	Weight fraction monomer	
φ_c	Theoretical weight fraction monomer	
φ / φ_m	Acid monomer fraction	
pH^*	Non-aqueous pH	
μ_{eff}	Effective mobility	$m^2V^{-1}s^{-1}$
L_d	Capillary length inlet - detector	m
L_t	Total capillary length	m
t_m	Migration time	s
t_{EOF}	EOF migration time	s
C_n	Number-average charge	φ
C_p	Charge at peak top	φ
$FWHM$	Full width at half peak height	φ
As	Assymetry factor	
n_{acid}	Number of acid groups	
ε	Pore volume fraction	
d	Column diameter	cm
L	Column length	cm
R_s	Peak resolution	

PUBLICATIONS (CO)AUTHORED

P

Publications (co)authored

Acid monomer analysis in waterborne polymer systems by targeted labeling of carboxylic acid functionality, followed by pyrolysis – gas chromatography (Chapter 2 of this thesis). Journal of Chrom A, 2018, T. Brooijmans, R. Okhuijsen, I. Oerlemans, P.J. Schoenmakers, R.A.H. Peters.

Applications of Charged Aerosol Detection for Characterization of Industrial Polymers (Chapter 15), Wiley Book Chapter, 2017, T. Brooijmans, P.J.C.H Cools.

Heterogeneity analysis of polymeric carboxylic acid functionality by selective derivatization followed by size exclusion chromatography (Chapter 3 of this thesis), Analytica Chimica Acta, 2019, T. Brooijmans, R. Okhuijsen, I. Oerlemans, B.W.J Pirok, P. J. Schoenmakers, R.A.H. Peters.

Charge-based separation of synthetic macromolecules by non-aqueous ion exchange chromatography (Chapter 4 of this thesis), Journal of Chrom A, 2020. T. Brooijmans, P. Breuer, P. J. Schoenmakers, R.A.H. Peters.

Charge-based separation of acid-functional polymers using non-aqueous capillary electrophoresis employing deprotonation and heteroconjugation approaches (Chapter 5 of this thesis), Analytical Chemistry, 2021, T. Brooijmans, P. Breuer, A. Schreuders, M. van Tilburg, P. J. Schoenmakers, R.A.H. Peters

Network Structure in Acrylate Systems: Effect of Junction Topology on Cross-Link Density and Macroscopic Gel Properties, Macromolecules, 2016, B. Wu, W. Chassé, R.A.H. Peters, T. Brooijmans, A. Dias, A. Heise, C. J. Duxbury, A.P.M. Kentgens, D. F. Brougham, V. M. Litvinov.

Separation and characterization of polyurethanes using (ultra-high pressure) gradient-elution liquid chromatography and mass-spectrometric techniques, PhD thesis E.Uliyanchanko, 2012, E. Uliyanchenko, P. J. C. H. Cools, P. J. Aarnoutse, T. Brooijmans, Sj. van der Wal, P. J. Schoenmakers.

Analysis of charged acrylic particles by on-line comprehensive two-dimensional liquid chromatography and automated data-processing, Analytica Chimica Acta, 2019, B.W.J.Pirok, N. Abdulhussain, T. Brooijmans, T. Nabuurs, J. de Bont, M.A.J. Schellekens, R.A.H. Peters, P. J. Schoenmakers.

Microstructural analysis of polymers employing two-dimensional solutions; coupling non-aqueous ion-exchange chromatography to size-exclusion chromatography (Chapter

6 of this thesis), Submitted to Journal of Chromatography A, 2022, T. Brooijmans, P. Camoiras Gonzalez, B.W. J. Pirok, P. J. Schoenmakers, R.A.H. Peters

ACKNOWLEDGEMENTS

A

Acknowledgements

Aha, busted! Not reading from the beginning, but went straight here to see your name, did you? I will give you a chance to start over, and I will see you back here tomorrow or the day after. For those that already read the whole thing: welcome, to the most-read part of a PhD thesis..

Ever since I can remember, I have had an interest in how things worked – no doubt resulting in many headaches for my parents. I guess my 'but why'-phase never ended... good grades got me into HAVO and subsequently VWO which was quite enjoyable since I basically did not have to do anything besides having fun with my friends, playing soccer in the parc or sneaking out for a beer before physics. After VWO, finally my interests in chemistry could be sated in the Bachelor program in Eindhoven – or at least so I thought. Turns out being lazy in HAVO and VWO could get you TO that level, but from there on out that did not work anymore. Also, the great times in the AOR, playing cards, the constant gaming (at two schools, both in Den Bosch and Eindhoven) also did not do wonders for my motivation to go to classes other than practical classes. Also having teachers read a full chapter of chemometrics, electrochemistry etc to the class - literally from the book - did not help a lot. So I flunked out – big time. My parents made it crystal clear at that time that the choice was fully mine. From that point on - the penny dropped and I finished my bachelor's degree 1 year late. At that point, it took me about 20 seconds to contemplate advancing my study for a Master's degree but being in classes for several more years was a severely depressing thought. So to find a job! Within a few weeks after graduation, I somehow successfully interviewed for a job at Analytico as an environmental analyst. After 2.5 years there, I felt I was done learning. NeoResins was looking for a technician in their analytical lab and I was really happy to get a job closer to home, which was new and challenging. To this day, I can still say that every day here is new and challenging – regardless of the name or logo we have on the building. The "but-why"-phase does not end here, and neither does it at the University of Amsterdam – where I was lucky enough to get a spot as an external PhD candidate. Although not nearly being there often enough, I thoroughly enjoy(ed) the discussions and collaborations and the general atmosphere of buzzing enthusiasm.

Although my name is on this book, there should actually be many names – as there are a lot of people that have been essential to my research, this thesis, my motivation, insights and personal developments. Quite frankly, this whole process and the road towards it has been a wonderous chain of events, in which all the people below play their own role.

Paul, you were the first one that mentioned to me that I should consider doing a PhD. I think I laughed in your face (loud) when you first mentioned it, but (as so often) you turned out to be right. When you took me under your wing and tried to educate me in the finesses of polymer chemistry, HPLC, SEC etc, I frequently went home with a pounding headache of all the information I tried to digest but I guess some of it sticked. I have taken over doing a "Paul Cools" in the lab, which means: someone else has tried to do something already 10 times, they finally ask you what they are doing wrong, you do the exact same thing they already did but now it works. Also the pink, glittery hula-hoop you bought us is still hanging proudly above my desk. Many people coming into my office have probably thought I have a weird hobby because of that thing but the people that are not too afraid to ask what the hell it means is leave the office with a smile. I am sincerely grateful for you educating me in polymer analysis, dragging me to DSP and other events and for mentoring me in many other aspects of this work. Also happy we can still discuss pretty much anything still, such as the wonderous world of the USA, politics and, of course, Ajax.

Peter, before we actually met I have been at many of your presentations at various events. These were thoroughly enjoyable, mixing chemistry and analytics with humor (sometime a bit towards the edge) and a touch of Belgian beer. I remember when I gave my first lecture at the DSP conference in Lelystad in 2014 and as if I was not nervous enough already, you also showed up. After the talk (I am sure I was babbling) you approached me in the break session and told me you liked the talk and encouraged me to continue this line of work. After more and more interactions like Elena's PhD, of course Ron joining our group and Bob's research, I was finally ready to ask you if you would be one of my promotors. You took the words out of my mouth that day, you probably knew for quite some time where this was going. Despite never having been to any of your classes, the atmosphere you created at the UvA is very inspiring and I rarely leave Science Park without several ideas, collaborations or feeling energized. Creating such an atmosphere is really the basis of good science in my opinion (and it is rather seldom encountered). I am very grateful for being able to contribute a small part to the awesome tools, insights and knowledge that have been developed at the UvA under your guidance. A special 'thank you' for helping me in the final days before submission of the final thesis is also in place!

Ron, I think it is safe to say this work would definitely not have been here without you. After you joined our lab, we did not take long to understand each other (no, I am not talking about accents here) and somewhat to my surprise you echoed the same recommendation Paul gave me about doing a PhD. That got me thinking, and after

careful consideration and some discussions with you, I figured that I should just try and see if this would be something for me. Your positive attitude with your full support (!) for (many) silly ideas I have had these last years have really provided me with enough confidence to tackle the hurdles that were encountered in this work. Even if we did not agree at first, you were always right (even about the Ion Exchange – which gave me serious headaches trying to envision how we could get that to work for non-aqueous systems). Your honest input in various stages of the research was immensely valuable, and really helped shaping the work itself, but also shaped me as a person / researcher. Thank you for your *full support*!!

Bob, I remember meeting you for the first time, at a UvA meeting about two-dimensional LC – must have been around the start of your Maniac time. You struck me as a smart, witty and extremely organized researcher (I actually felt quite intimidated by the level of detail of your meeting notes!) and you have amazed not only me with your research but the whole analytical world. I have really enjoyed our collaborations and conversations, and appreciate the honest feedback when something I did or wrote was crappy (or good). Should you ever need someone from industry for any of your future projects, feel free to give me a call – I owe you! Literally every time we discussed various topics over the years, you provided me with confidence, ideas or a general positive feeling about my research. At certain moments, this really pulled me through!

A special thanks goes out to my co-authors, which have helped me in various projects, research topics, interpretations etc:

Ingrid, besides doing an insane amount of pyrolysis work we probably drove half the lab insane with the weird voices we used to speak with (happy you grew up..). Your transformation from "Oh grutjes" to "Did I ask you something? No? Then shut your face" has been thoroughly amusing, but also helped you stand your ground in a difficult environment – which an industrial laboratory is. Always wanting to help out, and being (annoyingly) positive all the time – I am happy you still work with us!

Remco, you also started out as an intern at our lab a long time ago and I do not think anyone would recognize you if they would meet that guy now. Starting out very quiet, over time you have developed yourself to be proficient in almost every technique we have available – which is amazing by itself. Your coding skills helped me out a lot when we were developing the acid heterogeneity calculations, and your way of calmly explaining how those things work is very much appreciated – even now you have found a new place in the organization, you are still instrumental for the efficiency of our lab.

Also, your ultra-dry humor ("There is no 'our age', there is your age and there is my age") still cracks me up.

Pascal B, you had _the_ hardest job when we decided to explore charge-based separations. No literature, no prior art, nada. Turns out many of the things you started with were logical, although we did not completely understand what was going on. Coming by motorcycle every day from Leiden to Waalwijk for 9 months… I admire your motivation! Proud that you landed a PhD spot yourself.

Myrthe, nothing beats analysts from Waalwijk, right? Your awesome work on the capillary electrophoresis project brought us several steps closer to the end result, frustrating as it may have been at times. I have never seen anyone making purple NMP before.. I was genuinely sad when we could not keep you with us after your temporary contract, but I think you landed nicely… perhaps more will be in store in the future!

Aniek, yet another intern that stuck around – and again one to help the CE work along. I remember interviewing you for the ASTP program, you came back later for an industrial assessment and strangely enough you were not scared enough by us - so you applied for an internship and even a job after your bachelors' degree. You really have the capacity well beyond that degree though, but we are very happy with you joining our lab.

Pascal C, we met just before Covid hit – and every time we talked about doing 2DLC work at the UvA some kind of lockdown slammed our options. Your kind demeanor really is an asset to the UvA laboratories, have seen you helping 15-20 students a day with the most diverse sets of troubles you can think of. It is people like you that make projects or studies go well, and it is seldom appreciated! Also your humor is very much appreciated ("performing the Jesus" is a term I will never forget).

From DSM / Covestro, one of the people who cannot be forgotten is Koen. We had great times at Fontys as practicum buddies, I guess we still have the exact same roles now as we did back then! Still thankful for you mentioning there was a job opening at the analytics department. Sadly there is a dark side (pun alert) to anyone, as your love for stouts and porters is simply unacceptable.

Of course our entire analytical team should be mentioned. Together we have developed our lab to an expertise center that is recognized throughout the company and beyond. In many occasions, the type of support that we can deliver provided a competitive edge – but most importantly the working atmosphere we have is one of the key drivers of our

success. Thank you Qi, Jan, Harm, Anne-Mieke, Ingrid, Radko, Martin, Nico & Aniek, but also credits to the people that played a significant role in the past of our department (Maria, Alida, Ragna, Paul, Dorina (†), Marcel & Rob). Marcel, many thanks for hiring me although you did not have the official budget to do so at that time. Also Robert, Konraad, Ad and Jan H – thanks for your support. Either of you could have stopped this whole thing at any time in view of business priorities, and I would have understood. Combining a PhD with a challenging job in industry and a family is not something to be taken lightly, but you have given me the opportunity to at least try.

From (former) DSM sites, I really liked to collaborate with people like Ynze, Harry, Erwin and Jan. The knowledge you have on a broad scale of topics is amazing, and I have learnt a lot on separation mechanisms, equipment and derivatization protocols. Also enjoyed reconnecting with my supervisor Remco from my Organon internship again. Although analyzing cyclodextrines is something very different from industrial polymers, the application of 2DLC, capillary electrophoresis and ion-exchange chromatography somehow came full circle in this thesis.

These last years, I had many interactions the CASA group – which were without exception thoroughly enjoyable (Noor, Stef, Wouter, Jordy, Tijmen, Andrea, Govert, Rob and many, many more). The knowledge and talent there is simply staggering. Whether meeting at the universities or at symposia, I rarely left there without new ideas. All the talented people from CASA – thanks for making me feel welcome! This group of people and all the developments that are going on there are simply amazing - keep doing what you do!

Arian and Maarten, happy to have had you as my opponents in the learned discourse! Sjoerd and Cor, many thanks for proofreading this thesis, it is remarkable how many unforced errors I left in there. Your comments helped improving this work a lot! To all committee members (Arian, Maarten, Paul, Wolfgang, Sjoerd, Cor and Gert-Jan), thank you for agreeing to be on my committee - an impressive group of very knowledgeable experts!

Another celebrity in the field, Cari – we met in a feasibility discussion Agilent organized to assess our plans for capillary electrophoresis. “I do not see how it wouldn’t work” were your words, well we got it working but it turned out to be harder than expected. Thanks for introducing me to the wondrous world of electrophoresis, an absolutely fascinating technique.

Anita from Skinque.com – thank you for the awesome cover image of this thesis. It was a very pleasant collaboration, and I will definitely come back to you if I ever need another trash polka design – I highly recommend your work!

To my parents, I can imagine you did not know what to do with this strange kid at times (having kids now, I can totally relate). You gave me the room to develop myself in my own way, which probably was not the easiest for you or myself (stubborn as I may be). I do still think you should have kept me from growing long hair though.

My second family – the Drunen crew. I met some of you at VWO, HAVO, music school, sports, elementary school, or even before that. I consider myself lucky to have such a steady group of people to grow up with. Our times at HAVO / VWO are legendary, but also hanging out at the Cantu or of course Polonia were fun times. Very happy we still get together with the whole group (-1, we miss you Bèr †), although it is not nearly frequent enough in my opinion. Mark, Arno – thanks for supporting me as my paranymphs! Also, Twan, Bjorn, Jorg, Koen, Maarten, Michiel, Niels, Marijn, Rogier, Sander, Stefan W, Stefan K, Eric – thanks for the good times, hope we have much more of those!

Last but certainly not least, my own family. Jelle and Stan, I recognize myself in many parts of you – which is fun most times but sometimes confronting as well. For most of your life, I have been busy working on parts of this thesis but I tried to keep this as much away from you as possible. I hope you will also find out that there is nothing that you cannot do – as long as you put your mind to it, I will support you with whatever paths you choose. Monique, I can fully understand that it has been difficult sometimes with me choosing this path, albeit with your support from the start. The amount of time this has taken, is beyond description so I can imagine seeing the back of my laptop screen is something you can do without. I would definitely not have been able to do this without your support and patience. You also shaped me as a person, which I am eternally grateful for. To the three of you – I cannot imagine life without you. Thank you for everything!